THÈSE DE DOCTORAT
DE L'UNIVERSITE DE LYON

Préparée à l'Ecole Normale Supérieure de Lyon

Ecole Doctorale n°340 - Biologie Moléculaire Intégrative et Cellulaire (BMIC)

Discipline : Sciences de la Vie

par

Antoine Ducuing

Signalling and morphogenesis during *Drosophila* dorsal closure

---

Thèse présentée et soutenue publiquement à l'Ecole Normale Supérieure de Lyon, le

11 mars 2016

Directeur de thèse : Dr. Stéphane Vincent

Devant le jury composé de:

Dr. Yohanns Bellaïche, Directeur de Recherche, Institut Curie, Paris	Rapporteur
Dr. Krzysztof Jagla, Directeur de Recherche, GReD, Clermont-Ferrand	Rapporteur
Dr. Stéphane Vincent, Maître de Conférences, LBMC, ENS de Lyon	Directeur de Thèse
Pr. Arezki Boudaoud, Professeur, RDP, ENS de Lyon	Examinateur
Dr. Muriel Grammont, Chargée de Recherche, LBMC, ENS de Lyon	Examinatrice
Dr. Raphaël Rousset, Chargé de Recherche, IbV, Nice	Examinateur



On a deux vies. La deuxième commence le jour où on réalise qu'on en a juste une.

— Confucius

Acknowledgement

First of all, I would like to thank my two *rapporteurs*, Yohanns Bellaiche and Krzysztof Jagla for spending their time on reading my thesis. I also thank all my jury for letting me defend my thesis, for listening to my scientific presentation, and for future exciting scientific discussions.

I would also like to thank Stéphane for his mentoring, technical advice, exiting scientific discussions and patience over these four years spent together. I hope that the number and the quality of publications in which the two of us are involved will confirm that our association was stimulating and fructuous.

I also thank Muriel Grammont and Raphaël Rousset for participating to my "*Comités de suivi de thèse*" during which they provided me useful technical, conceptual and human feedbacks.

Many thanks to Dali Ma, who helped me to greatly improve my scientific writing.

I also thank all the persons that helped me during my thesis: Djamel Belgarbi (creating the embryo collection vials for instance), Christophe Chammot, Claire Lionnet and Elodie Chatre (members of the PLATIM facility, they helped me many times on diverse microscope and ImageJ plugins), all the fly persons for advice and discussion.

I also thank my wife Jennifer for critical and extensive reviewing of my thesis, for assistance when going to the lab on Sunday was mandatory, for scientific discussions about the overall relevance of my work from a non-specialist point of view and for her general support.

Unless otherwise indicated, cartoons are home-made, confocal pictures have been generated by me.

ABSTRACT

Drosophila dorsal closure is a key embryonic process during which the dorsal-most epidermal cells called leading edge cells differentiate and act in a coordinated manner to close a transient dorsal hole covered by the amnioserosa in a process reminiscent of wound healing. During dorsal closure, leading edge cells have a highly specialized cytoskeleton: leading edge cells are polarized, display strong adherent junctions, accumulate a dense microtubule network and produce a trans-cellular acto-myosin cable and filopodia. Leading edge cells receive both JNK and DPP (TGF-ß homolog) inputs where JNK induces DPP. These two signalling pathways are crucial for dorsal closure since embryos mutants for either JNK or DPP pathway components fail to undergo correct dorsal closure and exhibit a "dorsal open" phenotype. However, how JNK and DPP contribute to dorsal closure and how these signals are integrated in a robust manner remained unclear. I showed that JNK and DPP are wired in a network motif called 'feed-forward loop' (FFL) that controls leading edge cell specification and differentiation. The DPP branch of the FFL filters unwanted JNK activity that occurs during thermal stress. DPP here buffers against environmental challenges and canalizes cell identity, which is a novel function from its well-established ability to spread spatial information.

Next, I focused on the actin cable, a supra-cellular structure produced by the leading edge cells during dorsal closure or wound healing from fly to humans. Using Zasp52, one of the JNK/DPP feed-forward loop targets I identified, I noticed that the actin cable is a discontinuous structure and is dispensable for both dorsal closure and wound healing. This questions the main model in which the actin cable acts as a contractile purse string. My data suggest that the actin cable does not provide a major contractile force. Rather, the actin cable balances forces and stabilizes cell geometry so that closure resolves in a perfectly structured and scar-free tissue. The

absence of the cable leads to cell shape irregularities as well as patterning and planar cell polarity defects that are reminiscent of scarring. We propose that the cable prevents scaring by acting as a mechanical freeze field that protects fine cellular structures from the major closure forces that operate at tissue level.

I also showed that during dorsal closure, DPP does not prevent JNK-induced cell death but rather that the physiological cell death of the amnioserosa participates to the onset of the dorsal open phenotype in DPP signalling mutant embryos.

Last, I found that over time, abnormal tensions / stress can trigger ectopic JNK activity. This stress-induced JNK activity is crucial for embryonic wound healing.

Altogether, my work brings new insights on the signalling and morphogenesis during dorsal closure.

RESUME

La fermeture dorsale est un événement majeur de l'embryogénèse de la drosophile durant lequel les cellules les plus dorsales de l'épiderme se différencient et agissent de concert pour refermer une ouverture dorsale temporairement recouverte par l'amnioséreuse. Ce processus présente de nombreuses similarités avec la cicatrisation cellulaire. Pendant la fermeture dorsale, les cellules de la marge active ont un cytosquelette extrêmement dynamique : les cellules sont polarisées, elles accumulent de fortes jonctions adhérentes et un réseau de microtubule dense. Les cellules de la marge active produisent également un câble d'actine ainsi que des protrusions appelées filopodes. Pendant la fermeture dorsale, les cellules de la marge active sont régulées par les voix JNK et DPP (homologue à la voie TGB-ß), où JNK induit DPP. Ces deux voies sont nécessaires à la fermeture dorsale. En effet, dans les mutants de la voie JNK ou DPP, la fermeture dorsale ne se fait pas. Les embryons présentent un phénotype d'ouverture dorsale. Cependant, on ne connaît pas comment les signaux de la voie JNK et DPP sont intégrés par les cellules de la marge active pour permettre une fermeture dorsale robuste. J'ai montré que les voies JNK et DPP forment une boucle cohérente appelée « feed-forward loop » (boucle d'anticipation) qui contrôle la différentiation des cellules de la marge active. La branche DPP de cette boucle filtre les signaux non désirés de la voix JNK quand les embryons sont soumis à un stress thermique. DPP joue un rôle ici de tampon contre les variations environnementales, ce qui est une nouvelle fonction par rapport à son rôle bien décrit de morphogène.

Je me suis ensuite concentré sur le câble d'actine, une structure supra-cellulaire produite par les cellules de la marge active lors de la fermeture dorsal. Les cellules autour d'une plaie dans des embryons de Drosophile, de poulet ou même de souris produisent également ce câble d'actine. En me servant de Zasp52, l'une des

cibles de la boucle de régulation JNK / DPP, j'ai montré que le câble d'actine est une structure discontinue qui n'est pas nécessaire pour la fermeture dorsale ou pour la cicatrisation cellulaire. Ceci remet en cause le modèle principal selon lequel le câble d'actine agit comme un cordon de bourse qui se ferme. J'ai montré que le câble ne confère par une force contractile pendant la fermeture. Le câble d'actine homogénéise les forces et stabilise la géométrie cellulaire pour que la fermeture se fasse de manière parfaite et sans cicatrice. Sans le câble, les cellules ont une forme irrégulière, associé à des défauts de patterning et des défauts de polarité planaire qui ressemblent aux défauts que l'on trouve lors de la formation d'une cicatrice. Nous proposons donc que le câble empêche la formation de cicatrice en « congelant » les propriétés mécaniques des cellules afin de les protéger des forces qui agissent au niveau tissulaire lors de la fermeture dorsale.

J'ai également montré que lors de la fermeture dorsale, DPP ne protège pas contre la mort cellulaire induite par JNK. J'ai également montré que c'est plus vraisemblablement la mort cellulaire dans l'amnioséreuse qui participe à l'apparition du phénotype d'ouverture dorsale dans les mutants de la voie DPP.

Enfin, j'ai montré que les tensions anormales / le stress peuvent déclencher l'activation de la voie JNK. Cette activité de JNK induite par le stress est cruciale pour la cicatrisation cellulaire chez l'embryon.

En conclusion, mon travail apporte un regard neuf sur la signalisation et la morphogenèse lors de la fermeture dorsale de l'embryon de Drosophile.

INDEX

ABSTRACT 7

RESUME 9

INDEX 11

FIGURES INDEX 15

ABBREVIATIONS 17

INTRODUCTION 21

I. From Thomas Hunt Morgan to Today: *Drosophila melanogaster* as a powerful model organism to study signalling and morphogenesis 21

I.1 Thomas Morgan and his pioneer 'Fly Room' 21

I.2 Easy to grow, easy to keep: *Drosophila* as a versatile tool 22

I.3 A small but instructive genome 23

I.4 *Drosophila* genetics 25

I.5 Live imaging and *in vivo* techniques 26

II. *Drosophila* embryonic development 29

II.1 Early embryogenesis (Stage 1 – Stage 5) 29

II.2 Gastrulation (Stage 6 – Stage 7) 32

II.3 Germ band extension (Stage 8 – Stage 10) 35

II.4 Segmentation and trachea invagination (Stage 11) 37

II.5 Germ Band retraction (Stage 12) 41
II.6 Dorsal closure (Stage 13 – Stage 15) 43
II.7 Late embryogenesis (Stage 16 – Stage 17) 44

III. Morphogenesis during dorsal closure 45
III.1 An overview of dorsal closure 47
III.2 The amnioserosa 50
III.3 The actin cable 53
III.4 The filopodia 59
III.6 Dorsal closure has a model for wound healing 63

IV. Signalling during dorsal closure 65
IV.1 The JNK pathway: a stress-response and developmental pathway. 65
IV.2 The DPP pathway: a patterning and morphogenetic pathway. 70

V. Jupiter, Jaguar and Zasp52: 3 cytoskeletal-associated proteins that define the leading edge identity during dorsal closure 78
V.1 Jupiter, a microtubule-associated protein 79
V.2 JAGUAR, the Myosin VI homolog 82
V.3 Z band alternatively spliced PDZ-motif containing protein 52 84

RESULTS 88

1. A DPP-mediated feed-forward loop canalizes morphogenesis during *Drosophila* dorsal closure 88
1.1. The Article 88
1.2. Additional figures not included in the paper 89

2. Zasp52 paper 106

3. Stress-induced JNK story 142

4. Cell death paper 155

ADDITIONAL PAPERS 197

1. Absolute requirement of cholesterol binding for Hedgehog gradient formation in *Drosophila*. 198

2. Cholesterol-free and cholesterol-bound Hedgehog: Two sparring-partners working hand in hand in the Drosophila wing disc? 200

DISCUSSION 213

1. JNK and DPP form a coherent feed-forward loop during dorsal closure. 216

2. What is the leading edge? 220

3. Zasp52 is an upstream regulator of the actin cable 222

4. The actin cable: do not call me purse string. 224

5. Is JNK acting as a stress-mediator pathway in the embryo? 228

6. Conclusion 232

MATERIALS AND METHODS 234

1. Embryo collection 234

2. Fly stocks 236

3. Immunofluorescence 240

3.1 Regular immunofluorescence 240

3.2. Phalloidin stainings 242

3.3 Antibodies list 245

4. Live imaging and in vivo techniques 248

4.1. Aligning embryos for the Spinning disc 248

4.2 Setting up the Spining disc 250

4.3. Laser ablation experiments. 254

5. Quantifications 256

5.1. Closure dynamics 256

5.2. Recoil experiments 256

5.3. Leading edge straightness. 257

5.4 Quantification and statistical analyses. 257

6. Image processing 258

6.1 Live imaging 258

6.2 Immunofluorescence 259

REFERENCES 260

FIGURES INDEX

Figure 1. The *Drosophila melanogaster* life cycle. 22
Figure 2. WT and TM6 balancer chromosomes. 24
Figure 3. The UAS-Gal4 system. 25
Figure 4. Early *Drosophila* embryogenesis. 30
Figure 5 Antero-posterior axis specification. 31
Figure 6. Dorso-ventral axis specification. 32
Figure 7. Ventral furrow formation during *Drosophila* gastrulation. 33
Figure 8. Cell intercalation during germ-band extension. 36
Figure 9. *Drosophila* embryos during germ-band extension. 37
Figure 10. *Drosophila* segmentation. 39
Figure 11. *Drosophila* segment organization. 40
Figure 12. Stage 11 and 12 *Drosophila* embryos. 41
Figure 13. Trachea metamer. 42
Figure 14. *Drosophila* embryonic stages 45
Figure 15. *Drosophila* dorsal closure 47
Figure 16. Microtubules accumulation and cell elongation at the leading edge during dorsal closure. 48
Figure 17. Amnioserosa cell oscillations during dorsal closure. 50
Figure 18. Amnioserosa during the slow and fast phases. 51
Figure 19. Amnioserosa cell delamination. 52
Figure 20. Actin cable during dorsal closure. 53
Figure 21. Ena, Ed and Baz expression pattern during dorsal closure 54
Figure 22. Filopodia during dorsal closure. 60
Figure 23. Proposed model of zipping. 60
Figure 24. Actin cable and filopodia formation during human and *Drosophila* wound healing 63
Figure 25. JNK activity during *Drosophila* larval wound healing 64
Figure 26. Simplified view of the JNK pathway during dorsal closure. 67
Figure 27. The JNK signalling pathway during dorsal closure 70
Figure 28. DPP gradient in the wing imaginal disc 71
Figure 29. A simplified view of the DPP pathway 74
Figure 30. The DPP pathway during dorsal closure. 76
Figure 31. The dorsal open phenotype. 78

ABBREVIATIONS

Abl	Abelson
Aop	Anterior open
AS	Amnioserosa
Baz	Bazooka
Bnl	Branchless
BMP	Bone Morphogenetic Protein
Brk	Brinker
Bsk	Bsk
Btl	Breathless
Chic	Chicadee
Ci	Cubitus interruptus
Dad	Daughters against DPP
DB	Dorsal branch
DC	Dorsal closure
Dfd	Deformed
Dia	Diaphanous
Dl	Dorsal
Dok	Downstream kinase
DPP	Decapentaplegic
Dsh	Dishevelled
DTa	Dorsal Trunk anterior
Ed	Echinoid
En	Engrailed
Ena	Enabled
FGF	Fibroblast growth factor
GB	Ganglionic Branch

GFP	Green Fluorescent Protein
Hep	Hemipterous
Hh	Hedgehog
Hnt	Hindsight
JNK	Jun N-terminal Kinase
Jra	Jun-related antigen
Kay	Kayak
Kr	Kruppel
LE	Leading Edge
LT	Lateral Trunk
Mad	Mother against DPP
MAPK	Mitogen-activated protein kinase
Msn	Misshapen
Omb	Optomotor-blind
Pnr	Pannier
Puc	Puckered
RFP	Red Fluorescent Protein
ROS	Reactive oxygen species
Rpr	Reaper
Salm	Spalt
SB	Stublle
Scaf	Scarface
Shn	Schnurri
Slpr	Slipper
Sog	Short gastrulation
Sqh	Spaghetti Squash
TGF	Transforming Growth Factor

Tkv	Thickveins
Tld	Tolloid
TM6	Third Multipular 6
UAS	Upstream Activating Sequences
Ush	U-shaped
VB	Ventral Branch
Wg	Wingless
YFP	Yellow Fluorescent Protein
Zen	Zerknullt

INTRODUCTION

I. From Thomas Hunt Morgan to Today: *Drosophila melanogaster* as a powerful model organism to study signalling and morphogenesis

I.1 Thomas Morgan and his pioneer 'Fly Room'

Drosophila melanogaster has been a widely used model organism for more than a century. In the early 1920, Thomas Morgan's lab, nicknamed the 'Fly Room', pioneered the use of *Drosophila* as a model organism to understand genetics. At the origin, Morgan's lab was said to be has big as a broom closet. Thanks to *Drosophila*, Thomas Morgan made key contributions working on heredity, and sex-linked traits. This historic photo from the Betsey Bridges Family Collection is showing Calvin Bridges, one of Thomas Morgan's disciple in the fly room where they discovered *white* (*w*), the first X-linked mutation in *Drosophila* (Morgan et al., 1915).



I.2 Easy to grow, easy to keep: *Drosophila* as a versatile tool

Since Thomas Morgan, many scientists have been using *Drosophila* as a model organism. Indeed, *Drosophila* is cheap, easy to breed and has a short life-time generation that lasts only 10 days at 25°C. The embryogenesis starts right after egg laying and lasts for 24h to give rise to a ready-to-live larva. The newborn larvae go through 3 different stages during which they grow. Specifically, the imaginal discs will undergo cell proliferation and differentiation throughout the larval life to form the adult appendages. After a phase of growth, larvae enter into a quiescent pupal stage, during which metamorphosis takes place followed by the emergence of the new adult fly (**Figure 1**).

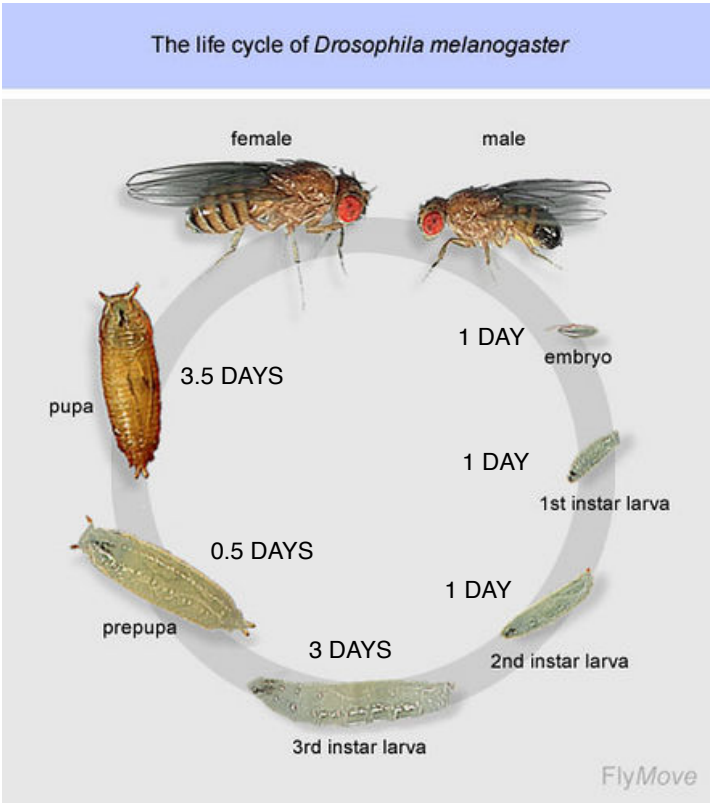

Figure 1. The *Drosophila melanogaster* life cycle.

At 25°C, the life cycle last ten days.

Source: http://flymove.uni-muenster.de

Flies are tiny (< 3 mm), and are therefore easy to keep. A female can produce between 750 and 1,500 eggs during its life when harvest with a *good* food medium. Therefore it is quite easy to generate hundreds of flies quickly.

I.3 A small but instructive genome

The *Drosophila* genome is composed of four pairs of chromosomes: X/Y, 2, 3 and 4. The fourth chromosome is very small and is not often studied, although some important genes are located on the fourth chromosome (e.g. *eyeless*, *cubitus interruptus*). Each chromosom (exept the X that has a single arm) is divided into a left and a right arm, and each arm is subdivided into segments. The *Drosophila* genome has little redundancy: by affecting a single gene, a complete function can be affected. *Drosophila* is therefore an excellent model for genetic screens. In 1980, Christiane Nüsslein-Volhard and Eric Wieschaus induced mutations in the entire genome and discovered key developmental genes including *patched* or *hedgehog* for instance (Nusslein-Volhard and Wieschaus, 1980). For these major discoveries, Christiane Nüsslein-Volhard and Eric Wieschaus are the 1995 recipients of the Physiology and Medicine Nobel Prize.

Although the *Drosophila* genome is simpler than more complex model organisms such as the mouse genome, 50% of *Drosophila* genes have a human homolog. There are multiple examples where *Drosophila* and mammalian genes display functional homology. A striking example is that in the absence of the BMP-4/BMP-2 *Drosophila* homologue called *Decapentaplegic* (*Dpp*), BMP4 ligand sequences can function in lieu of DPP in the *Drosophila* embryo (Padgett et al., 1993). Thus, human and *Drosophila* genes can display functional homologies.

A problem with mutations is that they are often homozygous lethal, and can only be maintained at heterozygous state. The issue is that, by breeding heterozygous flies, a third of the emerging progeny will not carry any copy of the mutation. Thus, over time, two populations – wild-type and heterozygous flies – can coexist. Considering that the mutation brings a natural disadvantage, even at heterozygous state, it is likely that over time, only the wild-type flies will remain in

the stocks. To overcome this difficulty, the fly community has set up the so-called 'balancer chromosomes'. Balancers are chromosomes that carry numerous chromosomal inversions, which prevent any meiotic recombination. Balancers carry a dominant marker and a recessive mutation. Balancers are therefore homozygous lethal (or sterile) and carry a visible marker.

Here are the advantages of the system:

- Because balancers are homozygous lethal, the only genotype maintained over the generations will be *Mutation* over *Balancer* (The combinations *Balancer/Balancer* and *Mutation/Mutation* are lethal, only the combination *Mutation/Balancer* is viable).
- Because balancers carry a dominant marker, the mutation can be counter selected when making crosses (the offspring either gets the mutation and therefore no makers, or the balancer AND the marker).
- Since flies, and especially females undergo meiotic recombination, the inversion of chromosomic sequences in the balancer prevents any recombination. This way, one can be sure that the mutation will never be on the same chromosome than the marker or the balancer.

TM6, Sb is a Balancer chromosome located on the third chromosome. TM stands for Third Multipular. ***TM6*** carries a recessive mutation, and the marker ***Sb***.

Sb (Stubble) is a homozygous lethal marker. It is not a balancer. Sb flies have short bristles, like the regrowth of a shaven beard (**Figure 2**).

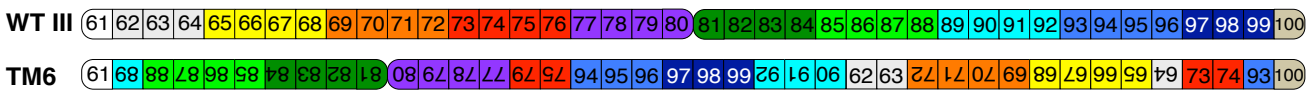

Figure 2. WT and TM6 balancer chromosomes.
The configuration of the TM6 balancer chromosome prevents recombination, apart from the 61 and 100 extremities.

I.4 *Drosophila* genetics

In addition of the mutant collections available, several genetic tools are available in *Drosophila*. Among them, Andrea Brand and Norbert Perrimon set up the UAS-Gal4 system, a powerful genetic tool that allows specific gene over-expression with temporal and spatial resolution (Brand et al., 1994).

The yeast transcriptional activator Gal4 is expressed under the control of an endogenous *Drosophila* enhancer. Cells within this domain can therefore activate transgenes controlled by Upstream Activating Sequences (UAS) (**Figure 3**). The system has many advantages:

- Expression of a given cDNA with temporal and spatial specificity.
- Almost infinite combination between Gal4 and UAS lines.
- Avoid the toxicity (the system is only active in the progeny, since UAS and Gal4 sequences are from yeast are therefore not interpreted by the fly genome).

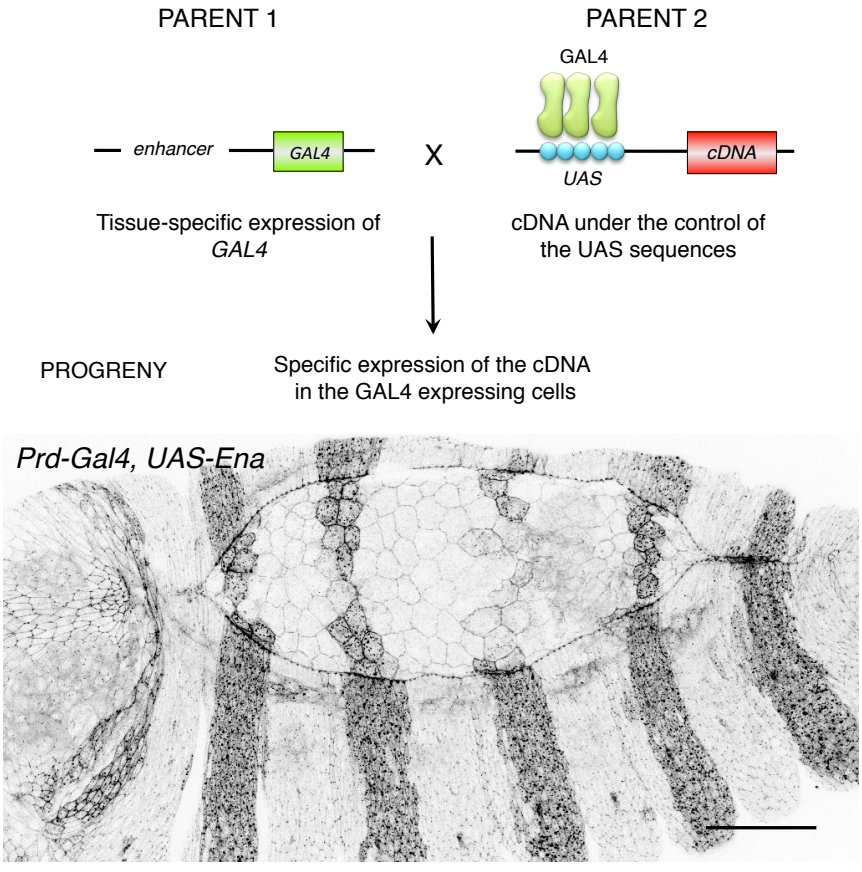

Figure 3. The UAS-Gal4 system.

Top: Cartoon depicting the UAS-Gal4 system. Inspired from (St Johnston, 2002).

Bottom: *Prd-Gal4, UAS-Ena* embryo marked with anti enabled (grey).

Prd-Gal4 drives expression in epidermal stripes. Ena is therefore over-expressed in epidermal stripes.

I.5 Live imaging and *in vivo* techniques

The genetic power of *Drosophila* also resides in the use of fluorescent-tagged proteins. The isolation of the green fluorescent protein (GFP) from the jelly fish *aequorea victoria* by Osamu Shimomura enabled Martin Chalfie to tag *C. Elegans* proteins with GFP and follow their behaviour *in vivo* (Chalfie et al., 1994). GFP and other derivatives (RFP, etc.) have been widely used in *Drosophila*. Expression of fluorescent reporters constitutes a convenient way to decipher or to mark the expression pattern of various Gal4 lines. GFP-exon trap screen also allowed the characterization of previously unknown genes for instance (Morin et al., 2001). In addition, the development of fluorescent balancers to easily sort out the mutant and the non mutant populations constitute a convenient – if not crucial – advance for in vivo studies (Le et al., 2006).

Importantly, the expression of GFP-tagged cytoskeletal markers has been extremely useful to better understand a variety of morphogenetic processes. For instance, it allowed a better understanding of cell junction rearrangement (Bardet et al., 2013), cell-mixing process like during tumour invasion (Levayer et al., 2015), local forces induced by apoptosis (Monier et al., 2015) or mechanical control of growth in the wing disc (Legoff et al., 2013). It also enabled the characterisation of actin-based protrusion called cytonemes, that appear more and more as a major mechanism of paracrine signalling (Roy et al., 2011; Roy et al., 2014). In the embryo, these reporters have been notably used to better understand the behaviour of various tissues during dorsal closure (Jacinto et al., 2000; Kiehart et al., 2000; Jacinto et al., 2001; Jacinto et al., 2002; Kaltschmidt et al., 2002; Franke et al., 2005; Jankovics and Brunner, 2006; Laplante and Nilson, 2006; Fernandez et al., 2007; Millard and Martin, 2008; Rodriguez-Diaz et al., 2008; Toyama et al., 2008; Solon et al., 2009; Wells et al., 2014; Ducuing et al., 2015). In addition, single junction cuts with a UV

laser has become a standard way to assess local tensions cells are subjected to, or to perturb ongoing morphogenesis.

New techniques are also emerging such as the development of light-sheet microscopy system (Saias et al., 2015), or the development of super-resolution microscopy.

II. *Drosophila* embryonic development

The *Drosophila* embryonic development is a complex process that lasts 22 hours at 25°C. All the embryonic stages are depicted at the end of this section in the **Figure 14**. In this section, I will describe the most important developmental processes, except dorsal closure that will be described in greater details in the next section.

II.1 Early embryogenesis (Stage 1 – Stage 5)

During the five first embryonic stages, the egg will undergo 13 round of synchronous nuclear divisions without cellular division. Nuclei then migrate to the periphery to eventually undergo a simultaneous cellularization to form a 8,000-cell blastula.

Initially, the egg is composed of a homogenous cytoplasm and contains yolk granules. The first stage of embryogenesis usually starts after the egg laying and last until the completion of the two first cleavages (Stage 1).

Then, the 5 next nuclear divisions (without cellular division) occur predominantly in the anterior part of the egg, leading to the formation of a cluster of nuclei (Stage 2). The nuclei progressively move towards the posterior pole of the embryo while the embryo constricts, leading to the formation of an unfilled space both at the anterior and the posterior part of the egg.

From the 8th nuclear division, the nuclei migrate progressively at the periphery to relocate under the vitelline membrane (Stage 3). The first 3 nuclei to reach the posterior pole divide and then cellularize to become the pole cells. These pole cells fill the posterior space created earlier and will constitute the germ line.

At Stage 4, the nuclei are migrating at the periphery, leading to the formation of a syncytial blastoderm: they share the same cytoplasm, but are excluded from the

central part of the egg due to the presence of the yolk. The duration of cleavage divisions 10-13 increases progressively, from approximately 8 min to 20 min.

Cellularization occurs during stage 5. Cellularization starts with the invagination of membrane furrows from the periphery towards the centre of the egg. Blastoderm cells are not completely isolated since they still connect with the yolk cytoplasm through cytoplasmic bridges. These bridges are lost later, during gastrulation. After cellularization, the blastoderm cells have a homogenous shape and size (**Figure 4**).

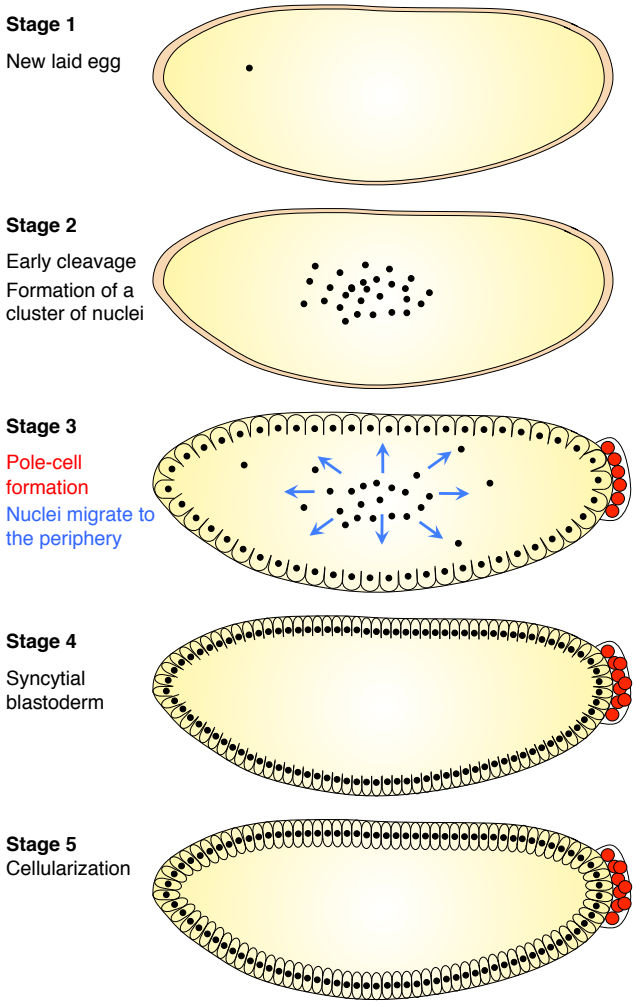

Figure 4. Early *Drosophila* embryogenesis.

Drawings representing the early stages of embryogenesis.

Stage 1: 0 – 15 min.

Stage 2: 15 – 80 min.

Stage 3: 80 – 90 min

Stage 4: 90 – 150 min.

Stage 5: 150 – 180 min.

During cellularization, the antero-posterior and the dorso-ventral axis are established. The antero-posterior axis is established by the formation of opposite gradients of four maternal-effect genes. Bicoid and Hunchback regulate the

production of anterior structures (Driever and Nusslein-Volhard, 1988; Struhl et al., 1992), while Nanos and Caudal regulate the formation of the posterior part of the embryo (Macdonald and Struhl, 1986; Nusslein-Volhard et al., 1987). The classical view is that *bicoid* mRNA is actively transported via microtubules towards the anterior part of the egg while *nanos* mRNA remains in the posterior part of the egg. Bicoid and Nanos then establish an opposite protein gradient. Nanos inhibits Hunchback transcription. Hunchback therefore adopts a gradient opposite to Nanos gradient. Similarly, Bicoid represses Caudal transcription. Caudal thus adopts a gradient opposite to Bicoid gradient (**Figure 5**).

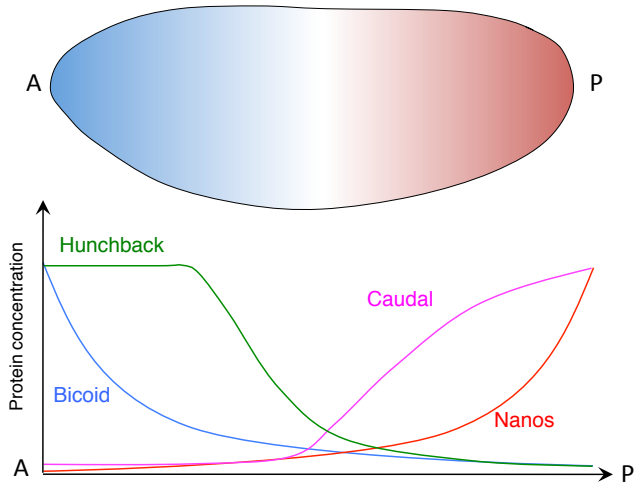

Figure 5 Antero-posterior axis specification.

Top: Bocoid and Nanos protein gradients.

Bottom: Bicoid inhibits Caudal while Nanos inhibits Hunchback, leading to the formation of opposite gradients.

The patterning of the dorsoventral axis is regulated by the mutually exclusive action of the two morphogenes Dorsal (Dl) and Decapentaplegic (Dpp). Dl is the determinant of the ventral axis and establishes a dorsoventral nuclear gradient with peak levels in the ventral nuclei (Roth et al., 1989; Steward, 1989). The ventral-most cells that display the highest nuclear concentration of Dl express *twist* and *snail*, two transcription factors that will specify the mesoderm. Specifically, *snail* represses the expression of *short gastrulation (sog)*, a determinant of the neurodermal fate. In more ventral cells where Snail in not expressed, lower nuclear levels of Dl can activate *sog*. Sog prevents in turn cells from becoming dorsal ectodermal cells by sequestering

Dpp. In the dorsal-most regions, Dl is absent from the nucleus: Dpp and Tolloid (Tld), a metalloprotease that cleaves Sog are expressed and secreted. In the future dorso ectodermal cells, Tld prevents Sog-dependant Dpp sequestration, thus allowing Dpp to specify the dorsal ectoderm. The amnioserosa is specified by *zerknullt (zen)*, a transcription-factor that is initially broadly expressed like Dpp, but that becomes restricted to the dorsal-most region in a Dpp-dependent manner (Doyle et al., 1986; Rushlow et al., 1987). Interestingly, Zelda is a uniformly expressed factor that would potentiate Dl gradient interpretation (Foo et al., 2014). Specifically, Zelda opens the chromatin of the genes that are induced by Dorsal. However, the number of Zelda binding sites per gene varies, thus modulating the ability of these genes to respond to various concentration of nuclear Dl (**Figure 6**).

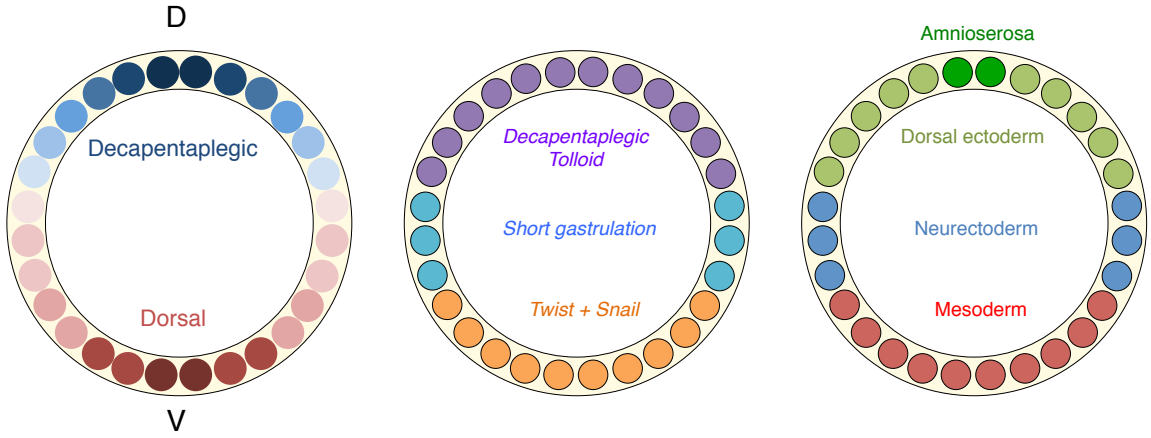

Figure 6. Dorso-ventral axis specification.

Cartoons represent cross-sections of a Stage 5 *Drosophila* embryo.

Left: opposite Dorsal and Decapentaplegic gradients. Nuclear (for Dorsal) and extra cellular (for Dpp) gradients are represented in a similar manner for the sake of simplicity.

Middle: High levels of nuclear Dorsal induce Twist and Snail (orange). Snail represses Short gastrulation. Medium levels of nuclear Dorsal in the absence of Snail induce Short gastrulation (blue). In the absence of Dorsal in the nucleus DPP and Tolloid are produced. Short gastrulation sequesters Dpp while Tolloid inhibit this sequestration, leading to the establishment of a Dpp gradient.

Right: Twist and Snail expressing cells form the mesoderm (red). Short gastrulation expressing cells form the neuro ectoderm. Dpp receving cells form the dorsal ectoderm. When Dpp activity pattern refines, *zerknullt* expression pattern refines to the dorsal-most cells, where the amnioserosa is specified.

II.2 Gastrulation (Stage 6 – Stage 7)

Gastrulation is a developmental phase during which a single-layered embryo becomes a three-layered embryo with formation of the ectoderm (future epidermis and nervous system), the mesoderm (future muscles) and the endoderm (future intestine). Gastrulation starts at Stage 6 by the formation of the three distinct furrows. The cephalic furrow, located in the first third of the embryo starts to fold. Second, the pole cells at the posterior part of the embryo progressively shifts dorsally and are engulfed in a pocket.

The most striking process during gastrulation is the formation of a ventral furrow (**Figure 7**). During this process, about 1000 future mesodermal cells progressively invaginate from the surface of the embryo in a coordinated manner to eventually form the mesodermal tube (Leptin, 1999). As the ventral furrow forms, the invaginating cells constrict apically and undergo cell elongation. At a morphogenetic level, the non-muscle myosin II (*spaghetti squash*, *sqh*) is localized apically. Sqh associates with actin to promote the apical constriction of the cells and allow their flattening *via* the association of the acto-myosin cytoskeleton to the apical adherens junctions (Dawes-Hoang et al., 2005). Once the furrow is formed, the future mesodermal cells go back to their original length, to end up in a wedge–like shape.

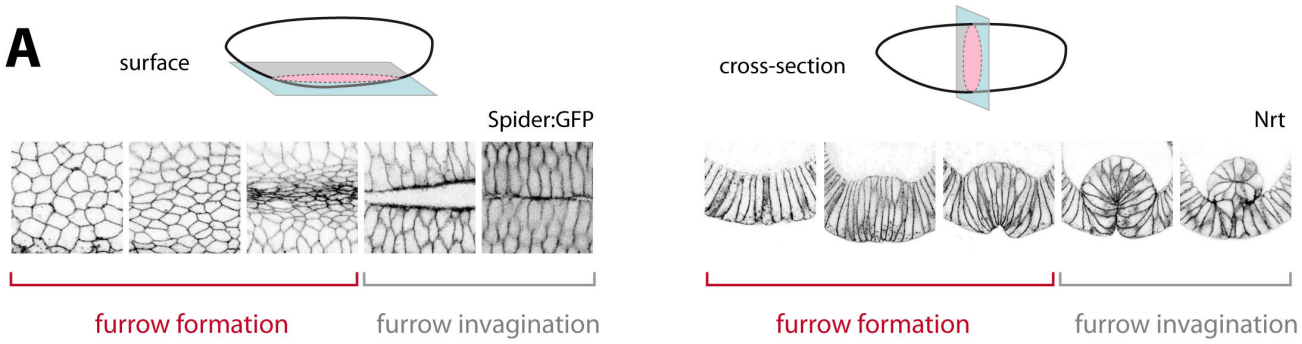

Figure 7. Ventral furrow formation during *Drosophila* gastrulation.
This figure is composed of surface sections (left) and cross-sections (right) of the ventral epithelium of the *Drosophila* embryo during ventral furrow formation and furrow invagination. This figure is taken from (Spahn and Reuter, 2013). Nrt: Neurtactin (surface glycoprotein). Spider-GFP is a casein kinase I encoded by the gene gilgamesh that associates with the plasma membrane and secretory vesicles destined for the plasma membrane.

The formation of the ventral furrow is controlled by the two transcription factors *twist* and *snail*. *snail* is a transcriptional repressor required for the initiation of the ventral furrow formation. It acts by repressing the neuroectodermal fate in the invaginating mesoderm. *twist* is a transcriptional activator that will control the proper expression of mesodermal genes. Interestingly, *snail* expression needs to be synchronous for correct gastrulation thanks to RNA Polymerase II pausing mechanism (Lagha et al., 2013). The mechanism of "paused Polymerase II" is a mechanism by which the RNA polymerase starts the initiation of the transcription, but does not proceed further to elongation due to the lack of additional factors. This way, the RNA Polymerase II is linked to the nascent RNA in a "ready-to-go" state (Adelman and Lis, 2012). The RNA Polymerase II pausing is essential for fast and synchronous *snail* expression in the presumptive mesoderm. Importantly, the paused RNA polymerase II mechanism determines the "time to synchrony", which is the time necessary for coordinating gene expression across a tissue (Lagha et al., 2013).

During the second part of gastrulation (Stage 7), the pole cells that are engulfed in a pocket of about 150 cells adopt a horizontal position compared with the dorsal egg surface. The cells that are immediately anterior to this pocket start to form a deep groove that becomes continuous with the ventral furrow. This is the proctodeum invagination. In addition, the stomodeum, composed of the anterior midgut primordium, invaginates. The mitosis are now non-synchronous and occur in so-called "mitotic domains" (Foe, 1989). The embryo is ready for the extension of its germ-band.

II.3 Germ band extension (Stage 8 – Stage 10)

At the end of stage 7, gastrulation is completed. The ventral furrow is closed, and the mesodermal tubes composed of a regular and structured epithelium. During stage 8, the mesodermal tube starts to disaggregate and the mesodermal cells undergo mitosis. In parallel, germ-band elongation (or germ-band extension) occurs.

Germ-band elongation is a morphogenetic process during which the epidermis doubles in length along the anterior-posterior axis while reducing its width along the dorsal-ventral axis thanks to medio-lateral to antero-posterior cell intercalation (Irvine and Wieschaus, 1994). During germ-band elongation, the posterior half of the trunk reaches the dorsal side of the embryo, while the anterior half constitutes the ventral side of the embryo (Irvine and Wieschaus, 1994). Germ-band elongation is divided into two phases: a first fast phase (25 minutes) during which most of the elongation occurs, and a slow phase (70 minutes) after which elongation is completed (da Silva and Vincent, 2007). The process of cell intercalation is the main driver of germ-band extension, as no cell division occurs during this period (**Figure 8**).

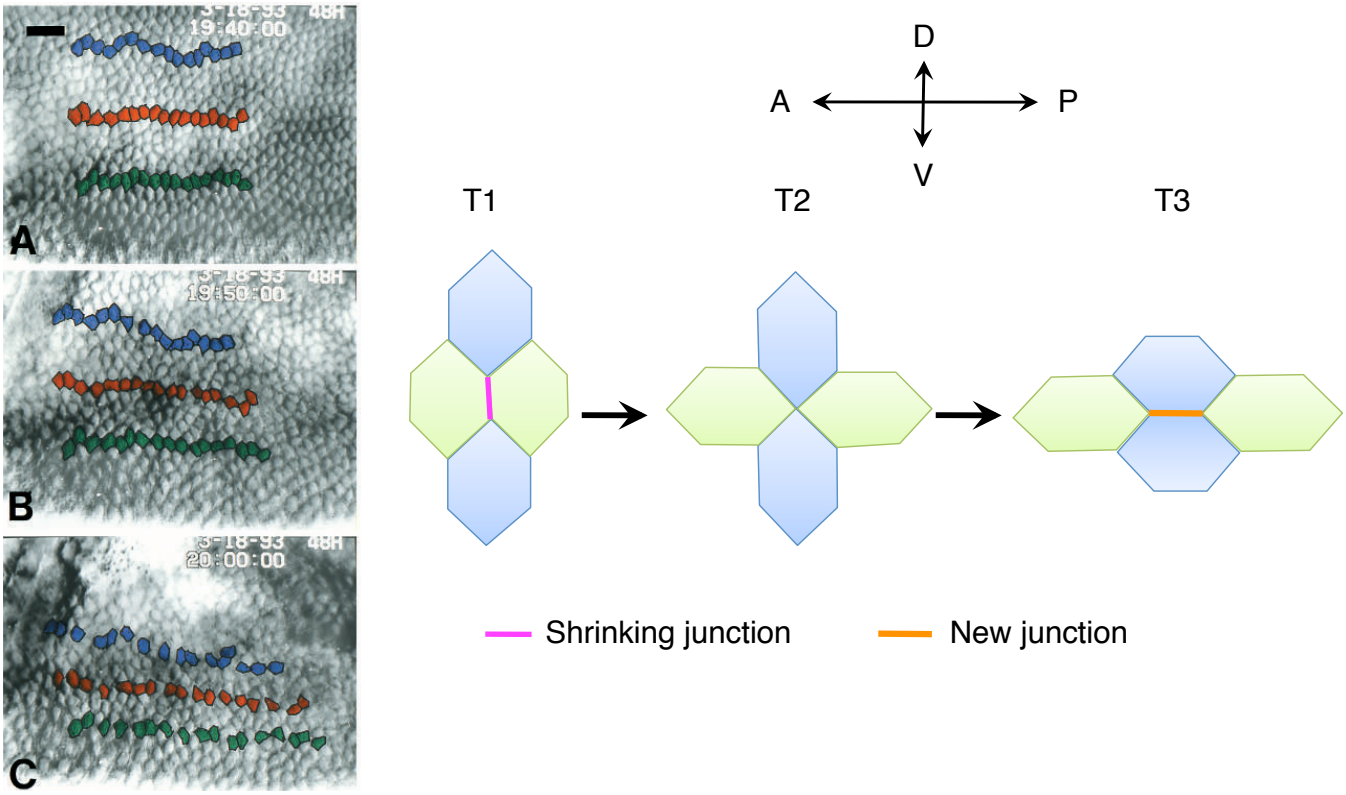

Figure 8. Cell intercalation during germ-band extension.

Left: Figure taken from Irvine and Wieschaus, 1994 showing the cell intercalation phenomenon during germ-band extension.
Right: Drawings representing the cell-intercalation process, in a T1-T2-T3 mechanism, with the shortening of the D/V orientated junction (T1), the formation of a rosette (T2), and the formation of a new A/P orientated junction (T3).

At the cellular level, the junction that undergoes the dorso-ventral orientated shrinkage has less E-Cadherin than their neighbours, but accumulates myosin-II and the Rho-kinase in response to tensions (Bertet et al., 2004; Fernandez-Gonzalez et al., 2009). Specifically, the polarized flow of actomyosin bursts towards dorso-ventral orientated junctions would be the key driver factor of cell-membrane shrinkage (Rauzi et al., 2010). In addition, the myosin phosphorylation constitutes an instructive cue to generate the proper tensions during cell rearrangement (Kasza et al., 2014).

In parallel, formation of the amnioserosa, an extra-embryonic tissue involved in dorsal closure occurs. As germ-band extension proceeds, the proctodeal invagination that was formed during gastrulation and that was containing amnioserosa primordium becomes deeper. The cells for the amnioserosa primordium become flat, elongated and are progressively engulfed between the tip of tail and the head (Campos-Ortega and Hartenstein, 1985; Frank and Rushlow, 1996).

During stage 9, germ-band extension continues. In parallel, the first neuroblasts start to delaminate from the ectoderm in three distinct waves (Campos-Ortega and Hartenstein, 1985). The mesoderm also rearrange to form a monolayer while undergoing mitosis (Campos-Ortega and Hartenstein, 1985).

The extension of the germ-band ends at Stage 10. At this stage, the stomodeum invaginates, which will give rise to the foregut. Neuroblasts start to undergo asymmetric cell divisions. The first signs of parasegmentation are also visible (**Figure 9**).

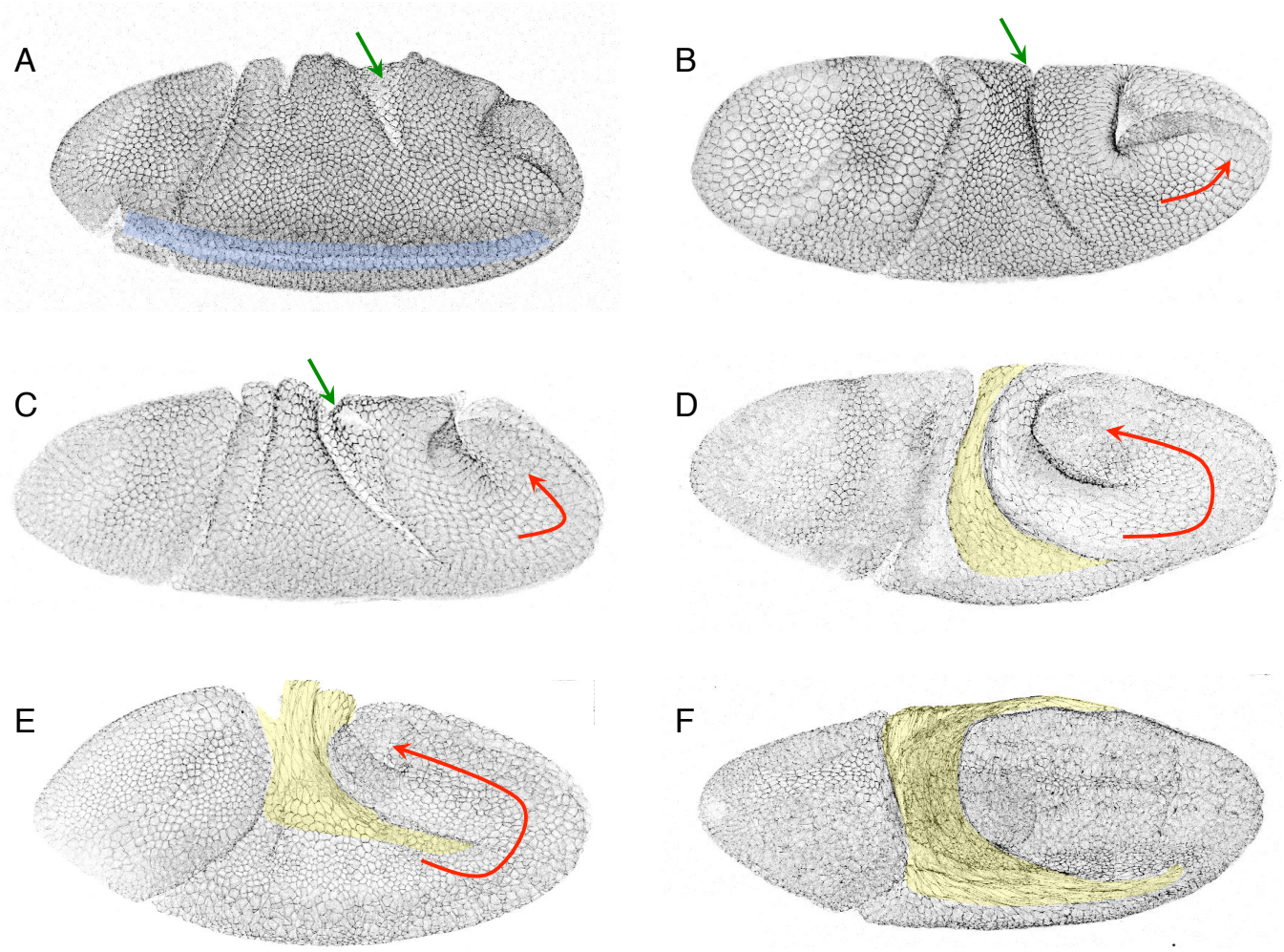

Figure 9. *Drosophila* embryos during germ-band extension.

All the embryos are marked with E-Cadherin. Green arrows indicate the proctodeal invagination that gets deeper over time. Red arrows indicate the extension of the germ band. The amnioserosa is in yellow.

A = Beginning of germ-band elongation (Stage 8), with the end of the ventral furrow invagination visible (blue)

B, C, D = Fast phase of elongation (Stage 8),

E = Slow phase of elongation (Stage 9),

F = End of elongation (Stage 9/10).

II.4 Segmentation and trachea invagination (Stage 11)

At stage 11, the metameric organisation of the embryo becomes apparent. The embryo is composed of 3 thoracic and 8 abdominal segments. Segmentation occurs by the progressive refining of the expression patterns of key determinant of the antero/posterior axis of each segment. Segmentation is therefore initiated earlier in development.

Initially, the egg contains maternal genes (inherited by the mother) such as *bicoid* or *nanos*. These maternal genes adopt a graded distribution to establish the antero-posterior axis.

The combination and the concentration of these morphogens regulate the expression pattern of 'gap genes' that divide the embryo into large regions. Mutations in these genes create 'gaps' in the segmentation. For instance, *krüppel* mutant embryos display only the 3 most-posterior abdominal segments (Nusslein-Volhard and Wieschaus, 1980).

These gap genes then control the expression of so-called 'pair-rule' genes that are expressed in large stripes and that establish pairs of segments. The pair-rule genes mutants lack either odd or even segments. For instance, embryos mutant for *fushi tarazu* exhibit only odd thoracic segments and even abdominal ones (Kankel et al., 2004).

The pair-rule genes finally control the 'segment polarity genes' that are expressed in narrow stripes in each segment and that control the antero-posterior organisation of the segments (**Figure 10**). A simplified view is to consider that during embryogenesis, these different classes of genes have a temporal hierarchy. However, the reality is more complex: for instance, seven stripes of the pair-rule gene *odd skipped* can be detected before the extension of the germ-band (Stage 7), but 14 stripes are detected at least until dorsal closure (Stage 14), when the segment

polarity genes are present (Vincent et al., 2008; Ducuing et al., 2013). Therefore, the temporal hierarchy of these classes of genes should be taken with caution.

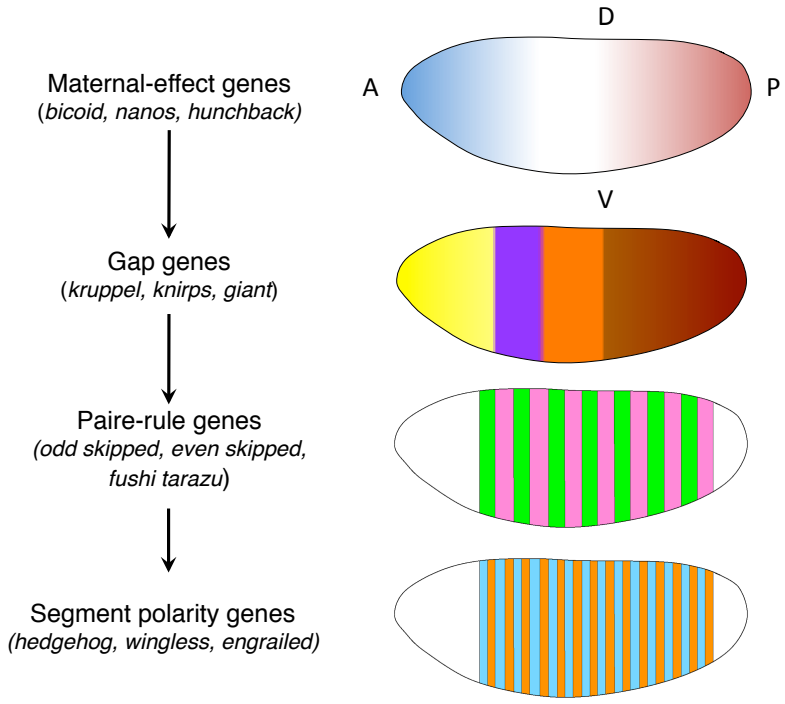

Figure 10. *Drosophila* segmentation.

Drawings representing maternal-effect, gap, pair-rule and segment-polarity genes.

Examples listed for each class of genes is not exhaustive.

The fine organisation of each segment is achieved by complex crosstalks between segment-polarity genes. Each segment is divided into the anterior and posterior compartment by analogy to the disc organisation fsignalwhere García-Bellido and colleagues proved the existence of a non physical boundary that divides the wing disc into an anterior and a posterior compartment (Garcia-Bellido et al., 1973). As it is the case in the wing disc, the posterior compartment of each segment in the *Drosophila* embryo expresses the transcription factor *engrailed* (*en*) (Fjose et al., 1985; Kornberg et al., 1985) and secretes Hedgehog (Hh), a double-lipid modified ligand (Kornberg et al., 1985; Tabata and Kornberg, 1994). Hh diffuses and induces its targets in the Cubitus interruptus (Ci)-expressing domains that border the En-expressing cells. Since Ci is the transcription factor of the Hh pathway and is never expressed in the En-domain, the En-expressing cells are competent to produce but not to interpret Hh (Aza-Blanc et al., 1997). In response to Hh signal, the Ci-

expressing cells that are anterior to the En cells maintain Wingless (Wg) expression, another secreted ligand (Baker, 1987; Alexandre et al., 1999). Wingless diffuses and in return maintains Engrailed in the posterior cells. The Wg and En cells form therefore a feedback loop and constitute the parasegmental organizer, by analogy to the Spemann organizer (Martinez-Arias and Lawrence, 1985). Posterior to the *engrailed*-cells, Hh diffuses and maintains the expression of the pair-rule gene *odd skipped* in the next segment that will constitute the groove cells (Vincent et al., 2008). Therefore, En and Odd cells define the segmental boundary (**Figure 11**).

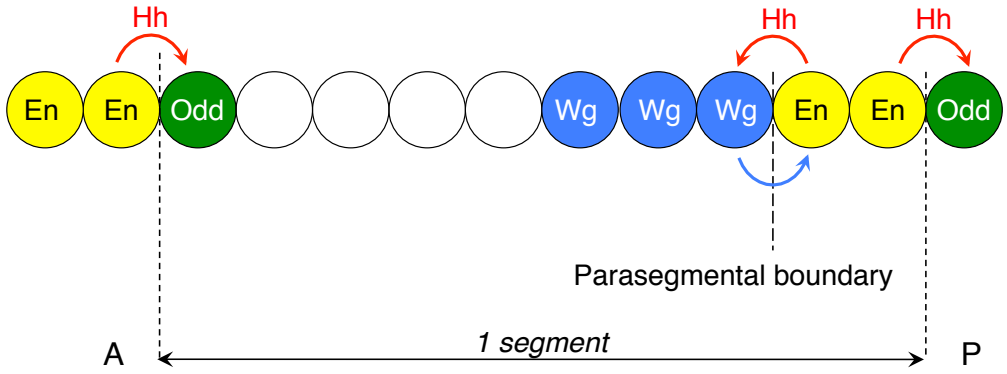

Figure 11. *Drosophila* segment organization.

En = Engrailed ; Wg = Wingless ; Odd = Odd skipped ; Hh = Hedgehog. Wg and En cells constitute the parasegmental organizer: En cells produce Hh that maintains Wg expression, while Wg maintains En cells. Posterior to the En cells, Hh maintains Odd expression that marks the groove cells.

During Stage 10, cells that constitute the tracheal placodes divide and invaginate at Stage 11 to form the tracheal pits (80 cells per pit). The anterior-most pits will give rise to the anterior spiracles while the posterior-most pits will form the posterior spiracles. The remaining pits will give rise to the tracheal tree without any cell division.

In parallel, cell death located between the epidermis and the nervous system occurs, leading to the formation of large clusters of neurons. It continues until Stage 12 (**Figure 12**).

II.5 Germ Band retraction (Stage 12)



Figure 12. Stage 11 and 12 *Drosophila* embryos.

Confocal pictures of a stage 11 and a stage 12 embryo marked with E-Cadherin. The second row represents lower Z-section to highlight the trachea.

At stage 12, the tail of the embryo retracts. The amnioserosa, wrinkled like an accordion at the end of Stage 11 starts to deploy to cover a transient dorsal gap. Grooves also start to form. These groove cells have a specific shape and cytoskeleton: groove cells display a ladder-like organisation, and accumulate adherent junction molecules such as Crumbs, aPKC or Ena (Vincent et al., 2008).

While neuronal cell death still occurs at Stage 12, the ventral cord separates from the epidermis and the first axons in the ventral nerve cord are visible.

During Stage 12, the invaginated trachea pits start to elongate and form the trachea. The tracheal metameres are composed of 5 branches: the dorsal branch (DB), the dorsal trunk anterior (DTa), the visceral branch (VB), the lateral trunk (LT) and the ganglionic branch (GB) (Samakovlis et al., 1996) (**Figure 13**).

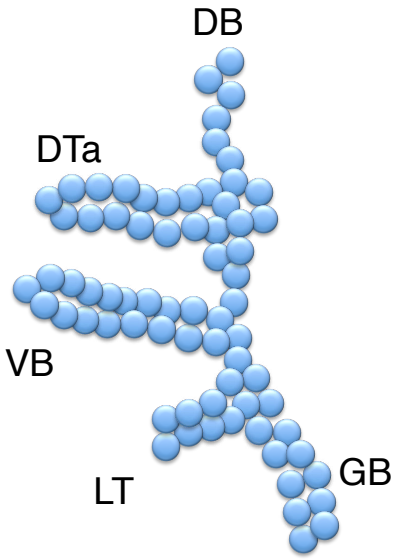

Figure 13. Trachea metamer.

Drawing representing a trachea metamer.

DB = Dorsal Branch
DTa = Dorsal Trunk anterior
VB = Ventral Branch
LT = Lateral Branch
GB = Ganglionic Branch

During trachea formation, the migration of the dorsal branches depends on the action of the FGF homolog Branchless (Bnl) and DPP (Vincent et al., 1997). The tracheas cell express the FGF receptor Breathless (Btl) and are therefore capable to interpret the Bnl produced by the organs that are "attracting" the migration of the branches.

DPP plays a dual role for the DB, LT and GB specification and migration. First, DPP repress *spalt* while activating *knirps* expression, whereas in other branches, the situation is the opposite: *knirps* is inhibited while *spalt* is transcribed (Vincent et al., 1997). Second, DPP controls Bnl expression for the proper migration of the DB, LT and GB. Consistently, in embryos where DPP signalling is impaired such as in the *thickveins (tkv)* mutant embryos, dorsal branches as well as lateral and ganglionic branches are absent (Vincent et al., 1997).

II.6 Dorsal closure (Stage 13 – Stage 15)

After the completion of the retraction of the germ band, dorsal closure takes place from Stage 13 to Stage 15. During dorsal closure, the transient dorsal gap covered by the amnioserosa is progressively closed by the fusion of the first row of dorsal epidermal cells called the leading edge at each extremity. I will detail dorsal closure in the next section. In parallel to dorsal closure, the head of the embryo invaginates.

During these stages, other layers continue to develop. The central and the peripheral nervous system (including sensilla and motor neurons) start to differentiate. The ventral nerve cord starts to condensate at Stage 14. The mesoderm also progressively differentiates: by stage 13, the fusion of myoblasts is completed. As the segments stretch during closure, the muscle fibres become distinguishable. The visceral mesoderm, attached to the somatic mesoderm at stage 12 is progressively attached to the midgut primordial at stage 13. It later spreads to encircle the developing gut. The trachea continue to migrate at Stage 13, the anterior-directed dorsal branches of all segments fuse to form the dorsal longitudinal tracheal trunk.

II.7 Late embryogenesis (Stage 16 – Stage 17)

The two last embryonic stages will give rise to a ready-to-live larva. The epidermis starts to secrete the cuticle, including the denticle belts that are enriched with actin. The diverse organs terminate their differentiation. The condensation of the ventral nerve cord, initiated at stage 14 continues until stage 17. During these last steps, the trachea become filled with air. The sensilla are differentiated and sensory axons are connected with the central nervous system. The motor axons are now connected to the muscles, leading to spontaneous movement of the embryo at mid-stage 17, until its eventual hatching (**Figure 14**).

	Stage	Time	Developemental Events
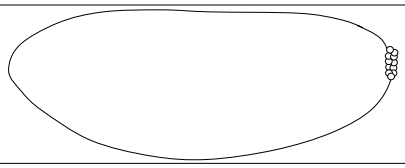	5	3h00	Cellularization
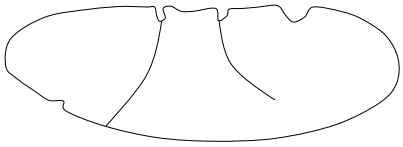	6-7	3h – 3h20	Gastrulation
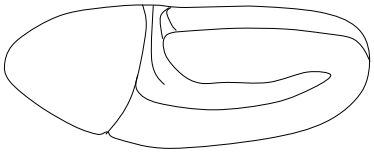	8-9	3h20 – 4h20	Germ band extension
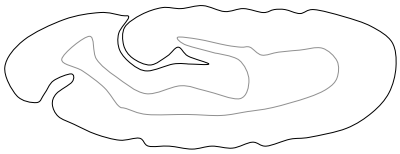	10	4h20 – 5h20	End of germ band extension Stomodeum invagination
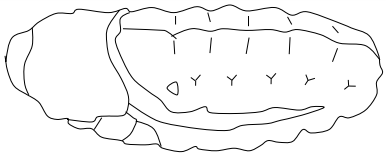	11	5h20 – 7h20	Trachea invagination Parasegmentation
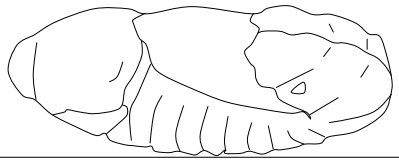	12	7h20 – 9h40	Germ band retraction
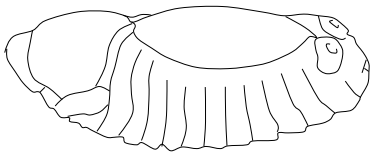	13	9h40 – 10h20	
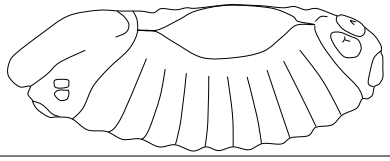	14	10h20 – 11h	Dorsal closure and head involution
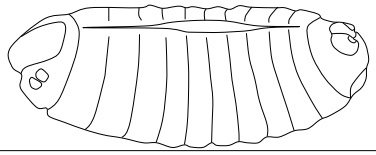	15	11h – 13h	
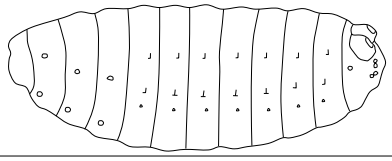	16-17	13h – 22h	Condensation of the nervous system Embryo ready to hatch

Figure 14. *Drosophila* embryonic stages.

Homemade drawings adapted from the Atlas of *Drosophila* development written by Volker Hartenstein. This figure depicts the key *Drosophila* embryonic stages at 25°C.

III. Morphogenesis during dorsal closure

III.1 An overview of dorsal closure

Dorsal closure is a key embryonic process during which the dorsal gap covered by the amnioserosa progressively disappears. As dorsal closure proceeds, the dorsal-most epidermal cells that constitute the leading edge, elongate dorso-ventrally, meet and zip at each extremity called canthus. Dorsal closure starts at Stage 13, once the retraction of the germ band is completed and ends at Stage 15 with a perfectly suturated embryo (**Figure 15**).

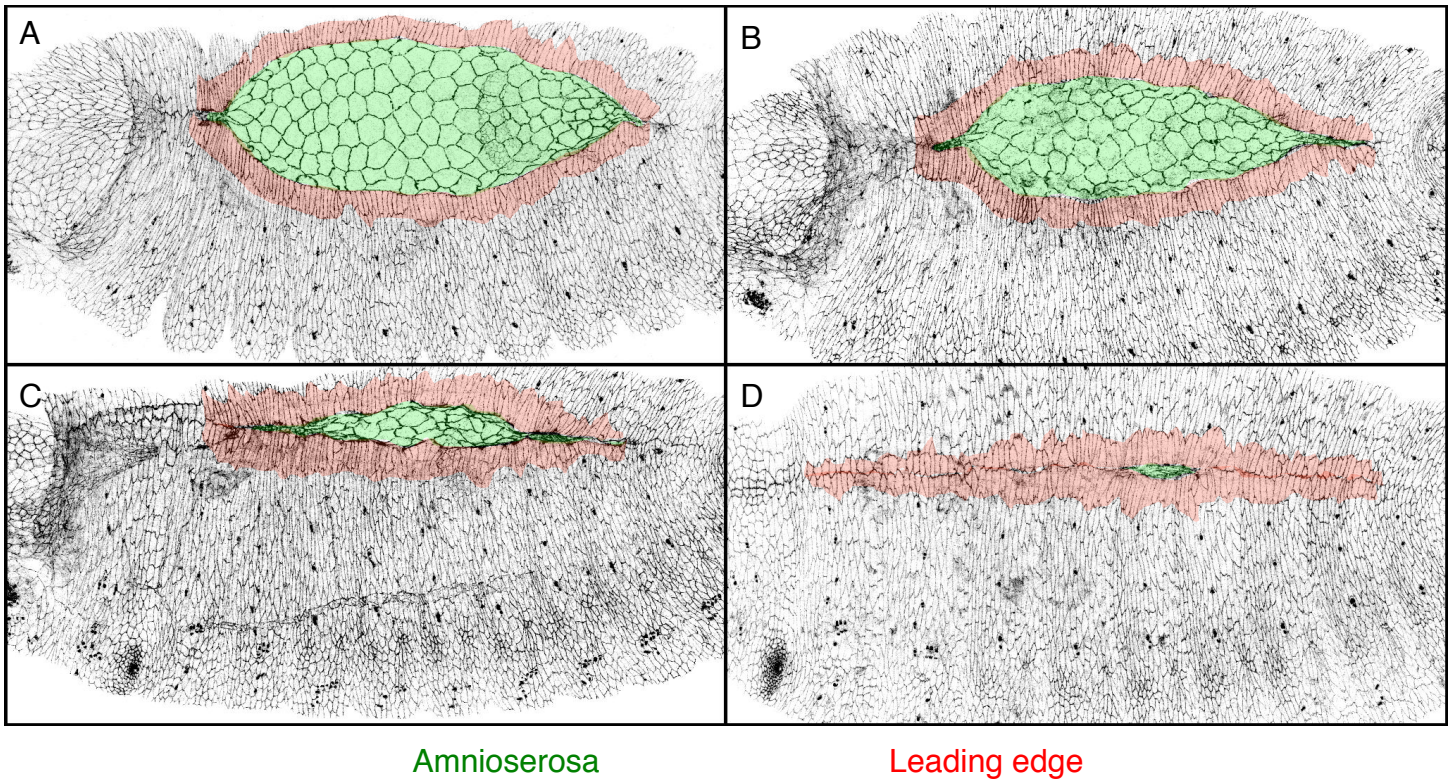

Figure 15. *Drosophila* dorsal closure.

(A-D) Wild-type embryos marked with E-Cadherin during dorsal closure. The amnioserosa is colour-coded in green. The first rows of epidermal cells in contact with the amnioserosa that constitute the leading edge are colour-coded in red. As closure proceeds, the amnioserosa progressively disappears while the leading edge of each epidermis fuse at the canthi.

During dorsal closure, the leading edge cells are polarized and have a highly dynamic cytoskeleton. As closure proceeds, leading edge cells elongate along the dorso-ventral axis and display strong adherens junctions (Kaltschmidt et al., 2002; Ducuing et al., 2015). They accumulate a dense apical microtubule network that is orientated dorso-ventrally (Kaltschmidt et al., 2002; Jankovics and Brunner, 2006) (**Figure 16**).

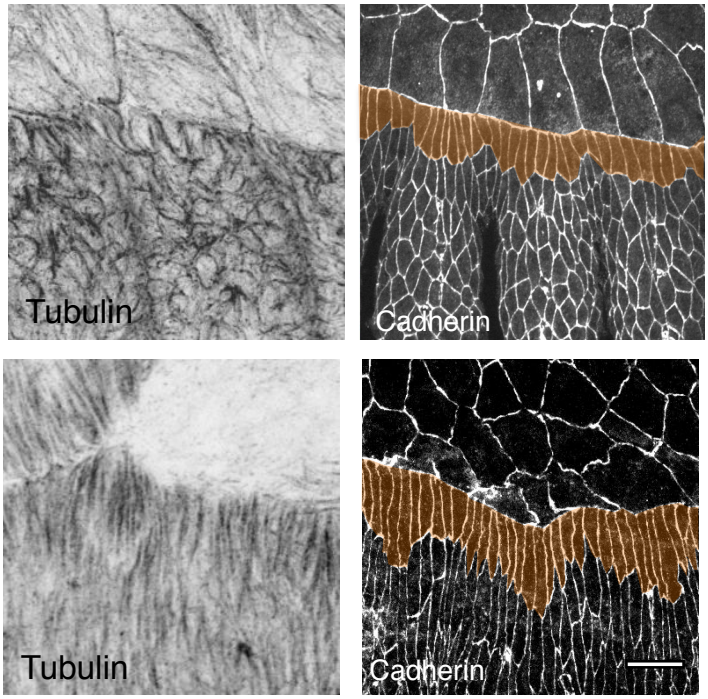

Figure 16. Microtubules accumulation and cell elongation at the leading edge during dorsal closure.

These four images have been obtained from for different wild-type embryos.

At the beginning of dorsal closure (top panels), microtubules are neither polarized, nor enriched at the leading edge. Leading edge cells are not elongated (orange cells).

As closure proceeds (bottom panels), microtubules accumulate and polarize along the dorso-ventral axis at the leading edge. Leading edge cells also elongate dorso-ventrally (orange cells).

In addition, leading edge cells produce a trans-cellular actin cable that circles the amnioserosa (Young et al., 1993; Jacinto et al., 2000; Jacinto et al., 2002). Leading edge cells also produce actin-based short protrusions called filopodia that are crucial for the zipping (Jankovics and Brunner, 2006; Millard and Martin, 2008).

Two major developmental pathways control dorsal closure: the stress response pathway JNK acts upstream and induces the Bone Morphogenetic Protein homologue Decapentaplegic (DPP) (Glise and Noselli, 1997; Hou et al., 1997; Kockel et al., 1997; Riesgo-Escovar and Hafen, 1997). Both JNK and DPP pathway are

crucial for dorsal closure since embryos where either JNK or DPP signalling is impaired fail to complete dorsal closure (Affolter et al., 1994; Glise et al., 1995).

There are three main driving forces of dorsal closure that will be detailed hereafter:

(1) Cell oscillation and delamination in the amnioserosa (Toyama et al., 2008; Solon et al., 2009; Muliyil et al., 2011).

(2) The actin cable that could either provide a contractile force or prevent the relaxation of leading edge cells (Young et al., 1993; Kiehart et al., 2000; Jacinto et al., 2002; Rodriguez-Diaz et al., 2008; Solon et al., 2009).

(3) The filopodia that make the zipping effective at each canthus (Jankovics and Brunner, 2006; Millard and Martin, 2008).

III.2 The amnioserosa

The amnioserosa is an extra-embryonic tissue composed of flat squamous cells that cover the yolk. During dorsal closure, the amnioserosa progressively disappears, hence participating to the progression of closure. Amnioserosa is specified during gastrulation by the transcription factor *zerknullt* (Doyle et al., 1986) and becomes sandwiched between the tail and the head of the embryo as germ-band extension proceeds.

Dorsal closure is divided into two phases (Gorfinkiel et al., 2009). During the first "slow" phase of dorsal closure, amnioserosa cells dynamically oscillate at the apical surface (Fernandez et al., 2007; Gorfinkiel et al., 2009; Solon et al., 2009; Blanchard et al., 2010; David et al., 2010; Sokolow et al., 2012) (**Figure 17**).

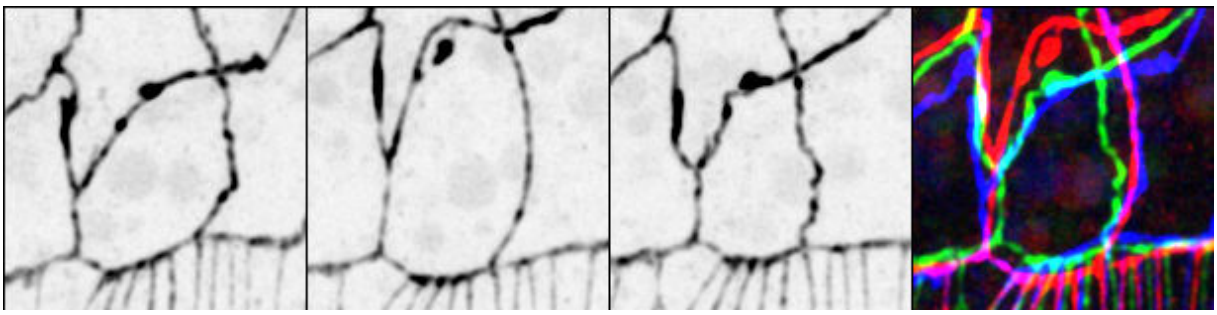

Figure 17. Amnioserosa cell oscillations during dorsal closure.

Closeup of a *shg ::GFP* embryo during dorsal closure. The three first images are still images from a time-lapse movie showing the oscillation of one amnioserosa cell. The last image is a composite where the three first images have been colour-coded and super-imposed.

Amnioserosa cell oscillation is driven by transient relocalisation of actin and non-muscle myosin II (*spaghetti squash*, *sqh*) at the centre of the cells (Franke et al., 2005; Blanchard et al., 2010). During the first "slow" phase, the myosin-actin flow is therefore pulsed and is regulated by the PAR complex (David et al., 2010), but also by Ca^{2+} flux (Hunter et al., 2014). Indeed, blocking of the Ca^{2+} channels subunits

generates defects in actomyosin structures, and prevents amnioserosa cell contraction (Hunter et al., 2014). These amnioserosa cell oscillations drive the progressive constriction of their apical domain (Solon et al., 2009). In addition, laser ablation of a single amnioserosa cell leads to a decrease in or a stop of the oscillation of neighbouring amnioserosa cells, indicating that local tensions are crucial for these oscillations (Solon et al., 2009).

During the second, "fast" phase, amnioserosa cells stop oscillating, concomitantly with the formation of the actin cable. Myosin accumulates in a more sustained manner in the amnioserosa (Blanchard et al., 2010). Amnioserosa cells continue to reduce their apical surface. This contributes to the progression of the leading edge since ablation of in the amnioserosa leads to a transient ventral-ward retraction of the leading edge (Kiehart et al., 2000). The amnioserosa cells located at the periphery start to flatten first, followed by the next row of cells shortly after (Gorfinkiel et al., 2009) (**Figure 18**).

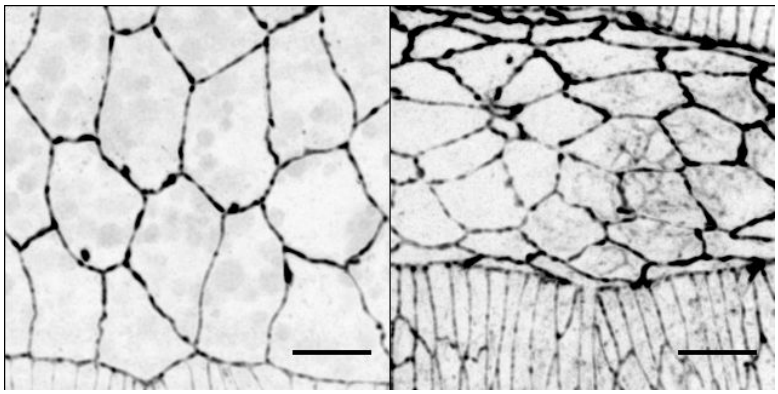

Figure 18. Amnioserosa during the slow and fast phases.

Still images of a *shg ::GFP* embryo during dorsal closure.
Left: amnioserosa during the slow phase. Right: Amnioserosa during the fast phase. Peripheral amnioserosa cells are flattened.

In addition, about 10 to 30% of the amnioserosa cells undergo apoptosis and delaminate in a stochastic fashion (Kiehart et al., 2000; Toyama et al., 2008). This occurs preferentially in the anterior part of the embryo during the "fast" phase (Muliyil et al., 2011). Enhancing or reducing apoptosis in the amnioserosa speeds or slows dorsal closure respectively, indicating that cell death in the amnioserosa tunes

the speed of closure (Toyama et al., 2008; Muliyil et al., 2011). This could be the main driving force of dorsal closure, since the ablation of the canthi that breaks the continuity of the actin cable does not stop the progression of the leading edge (Wells et al., 2014) (**Figure 19**).

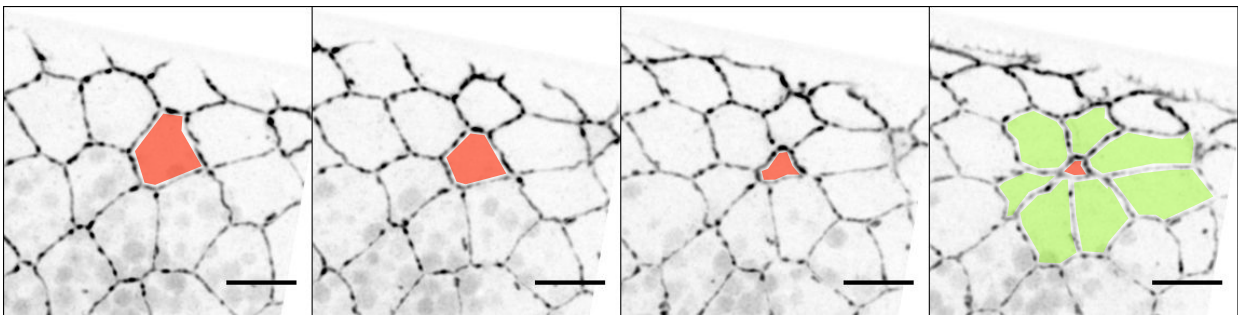

Figure 19. Amnioserosa cell delamination.

Still images of a *shg ::GFP* embryo during dorsal closure. The red cell progressively delaminates, leading to the formation of a so-called "rosette" (green cells). Scale bar: 10 µm.

Recently, it has been shown that stochastic generation of Reactive Oxygen Species (ROS) in the amnioserosa is necessary and sufficient to trigger cell delamination by acting on actomyosin and mitochondrial architecture (Muliyil and Narasimha, 2014). However, we currently do not understand the genetic program that control amnioserosa cell death and what controls ROS regulation.

Altogether, amnioserosa is a major driving force during dorsal closure. During the initial first "slow phase", pulses of actin and myosin in the centre of the cells drive rapid cell contraction and relaxation. This depends on the PAR complex and on the Ca^{2+} flux. While these cells oscillate, they progressively reduce their apical surface and volume. During the second "fast" phase, oscillations are reduced since myosin accumulates in the centre of cells in a sustained manner. Cells continue to reduce their apical surface and volume, while 10 to 30% undergo apoptosis due to ROS accumulation. In addition, the actin cable that circle the amnioserosa is also believed to be another major driving force during dorsal closure.

III.3 The actin cable

The actin cable is a remarkable supra-cellular structure that is present during the developmental morphogenesis of many tissues such amnion sac closure in the chick embryo (Tipping and Wilson, 2011), ventral enclosure in *C. elegans* (Williams-Masson et al., 1997; Martin and Parkhurst, 2004) or during *Drosophila* dorsal closure (Young et al., 1993; Jacinto et al., 2000; Jacinto et al., 2002). The presence of an actin cable has first been described in the 90's in cells around wounds in the chick embryo (Martin and Lewis, 1992). Shortly after, the presence of an actin cable has been also described in both vertebrate and invertebrate models of wound healing (Martin and Lewis, 1992; Brock et al., 1996; Davidson et al., 2002; Wood et al., 2002; Belacortu and Paricio, 2011). In the *Drosophila* embryo, at the beginning of dorsal closure, the leading edge cells that are in contact with the amnioserosa produce a dense trans-cellular actomyosin cable that can be easily visualized with a phalloidin staining that labels actin (**Figure 20**).

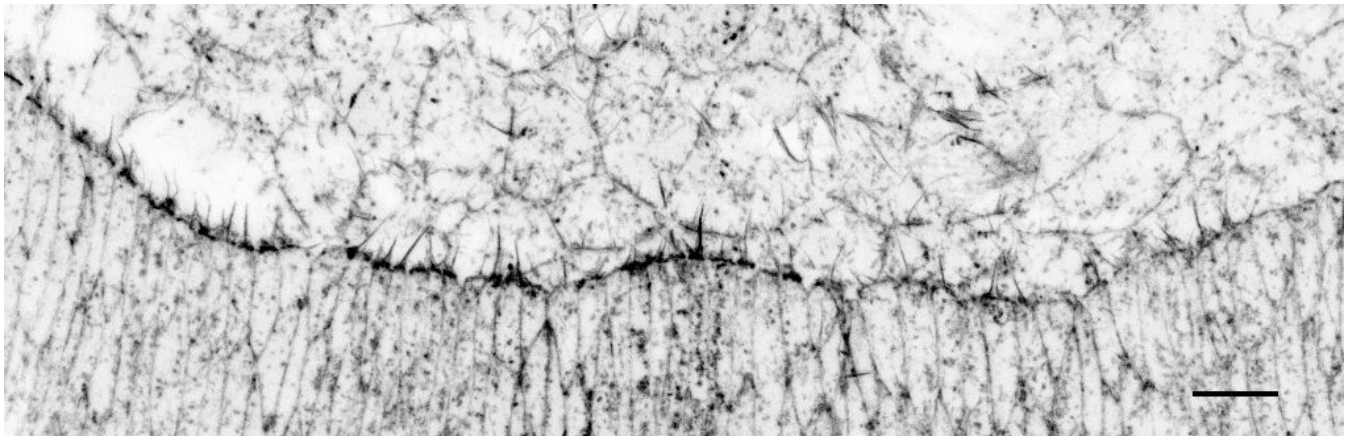

Figure 20. Actin cable during dorsal closure.

Closeup of a Stage 13/14 embryo marked with Phalloidin to label actin. Scale bar: 10 µm. Note the strong enrichment of actin at the amnioserosa / leading edge interface that corresponds to the actin cable. Filopodia produced by leading edge cells and pointing towards the amnioserosa are also visible.

The actin cable formed at stage 13 becomes stronger as closure proceeds. It accumulates filamentous actin and the non-muscle myosin II (*spaghetti squash*, *sqh*) (Young et al., 1993; Kiehart et al., 2000; Jacinto et al., 2002). In addition, the actin-capping molecule Enabled (Ena) is enriched at the actin cable during dorsal closure (Grevengoed et al., 2001; Gates et al., 2007), but also in tri-cellular junctions in the epidermis (Gates et al., 2007) and in groove cells (Vincent et al., 2008). Ena therefore constitutes an excellent marker to label the actin cable. In addition, the adhesion molecule Echinoid (Ed) is expressed in all the cells of the epidermis except in the junctions between the leading edge and the amnioserosa (Laplante and Nilson, 2006; Laplante and Nilson, 2011). This asymmetric distribution of Ed at the leading edge is crucial for actin cable formation since restoring a symmetric distribution of Ed by either depriving all cells from Ed or by ectopically expressing the Ed at the amnioserosa / leading edge interface results in similar actin cable defects (Laplante and Nilson, 2011) (**Figure 21**).

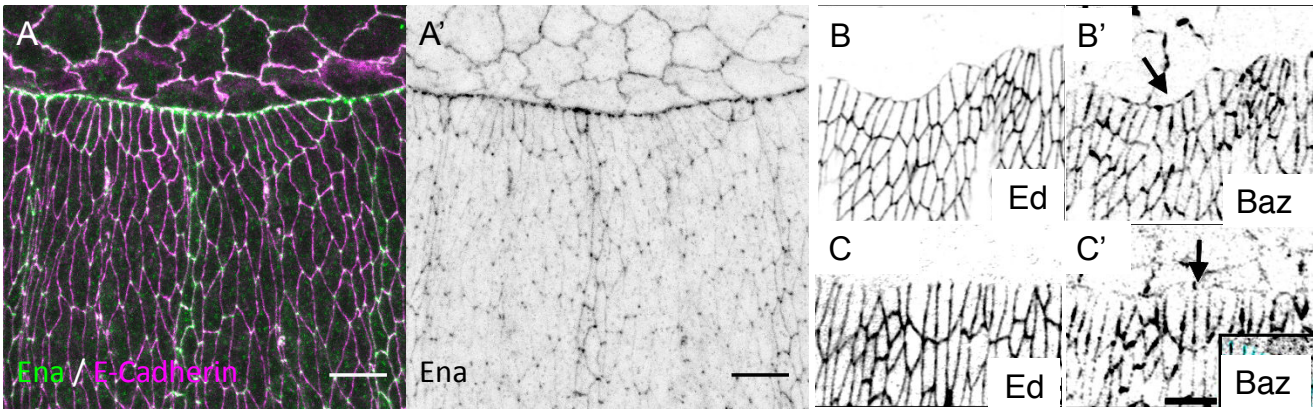

Figure 21. Ena, Ed and Baz expression pattern during dorsal closure.

(A-A') closeup of a Stage 14 embryo marked with Ena and E-Cadherin. Scale bar: 10 µm. Ena is enriched in tri-cellular junction, in groove cells but most importantly at the level of the actin cable (Gates et al., 2007).

(B-C') Closeup of embryos at the beginning (B-B') or at the middle of dorsal closure (C-C'). Ed and Baz are progressively excluded from the leading edge / amnioserosa interface as closure proceeds. These images are taken from (Laplante and Nilson, 2011) and have been processed on ImageJ.

Ed also controls the correct localisation of the scaffolding protein and apical determinant Par3/Bazooka (Baz) (Laplante and Nilson, 2011). During development, Baz localizes to adherens junctions but is lost from the leading edge / amnioserosa interface as closure proceeds. Baz is important for acto-myosin contractility during amnioserosa cell apical constriction (David et al., 2010; David et al., 2013; Pickering et al., 2013) as well as for actin-based protrusions. Since Baz exclusion from the amnioserosa / leading edge interface is Ed-dependant, Baz might directly control actin cable formation, although the molecular mechanism is unknown (Laplante and Nilson, 2011).

The actin cable is therefore a striking feature of the highly specialized cytoskeleton of the leading edge cells during dorsal closure. There are to main questions that have been addressed extensively but still remain unsolved:

(1) Is the actin cable required or dispensable for dorsal closure?

(2) What is the function of the actin cable during dorsal closure?

The requirement or dispensability of the actin cable during dorsal closure remains puzzling. Indeed, embryos where the cable is affected are showing a range of different phenotypes, probably because the missing components are not expressed solely at the leading edge but also in other tissues such as the amnioserosa. For instance, in embryos lacking zipper, the motor protein non-muscle myosin heavy chain, the actin cable is affected and dorsal closure often fails (Young et al., 1993). Alternatively, in embryos deficient for the non-receptor tyrosine kinase *Abelson* (*Abl*) where the actin cable formation is perturbed, a subset of Abl mutant embryos either close slowly or fail to complete dorsal closure, suggesting that the actin cable could be either dispensable or strictly required for dorsal closure (Grevengoed et al., 2001). Last, the asymmetric distribution of Ed at the leading edge is crucial for the actin cable formation (Laplante and Nilson, 2011). In embryos that are zygotically lacking Ed, dorsal closure is completed, although terminating with discontinuities and puckering

at the dorsal midline (Laplante and Nilson, 2006). This suggests that the cable would be dispensable for closure. In addition, laser ablation experiments showed that breaking the continuity of the cable does not prevents closure, although the continuity of the cable is restored shortly after the cut (Kiehart et al., 2000; Hutson et al., 2003; Rodriguez-Diaz et al., 2008). Altogether, the requirement of actin cable during dorsal closure is unclear. With the model we set up, we provide an unambiguous proof that the actin cable is dispensable for dorsal closure (Results section). Using our model, we then further investigated the effect of the absence of the acting cable during dorsal closure.

In *Drosophila*, two main models have been proposed to account for the function of the actin cable during dorsal closure. First, the actin cable has been proposed to operate as a contractile purse-string (Young et al., 1993; Kiehart et al., 2000; Jacinto et al., 2002; Rodriguez-Diaz et al., 2008). The name purse string refers to the analogy of the purse string procedure in medicine where a string surrounding a wound is pulled by the surgeon to artificially close the wound. In this model, the actin cable provides a contractile force to ensure the dorsal-ward migration of leading edge cells. This is supported by the observation that in embryos lacking the actin cable, dorsal closure often fails to complete (Young et al., 1993; Grevengoed et al., 2001). A prediction of this model is that leading edge cells should be under tensions, since the cable should be pulled along the antero-posterior axis. This has been confirmed by laser ablation experiments where cutting the actin cable leads to a retraction of the neighbouring leading edge cells (Kiehart et al., 2000; Hutson et al., 2003; Rodriguez-Diaz et al., 2008). However, laser ablation of the actin cable does not prevent dorsal closure, indicating that the actin cable is not the only driving force during dorsal closure (Kiehart et al., 2000). In addition, the purse string mechanism relies on the geometry of the system: the movement should be proportional to the curvature of the cable and no movement should proceed when the cable is straight. It has been

shown that two parallel actin cables can still progress towards each other, suggesting that the cable does not drive dorsal closure (Wells et al., 1999) and that other forces are at work.

Recently, the decrease in the amnioserosa cell volume at the onset of cell death has been shown to ensure correct dorsal closure kinetics, together with the actin cable tension (Saias et al., 2015). In addition to their delamination, amnioserosa cells contract and relax in a pulsed manner (Solon et al., 2009). To potentiate the energy provided by amnioserosa cell contraction, the actin cable has been proposed to act in a ratchet-like mechanism (Solon et al., 2009), rather than acting as a purse-string. In this model, during amnioserosa cell contraction, the cable is passive and leading edge cells progress dorsally. However, during the relaxation of the amnioserosa, the actin cable prevents the subsequent relaxation of the leading edge, thus suppressing unwanted ventral-ward movement of the cells (Solon et al., 2009). However, clear experimental evidence confirming this model is lacking.

Altogether, the function of the actin cable during dorsal closure remains elusive. The main issue to assess the function of the actin cable during dorsal closure is that a powerful experimental setting is lacking. The use of laser microsurgery is useful to get an instantaneous picture of the forces present at the level of the leading edge. However, within 10 minutes after the cut, a new cable forms, thus restoring the continuity of the actin cable. Thus, the system does not provide information on the effect of a missing actin cable during the full process of dorsal closure (Kiehart et al., 2000; Hutson et al., 2003; Rodriguez-Diaz et al., 2008). In addition, laser ablation experiments not only affect the actin cable, but in addition the leading edge cells themselves (including possibly filopodia, adherent junctions, etc.). Alternatively, mutant embryos lacking the cable should provide an elegant way to assess to function of the actin cable during dorsal closure. A difficulty is that in embryos deficient for either JNK or DPP signalling, the actin cable formation is affected, but

also many other morphogenetic processes that, together with actin cable formation defects, are likely to contribute to the "dorsal open" phenotype (Affolter et al., 1994; Glise et al., 1995; Kaltschmidt et al., 2002; Fernandez et al., 2007). On the other hand, embryos lacking components of the cable such as actin or myosin are also difficult to analyse since these components are broadly expressed in the embryo and affect other cell types (Hutson et al., 2003; Houssin et al., 2015). In addition, in embryos lacking the small GTPase Rho1, the actin cable is affected, but the number and the length of filopodia is modified (Jacinto et al., 2002). Thus Rho1 mutant embryos have two components crucial for dorsal closure simultaneously affected. Last, although Ena constitutes a nice marker of the actin cable, embryos lacking Ena show a normal accumulation of phalloidin at the amnioserosa / leading edge interface, indicating the actin cable is only mildly – if not – affected in *ena* mutants (Gates et al., 2007).

Therefore, a perfect model would be an embryo lacking a component of the actin cable that is solely expressed in the leading edge cells. This what we set up with Zasp52 (results section).

In addition of the actin cable, leading edge cells also produced actin-based protrusion (the filopodia) that are crucial for the zippering.

III.4 The filopodia

The filopodia are actin-based protrusions that are produced by the leading edge cells and that point towards the amnioserosa (Jacinto et al., 2000). Filopodia were first characterized in the sea urchin embryo during gastrulation. Indeed, mesenchymal cells extend filopodia towards cells of the ectoderm so they can migrate during invagination of the sea urchin endoderm. During *Drosophila* dorsal closure, leading edge cells produce filopodia that are up to 10-µm long and are crucial during the zippering phase. Filopodia from each leading edge fuse the two edges when they are close enough (e.g. at the canthi) (Jacinto et al., 2000; Jankovics and Brunner, 2006; Millard and Martin, 2008). Filopodia are highly dynamic structures that establish stable interactions with filopodia from the opposite cell type (e.g. *engrailed*-expressing cells for instance), hence ensuring a perfect segment matching (Jacinto et al., 2000; Millard and Martin, 2008) (**Figure 22**).

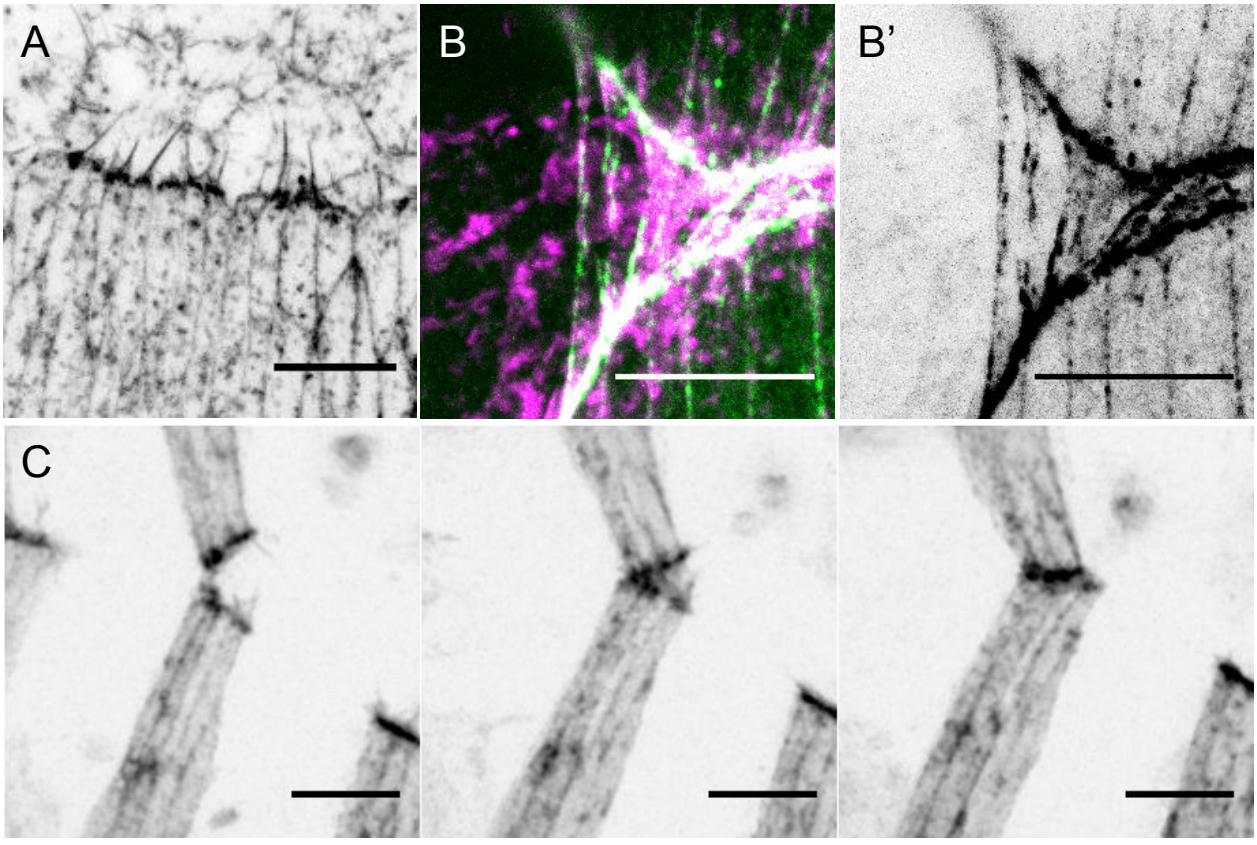

Figure 22. Filopodia during dorsal closure.

(A) Wild-type embryo marked with Phalloidin. Filopodia produced by the leading edge cells point towards the amnioserosa. (B-B') *Zasp52::GFP* embryo marked with Phalloidin (magenta) and Zasp52 (green in B, grey in B').
(C) Still images from a *engrailed-Gal4, UAS-Actin::RFP* embryo showing the segment matching. Scale bar for all panels: 10 µm.

Although filopodia are for the moment considered as dispensable for the dorsal-ward progression of the leading edge cells, they are crucial to terminate dorsal closure: in embryos lacking filopodia, the two edges get closer without fusing (Jankovics and Brunner, 2006). In addition, a complex cytoskeleton reorganisation occurs within the filopodia during the zippering (Eltsov et al., 2015)(**Figure 23**). After a phase of lamellar 'roof tile'-like overlap, the horizontal membrane interaction rotates into a vertical orientation due to the shortening and the thickening of the filopodia. This is achieved by the replacement of actin bundles by microtubules.

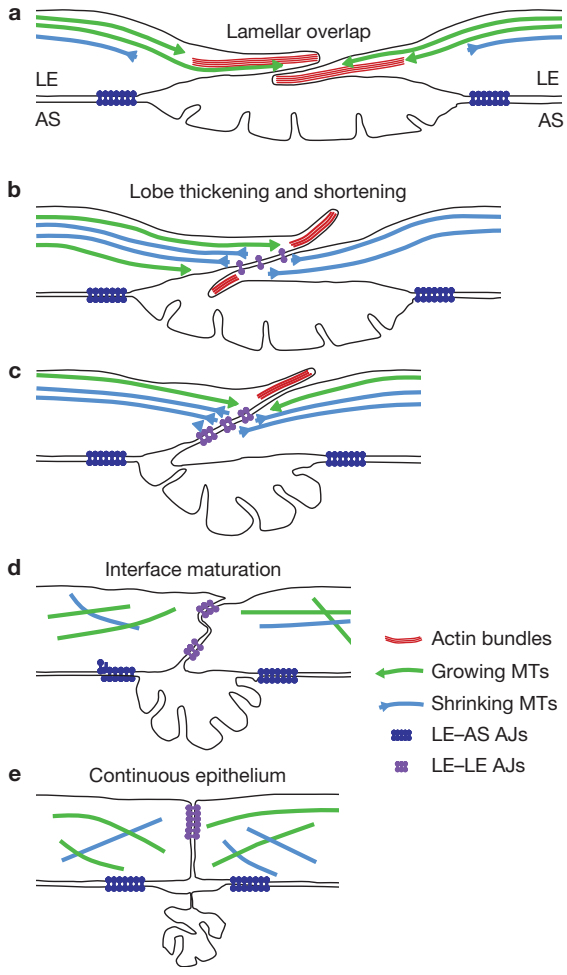

Figure 23. Proposed model of zipping.

Cartoon taken from (Eltsov et al., 2015) deciphering the main phases of zippering.

Filopodia formation is under the control of the JNK pathway. Indeed, in JNK signalling mutant embryos, filopodia are missing, associated with segment mismatching (Jacinto et al., 2000). In addition, the small GTPases Rho1 and Cdc42 regulate the abundance and the length of filopodia: *Rho1* mutant embryos display more abundant and longer filopodia compared with WT embryos, while Cdc42 overexpression decreases the number of filopodia (Jacinto et al., 2000; Jacinto et al., 2002). Importantly, either an increase or a reduction of the number of filopodia leads to segment mismatching, indicating that the number and the length of filopodia have to be finely tuned.

In addition, filopodia length and dynamic are also regulated by the actin-associated molecules Ena and Diaphanous (Dia) in an opposite manner. Dia induces filopodia, while Ena decreases Dia-induced filopodia (Homem and Peifer, 2009).

A conundrum about filopodia is how they connect the correct opposite ones remains mysterious. We know that when JNK signalling is impaired, it can lead to segment mismatching where for instance *engrailed*-positive cells from a segment match with the *engrailed*-positive cells of the next opposite segment (Gettings et al., 2010). In some cases, fusion of two stripes of *engrailed*-positive cells from the same edge can occur (see the Zasp52/Actin cable paper). This raises several questions:

(1) What mechanism enables filopodia from one cell type to connect the correct filopodia from the very same cell type of the opposite edge?

(2) When the same type of cells (e.g. *engrailed*-positive cells) from the same edge are in close vicinity, what prevents / delays their "auto"-matching?

An attractive hypothesis would be that filopodia can transport signalling ligands and/or receptors, as it is the case for actin-long protrusions called cytonemes in the wing imaginal disc (Ramirez-Weber and Kornberg, 1999; Roy et al., 2011; Roy et al.,

2014) or in the *Drosophila* testis (Inaba et al., 2015). For instance, in the wing imaginal disc, anterior cells send specific cytonemes toward the posterior compartment on which Hh or Dpp are routed (Roy et al., 2014). However, such hypotheses remain to be tested.

It is worth noting that both filopodia and the actin cable are also produced by cells around a wound. Dorsal closure is thus considered as a process reminiscent of wound healing.

III.6 Dorsal closure has a model for wound healing

Wound healing is a key morphogenetic process that allows the restoration of tissue continuity without proliferation. There are two types of wound healing: the embryonic wound healing, associated with little or no inflammatory response, that leaves no scar, and the adult wound healing with an inflammatory response, associated with the formation of a scar (Belacortu and Paricio, 2011).

Although pioneer wound healing studies have been conducted in vertebrates, the genetic power combined with live-imaging techniques in *Drosophila* enabled the better cellular characterization of morphogenetic events during wound healing. Indeed, both *Drosophila* wound healing and dorsal closure shares similar properties with vertebrate wound healing.

First, both the presence of an actin cable and filopodia have been reported to be present during wound healing in *Drosophila* (Wood et al., 2002; Martin and Parkhurst, 2004; Belacortu and Paricio, 2011) but also in a wide range of vertebrate species including the chick (Martin and Lewis, 1992; Brock et al., 1996), the *Xenopus* embryo (Davidson et al., 2002), the adult mice cornea (Danjo and Gipson, 1998) or even in human cultured cells (Bement et al., 1993; Jacinto et al., 2000) (**Figure 24**).

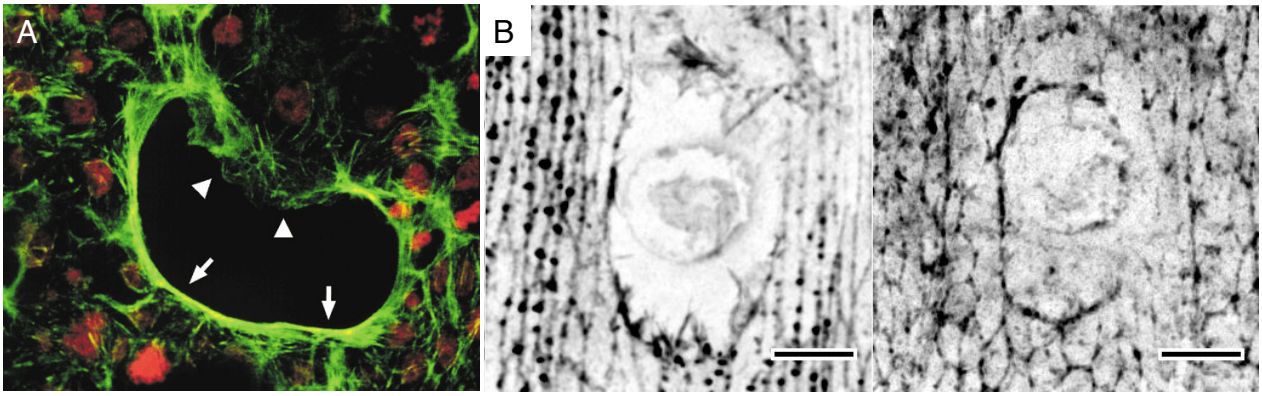

Figure 24. Actin cable and filopodia formation during human and *Drosophila* wound healing.

(A): Figure from (Jacinto et al., 2001) showing the actin cable formation after a wound in Caco-2BBE cells. (B): Wounds in Moesin::GFP embryos with filopodia and actin cable formation.

In addition, the JNK pathway that controls dorsal closure is also controlling wound healing both in *Drosophila* and in mammals. In *Drosophila*, lacZ reporters of the JNK target *puckered* (puc) as well as the JNKKKK *misshapen* (*msn*) accumulate around wounds in larvae or in adults (Ramet et al., 2002; Galko and Krasnow, 2004), as well as after ablation of a part of the wing imaginal disc (Bosch et al., 2005) (**Figure 25**). In mammals, inhibition of JNK signalling leads to defects in fibroblasts migration during wound healing (Grose, 2003; Javelaud et al., 2003; Li et al., 2003). JNK signalling is also required for zebrafish regeneration (Kawakami, 2010).

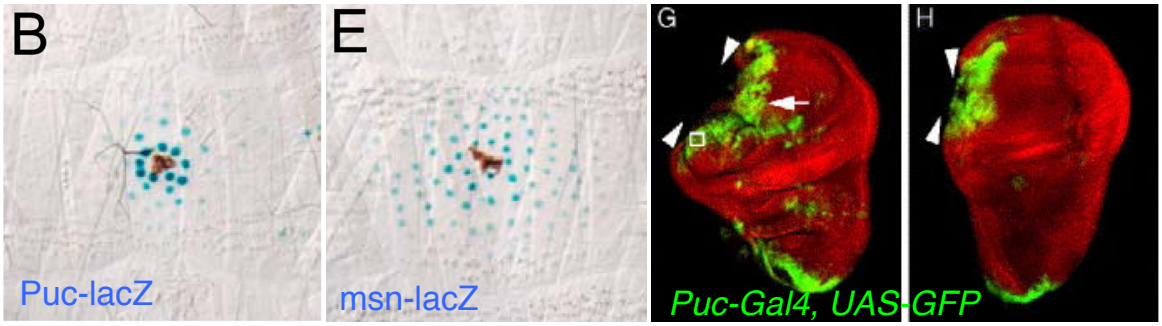

Figure 25. JNK activity during *Drosophila* larval wound healing.

(B and E): Figure from (Galko and Krasnow, 2004) showing puc-lacZ and msn-lacZ accumulation around larval puncture wounds. (G and H): Figure from (Bosch et al., 2005) showing Puc-Gal4 expressing cells after a wound in a wing imaginal disc.

Altogether, *Drosophila* dorsal closure in an excellent model to understand wound healing since it shares structural and signalling properties with both *Drosophila* and vertebrate wound healing. However, a major difference is that while the amnioserosa plays a crucial role during dorsal closure, there is no such equivalent structure in both *Drosophila* and vertebrate wound healing. Interestingly, it been proposed that the fibroblasts of the granulation tissue have contractile movements and play a role in the zippering, thus functionally resembling to the amnioserosa (Martin and Parkhurst, 2004).

IV. Signalling during dorsal closure

IV.1 The JNK pathway: a stress-response and developmental pathway.

The Jun N-terminal Kinase pathway (JNK) is an eukaryotic evolutionary conserved stress-response pathway that also controls developmental processes. While JNK initially acted as a stress-mediator pathway, it acquires during evolution developmental functions (Rios-Barrera and Riesgo-Escovar, 2013). In *Drosophila*, the JNK pathway acts as a stress mediator in a variety of cellular and homeostatic mechanisms. For instance, JNK induces apoptosis in response to UV or gamma-irradiation in larvae and adults (Leppa and Bohmann, 1999; McEwen and Peifer, 2005; Igaki, 2009). The JNK pathway is also involved in the healing of larval and adult wounds (Ramet et al., 2002; Galko and Krasnow, 2004; Belacortu and Paricio, 2011), as well as triggering compensatory proliferation (Ryoo et al., 2004) or regeneration following an injury (Bosch et al., 2005). It also controls several morphogenetic processes, including dorsal closure (Glise et al., 1995; Glise and Noselli, 1997; Hou et al., 1997; Kockel et al., 1997; Riesgo-Escovar and Hafen, 1997) but also follicle cell morphogenesis, thorax closure and genital disc rotation (Rousset et al., 2010).

The JNK pathway is a conserved type of Mitogen-Activated Protein Kinase pathway (MAPK), with a core pathway composed of three kinases where each component phosphorylates and subsequently activates its downstream partner. The MAPKKK is a Serine/Threonine kinase that phosphorylates the MAPKK. The MAPKK in turn phosphorylates the MAPK, a Serine/ Threonine kinase. Last, the MAPK phosphorylates transcription factors to control specific gene expression. In *Drosophila*, the core JNK module comprises the JNKK *hemipetrous* (*hep*) that

phosphorylates the JNK *basket* (*bsk*). In turn, Bsk phosphorylates at its N-termini Jun-related-antigen (Jra or D-Jun), the only *Drosophila* c-Jun homolog. Phosphorylated Jra subsequently associates with Kayak (Kay, DFos) to form the AP-1 complex that controls specific gene expression.

JNK is crucial for dorsal closure since embryos mutant for components of the JNK pathway fail to close dorsally and exhibit the so-called dorsal open phenotype. In these embryos, dorsal closure is aborted, leading edge cells fail to elongate, the zippering does not occur since actin cable and filopodia are not present. In addition, the amnioserosa is ripped away, and the digestive organs extruded dorsally (Affolter et al., 1994). This raises two questions:

(1) What are the upstream components that control JNK pathway?

(2) What are the JNK targets during dorsal closure?

(1) What are the upstream components that control JNK pathway?

Because embryos exhibiting a dorsal hole are easy to identify, this led the rapid progress in the identification of JNK core pathway upstream and downstream components (Nusslein-Volhard et al., 1987; Glise and Noselli, 1997; Hou et al., 1997; Kockel et al., 1997; Riesgo-Escovar and Hafen, 1997). It is known that the JNKKKK Misshapen (Msn) phosphorylates the mixed-lineage kinase (MLK)/ JNKKK Slipper (Slpr) that in turn phosphorylates Hep. Indeed, mutations in both kinases, Slpr and Msn, lead to the dorsal open phenotype (Su et al., 2000; Stronach and Perrimon, 2002).

This raises the question of the regulation of Msn. However, a striking conundrum in the dorsal closure field is that neither extracellular molecules nor membrane receptors leading to JNK activation have been identified. Interestingly, Shark is a non-receptor tyrosine kinase, that, when mutated in the embryo causes dorsal closure defects (Fernandez et al., 2000). Shark has been proposed to interact

with the *Drosophila* homolog *downstream of a kinase* (Dok). Dok mutant embryos display also some dorsal closure defects including absence of proper actin cable formation (Biswas et al., 2006). Based on these observations and S2 cells *in vitro* experiments, it has been proposed that the non-receptor tyrosine kinase Src42A phosphorylates Dok that in turn recruits Shark (Biswas et al., 2006). However, how Shark controls the downstream components remains elusive. In addition additional kinases have been shown to activate Msn expression when ectopically expressed. For instance, overexpression of the JNKKK dTAK1 induces ectopic expression of DPP and Puc (Takatsu et al., 2000; Mihaly et al., 2001). However, dTAK1 mutant embryos do not exhibit dorsal closure defects, suggesting that dTAK1 does not participate to dorsal closure *in vivo* (Mihaly et al., 2001) (**Figure 26**).

Altogether, the core JNK pathway consists in a signalling cascade of kinases. However, the very upstream components that regulate JNK activity remain elusive.

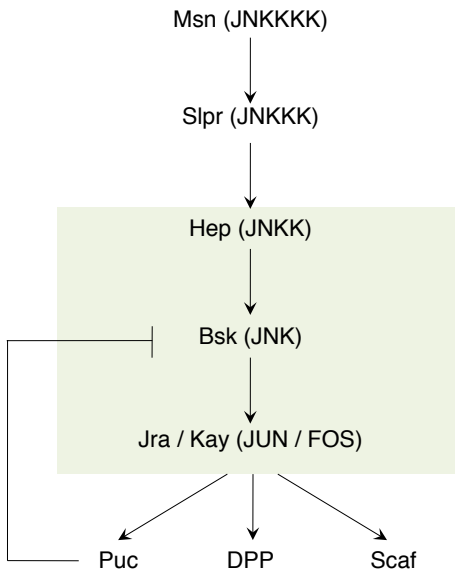

Figure 26. Simplified view of the JNK pathway during dorsal closure.

The core JNK pathway is in green.

Msn: Misshapen

Slpr: Slipper

Hep: Hemipterous

Bsk: Basket

Jra/Kay: Jun-related antigen / Kayak

Puc: Puckered

Scaf: Scarface

(2) What are the JNK targets during dorsal closure?

Genetic screens and microarrays enabled the identification of JNK targets. The main JNK target is DPP, that signals in the amnioserosa and the lateral

epidermis. DPP is crucial also for dorsal closure since embryos mutant for DPP pathway components display the dorsal open phenotype (Affolter et al., 1994; Simin et al., 1998). DPP is downstream of JNK signalling: DPP leading edge mRNA is lost in various JNK signalling mutant embryos (Glise and Noselli, 1997; Hou et al., 1997; Kockel et al., 1997; Riesgo-Escovar and Hafen, 1997). In addition, JNK pathway activates *puckered* (*puc*) expression, a phosphatase that provides a negative feedback on the JNK pathway by dephosphorylating Bsk (Martin-Blanco et al., 1998). Mutations in the *puc* gene lead to dorsal closure defects: closure completes but with a puckering of the epidermis toward the dorsal midline, associated with a salt and pepper JNK signalling. Therefore, excess and / or non-uniform JNK expression leads to closure defects. Interestingly, the Puc-lacZ reporter line has been widely used as a readout of JNK signalling and leading edge cell identity. Another JNK target is Scarface (Scaf), a secreted serine-protease homologue family member that provides a negative feedback on the JNK pathway (Rousset et al., 2010). These three targets are specifically expressed during germ-band retraction (Stage 12), onwards, indicating that JNK is active before dorsal closure. Last, in certain conditions, JNK would induce the pro-apoptotic gene *reaper* (*rpr*) at the leading edge. However, leading edge cells would be protected against this JNK-apoptosis because of the presence of DPP that inhibits rpr transcription (Beira et al., 2014).

In addition, JNK signalling also controls the expression of genes that are not expressed at the leading edge. First, JNK is required for the accumulation of the actin cytoskeleton regulator Chickadee (Chic), the *Drosophila* homolog of the vertebrate profilins (Jasper et al., 2001). JNK is also required for the accumulation of Cabut, a zinc finger transcription factor expressed in the yolk sac (Munoz-Descalzo et al., 2005).

Interestingly, the negative feedback loop mediated by the JNK targets Puc and Scaf indicates that JNK signal is tightly controlled. In addition of these negative

feedback loops, JNK signal is negatively regulated by several proteins. Anterior open (Aop, a.k.a Yan) is a transcriptional repressor of the RAS/MAPK pathway (Rebay and Rubin, 1995; Riesgo-Escovar and Hafen, 1997). Aop is a nuclear repressor constitutively expressed that gets degraded by the proteasome by Bsk. Contrary to other JNK pathway components, *aop* mutant embryos do not exhibit a "dorsal open" phenotype but rather an anterior hole.

Two other genes, Raw and Hindsight (Hnt, a.k.a Pebelled), are other negative regulators of the pathway, but their molecular actions remain unclear (Byars et al., 1999; Reed et al., 2001; Bates et al., 2008). Epistatic studies confirmed that Raw is downstream of Bsk and upstream of Jra, suggesting that Raw could act in parallel of Bsk (Bates et al., 2008). In addition, Hnt is a zinc-finger protein that is specified by early Dpp to promote the correct survival of the amnioserosa. Later, Hnt expression in the amnioserosa prevents JNK signalling (Reed et al., 2001). In this case, one could argue that Hnt antagonizes the stress-related JNK, since Hnt mutants exhibit premature apoptosis of amnioserosa cells before germ-band retraction (Reed et al., 2001; Rios-Barrera and Riesgo-Escovar, 2013).

A comprehensive view of the JNK pathway during dorsal closure is depicted in **Figure 27**. Upstream regulators of the JNK pathway are unknown. During dorsal closure, JNK induces targets. Chief among them is DPP, a key signalling ligand that is also crucial during dorsal closure.

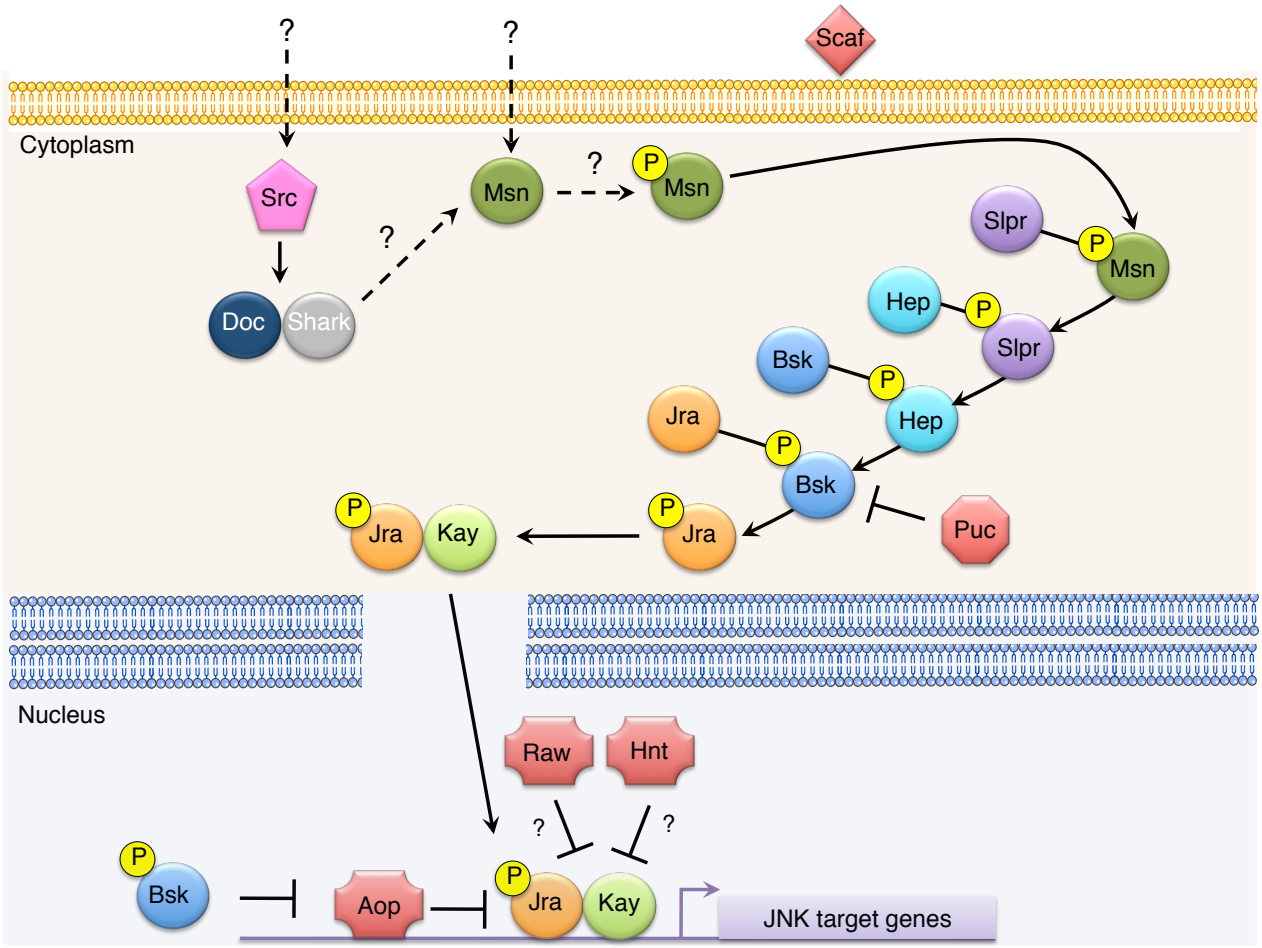

Figure 27. The JNK signalling pathway during dorsal closure.

Jra: Jun-related antigen; Kay: Kayak (D-Fos); Bsk: Basket; Hep: Hemipterous; Slpr: Slipper ; Msn: Misshapen. Negative regulators of the JNK pathway are in red. Aop: Anterior open (a.k.a. Yan); Hnt: Hindsight (a.k.a Pebbled); Puc: Puckered (a JNK target); Scaf: Scarface (another JNK target that provides a negative feedback on the JNK pathway); Dok: Downstream kinase; Src: Sarc.

The link between Doc / Shark activation and Msn activation is unknown. Signals that control Msn and / or Src activation remain unknown too. The negative regulation exerted by Raw and Hnt is not understood.

IV.2 The DPP pathway: a patterning and morphogenetic pathway.

The Decapentaplegic (DPP) protein is the *Drosophila* homologue of the TGB-ß super-family members BMP-2 and BMP-4. DPP is one of the best example of a morphogene, *i.e.* a diffusible ligand that spreads at a distance and induces targets in a concentration-dependent manner. In the larval wing imaginal disc, DPP is produced in a stripe of cells abutting the antero/posterior boundary and induces its targets Spalt (Salm) and Optomotor-Blind (Omb) at a distance to ensure correct growth (Affolter and Basler, 2007) (**Figure 28**). Indeed, impairing DPP expression in the wing disc reduces the wing to a small stump (Spencer et al., 1982; Zecca et al., 1995). Conversely, ectopic DPP signalling activity in a group of cells leads to strong overgrowth that can lead to a wing duplication (Capdevila and Guerrero, 1994; Zecca et al., 1995; Lecuit et al., 1996; Nellen et al., 1996). Hence, DPP is required and sufficient for the correct wing organisation and growth (Affolter and Basler, 2007).

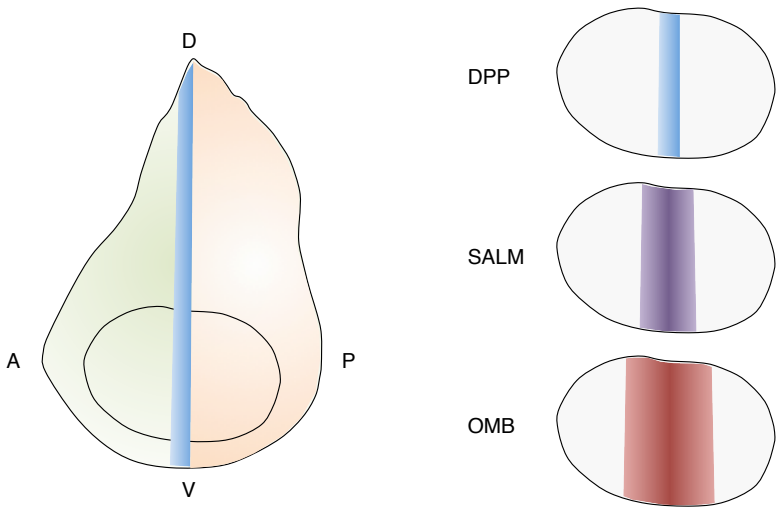

Figure 28. DPP gradient in the wing imaginal disc.

Left: wing disc. DPP (blue) is produced in a narrow stripe of anterior cells (green) abutting the A/P boundary. Right: wing pouch with DPP, Salm and Omb expression pattern.

In addition of its patterning activity, DPP also controls morphogenesis. For instance, in the wing imaginal disc, DPP not only acts as a morphogene, but is important for the cuboidal-to-squamous cell shape transition in the peripodial membrane, a layer of flat cells that covers the disc and that constricts to evert the

wing (McClure and Schubiger, 2005). DPP also prevents cell extrusion in columnar epithelium that will become the wing blade. Indeed, lack of DPP signalling in clones of cells induces the extrusion of these clones out of the epithelium, associated with a loss of apical microtubules (Gibson and Perrimon, 2005; Shen and Dahmann, 2005). In the ovary, DPP also controls flattening of the follicular cells (Brigaud et al., 2015). However, DPP has been the best described as a regulator of morphogenesis during dorsal closure.

In the *Drosophila* embryo, during cellularization, DPP is produced by the dorsal cells and establishes a dorso-ventral gradient. Early DPP is crucial for specifying the dorsal ectodermis and the amnioserosa since embryos mutant for DPP are ventralized (Irish and Gelbart, 1987; St Johnston and Gelbart, 1987). During dorsal closure, JNK signalling induces DPP expression in leading edge cells (Glise and Noselli, 1997; Hou et al., 1997; Kockel et al., 1997; Riesgo-Escovar and Hafen, 1997) and is active in the first four rows of dorsal epidermal cells. DPP is crucial for dorsal closure, since embryos where DPP signalling is impaired have a "dorsal open" phenotype (Affolter et al., 1994). Genetic screens in embryos enabled rapid the identification of the DPP pathway components (Nusslein-Volhard and Wieschaus, 1980; Affolter et al., 1994).

DPP binds to its Serine / Threonine kinase receptors Thickveins (Tkv) and Punt, the homologues of the TGF-ß receptor type I and II respectively (Brummel et al., 1994; Penton et al., 1994; Letsou et al., 1995; Ruberte et al., 1995; Nellen et al., 1996). Upon DPP binding, Punt phosphorylates Tkv, that in turns promotes the formation of a transcription factor complex composed of Mother against DPP (Mad) and Medea, the two *Drosophila* homologues of the receptor SMAD (r-Smad) and common-mediator Smad (co-Smad) respectively. Indeed, mutations in either Mad or Medea enhance an hypomorphic DPP mutant phenotype, suggesting that these genes are positive regulators of DPP signalling (Raftery et al., 1995; Sekelsky et al.,

1995). Specifically, activated Tkv receptor phosphorylates Mad, than in turn associates with Medea. Mad–Medea complex subsequently translocate into the nucleus. There, it associates with the transcription factor Schnnuri (Shn) to repress Brinker (Brk), a transcriptional repressor that silences most DPP target genes in the absence of DPP (Marty et al., 2000). Indeed, in the absence of Shn, cells fail to respond to DPP signalling, even upon ectopic activation of Tkv (Arora et al., 1995; Grieder et al., 1995; Staehling-Hampton et al., 1995). Furthermore, Brk was identified as a transcriptional repressor that is negatively regulated by DPP (Campbell and Tomlinson, 1999; Jazwinska et al., 1999; Minami et al., 1999). Indeed, *brk* mutant clones in the wing disc lead to the expansion of Salm and Omb expression pattern (Jazwinska et al., 1999). In addition, in the absence of Brk, Mad is not required for the activation of Dpp target genes, confirming that Mad actively acts on Brk repression (Jazwinska et al., 1999).

Importantly, DPP has several types of targets. For a first class of target genes such as Omb, removal of Brk is sufficient to trigger transcription. These genes constitute the 'depressed targets' class of genes. The expression of the second set, however, requires the additional activation by Mad / Medea transcription factor complex in addition of Brk repression. Such genes including Salm constitute the 'depressed and induced' set of targets (**Figure 29**). During dorsal closure, the loss of Brk is sufficient to rescue dorsal closure in the absence of pathway activation, suggesting that the DPP targets required for dorsal closure are expressed upon Brk de-repression only (Marty et al., 2000). A comprehensive view of the DPP pathway is depicted in **Figure 30**.

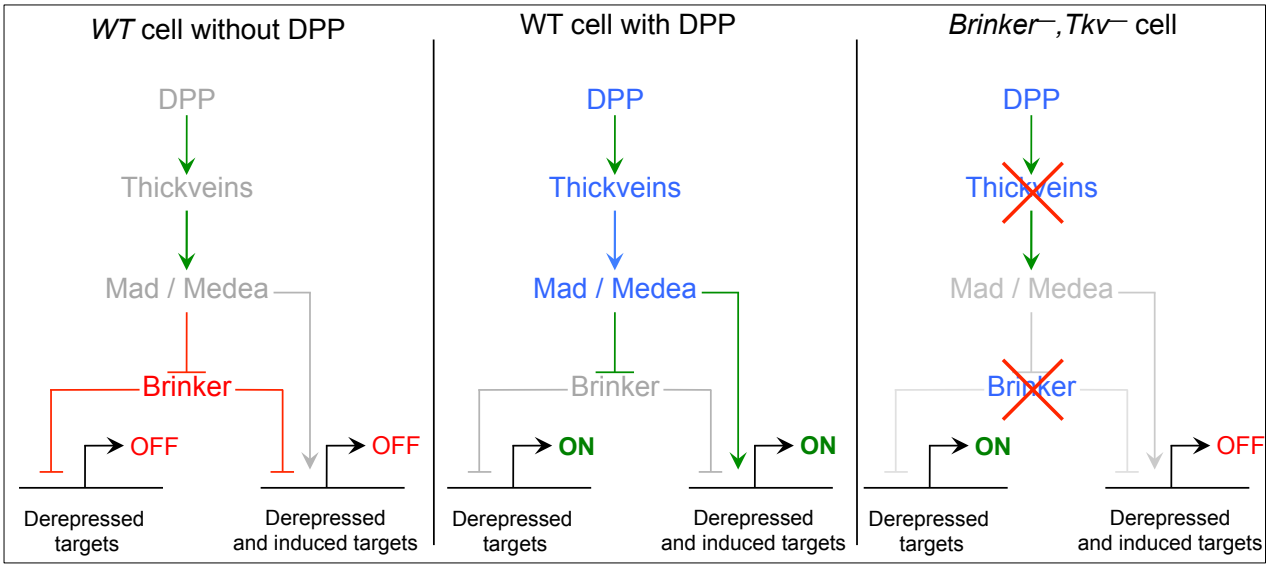

Figure 29. A simplified view of the DPP pathway.

Left and Middle: Simplified view of the DPP pathway with or without DPP.

Right : *Brinker*⁻, *Tkv*⁻ cell. Absence of Tkv prevents the formation of the Mad/Medea complex. The 'Derepressed and induced targets' are not expressed. Brk genetic removal leads to the activation of the 'Derepressed targets'. Analysis of the expression pattern of any potential DPP target in *Brinker*⁻, *Tkv*⁻ cells therefore reveals to which set of targets the tested target belongs.

Shortly after the identification of DPP pathway components, DPP targets were identified in the wing disc. However, DPP targets involved in dorsal closure - and especially genes controlling the cytoskeleton of the leading edge cells - remained elusive.

First, DPP induces *daughters against DPP* (Dad), an inhibitory *Drosophila* SMAD that acts as a negative regulator of the DPP pathway (Tsuneizumi et al., 1997; Marty et al., 2000). Dad is induced during dorsal closure and in the wing disc. Specifically, Dad binds to Tkv and prevents Mad phosphorylation (Inoue et al., 1998).

In the embryo, DPP induces the transcription factor of the GATA family *pannier* (*pnr*) in the dorsal part of the embryo just after cellularization (Winick et al., 1993; Heitzler et al., 1996; Ashe et al., 2000). As development progresses, *pnr* expression pattern is refined to the dorsal epidermis and the amnioserosa. From germ-band retraction onwards, Pnr is expressed in the first ten rows of dorsal epidermal cells but is excluded from the amnioserosa (Winick et al., 1993; Heitzler et al., 1996). Pnr is required for dorsal closure since *pnr* embryos display dorsal closure defects (Heitzler et al., 1996). Strikingly, DPP and *pnr* epistatic relation is reversed during dorsal closure: Pnr is upstream and is required for DPP leading edge expression independently of JNK (Herranz and Morata, 2001). Indeed, in *pnr* mutant embryos during dorsal closure, DPP leading edge expression is lost. Conversely, over-expression of Pnr in stripes lead to ectopic DPP during dorsal closure. (Herranz and Morata, 2001).

Recently, the Martinez-Arias lab performed a microarray analysis screen to identify DPP targets during dorsal closure. They identified that the transcription factor *U-shaped* (*Ush*) is downstream of DPP. Indeed, Ush levels are reduced in *tkv* mutant embryos, while overexpression of an activated form of Tkv in the entire epidermis leads to elevated Ush levels (Fernandez et al., 2007; Lada et al., 2012). Ush is expressed in the amnioserosa and in the first ten rows of cells in the lateral epidermis. It is worth noting that Ush expression domain is broader than the DPP activity domain (stated by phospho-mad staining), resembling to Pnr expression domain. Embryos mutant for *ush* exhibit defects in germband retraction and dorsal closure (Frank and Rushlow, 1996; Goldman-Levi et al., 1996). However, Ush targets remain elusive. A possible explanation is that Ush is regulated by the early DPP that acts during gastrulation to specify the dorsal side of the embryo.

Altogether, during dorsal closure, DPP is induced upon JNK at the leading edge. DPP targets remain elusive: only the transcription factor Ush appear to be

downstream of DPP during dorsal closure. During my thesis, I identified JNK and DPP targets that are likely to play an important role during dorsal closure.

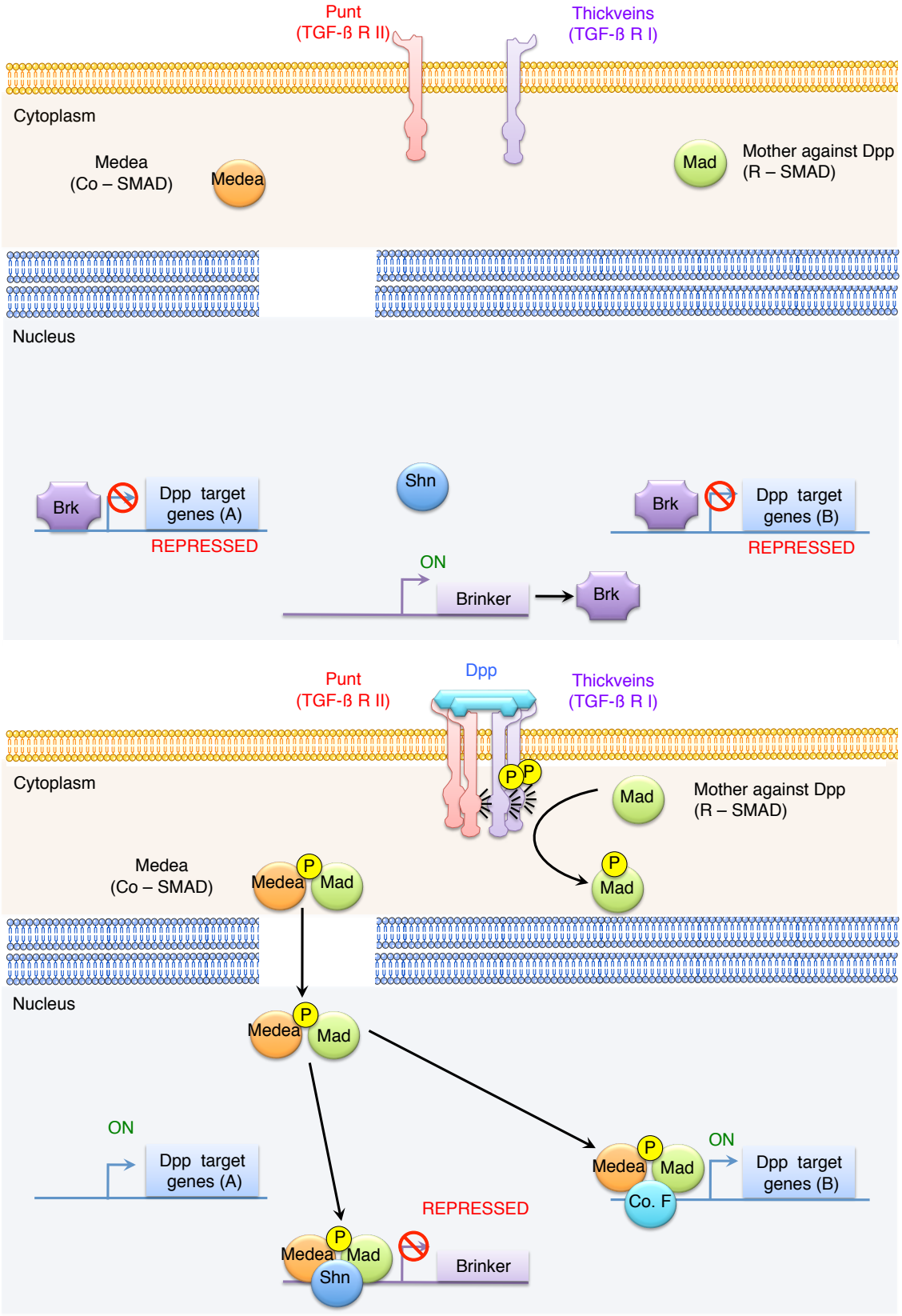

Figure 30. The DPP pathway during dorsal closure.

Brk: Brinker; Mad: Mother against DPP; Shn: Shnurri; Co.F: Co Factor.

Top: In the absence of DPP, Brk represses both sets of target genes.

Bottom: DPP binds to its receptors, leading to Mad phosphorylation. Mad and Medea associate with Shn to represses Brinker. This is sufficient for a first set of targets (A). A second set of targets require in addition of Brk repression activation by Mad and Medea (B).

V. Jupiter, Jaguar and Zasp52: 3 cytoskeletal-associated proteins that define the leading edge identity during dorsal closure

It is known for long that JNK and DPP pathways are active at the leading edge during dorsal closure (Glise and Noselli, 1997; Hou et al., 1997; Kockel et al., 1997; Riesgo-Escovar and Hafen, 1997). Indeed, embryos mutant for either JNK or DPP components fails to complete dorsal closure and exhibit the so-called 'dorsal open' phenotype (Affolter et al., 1994; Glise et al., 1995). In these mutant embryos, microtubule accumulation, actin cable formation, filopodia formation as well as dorso-ventral elongation of the leading edge cells are affected, suggesting that JNK and DPP influence the cytoskeleton of these leading edge cells (Jacinto et al., 2000; Jacinto et al., 2001; Jacinto et al., 2002; Kaltschmidt et al., 2002; Jankovics and Brunner, 2006; Fernandez et al., 2007; Millard and Martin, 2008; Solon et al., 2009) (**Figure 31**).

However two main questions remained unsolved:

(1) How are JNK and DPP integrated by the leading edge cells to promote a robust closure?

(2) What are the JNK and/or DPP targets that directly control the cytoskeleton of the leading edge cells during dorsal closure?

The difficulty to address these questions is that so far, markers expressed at the leading edge are missing. In the embryo, the only JNK targets are DPP itself, *puc* and Scaf, two phophatases providing a negative feedback on the JNK pathway (Glise and Noselli, 1997; Hou et al., 1997; Kockel et al., 1997; Riesgo-Escovar and Hafen, 1997; Rousset et al., 2010). Second, no clear DPP targets have been identified during dorsal closure. Thus, understanding how JNK and DPP control dorsal closure remained a conundrum. During my thesis, I focused on three exciting proteins:

(1) Jupiter, a microtubule associated protein that I observed to be enriched at the leading edge during dorsal closure.

(2) Jaguar, the Myosin VI homolog that is also enriched at the leading edge.

(3) Zasp52, an actin-associated protein that is expressed in muscles but also enriched at the leading edge during dorsal closure.

These three proteins were promising since they are all enriched at the leading edge during dorsal closure, and since they are associated with the cytoskeleton. Thus, I used these markers to understand how JNK and DPP inputs are integrated by the leading edge cells, and I persued on the role of Zasp52 during dorsal closure, the most promising target.

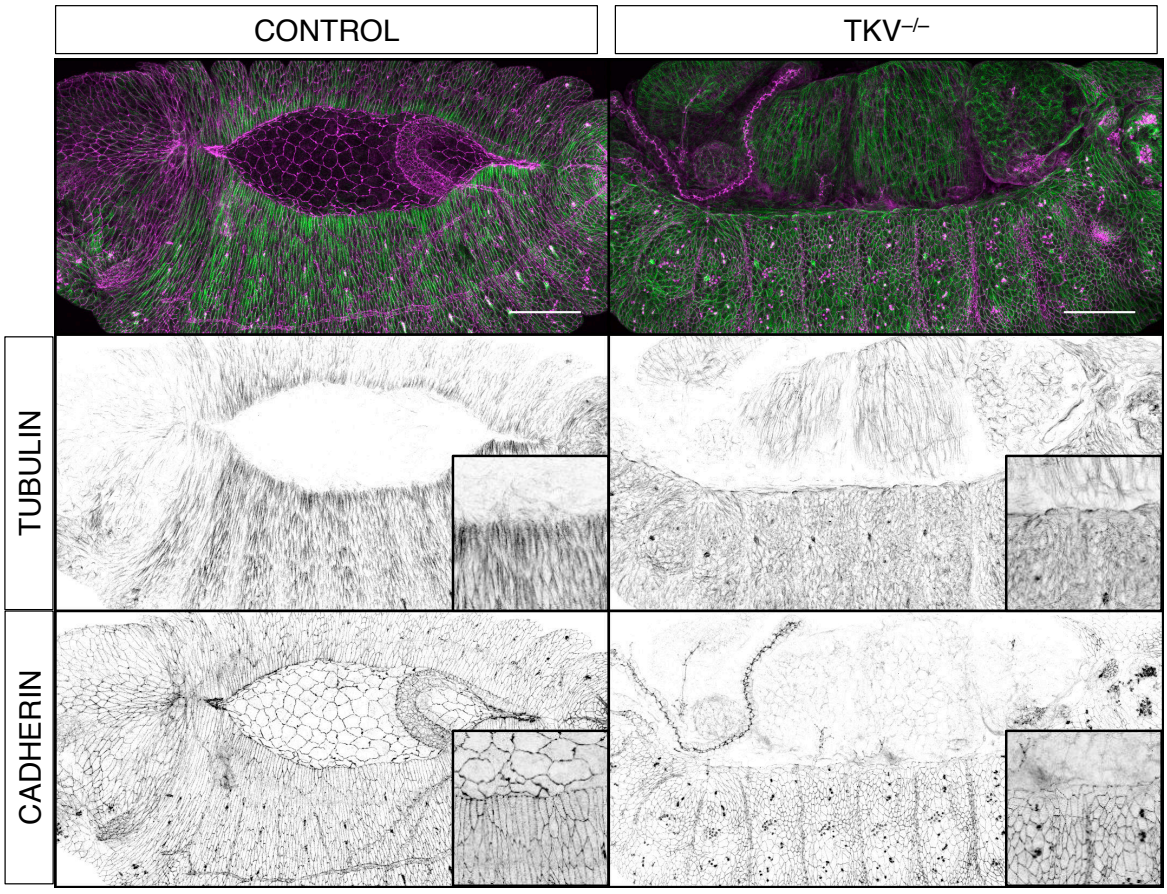

Figure 31. The dorsal open phenotype.

Left: Control embryo marked with E-Cadherin and Tubulin. Leading edge cells are elongated and have enriched, polarized apical microtubules. Right: *tkv* mutant embryo with the dorsal open phenotype. The zippering did not proceed, the amnioserosa is absent, leading edge cells are not elongated and failed to accumulate apical microtubules.

V.1 Jupiter, a microtubule-associated protein

Jupiter is a protein associated with microtubules (Karpova et al., 2006). It is not a proper MAP (Microtubule Associated Protein), although Jupiter contains two Proline-Proline-Glycine-Glycine (PPGG) motifs that are reminiscent of the domains of the microtubule-binding motif PGGG of Tau, MAP2 and MAP4 (Karpova et al., 2006). To study Jupiter, a Jupiter::GFP line has been set up by the Chia lab (Morin et al., 2001). It is a GFP knock-in generated with a GFP-exon trap strategy where the GFP has been flanked with spliced donor (SD) and spliced acceptor (SA) sites. This way, when inserted in an intronic sequence of the fly genome, the P-element carrying the GFP is recognised as an exon, thus creating a GFP knock-in (Morin et al., 2001). In the case of Jupiter::GFP, the flies are homozygous viable and do not display developmental delays, suggesting that GFP is not affecting dramatically Jupiter function. The Jupiter::GFP construct is a very useful line: the GFP fluorescence is bright and does not require any GFP antibody in immunofluorescence. Second, the fluorescence is bright enough to overcome the chorion autofluorescence. Thus, Jupiter::GFP embryos can be imaged in live without removing the chorion for a longer period that other GFP-tagged markers that require chorion removal. Using this line, Karpova and colleagues reported that Jupiter::GFP is expressed in the mitotic spindle during synchronous cell division in the early embryo, in larval nervous system, in the eye imaginal disc and in the adult ovary (Karpova et al., 2006). In addition, we observed that Jupiter::GFP also accumulates at the leading edge during dorsal closure (Ducuing et al., 2015). Thus Jupiter is a useful marker to follow the leading edge identity.

The limitation in studying Jupiter function is that few tools are available. The only Jupiter antibody was developed by the Alain Debec's lab. This antibody works in western blots but not in immunofluorescence, neither in Alain Debec's nor in my

hands. In addition, the Jupiter locus is characterized by large introns but very close neighbouring genes. For instance Jupiter and its neighbouring gene CG14710 are only separated by 150 bp. For these reasons, generating a mutant at the beginning on my thesis was a failure. With the new generations of genome-editing strategies, Sakuma and colleagues generated Jupiter mutant lines by targeted the inserted GFP in Jupiter::GFP flies with the out-to-date TALEN strategy (Sakuma et al., 2013). However, despite my multiple and repeated demands, the Takashi Yamamoto lab has always been reluctant to share the putative Jupiter mutants lines.

Altogether, Jupiter is a microtubule-associated protein enriched at the leading edge during dorsal closure. It is therefore an excellent marker to mark the leading edge identity. We used it to understand the integration of JNK and DPP signals at the leading edge. However, because of several technical issues mentioned above, I did not pursue on investigating Jupiter function during dorsal closure.

V.2 JAGUAR, the Myosin VI homolog

Myosin VI belongs to the super-family of unconventional myosins. Myosin VI are actin-based motor proteins that move towards the minus end of actin filaments (Wells et al., 1999). As a member of unconventional myosin, Myosin VI head domain contains a motor domain, an ATP-binding and an actin-binding domain that allow the myosin to move. Mutation in the Myosin VI gene leads to deafness in Snell's Waltzer mice or to nonsyndromic dominant form of deafness (NSAD) in humans (Avraham et al., 1995; Avraham et al., 1997).

In *Drosophila*, *jaguar* (*jar*) encodes the uncoventional myosin VI, Myosin 95F (Castrillon et al., 1993; Hicks et al., 1999). Jaguar was originally discovered in a genetic screen using P-element mutagenesis to identify male-sterile mutants (Castrillon et al., 1993). Jaguar has then been reported to play a key role in sperm individualization in the *Drosophila* testis (Hicks et al., 1999). During sperm individualization, a syncytial membrane of 64 spermatids is remodelled to contain every individual sperm. Interestingly, Myosin VI colocalizes with the individualization complex, an actin complex that assembles at the spermatid heads at the beginning of sperm individualization (Hicks et al., 1999). Specifically, Jar and dynamin, a protein that allows endocytosis in eukaryotes, would function in parallel pathways to regulate actin dynamic during spermatogenesis (Rogat and Miller, 2002). In addition, *jar* is required for the accumulation of the Cortactin and the Arp2/3 complex that control actin polymerisation. Thus, it has been proposed that myosin VI stabilizes a branched actin network in cones to mediate the separation of the syncytial spermatids (Noguchi et al., 2006).

Jar is also crucial for both imaginal disc and ovary morphogeneis. In the ovary, *jar* is expressed in the border cells, which migrate from the nurse cells towards the anterior part of the ovocyte (Deng et al., 1999). Jar knock-down leads to both

abnormal follicle cell-shape and migration (Deng et al., 1999; Geisbrecht and Montell, 2002). Specifically, in border cells lacking Jar, both ß-catenin and E-Cahderin levels where reduced (Geisbrecht and Montell, 2002). Similarly, in cells lacking E-cadhrin or ß-catenin, Jar levels where reduced. The proposed model is that Jar would be required for border cell migration by stabilizing ß-catenin and E-cadherin (Geisbrecht and Montell, 2002). Last, *jar* knock-down during metamorphosis in imaginal discs leads to misshapen legs and wings (Deng et al., 1999).

Altogether jar was accumulates in regions where actin assembly is coupled to membrane dynamic, cell-shape changes and migration.

In the *Drosophila* embryo, Jar is enriched at the leading edge during dorsal closure (Millo et al., 2004; Ducuing et al., 2015). Mutations in the *jar* promoter (jar^{R39} and jar^{R235}) cause a loss of myosin VI expression and result in variable phenotypes. Many embryos complete closure but die before hatching. Some embryos present closure defects: the leading edge is not straight and the amnioserosa is detached from the leading edge. Last, some embryos fail to complete germ band-retraction. However, the precise quantification of the penetrance of the phenotype is not documented (Millo et al., 2004). In addition, expression of a dominant negative form of Jar lacking the ATP-binding site leads to various closure defects: some embryos initiate closure, but the zippering is incomplete. In addition, some embryos present amnioserosa / leading edge disruption (Millo et al., 2004). A null allele of *jar* (jar^{322}) has been reported to causes defects in neural fate determination since the asymmetric localization of Miranda is affected (Petritsch et al., 2003). This null allele would constitute the perfect tool to deeply analyse Jar contribution to dorsal closure. However, jar^{322} mutation has been shown to affect both *jar* and a neighbouring gene, *CG5706*, thus making the analysis complex (Morrison and Miller, 2008). Altogether, Jar is enriched at the leading edge during dorsal closure and is an excellent marker of

the leading edge identity. I did not pursue the analysis the of Jar function during dorsal closure since we did not have a clear null Jar mutant.

V.3 Z band alternatively spliced PDZ-motif containing protein 52

During my thesis, I worked extensively on *Z band alternatively spliced PDZ-motif containing protein 52* (*Zasp52*), a *Drosophila* member of the Alp/Enigma family. The Alp/Enigma family is conserved throughout evolution and encodes proteins that associate with the actin cytoskeleton (te Velthuis and Bagowski, 2007; Krcmery et al., 2010). Alp/Enigma family proteins are found in different systems in actin-rich complexes such as stress fibres, adherens junctions or in muscles (Zhou et al., 1999; Vallenius et al., 2000; Zhou et al., 2001; Torrado et al., 2004; Vallenius et al., 2004; Loughran et al., 2005; Jani and Schock, 2007).

These proteins have in common a PDZ domain at the N-terminus that directly binds to alpha-actinin. Second, they have at their C-terminus several LIM motifs that define Zinc-binding proteodomains (Michelsen et al., 1993) so they can associate to different transcription factors (Krcmery et al., 2010). Interestingly, some proteins of the Alp/Enigma family are able to travel from the cytoskeleton to the nucleus (Krcmery et al., 2010). In mammals, the Alp subfamily proteins contain a single PDZ motif and a single LIM domain. On the other hand, the Enigma proteins contain a signle PDZ motif and three LIM domains including Cypher, the mamalian Zasp homologs (Zhou et al., 1999).

In mammals Cypher/Zasp is expressed in both striated and cardiac muscles and binds to alpha-actinin-2 to stabilize Z-lines (Faulkner et al., 1999; Zhou et al., 1999; Zhou et al., 2001). Zasp knock-out mice display severe cardiomyopathies or congenital myopathies with defects in Z-line maintenance (Pashmforoush et al., 2001; Zhou et al., 2001). In addition, mutations in human Zasp leads to both myofibrillar

and cardio-vascular myopathies (Vatta et al., 2003; Arimura et al., 2004; Selcen and Engel, 2005), sometimes referred as 'Zaspopaties' (Lin et al., 2014). Zasp is therefore a crucial actin cytoskeleton network component present in highly specialized structures.

In *Drosophila*, Zasp52 is spliced into 13 different isoforms (Katzemich et al., 2011) and is expressed in both larval and adult muscles (Jani and Schock, 2007; Katzemich et al., 2011; Katzemich et al., 2013; Stronach, 2014). Zasp52 isoforms are composed of an N-terminal PDZ domain followed by a Zasp-like motif (ZM), and four LIM domains at the C-terminus (Stronach, 2014). Specifically, Zasp52 binds to alpha-actinin and genetically interacts with integrins (Jani and Schock, 2007). Interestingly, *Zasp*Δ, a Zasp52 null allele is larval lethal. *Zasp*Δ L1 larvae die because of defects in muscle attachment and sarcomeric organisation. Indeed, *Zasp*Δ mutant larvae do not form the Z-line properly, eventually leading to muscle disruption at the myotendinous junction during spontaneous muscle contractions at the end of embryogenesis (Jani and Schock, 2007).

In the *Drosophila* embryo, Zasp52 starts to accumulate at the leading edge at the beginning of germ-band retraction (Stage 12) and is highly expressed during dorsal closure (Jani and Schock, 2007; Ducuing et al., 2015). An elegant tool to asses Zasp52 function is the *Zasp52::GFP* line (a.k.a ZCL423), a GFP knock-in that recapitulates Zasp52 expression pattern during dorsal closure (Morin et al., 2001; Stronach, 2014; Ducuing et al., 2015). Interestingly, Zasp52::GFP is enriched at the leading edge and more importantly at the level of the actin cable.

Altogether, Zasp52 is an actin-associated protein conserved across species, and is required for the actin cytoskeleton organisation in many instances. During dorsal closure, Zasp52 is enriched at the leading edge and at the level of the actin cable. For these reasons, Zasp52 constituted another nice marker of the leading edge identity,

as well as a promising potential candidate gene that organises the actin cable. I therefore decided to focus on this gene.

RESULTS

1. A DPP-mediated feed-forward loop canalizes morphogenesis during *Drosophila* dorsal closure

1.1. The Article

I started this project in September 2012. Initially, Stéphane noticed that Jupiter::GFP was enriched at the leading edge where DPP is active during dorsal closure. I also noticed that Jupiter::GFP was enriched in the peripodial membrane of the wing imaginal disc (Fig. JCB_SUP1), where DPP is required for a cuboidal-to-squamous cell shape transition (McClure and Schubiger, 2005). Jupiter::GFP is therefore expressed in two tissues where DPP regulates morphogenesis. We thought at that time that Jupiter was a major DPP target controlling morphogenesis, hence bridging the gap between signalling and morphogenesis. I soon established that Jupiter::GFP leading edge expression requires DPP activity. Then, I spent quite some time trying to rescue the *tkv*$^{-}$, dorsal open phenotype by ectopically expressing Jupiter with a number of drivers, without being able to observe a clear rescue of the phenotype or the alignment of microtubules. Facing a dead end, we admitted that DPP was not only controlling Jupiter expression but also bother unknown targets. We then ectopically activated DPP pathway but we did not observe any ectopic accumulation of Jupiter. We thus reasoned that another factor was required for Jupiter::GFP expression. Since JNK pathway is also active at the leading edge, we hypothesised that Jupiter may require both JNK and DPP inputs. Hence we fell into the feed-forward hypothesis.

Published January 19, 2015

A DPP-mediated feed-forward loop canalizes morphogenesis during *Drosophila* dorsal closure

Antoine Ducuing,[1] Charlotte Keeley,[2] Bertrand Mollereau,[1] and Stéphane Vincent[1]

[1]Laboratory of Molecular Biology of the Cell, UMR5239, Ecole Normale Supérieure de Lyon, Centre National de la Recherche Scientifique, 69007 Lyon, France
[2]Department of Biological Engineering, Massachusetts Institute of Technology, Cambridge, MA 02139

Development is robust because nature has selected various mechanisms to buffer the deleterious effects of environmental and genetic variations to deliver phenotypic stability. Robustness relies on smart network motifs such as feed-forward loops (FFLs) that ensure the reliable interpretation of developmental signals. In this paper, we show that Decapentaplegic (DPP) and JNK form a coherent FFL that controls the specification and differentiation of leading edge cells during *Drosophila melanogaster* dorsal closure (DC). We provide molecular evidence that through repression by Brinker (Brk), the DPP branch of the FFL filters unwanted JNK activity. High-throughput live imaging revealed that this DPP/Brk branch is dispensable for DC under normal conditions but is required when embryos are subjected to thermal stress. Our results indicate that the wiring of DPP signaling buffers against environmental challenges and canalizes cell identity. We propose that the main function of DPP pathway during *Drosophila* DC is to ensure robust morphogenesis, a distinct function from its well-established ability to spread spatial information.

Introduction

Mechanisms that achieve robustness evolved to cope with environmental stress or genomic instability. This buffering process, known as canalization (Waddington, 1959), stores genotypic diversity and minimizes phenotypic plasticity (Paaby and Rockman, 2014). When canalization is overwhelmed, cryptic genetic variations are unleashed for natural selection to act upon (Rutherford and Lindquist, 1998; Rohner et al., 2013). A well-known biological network that conveys robustness is the feed-forward loop (FFL), in which molecule A controls the expression of a branch component B, and A and B together act on a common target (Milo et al., 2002; Mangan and Alon, 2003). FFLs control patterning both in the *Drosophila melanogaster* embryo (Xu et al., 2005), the wing imaginal disc (Zecca and Struhl, 2007), and in the developing eye (Tsuda et al., 2002). In addition, miRNAs have been shown to form FFLs that regulate canalization (Posadas and Carthew, 2014).

Dorsal closure (DC) in the *Drosophila* embryo provides an elegant system to study robustness: hundreds of leading edge (LE) cells differentiate and act in concert to seal the dorsal opening in a process reminiscent of wound healing (Martin and Parkhurst, 2004; Belacortu and Paricio, 2011). LE cells are polarized, display strong adherent junctions, accumulate a dense microtubule network, and produce a trans-cellular actomyosin cable and filopodia (Jacinto et al., 2000, 2002; Kaltschmidt et al., 2002; Jankovics and Brunner, 2006; Fernández et al., 2007; Millard and Martin, 2008; Solon et al., 2009). The closure dynamics are highly reproducible at a given temperature, indicating that DC is a robust and quantifiable process (Kiehart et al., 2000; Hutson et al., 2003).

Two major developmental pathways control DC: the stress response pathway JNK acts upstream and induces the bone morphogenetic protein homologue Decapentaplegic (DPP; Glise and Noselli, 1997; Hou et al., 1997; Kockel et al., 1997; Riesgo-Escovar and Hafen, 1997). These two signaling pathways are crucial for DC since embryos mutant for either JNK or DPP pathway components fail to close dorsally and exhibit a dorsal open phenotype (Affolter et al., 1994; Glise et al., 1995). However, how JNK and DPP contribute to DC and how the signals are integrated in a robust manner remain unclear (Riesgo-Escovar and Hafen, 1997; Martin and Parkhurst, 2004; Ríos-Barrera and Riesgo-Escovar, 2013).

Here we report that DPP and JNK are wired in a coherent FFL that controls LE cell identity and differentiation. At the

Correspondence to Stéphane Vincent: stephane.vincent11@ens-lyon.fr

Abbreviations used in this paper: ANOVA, analysis of variance; Brk, Brinker; DC, dorsal closure; DPP, Decapentaplegic; FFL, feed-forward loop; Jar, Jaguar; LE, leading edge; *tkv*, *thick veins*; UAS, upstream activation sequence.

© 2015 Ducuing et al. This article is distributed under the terms of an Attribution–Noncommercial–Share Alike–No Mirror Sites license for the first six months after the publication date (see http://www.rupress.org/terms). After six months it is available under a Creative Commons License (Attribution–Noncommercial–Share Alike 3.0 Unported license, as described at http://creativecommons.org/licenses/by-nc-sa/3.0/).

Supplemental Material can be found at:
http://jcb.rupress.org/content/suppl/2015/01/15/jcb.201410042.DC1.html

The Rockefeller University Press $30.00
J. Cell Biol. Vol. 208 No. 2 239–248
www.jcb.org/cgi/doi/10.1083/jcb.201410042

THE JOURNAL OF CELL BIOLOGY

Downloaded from jcb.rupress.org on June 12, 2015

Published January 19, 2015

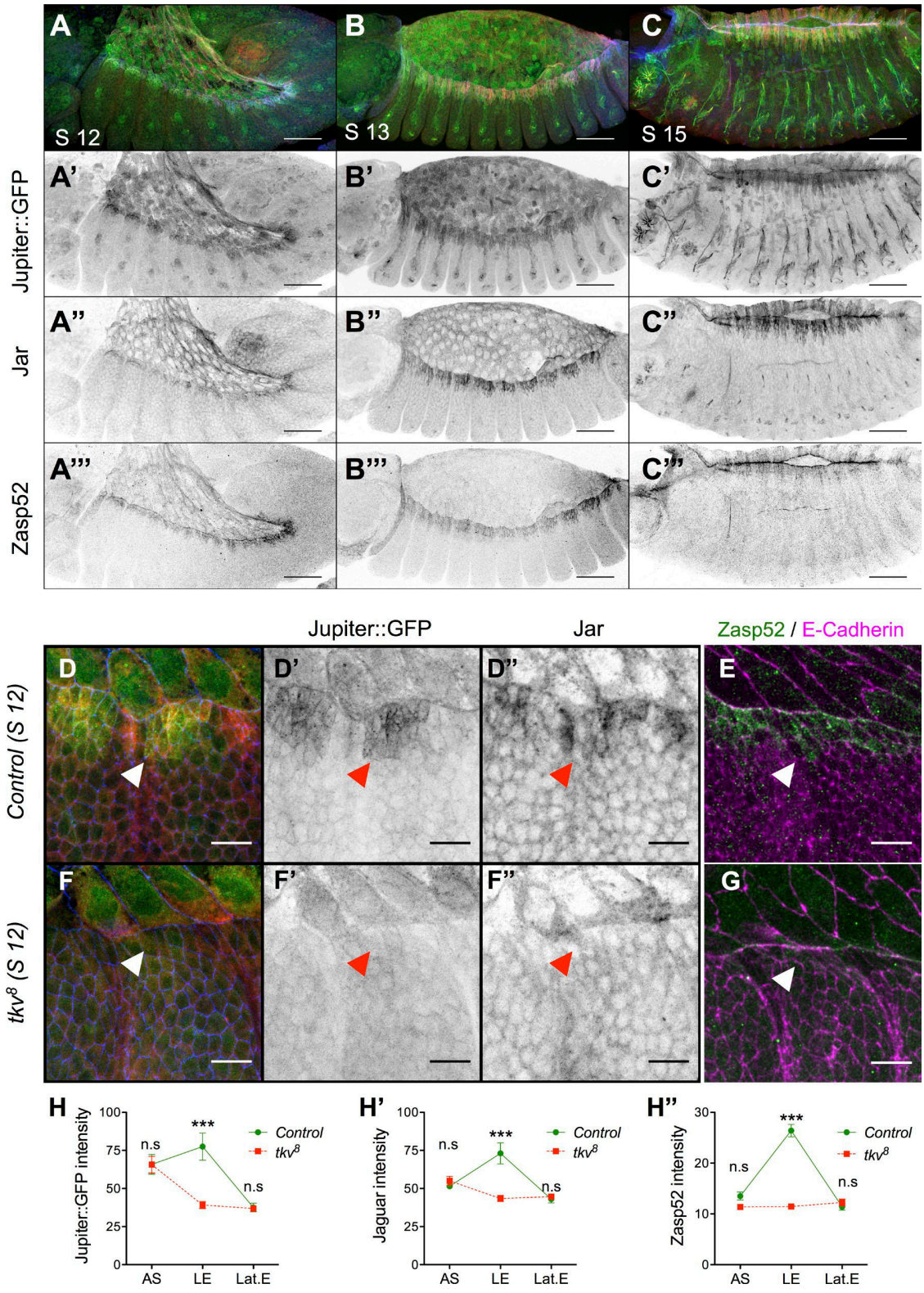

Figure 1. **DPP signaling is required for Jupiter, Jar, and Zasp52 LE expression during DC.** (A–C‴) Embryos at stage (S) 12 (A), 13 (B), and 15 (C) displaying Jupiter::GFP (green; gray in A′, B′, and C′), Jar (red; gray in A″, B″, and C″), and Zasp52 (blue; gray in A‴, B‴, and C‴). Bars, 50 µm. (D–G) Control (D and E) and tkv^8 (F and G) stage 12 embryos marked for Jupiter::GFP (green in D and F; gray in D′ and F′), Jar (red in D and F; gray in D″ and F″) and E-Cadherin (blue in D and F), or Zasp52 (green in E and G) and E-Cadherin (magenta in E and G). Bars, 10 µm. (H–H″) Plot profile of Jupiter::GFP ($n = 8$), Jar ($n = 8$), and Zasp52 ($n = 10$) intensity in control and tkv^8 embryos. AS, amnioserosa; LE, leading edge; Lat.E, lateral epidermis. (Two-way ANOVA and Bonferroni post-hoc test: ***, $P < 0.001$.) Accumulation of Jupiter::GFP, Jar, and Zasp52 at the LE is lost in tkv^- embryos (arrowheads). Error bars are means ± SEM.

Downloaded from jcb.rupress.org on June 12, 2015

Published January 19, 2015

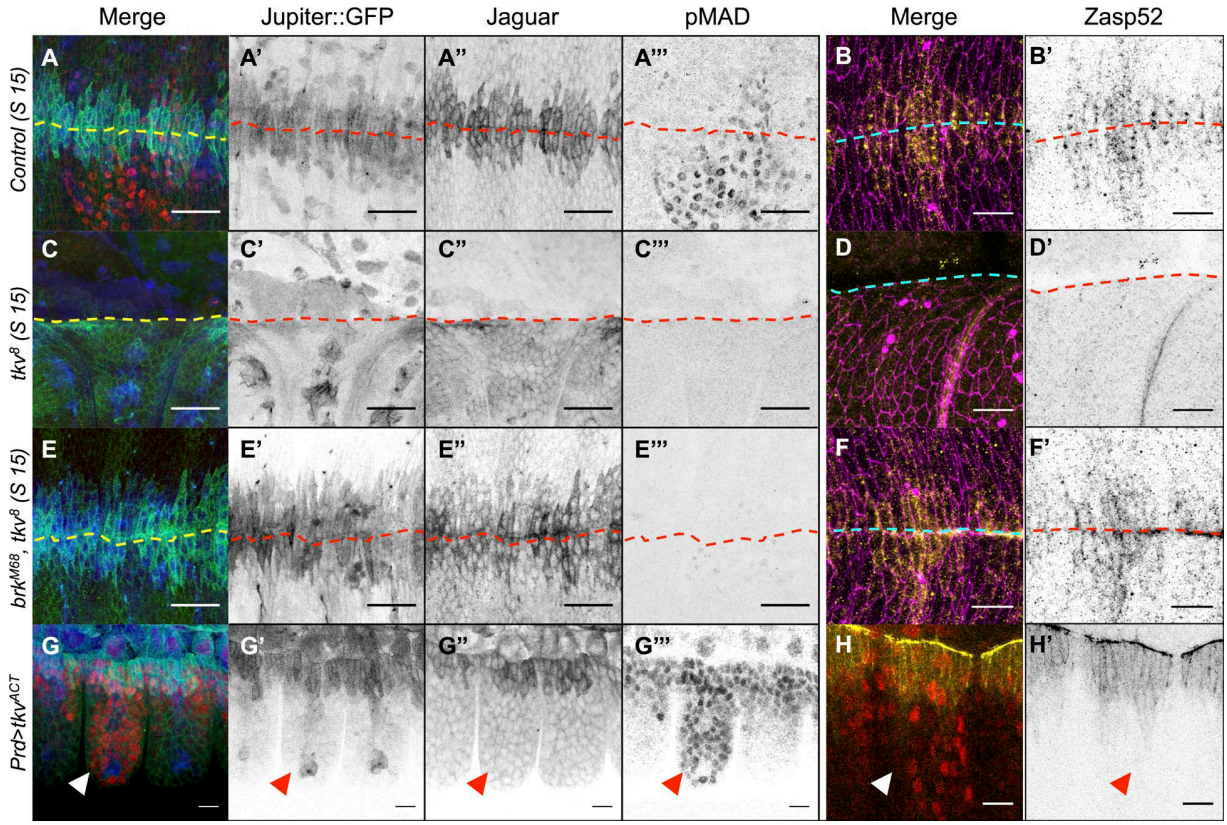

Figure 2. **DPP is required to derepress Jupiter, Jar, and Zasp52 but cannot induce them ectopically.** (A–F′) Control (A and B), tkv^{8} (C and D), and brk^{M68}, tkv^{8} (E and F) stage (S) 15 embryos marked for Jupiter::GFP (blue in A, C, and E; gray in A′, C′, and E′) Jar (green in A, C, and E; gray in A″, C″, and E″), phospho-Mad (pMad; red in in A, C, and E; gray in A‴, C‴, and E‴), Zasp52 (yellow in B, D, and F; gray in B′, D′, and F′), and E-Cadherin (magenta). The dashed lines delineate the midline. Accumulation of Jupiter::GFP, Jar, and Zasp52 at the LE is lost in tkv^{8} mutant embryos and restored in brk^{M68}, tkv^{8} embryos. (J and K) *Prd-Gal4*, *UAS-*tkv^{ACT} embryos marked for Jupiter::GFP (blue in G; gray in G′), Jar (green in G; gray in G″), phospho-Mad (red in G; gray in G‴), or Zasp52::GFP (yellow in H; gray in H′) and phospho-Mad (red). Ectopic activation of the DPP pathway does not lead to Jupiter, Jar, or Zasp52 accumulation (arrowheads). Bars, 10 µm.

mechanistic level, we provide evidence that derepression by the transcription factor Brk is sufficient to mediate DPP input. We show that the DPP/Brk indirect branch of the FFL does not pattern the LE but can filter unwanted JNK signaling so that the developmental JNK input remains preserved. Interestingly, although the DPP/Brk indirect branch of the FFL is dispensable for DC at 25°C, it is critical at 32°C. We propose that DPP function during DC is to ensure the robust interpretation of the positional information provided by JNK. By being wired into the FFL, DPP signaling acts as a filter rather than a positional signal and fosters the canalization of morphogenesis.

Results

DPP is required for Jupiter, Jaguar (Jar), and Zasp52 accumulation at the LE

We first analyzed three markers that display a strong accumulation at the LE during DC: the myosin VI homologue Jar (Kellerman and Miller, 1992), the microtubule binding molecule Jupiter (Morin et al., 2001; Karpova et al., 2006), and Zasp52, which promotes integrin-mediated adhesion (Morin et al., 2001; Jani and Schöck, 2007). To determine whether DPP signaling is required for their accumulation, we analyzed these three markers in embryos mutant for the DPP receptor *thick veins* (*tkv*) at stage 12, during which morphological defects are not yet detected. We observed that the LE accumulation of all three markers is lost in *tkv* mutant embryos compared with controls (Fig. 1, D–G; see Fig. 1, H–H″ for quantifications). Therefore, LE accumulation of all three targets requires DPP activity.

We next wondered how DPP mediates its effect on the markers. Indeed, DPP is known to induce two classes of targets that are both repressed by *brinker* (*brk*). Upon DPP action, Brk is transcriptionally repressed (Jaźwińska et al., 1999), leading to the induction of the first set of targets. The expression of the second set, however, requires the concomitant activation by the SMAD family of transcriptional activators (Affolter and Basler, 2007). Interestingly, loss of Brk is sufficient to rescue DC in the absence of pathway activation, suggesting that the DPP targets required for DC are expressed upon Brk derepression only (Marty et al., 2000). We hence tested whether removing Brk activity in the absence of DPP activation rescues Jar, Jupiter, and Zasp52 expression at the LE. To do so, we generated embryos double mutant for *brk* and *tkv*, to simultaneously disable DPP activation and prevent repression by Brk (Fig. S1 A). In these embryos, Jar, Jupiter, and Zasp52 expression is restored to wild type (Fig. 2, A–F′). In addition, *brk* overexpression represses

Downloaded from jcb.rupress.org on June 12, 2015

Published January 19, 2015

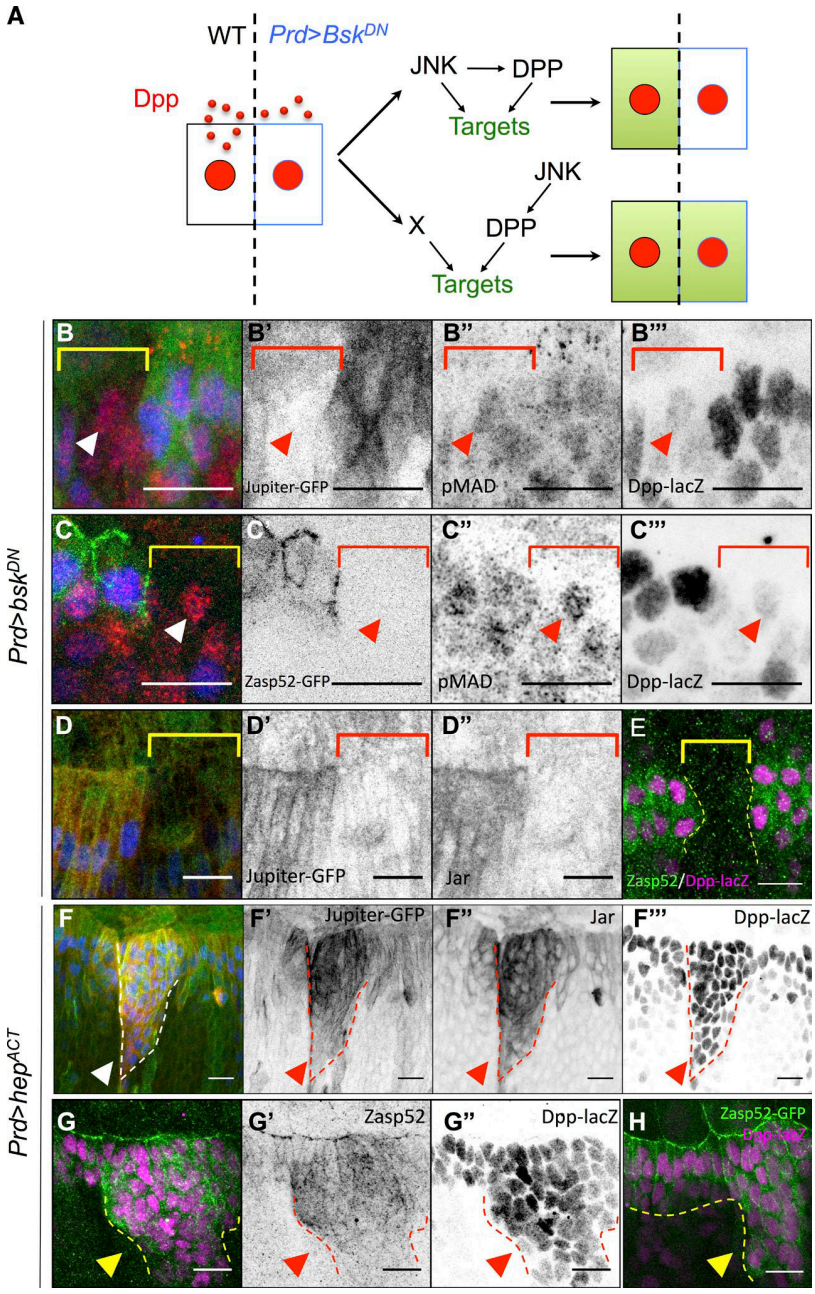

Figure 3. **JNK and DPP form a coherent FFL that regulates cell differentiation.** (A) Experimental design. The wild-type (WT) cell (black rectangle) secretes DPP (red dots) that induces its pathway in all cells (red nuclei). The absence of target (green) in the Prd>Bsk^{DN} cell abutting the wild-type cell indicates the presence of a JNK/DPP FFL. (B–C‴) *Prd-Gal4*, *UAS-bsk*^{DN}, *Dpp-lacZ* embryos marked for Jupiter::GFP (green in B; gray in B′) or Zasp52::GFP (green in C; gray in C′), phospho-Mad (red in B and C; gray in B″ and C″), and lacZ (blue in B and C; gray in B‴ and C‴). The brackets indicate the Bsk^{DN} domain, where *DPP-lacZ* (blue) is off. Anti–phospho-Mad (red) indicates that all cells receive DPP. Jupiter (B) and Zasp52 (C) in green are excluded from the Bsk^{DN} territory, even though DPP signaling is active (arrowheads), indicating that JNK acts also in parallel of DPP. (D–D″) *Prd-Gal4*, *UAS-bsk*^{DN}, *Dpp-lacZ* embryos marked for Jupiter::GFP (green in D; gray in D′) Jar (red in D; gray in D″) and lacZ (blue in D; gray in D‴). (E) *Prd-Gal4*, *UAS-bsk*^{DN}, *Dpp-lacZ* embryos marked for Zasp52::GFP and lacZ. All the markers are lost in the entire Bsk^{DN} territory (brackets in B–D or dotted lines in E). (F) *Prd-Gal4*, *UAS-hep*^{ACT}, *Dpp-lacZ*, *Jupiter::GFP* embryos marked for Jupiter::GFP (green in F; gray in F′), Jar (red in F; gray in F″), and lacZ (blue in F; gray in F‴). (G–H) *Prd-Gal4*, *UAS-hep*^{ACT}, *Dpp-lacZ* embryos marked for lacZ (magenta in G and H; gray in G″) and Zasp52 (green in G; gray in G′) or Zasp52::GFP (green in H). Ectopic JNK activity (dotted lines) induces Jar, Jupiter, and Zasp52 accumulation (arrowheads). Bars, 10 µm.

the three markers (Fig. S1, B–B‴). We conclude that repression of *brk* alone is sufficient for the accumulation of Jar, Jupiter, and Zasp52 at the LE.

DPP does not delineate Jupiter, Jar, and Zasp52 expression pattern

DPP is the best example of a secreted morphogen, a factor that patterns gene expression in a concentration-dependent manner (Nellen et al., 1996). In the wing imaginal disc, Brk activity dictates the boundaries of the DPP targets Salm and Omb, whose expression patterns expand in *brk*$^{-}$ clones (Jaźwińska et al., 1999). In contrast, at the LE, the expression patterns of Jar, Jupiter, and Zasp52 remain unchanged in *tkv brk* or *brk* embryos (Fig. 2, E–F′; and Fig. S1, C–H‴). In addition, the phospho-Mad pattern is broader than the Jupiter, Jar, and Zasp52 pattern, suggesting that, instead of delineating the boundaries of the expression of these targets, DPP may fulfill a function different from its well-established patterning activity (Fig. 2, G and H; Dorfman and Shilo, 2001). We further confirmed that ectopic activation of the DPP pathway in *paired* stripes fails to induce these targets outside the LE, indicating that DPP does not define the boundary of the expression patterns of the three markers during DC (Fig. 2, G–H′). What then, is the factor that limits their expression pattern, and what is the biological significance of DPP control of Jar, Jupiter, and Zasp52?

Downloaded from jcb.rupress.org on June 12, 2015

Published January 19, 2015

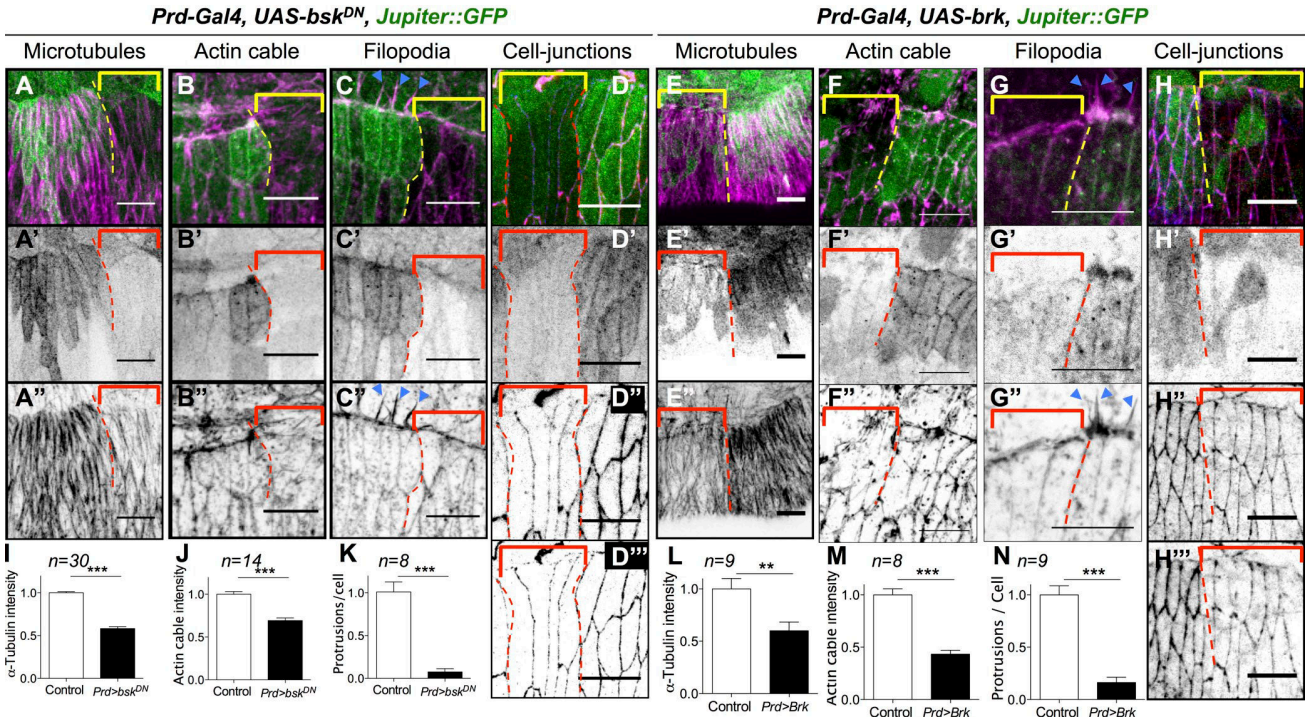

Figure 4. **Cytoskeletal components crucial for DC are also regulated by the JNK/DPP FFL.** (A–H‴) *Prd-Gal4, UAS-bsk*^{DN}*, Jupiter::GFP* embryos (A–D″) and *Prd-Gal4, UAS-brk, Jupiter::GFP* (E–H‴) marked for Jupiter::GFP (green in all panels; gray in A′–H′), α-tubulin (magenta in A and E; gray in A″ and E″) or actin (magenta in B, C, F, and G; gray in B″, C″, F″, and G″), or β-catenin (red in D and H; gray in D″ and H″) and E-Cadherin (blue in D and H; gray in D‴ and H‴). In all panels, the Bsk^{DN} or the Brk overexpression territory is marked by the absence of Jupiter::GFP (brackets), and the border between the wild-type and the Bsk^{DN} or Brk overexpression territory is delineated by the dotted lines. (I–N) Quantification of microtubule intensity, actin cable intensity, and filopodia numbers. Error bars: ±SEM (for all panels, Mann–Whitney's *U* test: **, $P < 0.01$; ***, $P < 0.001$). *bsk*^{DN} or *brk* overexpression affects microtubules, β-catenin, and DE-Cadherin accumulation as well as actin cable formation at the LE and filopodia (arrowheads in C″ and G″). Bars, 10 µm.

JNK and DPP are wired into a coherent FFL that controls LE cell differentiation

JNK acts upstream of DPP and determines LE identity (Glise and Noselli, 1997; Hou et al., 1997; Kockel et al., 1997; Riesgo-Escovar and Hafen, 1997). To test whether JNK activates the targets in parallel to DPP, we expressed a dominant-negative form of the JNK homologue *basket* (*bsk*) in *paired* stripes so that cells in the *paired* domain are deficient for JNK signaling but still receive DPP from their wild-type neighbors by diffusion (Fig. 3 A). We reasoned that if the expression of the markers does not require JNK activity in parallel to DPP, the markers should remain expressed in the cells in which JNK is affected as long as they receive DPP. We found that DPP produced by the neighboring cells efficiently induces Mad phosphorylation in the *paired* domain, yet the targets are not expressed (Fig. 3, B–E). Therefore, JNK acts both upstream and in parallel to DPP to control Jar, Jupiter, and Zasp52. To confirm that JNK directs the pattern of Jar, Jupiter, and Zasp52, we induced ectopic JNK signaling in paired stripes and used DPP-lacZ as a reporter of JNK activity. All the cells in which DPP-lacZ is induced also express Jar, Jupiter, and Zasp52 (Fig. 3, F–H). These observations indicate that JNK and DPP form a coherent FFL, in which JNK induces DPP, and both signals are absolutely required for target gene expression.

We next asked whether the FFL controls LE cell differentiation. We selectively inactivated in *paired* stripes, either JNK by using *bsk*^{DN} (Fig. 4, A–D‴) or DPP input by overexpressing *brk* (Fig. 4, E–H‴) and analyzed microtubule polarization, actomyosin cable, filopodia formation, and junctional integrity. Impairing either JNK or DPP signal affects the hallmarks of LE cell differentiation: First, microtubules fail to polarize and to accumulate (Fig. 4, A″ and E″). Second, filopodia and the actomyosin cable are absent (Fig. 4, B″, C″, F″, and G″). Last, both E-Cadherin and β-catenin expression are reduced, indicating weaker adhesion (Fig. 4, D″, D‴, H″, and H‴; see Fig. 4, I–N for quantifications). We conclude that both branches of the FFL are absolutely required for LE cell differentiation and morphogenesis.

A prediction of this model is that ectopic JNK, but not ectopic DPP, should redirect lateral cells to the LE cell identity and path of differentiation. We tested this prediction by inducing either JNK activity or DPP signaling in stripes (Fig. 5, A–D″ and E–H″, respectively). As expected for an FFL, ectopic JNK induces ectopic accumulation of microtubules (Fig. 5, A–A″) and actin (Fig. 5, B–B″) as well as E-Cadherin and β-catenin (Fig. 5, C–D″). Conversely, ectopic activation of the DPP pathway has no effect on microtubules, actin, E-Cadherin, or β-catenin accumulation (Fig. 5, E–H″). Altogether, these data indicate that we identified a novel FFL that plays a pivotal role in LE cells specification and differentiation.

Downloaded from jcb.rupress.org on June 12, 2015

Published January 19, 2015

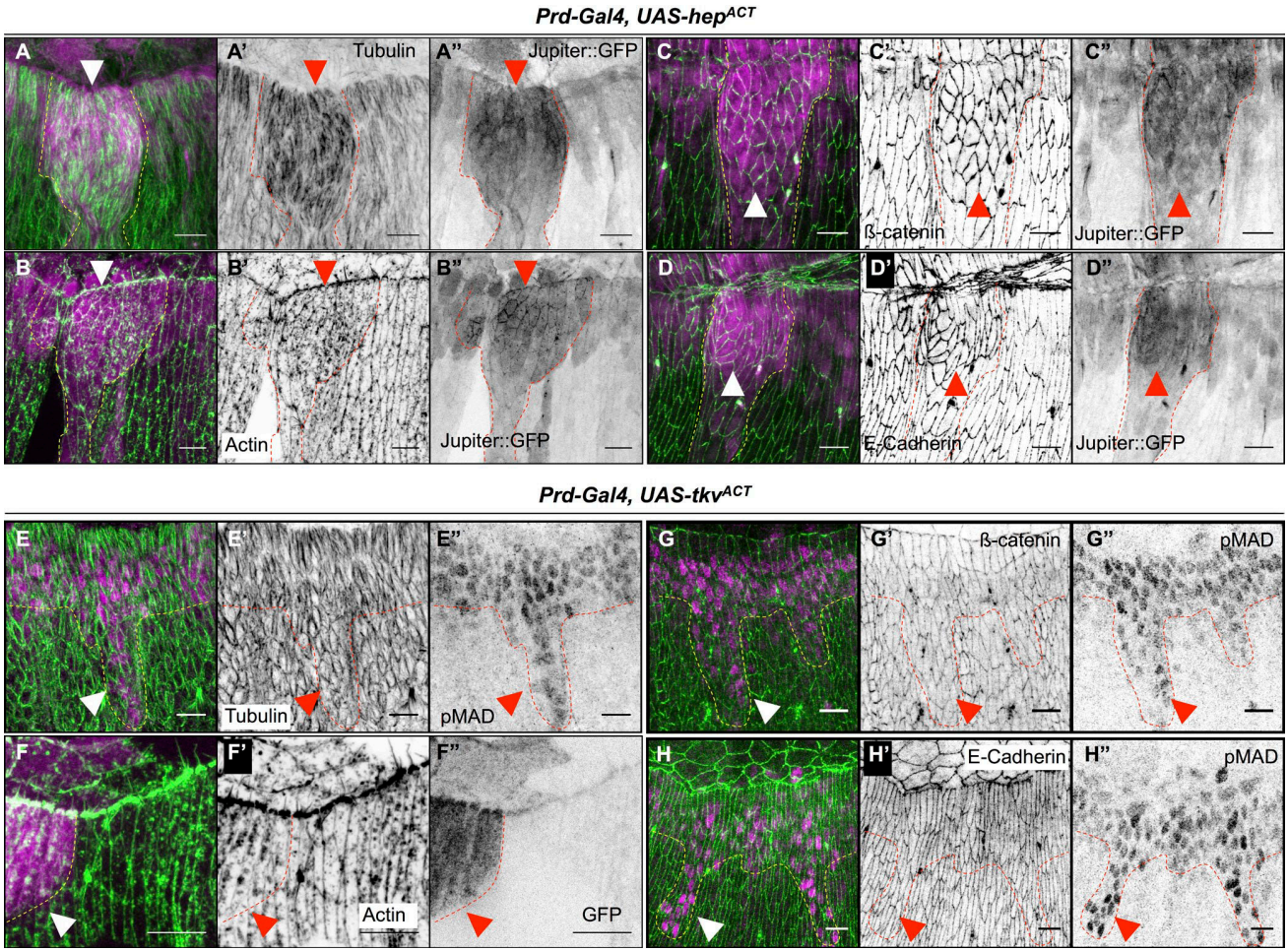

Figure 5. **Ectopic JNK but not ectopic DPP activity leads to accumulation of cytoskeletal components crucial for DC.** (A–D″) *Prd-Gal4, UAS-hep*^{ACT}, *Jupiter::GFP* embryos marked for Jupiter::GFP (magenta in A–D; gray in A″–D″) and α-tubulin (green in A; gray in A′) or actin (green in B; gray in B′), β-catenin (green in C; gray in C′), or DE-Cadherin (green in D; gray in D′). In all panels, the ectopic JNK activity is marked by the ectopic accumulation of Jupiter::GFP (arrowheads) and is delineated by dotted lines. Ectopic JNK signaling leads to accumulation of microtubules, β-catenin, DE-Cadherin, and actin. (E–E″) *Prd-Gal4, UAS-tkv*^{ACT} embryo stained for phospho-Mad (magenta in E; gray in E″) and α-tubulin (green in E; gray in E′). (F–F″) *Prd-Gal4, UAS-tkv*^{ACT}, *UAS-GFP* embryos marked for GFP (magenta in F; gray in F″) and actin (green in F; gray in F′). (G–H″) *Prd-Gal4, UAS-tkv*^{ACT} embryos stained for phospho-Mad (pMad; magenta in G and H; gray in G″ and H″) and β-catenin (green in G; gray in G′) or E-Cadherin (green in H; gray in H′). In all panels, the ectopic DPP activity is marked by either ectopic phospho-Mad nuclei or the presence of GFP (arrowheads) and is delineated by dotted lines. Ectopic DPP signaling activity does not lead to any accumulation of microtubules, β-catenin, E-Cadherin, or actin. Bars, 10 µm.

The JNK/DPP FFL can filter unwanted JNK signaling

FFLs can act as filters of short bursts of signaling (Milo et al., 2002; Mangan and Alon, 2003), which are random noises that make biological processes error prone if unchecked. In this paradigm, signaling robustness is achieved in that the synchrony between the two branches of the FFL is absolutely required for a response to occur. If the direct signal switches off before the indirect signal fires, no response can be elicited. We reasoned that in the JNK/DPP FFL, *brk*-mediated repression is the sentinel that prevents unwanted JNK activity from specifying ectopic LE identity. To test this hypothesis, we needed to first produce a source of ectopic JNK signal that is nonuniform and subsequently verify whether the FFL can indeed filter out such unwanted JNK activity to canalize LE identity. A previous study and our observations indicate that *puc* mutant embryos display a salt-and-pepper pattern of ectopic JNK activation throughout the lateral epidermis, suggesting the presence of nonuniform, ectopic JNK signal that varies in strength (Martín-Blanco et al., 1998). To test whether the FFL can filter the ectopic JNK signal in *puc* embryos, we generated *puc brk* double mutants and found that the ectopic Jar expression and the morphological defects are magnified compared with *puc* single mutants, suggesting that more cells respond erroneously to the action of the unwanted JNK signal when the FFL is disabled (Fig. 6, A–D). A critical aspect of the FFL is that the filtering ability depends on the delay between the activation of the direct and the indirect branch: any signal shorter than the delay is filtered out. We reasoned that the uneven JNK activity pattern reflects signal duration and could provide us with a nice system to test whether transient and robust JNK inputs are discriminated by the FFL: weak Jun staining corresponds to short accumulation of Jun and reveals transient signaling; strong Jun staining corresponds to an accumulation of Jun synthesis over

Downloaded from jcb.rupress.org on June 12, 2015

Published January 19, 2015

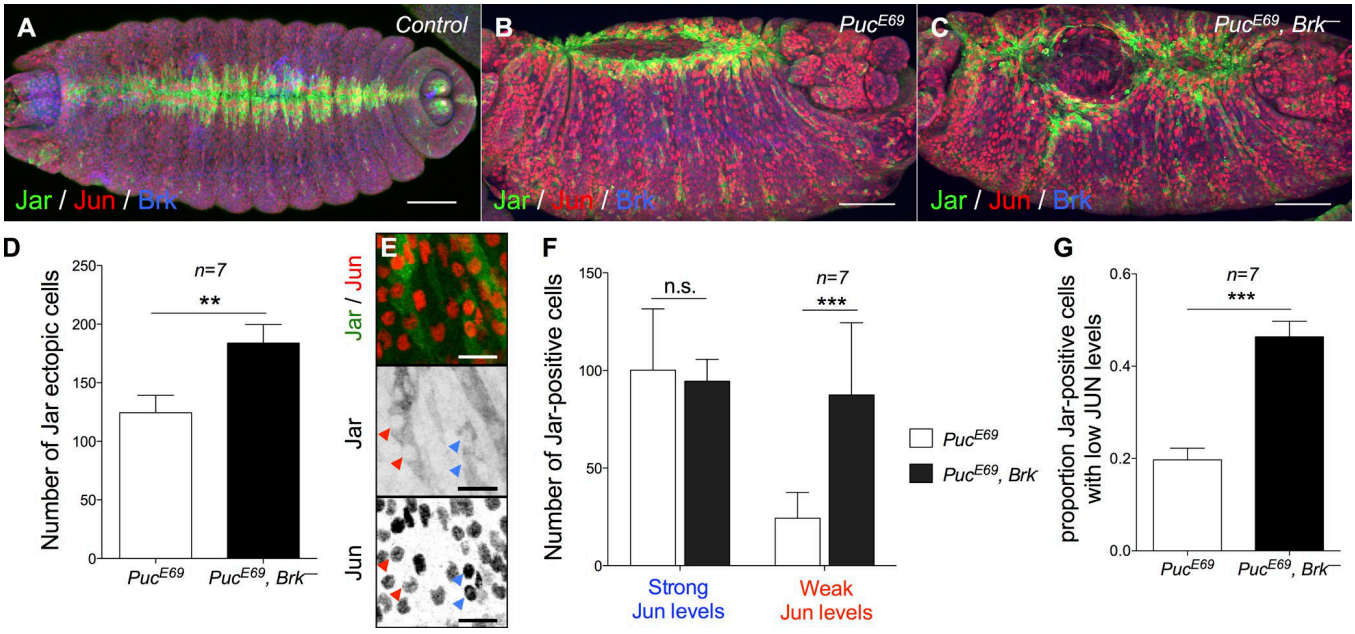

Figure 6. **The JNK/DPP FFL filters weak ectopic JNK activity.** (A–C) Control (A), Puc^{E69} (B), and Puc^{E69}, brk^{M68} (C) stage 15 embryos stained for Jar, Jun, and Brk. Bars, 50 µm. (D) Quantification of Jar ectopic cells in the lateral epidermis. ($n = 7$; Mann–Whitney's U test: **, $P < 0.01$.) Error bars: ±SEM. (E) Close-up of the lateral epidermis of a Puc^{E69} embryo showing weak (red arrowheads) or strong (blue arrowheads) Jun expression. Bars, 10 µm. (F and G) Quantification of Jar expression in cells expressing low or high Jun levels in Puc^{E69} versus Puc^{E69}, brk^{M68} embryos. (F: two-way ANOVA and Bonferroni post-hoc test: ***, $P < 0.001$; G: Mann–Whitney's U test: ***, $P < 0.001$.) Error bars: ±SEM. Brk represses Jar in about two thirds of the cells displaying weak Jun expression.

time and indicates robust signaling. We therefore compared Jar induction in cells displaying robust and weak Jun staining: although Brk activity does not modify Jar induction by robust ectopic JNK signaling, a cell that receives weak JNK signaling is ∼2.5 times more likely to wrongfully express Jar in a *brk* mutant (Fig. 6, E–G). We conclude that the FFL buffers weak ectopic JNK signaling to prevent the ectopic differentiation of lateral cells into LE cells.

The JNK/DPP FFL canalizes DC

Having confirmed that the FFL filters unwanted JNK noise, we sought to test whether the indirect branch of the FFL canalizes morphogenesis in the presence of environmental perturbations. We compared how wild-type or FFL-deficient (brk^{-}) embryos cope with thermal stress, a classical assay for robustness in *Drosophila* (Perry et al., 2010). At 25°C, *brk* mutants show wild-type Jar and Zasp52 expression and microtubule accumulation (Fig. 7, A–F). In contrast, *brk* mutants raised at 32°C display cells that ectopically express Jar and Zasp52 and accumulate microtubules, indicating that they differentiate into LE cells erroneously (Fig. 7, G–M; and Fig. S2, A–M). Therefore, *brk* canalizes LE specification by counteracting the deleterious effects of environmental stress. Next, we quantified DC dynamics in *brk* mutants at 32°C. Although closure speed is undistinguishable between wild-type and *brk* embryos at 25°C, a 1-h delay is recorded in *brk* at 32°C compared with wild type (Fig. 7, N and N′; Fig. S3; and Videos 1 and 2). Hence, *brk* activity renders embryonic morphogenesis more resilient to environmental challenge. Altogether, our data indicate that during DC, the DPP-mediated FFL canalizes LE identity to foster DC robustness (Fig. 8).

Discussion

We present a novel mechanism that weaves two classic signaling pathways into an FFL to canalize morphogenesis. This FFL is coherent as both JNK and DPP act positively and belong to the "and" type, as either signal alone does not trigger a response. Both experimental and computational evidence indicate that the general function of the indirect branch of a coherent FFL is to filter the input received by the direct branch (Mangan and Alon, 2003). Here, we find that during DC, patterning information is given by JNK, and the DPP/Brk branch filters this spatial information. In the presence of ectopic JNK generated by *puckered* loss of function, Brk filters out unwanted JNK signaling in two thirds of the cells displaying weak, but not strong, JNK activation. This is a prediction of the FFL model in which the network filters out only short bursts of signal and not longer, more robust signaling events. Interestingly, under normal laboratory conditions, at 25°C, Brk activity is not required for DC to proceed normally; LE markers are patterned correctly, and the dynamics of DC are nearly wild-type. Conversely, when embryos are subjected to thermal stress, at 32°C, Brk becomes critical to prevent the presence of ectopic LE cells in the lateral epidermis and to ensure proper closure dynamics. These observations provide strong evidence to support that DPP function during DC is to provide robustness to the system: under difficult conditions, phenotypic variation remains minimal, and cell identity remains canalized.

miRNAs are major players in the canalization of cell decisions in the face of environmental challenges (Posadas and Carthew, 2014): mir-7 stabilizes gene expression and allows the correct determination of sensory organs in flies subjected to temperature fluctuations (Li et al., 2009). miRNAs are

Downloaded from jcb.rupress.org on June 12, 2015

Published January 19, 2015

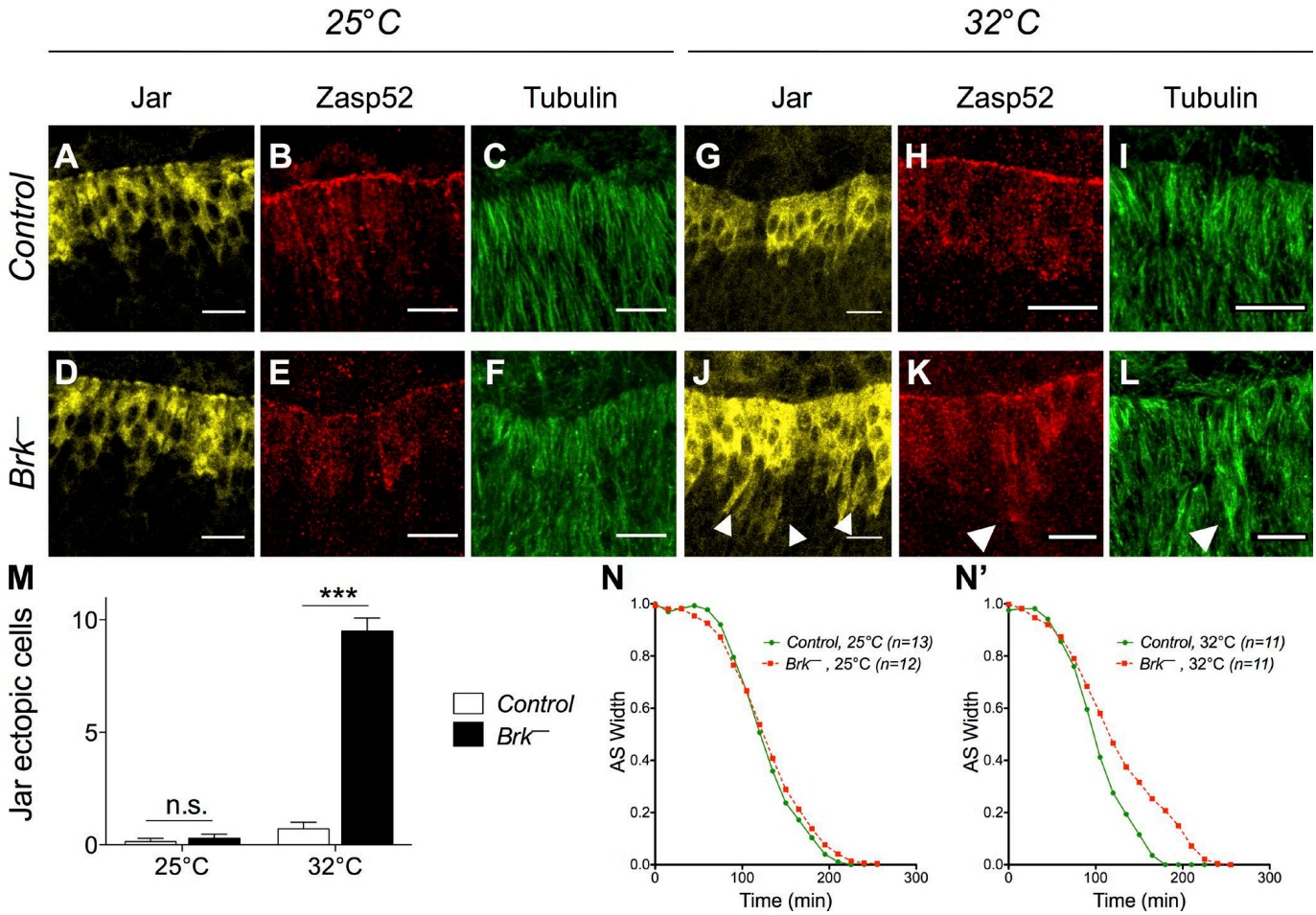

Figure 7. **The JNK/DPP FFL canalizes LE specification and fosters DC robustness.** (A–L) Control (top) and brk^{M68} (bottom) embryos at 25°C (left) or 32°C (right) marked for Jar (yellow), Zasp52 (red), and Tubulin (green). Ectopic Jar, Zasp52, and microtubule accumulations are detected only in brk^{M68} embryos at 32°C (arrowheads). Bars, 10 µm. (M) Quantification of Jar ectopic cells in control and brk^{M68} embryos at 25°C or 32°C. Only brk^{M68} embryos at 32°C exhibit Jar ectopic cells. $n \geq 7$. Two-way ANOVA and Bonferroni post-hoc test: ***, $P < 0.001$. (N and N') Width of the dorsal opening measured over time of control and brk^{M68} embryos imaged at 25°C or 32°C. Only brk^{M68} embryos at 32°C exhibit slower closure dynamics.

posttranscriptional regulators that produce moderate but rapid effects on gene expression. This rapid action appears to have favored their recruitment into network motifs dedicated to tune gene expression in a prompt manner: a transcription factor controls the miRNA and both together control a common target, forming an FFL. The major difference between miRNA and DPP-mediated FFL is the time scale: compared with the swift-acting miRNAs, DPP needs to be translated, secreted, reach a threshold to activate its pathway, to finally repress *brk* transcription. The prediction is that DPP-mediated FFL filters JNK inputs that are on a long time scale: DPP would not only filter out JNK noise but could also filter out authentic JNK signaling that is important for nonpatterning functions. JNK is the main messenger of stress, and mechanisms must exist to distinguish stress-related and development-related JNK inputs within a given cell. This would explain why *brk* mutants close normally in favorable conditions. Environmental perturbations such as temperature excess are bound to have pleiotropic effects on biological systems. The FFL appears as the generic remedy to enforce robustness at several levels. Factors acting at specific kinetics form the indirect branches of FFLs adapted to specific needs: miRNAs cancel noise, and DPP ensures the proper interpretation of JNK signaling.

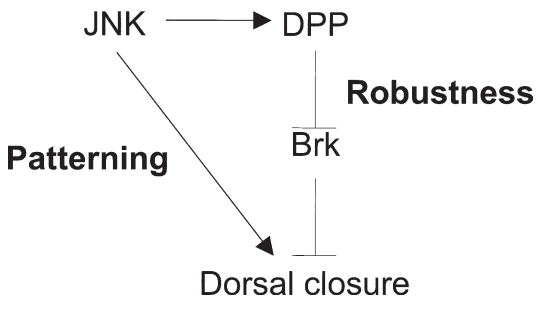

Figure 8. **Model of JNK and DPP wiring during DC.** JNK and DPP form a coherent FFL that ensures a canalized and robust DC.

DPP is one of the main architects of fly development and as such fulfills many functions during embryogenesis: DPP specifies dorsal tissues, including the amnioserosa early and the dorsal epidermis at midembryogenesis (Ferguson and Anderson, 1992; Xu et al., 2005) and also directs dorsal tracheal migration (Vincent et al., 1997). At stage 5, DPP induces *zerknüllt*, and both DPP and Zerknüllt control the amnioserosa-specific gene *Race*, thus forming a coherent FFL (Xu et al., 2005). In addition,

Downloaded from jcb.rupress.org on June 12, 2015

Published January 19, 2015

DPP also controls the spatial distribution of targets such as *Ush-aped*, in both the dorsal epidermis and the amnioserosa (Lada et al., 2012). This regulation is important for the interaction between these two tissues that is critical for DC. Recently, a study reported how DPP can protect from JNK-induced apoptosis in the dorsal epidermis (Beira et al., 2014). They show that the DPP pathway repressor Schnurri directly represses the pro-apoptotic gene *reaper*. Therefore, JNK fails to induce *reaper* expression or apoptosis in the *pannier* domain. This indicates that JNK and DPP signaling pathways are reiteratively integrated during *Drosophila* embryogenesis. To get a full picture of this network, we will also need to integrate the two negative feedback loops mediated by Puc and scarface that dampen JNK activity (Martín-Blanco et al., 1998; Rousset et al., 2010). A likely possibility is that these feedback loops improve fidelity in signaling. Altogether, the dorsal epidermis provides an elegant model system to understand how different inputs are integrated to modulate cell decisions during development. Although some of these functions are paramount to cell specification, we show that some, such as the JNK/DPP FFL, can also counteract deleterious environmental stimuli and canalize development, a function distinct from DPP well-established, non–cell-autonomous patterning activity.

Materials and methods

Fly strains and genetics

We used the following lines: Canton-S (wild type), tkv^{8} (amorphic allele; Bloomington Stock Center [BL] 34509), Brk^{M68} (loss-of-function allele, see Jaźwińska et al., 1999), gift from M. Affolter (University of Basel, Basel, Switzerland), Puc^{E69} (loss-of-function allele, see Martín-Blanco et al., 1998), *Prd-Gal4* (BL 1947), upstream activation sequence (*UAS*)–tkv^{ACT} (BL 36537), gift from M. Grammont (Université de Lyon, Lyon, France), *UAS-*bsk^{DN} (BL 6409), *UAS-*hep^{ACT} (BL 9306), *UAS-brk* (*brk* coding sequence under the control of a promoter containing UAS sequence), gift from J. de Celis (Centro de Biología Molecular "Severo Ochoa," Madrid, Spain), *UAS-*GFP^{NLS} (BL 4776), *Jupiter::GFP* (GFP knock-in; BL 6836), Zasp52::GFP (GFP knock-in; BL 6838), and *DPP-*$lacZ^{NUCLEAR}$ (lacZ-NLS coding sequence cloned after the *BS 3.0* promoter of DPP, see Blackman et al., 1991). Unless otherwise indicated, all crosses were performed at 25°C.

Immunofluorescence and quantification

We used standard techniques of immunohistofluorescence as described in Ducuing et al. (2013). Embryos were dechorionated with bleach, fixed in a 1:1 mix of 4% PFA–heptane. Embryos were subsequently devitellinized by replacing the 4% PFA with methanol. Samples were incubated with primary antibodies, with fluorescent-coupled secondary antibodies and mounted in Vectashield.

We used the following primary antibodies: rabbit anti-lacZ (1:1,000; Cappel), mouse anti-lacZ (1:250; G4644; Sigma-Aldrich), guinea pig anti-Brk (1:500; gift from G. Morata, Centro de Biología Molecular "Severo Ochoa," Madrid, Spain), mouse anti-Jar 3C7 (1:100; Kellerman and Miller, 1992), rabbit anti-pMad (1:1,500; gift from P. ten Dijke, Leids Universitair Medisch, Leiden, Netherlands), rat anti–DE-Cadherin (1:333; Developmental Studies Hybridoma Bank [DSHB]), mouse anti-Armadillo (1:250; DSHB), mouse anti–α-tubulin (1:1,000; T6199; Sigma-Aldrich), rabbit anti-Jun (1:10; Santa Cruz Biotechnology, Inc.), and rabbit anti-Zasp52 (1:400; gift from F. Schöck, McGill university, Montreal, Quebec). For Brk, pMad, Jar, and Zasp52, antigen was a full-length protein. Secondary antibodies are from Invitrogen and were used at 1:500. We used the following secondary antibodies: Alexa Fluor donkey anti–mouse 488, Alexa Fluor goat anti–mouse 633, Alexa Fluor goat anti–rat 546, Alexa Fluor donkey anti–rabbit 488, Alexa Fluor goat anti–rabbit 546, and Alexa Fluor goat anti–guinea pig 488. For 32°C experiments, embryos where first grown at 25°C and then shifted for 4 h at 32°C and immediately fixed after.

Phalloidin staining

Embryos were dechorionated with bleach and fixed in a 1:1 mix of 4% PFA–heptane. After PFA removal, embryos were stuck on double-sided tape, immerged in 0.1% Triton X-100 and PBS with Rhodamine Phalloidin (1:500; Sigma-Aldrich), and hand devitellinized with a needle. Devitellinized embryos were quickly rinsed twice with 0.1% Triton X-100 and PBS and mounted in Vectashield.

Image processing

Images were acquired on the acousto-optical beam splitter confocal laser-scanning microscope (SP5; Leica) with the following objectives: HC Plan Fluotar 20×, 0.5 multi-immersion (numerical aperture: 0.7), HCX Plan Apochromat 40× 1.25–0.75 oil (numerical aperture: 1.25), and HCX Plan Apochromat 63× 1.4–0.6 oil (numerical aperture: 1.4) using the acquisition software LAS AF (Leica) at the PLATIM imaging facility and analyzed with ImageJ (National Institutes of Health). Unless otherwise indicated, all images are projections of confocal sections.

Live imaging

Unless otherwise indicated, all crosses were performed at 25°C. Stage 10 or 11 embryos were staged and aligned in Halocarbon oil 27 (Sigma-Aldrich) and then imaged at 25°C or 32°C with a spinning disk (Leica), with a 20× dry objective (numerical aperture: 0.4) and a camera (iXon3; Andor Technology) using the acquisition software MetaMorph (Molecular Devices). brk^{M68}*/FM7* females were crossed with *Jupiter::GFP* males. In addition, *wild-type* females were crossed with *Jupiter::GFP* males as controls. *Brk* mutant embryos were identified by the absence of spontaneous movements at stage 17 and confirmed by the absence of hatching. For every sample, the length and width over time were normalized with the maximal length or maximal width, respectively.

Quantification and statistical analyses

We used the Prism software (GraphPad Software) to generate graphs. For Figs. 1, 4, 6, and 7 M, bar graphs represent means ± SEM. For Figs. 7 (N and N') and S4, graphs represent the mean. Mann–Whitney's *U* test was used to determine significant differences for Figs. 4 and 6 (D and G). For Figs. 1 (H–H"), 6 F, and 7 M, we used a two-way analysis of variance (ANOVA) followed by a Bonferroni post-hoc test. **, $P < 0.01$; ***, $P < 0.001$.

Online supplemental material

Fig. S1 describes the experimental strategy used to determine whether the three targets belong to the derepressed only or to the derepressed and induced class of DPP targets as well as the effects of the overexpression and the loss of function on the targets' expression. Fig. S2 reports the effects of temperature on *brk* mutants. Fig. S3 displays the analysis of the dynamics of DCs in *brk* mutants at 25°C and 32°C. Video 1 is a live recording of the closure of embryos representative of the controls and *brk* mutants we analyzed at 25°C. Video 2 is a live recording of the closure of embryos representative of the controls and *brk* mutants we analyzed at 32°C. Online supplemental material is available at http://www.jcb.org/cgi/content/full/jcb.201410042/DC1.

We thank the DROSO-TOOLS and PLATIM facilities of the UMS3444 and Bloomington and the Developmental Studies Hybridoma Bank for reagents. We thank Dali MA for the critical reading of this manuscript and Markus Affolter, Uri Alon, and Arezki Boudaoud for discussions.

This work was supported by a Chair from the Centre National de la Recherche Scientifique to S. Vincent.

The authors declare no competing financial interests.

Submitted: 10 October 2014
Accepted: 9 December 2014

References

Affolter, M., and K. Basler. 2007. The Decapentaplegic morphogen gradient: from pattern formation to growth regulation. *Nat. Rev. Genet.* 8:663–674. http://dx.doi.org/10.1038/nrg2166

Affolter, M., D. Nellen, U. Nussbaumer, and K. Basler. 1994. Multiple requirements for the receptor serine/threonine kinase thick veins reveal novel functions of TGF β homologs during *Drosophila* embryogenesis. *Development.* 120:3105–3117.

Beira, J.V., A. Springhorn, S. Gunther, L. Hufnagel, G. Pyrowolakis, and J.P. Vincent. 2014. The Dpp/TGFβ-dependent corepressor schnurri protects

Downloaded from jcb.rupress.org on June 12, 2015

Published January 19, 2015

epithelial cells from JNK-induced apoptosis in *Drosophila* embryos. *Dev. Cell*. 31:240–247. http://dx.doi.org/10.1016/j.devcel.2014.08.015

Belacortu, Y., and N. Paricio. 2011. *Drosophila* as a model of wound healing and tissue regeneration in vertebrates. *Dev. Dyn.* 240:2379–2404. http://dx.doi.org/10.1002/dvdy.22753

Blackman, R.K., M. Sanicola, L.A. Raftery, T. Gillevet, and W.M. Gelbart. 1991. An extensive 3′ cis-regulatory region directs the imaginal disk expression of decapentaplegic, a member of the TGF-β family in *Drosophila. Development*. 111:657–666.

Dorfman, R., and B.Z. Shilo. 2001. Biphasic activation of the BMP pathway patterns the *Drosophila* embryonic dorsal region. *Development*. 128: 965–972.

Ducuing, A., B. Mollereau, J.D. Axelrod, and S. Vincent. 2013. Absolute requirement of cholesterol binding for Hedgehog gradient formation in *Drosophila. Biol. Open*. 2:596–604. http://dx.doi.org/10.1242/bio.20134952

Ferguson, E.L., and K.V. Anderson. 1992. Decapentaplegic acts as a morphogen to organize dorsal-ventral pattern in the *Drosophila* embryo. *Cell*. 71:451–461. http://dx.doi.org/10.1016/0092-8674(92)90514-D

Fernández, B.G., A.M. Arias, and A. Jacinto. 2007. Dpp signalling orchestrates dorsal closure by regulating cell shape changes both in the amnioserosa and in the epidermis. *Mech. Dev.* 124:884–897. http://dx.doi.org/10.1016/j.mod.2007.09.002

Glise, B., and S. Noselli. 1997. Coupling of Jun amino-terminal kinase and Decapentaplegic signaling pathways in *Drosophila* morphogenesis. *Genes Dev.* 11:1738–1747. http://dx.doi.org/10.1101/gad.11.13.1738

Glise, B., H. Bourbon, and S. Noselli. 1995. *hemipterous* encodes a novel *Drosophila* MAP kinase kinase, required for epithelial cell sheet movement. *Cell*. 83:451–461. http://dx.doi.org/10.1016/0092-8674(95)90123-X

Hou, X.S., E.S. Goldstein, and N. Perrimon. 1997. *Drosophila* Jun relays the Jun amino-terminal kinase signal transduction pathway to the Decapentaplegic signal transduction pathway in regulating epithelial cell sheet movement. *Genes Dev.* 11:1728–1737. http://dx.doi.org/10.1101/gad.11.13.1728

Hutson, M.S., Y. Tokutake, M.S. Chang, J.W. Bloor, S. Venakides, D.P. Kiehart, and G.S. Edwards. 2003. Forces for morphogenesis investigated with laser microsurgery and quantitative modeling. *Science*. 300:145–149. http://dx.doi.org/10.1126/science.1079552

Jacinto, A., W. Wood, T. Balayo, M. Turmaine, A. Martinez-Arias, and P. Martin. 2000. Dynamic actin-based epithelial adhesion and cell matching during *Drosophila* dorsal closure. *Curr. Biol.* 10:1420–1426. http://dx.doi.org/10.1016/S0960-9822(00)00796-X

Jacinto, A., W. Wood, S. Woolner, C. Hiley, L. Turner, C. Wilson, A. Martinez-Arias, and P. Martin. 2002. Dynamic analysis of actin cable function during *Drosophila* dorsal closure. *Curr. Biol.* 12:1245–1250. http://dx.doi.org/10.1016/S0960-9822(02)00955-7

Jani, K., and F. Schöck. 2007. Zasp is required for the assembly of functional integrin adhesion sites. *J. Cell Biol.* 179:1583–1597. http://dx.doi.org/10.1083/jcb.200707045

Jankovics, F., and D. Brunner. 2006. Transiently reorganized microtubules are essential for zippering during dorsal closure in *Drosophila melanogaster*. *Dev. Cell*. 11:375–385. http://dx.doi.org/10.1016/j.devcel.2006.07.014

Jaźwińska, A., N. Kirov, E. Wieschaus, S. Roth, and C. Rushlow. 1999. The *Drosophila* gene brinker reveals a novel mechanism of Dpp target gene regulation. *Cell*. 96:563–573. http://dx.doi.org/10.1016/S0092-8674(00)80660-1

Kaltschmidt, J.A., N. Lawrence, V. Morel, T. Balayo, B.G. Fernández, A. Pelissier, A. Jacinto, and A. Martinez Arias. 2002. Planar polarity and actin dynamics in the epidermis of *Drosophila*. *Nat. Cell Biol.* 4:937–944. http://dx.doi.org/10.1038/ncb882

Karpova, N., Y. Bobinnec, S. Fouix, P. Huitorel, and A. Debec. 2006. Jupiter, a new *Drosophila* protein associated with microtubules. *Cell Motil. Cytoskeleton*. 63:301–312. http://dx.doi.org/10.1002/cm.20124

Kellerman, K.A., and K.G. Miller. 1992. An unconventional myosin heavy chain gene from *Drosophila melanogaster*. *J. Cell Biol.* 119:823–834. http://dx.doi.org/10.1083/jcb.119.4.823

Kiehart, D.P., C.G. Galbraith, K.A. Edwards, W.L. Rickoll, and R.A. Montague. 2000. Multiple forces contribute to cell sheet morphogenesis for dorsal closure in *Drosophila*. *J. Cell Biol.* 149:471–490. http://dx.doi.org/10.1083/jcb.149.2.471

Kockel, L., J. Zeitlinger, L.M. Staszewski, M. Mlodzik, and D. Bohmann. 1997. Jun in *Drosophila* development: redundant and nonredundant functions and regulation by two MAPK signal transduction pathways. *Genes Dev.* 11:1748–1758. http://dx.doi.org/10.1101/gad.11.13.1748

Lada, K., N. Gorfinkiel, and A. Martinez Arias. 2012. Interactions between the amnioserosa and the epidermis revealed by the function of the u-shaped gene. *Biol. Open*. 1:353–361. http://dx.doi.org/10.1242/bio.2012497

Li, X., J.J. Cassidy, C.A. Reinke, S. Fischboeck, and R.W. Carthew. 2009. A microRNA imparts robustness against environmental fluctuation during development. *Cell*. 137:273–282. http://dx.doi.org/10.1016/j.cell.2009.01.058

Mangan, S., and U. Alon. 2003. Structure and function of the feed-forward loop network motif. *Proc. Natl. Acad. Sci. USA*. 100:11980–11985. http://dx.doi.org/10.1073/pnas.2133841100

Martin, P., and S.M. Parkhurst. 2004. Parallels between tissue repair and embryo morphogenesis. *Development*. 131:3021–3034. http://dx.doi.org/10.1242/dev.01253

Martín-Blanco, E., A. Gampel, J. Ring, K. Virdee, N. Kirov, A.M. Tolkovsky, and A. Martinez-Arias. 1998. *puckered* encodes a phosphatase that mediates a feedback loop regulating JNK activity during dorsal closure in *Drosophila*. *Genes Dev.* 12:557–570. http://dx.doi.org/10.1101/gad.12.4.557

Marty, T., B. Müller, K. Basler, and M. Affolter. 2000. Schnurri mediates Dpp-dependent repression of brinker transcription. *Nat. Cell Biol.* 2:745–749. http://dx.doi.org/10.1038/35036383

Millard, T.H., and P. Martin. 2008. Dynamic analysis of filopodial interactions during the zippering phase of *Drosophila* dorsal closure. *Development*. 135:621–626. http://dx.doi.org/10.1242/dev.014001

Milo, R., S. Shen-Orr, S. Itzkovitz, N. Kashtan, D. Chklovskii, and U. Alon. 2002. Network motifs: simple building blocks of complex networks. *Science*. 298:824–827. http://dx.doi.org/10.1126/science.298.5594.824

Morin, X., R. Daneman, M. Zavortink, and W. Chia. 2001. A protein trap strategy to detect GFP-tagged proteins expressed from their endogenous loci in *Drosophila*. *Proc. Natl. Acad. Sci. USA*. 98:15050–15055. http://dx.doi.org/10.1073/pnas.261408198

Nellen, D., R. Burke, G. Struhl, and K. Basler. 1996. Direct and long-range action of a DPP morphogen gradient. *Cell*. 85:357–368. http://dx.doi.org/10.1016/S0092-8674(00)81114-9

Paaby, A.B., and M.V. Rockman. 2014. Cryptic genetic variation: evolution's hidden substrate. *Nat. Rev. Genet.* 15:247–258. http://dx.doi.org/10.1038/nrg3688

Perry, M.W., A.N. Boettiger, J.P. Bothma, and M. Levine. 2010. Shadow enhancers foster robustness of *Drosophila* gastrulation. *Curr. Biol.* 20: 1562–1567. http://dx.doi.org/10.1016/j.cub.2010.07.043

Posadas, D.M., and R.W. Carthew. 2014. MicroRNAs and their roles in developmental canalization. *Curr. Opin. Genet. Dev.* 27:1–6. http://dx.doi.org/10.1016/j.gde.2014.03.005

Riesgo-Escovar, J.R., and E. Hafen. 1997. *Drosophila* Jun kinase regulates expression of decapentaplegic via the ETS-domain protein Aop and the AP-1 transcription factor DJun during dorsal closure. *Genes Dev.* 11:1717–1727. http://dx.doi.org/10.1101/gad.11.13.1717

Ríos-Barrera, L.D., and J.R. Riesgo-Escovar. 2013. Regulating cell morphogenesis: the *Drosophila* Jun N-terminal kinase pathway. *Genesis*. 51:147–162. http://dx.doi.org/10.1002/dvg.22354

Rohner, N., D.F. Jarosz, J.E. Kowalko, M. Yoshizawa, W.R. Jeffery, R.L. Borowsky, S. Lindquist, and C.J. Tabin. 2013. Cryptic variation in morphological evolution: HSP90 as a capacitor for loss of eyes in cavefish. *Science*. 342:1372–1375. http://dx.doi.org/10.1126/science.1240276

Rousset, R., S. Bono-Lauriol, M. Gettings, M. Suzanne, P. Spéder, and S. Noselli. 2010. The *Drosophila* serine protease homologue Scarface regulates JNK signalling in a negative-feedback loop during epithelial morphogenesis. *Development*. 137:2177–2186. http://dx.doi.org/10.1242/dev.050781

Rutherford, S.L., and S. Lindquist. 1998. Hsp90 as a capacitor for morphological evolution. *Nature*. 396:336–342. http://dx.doi.org/10.1038/24550

Solon, J., A. Kaya-Copur, J. Colombelli, and D. Brunner. 2009. Pulsed forces timed by a ratchet-like mechanism drive directed tissue movement during dorsal closure. *Cell*. 137:1331–1342. http://dx.doi.org/10.1016/j.cell.2009.03.050

Tsuda, L., R. Nagaraj, S.L. Zipursky, and U. Banerjee. 2002. An EGFR/Ebi/Sno pathway promotes delta expression by inactivating Su(H)/SMRTER repression during inductive notch signaling. *Cell*. 110:625–637. http://dx.doi.org/10.1016/S0092-8674(02)00875-9

Vincent, S., E. Ruberte, N.C. Grieder, C.K. Chen, T. Haerry, R. Schuh, and M. Affolter. 1997. DPP controls tracheal cell migration along the dorsoventral body axis of the *Drosophila* embryo. *Development*. 124:2741–2750.

Waddington, C.H. 1959. Canalization of development and genetic assimilation of acquired characters. *Nature*. 183:1654–1655. http://dx.doi.org/10.1038/1831654a0

Xu, M., N. Kirov, and C. Rushlow. 2005. Peak levels of BMP in the *Drosophila* embryo control target genes by a feed-forward mechanism. *Development*. 132:1637–1647. http://dx.doi.org/10.1242/dev.01722

Zecca, M., and G. Struhl. 2007. Recruitment of cells into the *Drosophila* wing primordium by a feed-forward circuit of vestigial autoregulation. *Development*. 134:3001–3010. http://dx.doi.org/10.1242/dev.006411

Downloaded from jcb.rupress.org on June 12, 2015

Ducuing et al., http://www.jcb.org/cgi/content/full/jcb.201410042/DC1

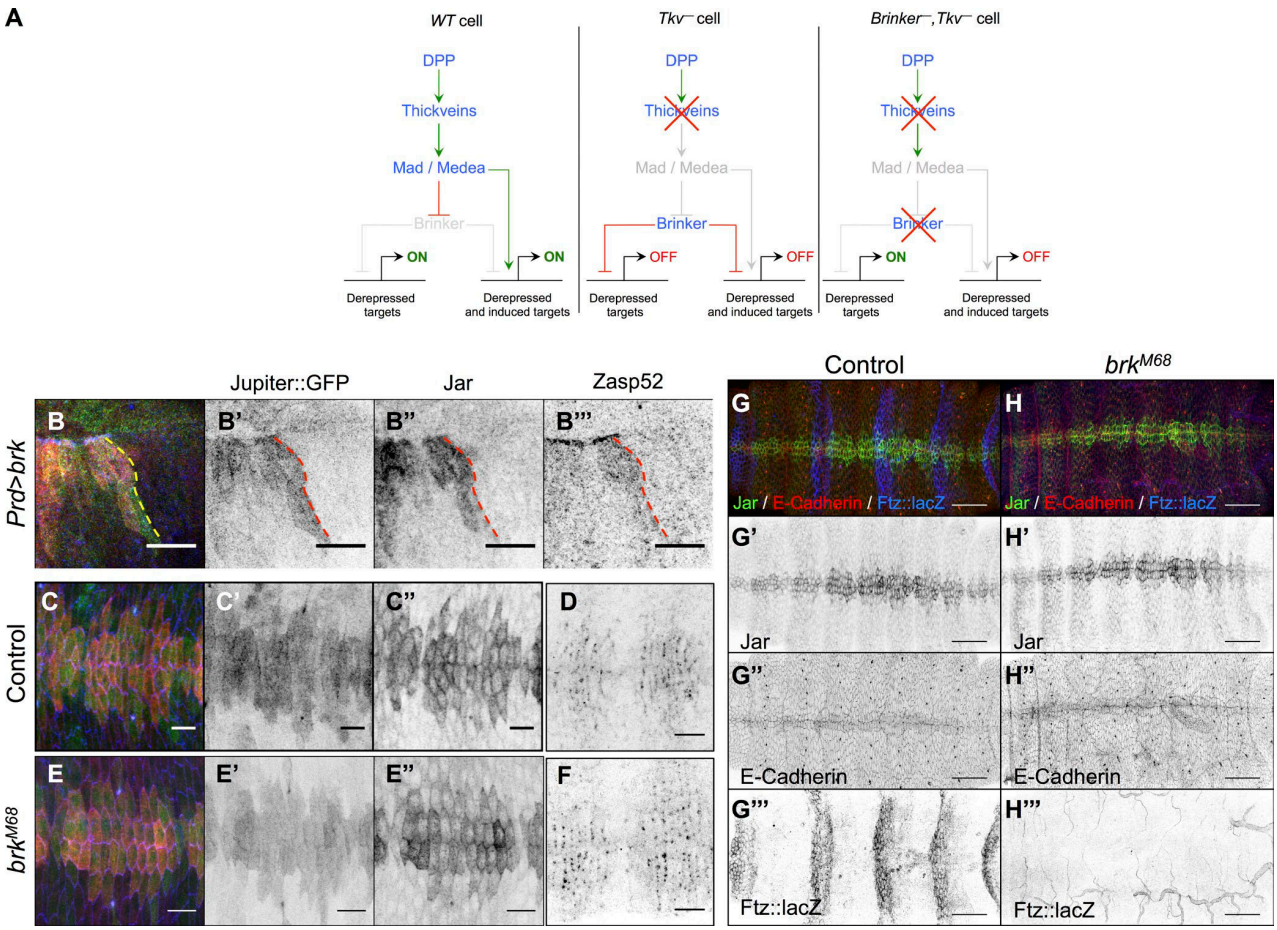

Figure S1. **Effects of Brk loss of function and overexpression on Jupiter, Jar, and Zasp52.** (A) Experimental strategy. As indicated on the figure, DPP pathway has two sets of targets: targets that only require Brk repression (derepressed targets) and targets that required Brk repression and subsequent activation by the Mad–Medea complex (derepressed and induced targets). In *brk*⁻, *tkv*⁻ double mutant embryos, only derepressed targets are restored. (B–B″) *Prd-Gal4*, *UAS-brk*, *Jupiter::GFP* embryos marked for Jupiter::GFP (green in B; gray in B′), Jar (red in B; gray in B″), and Zasp52 (blue in B; gray in B‴). Brk overexpression leads to a decrease of Jupiter::GFP, Jar, and Zaps52 expression. (C–H‴) Control (C, D, and G) and brk^{M68} (E, F, and H) embryos marked for Jupiter::GFP (green in C and E; gray in C′ and E′), Jar (red in C and E; gray in C″ and E″), and E-Cadherin (blue in C and E) or Zasp52 (gray in D and F) or for Jar (gray in G′ and H′), E-Cadherin (gray in G″ and H″), and Ftz (fushi tarazu)-lacZ to detect the balancer chromosome (blue in G and H; gray in G‴ and H‴). The Jupiter::GFP, Jar, and Zasp52 expression pattern is similar in both control and brk^{M68} embryos. Bars, 10 µm. WT, wild type.

THE JOURNAL OF CELL BIOLOGY

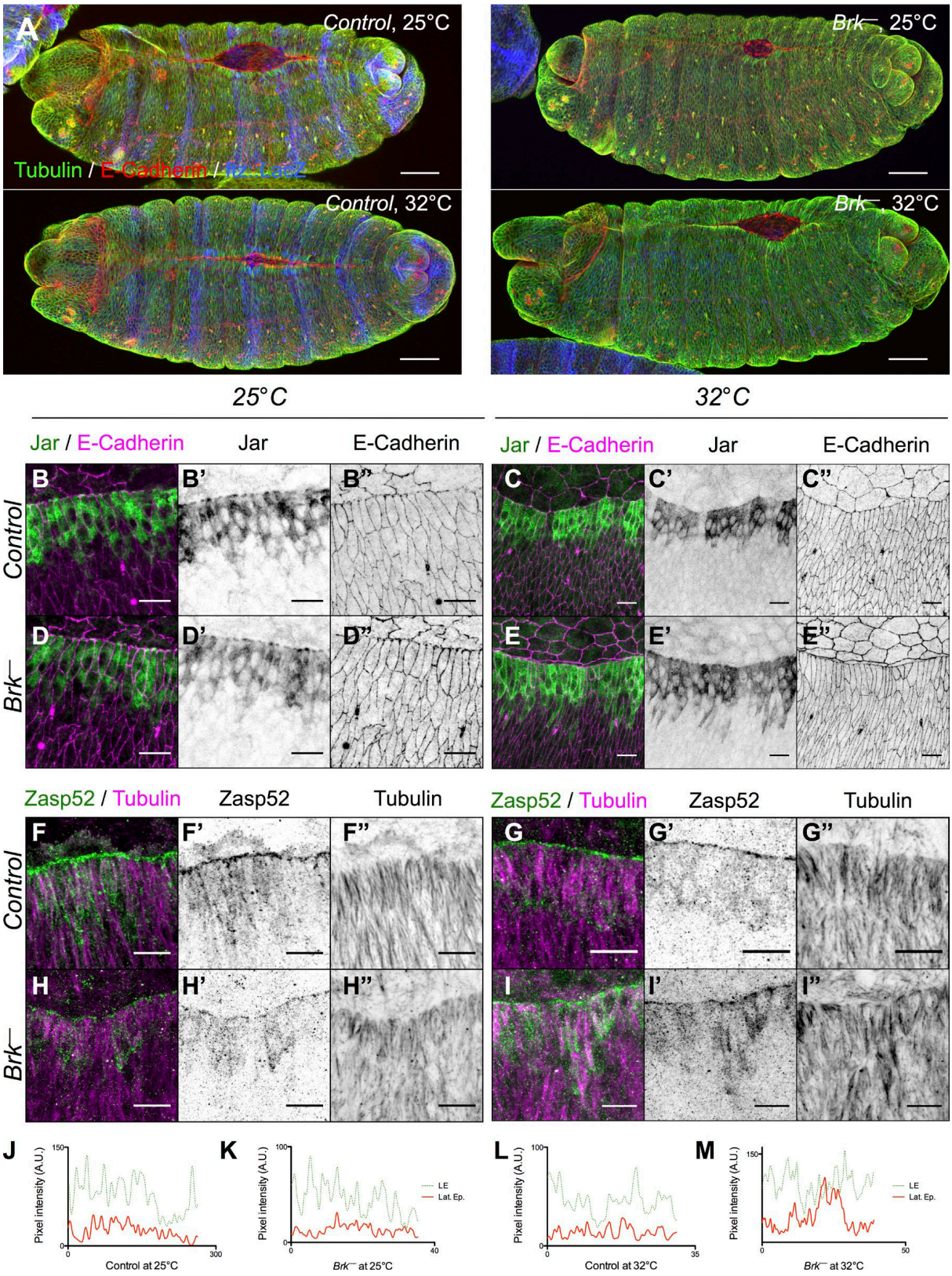

Figure S2. **Extended data of Fig. 7 (A–L).** (A) Control and *brk*^{M68} mutant embryos at 25°C or 32°C and stained for tubulin, cadherin, and lacZ. Bars, 50 µm. *Brk*^{M68} embryos exhibit closure and head involution defects only at 32°C. (B–E″) Control and *brk*$^{-}$ embryos at 25°C or 32°C marked for Jar (gray in B′–E′) and E-Cadherin (gray in B″–E″). (F–I″) *Control* and *brk*$^{-}$ embryos at 25°C or 32°C marked for Zasp52 (gray in F′–I′) and Tubulin (gray in F″–I″). Bars, 10 µm. At 25°C *control* and *brk*$^{-}$ embryos have similar expression pattern. Only *brk*^{M68} embryos at 32°C display ectopic Jar, Zasp52, and microtubule accumulation. (J–M) Zasp52 pixel intensity at the leading edge (LE) or in the lateral epidermis (Lat. Ep.) using the ImageJ plot profile function of the corresponding control (J and L) or *brk*^{M68} (K and M) embryos at 25°C (J and K) or 32°C (L and M). Only *brk*$^{-}$ embryos at 32°C exhibit ectopic Zasp52 in the lateral epidermis that reaches Zasp52 LE levels. A.U., arbitrary unit.

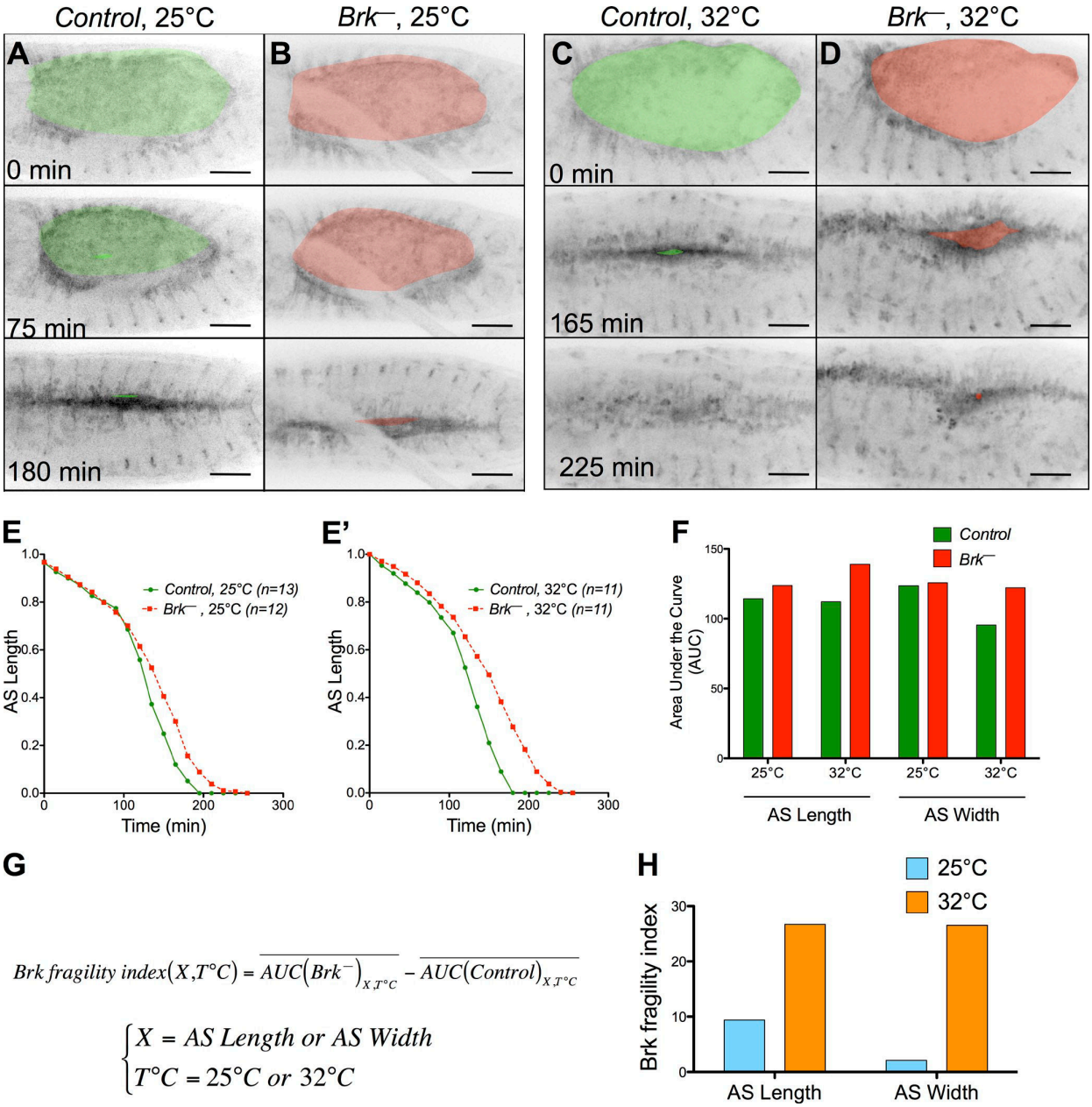

Figure S3. **Extended data of Fig. 7 (N and N').** (A–D) Still image of *Jupiter::GFP/+* (A and C) and *brk*^{M68}, *Jupiter::GFP/+* (C and D) embryos imaged at 25°C or 32°C. Bars, 50 µm. See also Videos 1 and 2. (E and E') Dorsal opening length over time. Only *brk*^{M68} embryos at 32°C exhibit slower closure dynamics. AS, amnioserosa. (F) Area under the curve of dorsal opening length and width graphs. (G) Brk fragility index defined as the difference of the mean Area Under the Curve (AUC) of *brk*$^{-}$ minus the mean Area Under the Curve of *control* for a given temperature. (H) Brk fragility index. At 32°C, *brk*$^{-}$ embryo robustness is much more affected than at 25°C.

1.2. Additional figures not included in the paper

Figure JCB_Sup1. Jupiter::GFP expression in the wing disc.

Top: Anaglyph image of a wing imaginal disc marked with Cadherin (top sections only to show the peripodial membrane). Cells delimited by the orange dotted lines are the ones that undergo a DPP-dependent cuboidal-to-squamous cells-shape transition (McClure and Schubiger, 2005). Botom: Wing disc marked for Jupiter::GFP, Phalloidin and Dpp-lacZ^{NUC} (Blackman et al., 1991). Jupiter::GFP accumulates in the peripodial cells undergoing the transition that are marked with Dpp-lacZ.

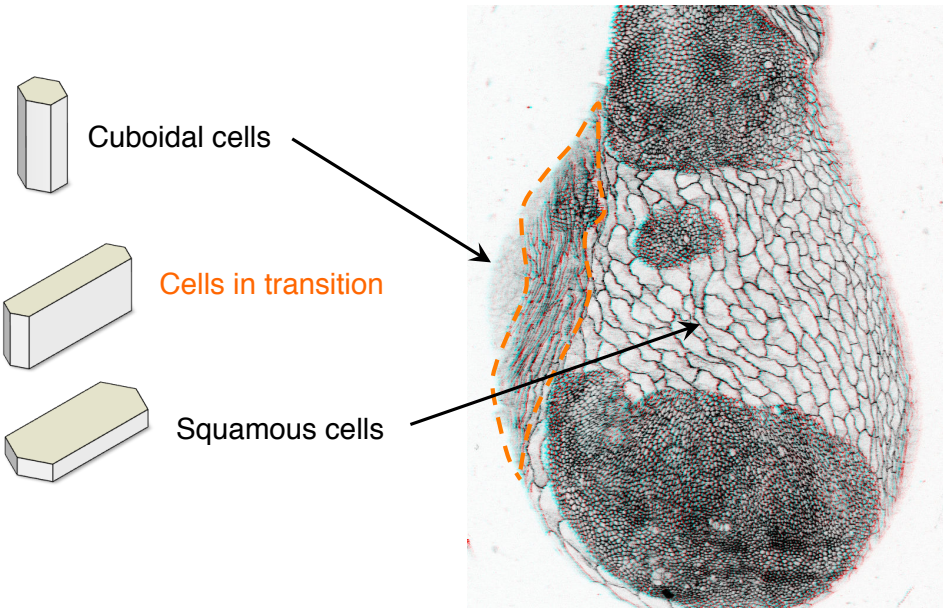

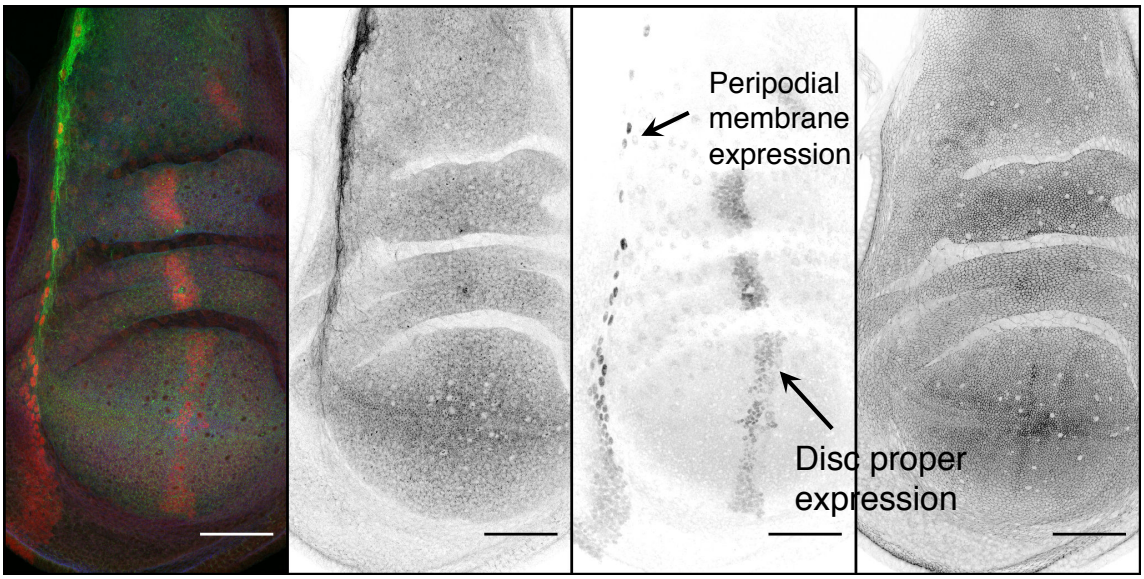

Figure JCB_Sup2. Jupiter::GFP requires both JNK and DPP inputs. *Prd-Gal4, UAS-Bsk^{DN}, UAS-tkv^{ACT}, Jupiter::GFP, Dpp-lacZ* embryo marked for Jupiter::GFP (green), pMAD (red) and Dpp-lacZ (blue). Scale bar: 10 µm.

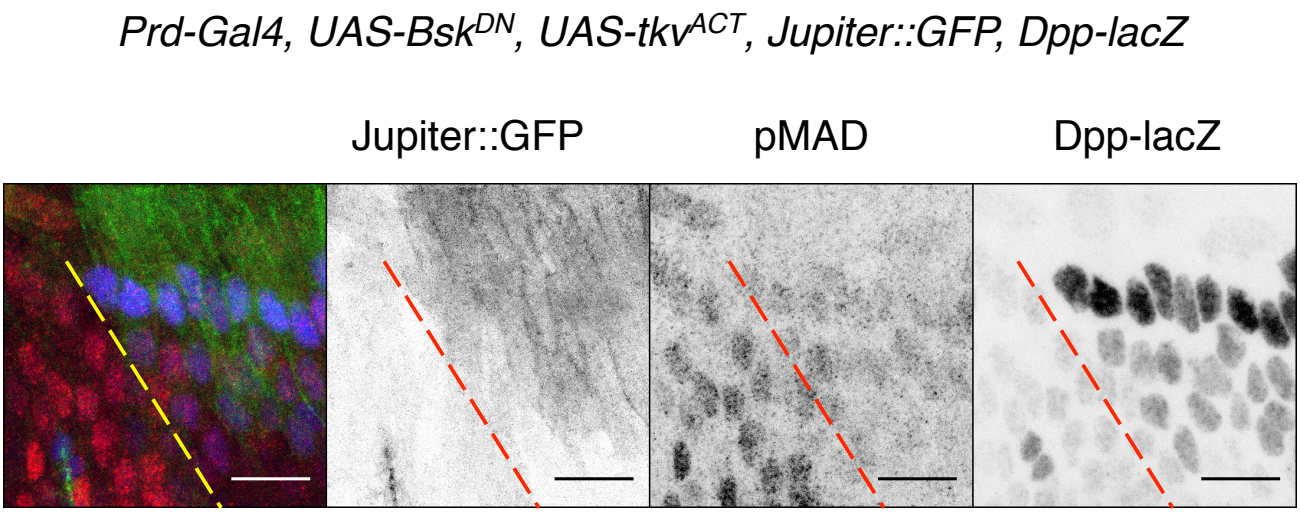

Cells on the left of the dashed lines are deprived of JNK activity (Dpp-lacZ negative), but high-ectopic DPP activity is genetically restored (increased pMAD staining compared with WT counterparts). Still, Jupiter::GFP expression is lost. These data rule out the possibility that levels of DPP signalling where not sufficient in the experiment depicted in Figure 3 of the JCB paper.

Figure JCB_Sup3. Puc-lacZ and Scarface require DPP input.

Control (A and C) and *tkv*^{8} (B and D) embryos marked with E-Cadherin (magenta) and Puc-lacZ (green in A and B) or Scaf (green in C and D). Scale bar: 50 µm. Both Puc-lacZ and Scaf expression at the leading edge are lost in *tkv*^{8} mutant embryos.

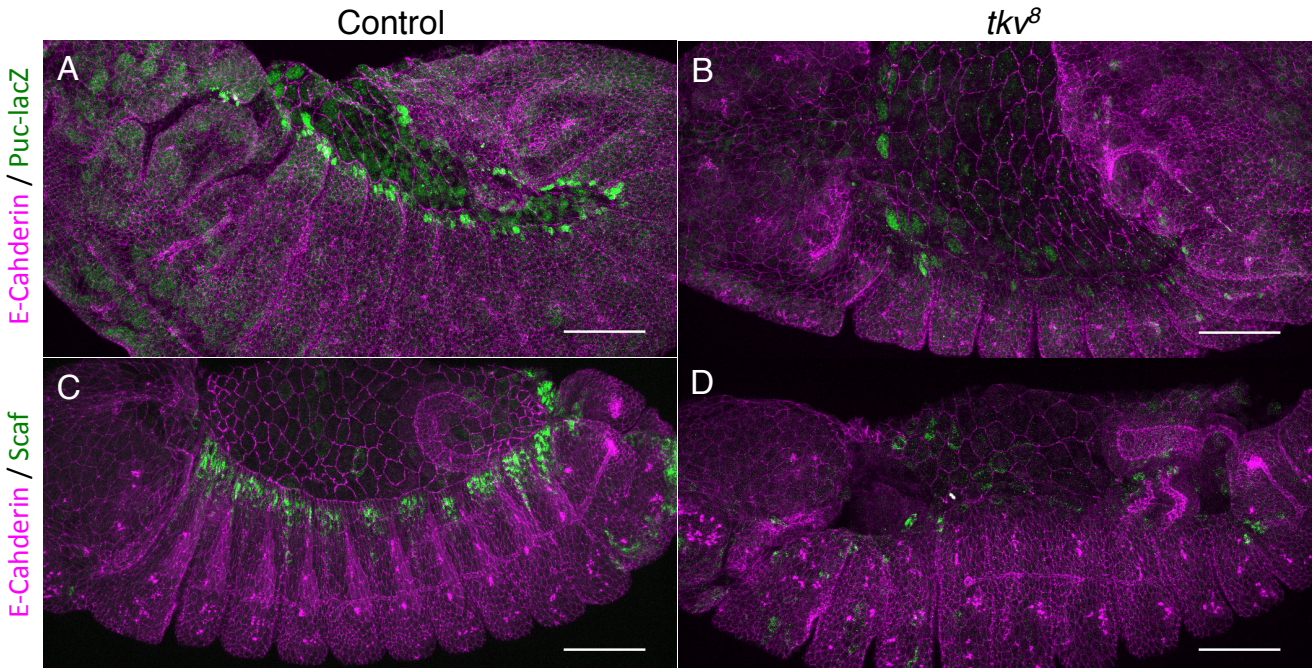

Puckered and Scarface are two JNK targets that provide a negative feedback on JNK inputs. This is based on the following observation:

- Scaf and Puc expression are lost in JNK signalling mutant embryos.
- Ectopic JNK activity leads to ectopic Scaf and Puc expression.
- Ectopic DPP activity does not lead to ectopic Scaf or Puc expression.

By showing that both Scaf and Puc are lost in DPP signalling mutant embryo, we demonstrate that these two genes are under the control of the JNK / DPP feed-forward loop we depicted in this paper.

2. Zasp52 paper

While deciphering the JNK/DPP feed-forward loop, I decided to go back to the original paper where the Jupiter::GFP line was published (Morin et al., 2001). In this paper, Morin and colleagues also published a line where the GFP is tagged to the actin cable. After efforts to find the gene that was targeted, I found that it was Zasp52. Zasp52 has been extensively studied in the muscles. Interestingly, the Frieder Schock lab showed that it was expressed at the leading edge during dorsal closure (Jani and Schock, 2007). I thus asked him for the antibody and the mutant that – according to him – was showing only a mild phenotype during dorsal closure. I repeated all the feed-forward loop experiments I did on Jaguar and Jupiter. This was published in the JCB paper. In addition, I analysed *Zasp52* mutant embryos and rapidly noticed that the actin cable was affected but that dorsal closure was completed. This was surprising regarding the current models of the function of the actin cable that predict that the actin cable is required for dorsal closure. Hence I decided to analyse the function of the actin cable during dorsal closure.

The actin cable is dispensable to regulate dorsal closure dynamics but neutralizes mechanical stress to prevent scaring in the *Drosophila* embryo

Antoine Ducuing[1] and Stéphane Vincent[1,*].

[1] LBMC, UMR5239 CNRS/Ecole Normale Supérieure de Lyon, SFR 128 Biosciences Lyon Gerland, Université de Lyon, Lyon, France

* Corresponding author: stephane.vincent11@ens-lyon.fr

Stéphane Vincent, Ph.D

LBMC, Ecole Normale Supérieure de Lyon

46 Allée d'Italie

69007 Lyon

France

Phone: +33 (0)4 72 72 85 74

Fax: +33 (0)4 72 72 86 74

ABSTRACT

A long-standing enigma in regenerative medicine is that certain developing tissues such as those in the embryo heal wounds perfectly while adult tissues produce scars. Interestingly, perfect healing correlates with the presence of an actin cable that surrounds the wound. Here we demonstrate for the first time that specific targeting of the cable induces scaring. The current model suggests that the cable functions as a contractile purse string to accelerate closure thus preventing inflammation and scarring. Using fly genetics and 4D imaging, we show that the cable does not act on closure dynamics. We further demonstrate that the actin cable balances forces and stabilizes cell geometry so that closure resolves in a perfectly structured and scar-free tissue. The absence of cable leads to cell shape irregularities as well as patterning and planar cell polarity defects that are typical of scarring. We propose a new mechanism where the cable acts as a static force field that protects cellular geometries from robust morphogenetic forces that operate at tissue level.

INTRODUCTION

Wound healing is a key homeostatic mechanism that restores tissue integrity after injury. Wound healing must be fast to prevent intrusion from pathogens, and perfect so that the tissue maintains its properties. Importantly, healing is efficient in embryos but imperfect in adults, where it leads to scar formation. Martin and Lewis described in 1992 in chick embryos a supra-cellular structure that accumulates at the border of wounds, the actin cable (AC) [1]. The founder model is that the AC acts as a purse string that constricts to close the wound. Since adult wound healing does not involve a prominent AC, they hypothesized that in the absence of an AC in adult tissues, closure is slower, leading to inflammation and scarring. To our knowledge this elegant model has not been demonstrated yet and is only supported by correlations. Strikingly, the AC is conserved from invertebrates to human [1-10] and is also present during normal development in processes such as *Drosophila* dorsal closure (DC) [11-13]. During DC, the right and left epidermis meet to close a transient dorsal gap covered by a layer of flat, squamous cells called the amnioserosa (AS) that generates the main driving force of closure. Specifically, the dorsal-most cells of the epidermis, called the leading edge (LE) cells, produce an AC as well as actin-based filopodia that are crucial for the seamless zippering of the epithelium[12-14]. The AC is therefore conserved through evolution and is a remarkable feature of embryonic epithelial closure.

Besides its conspicuous presence, the specific action of the AC remains unclear and several overlapping functions have been proposed to explain its participation to dorsal closure. First, the AC could work as a purse string that enhances the dynamics of closure [11, 13-15]. It could also work as a ratchet to enable

the transmission of forces from the oscillating AS cells to the epidermis [16]. In addition it could keep the LE straight to facilitate the zippering phase [13]. However, the inherent robustness of DC complicates the analysis of the precise contribution of the AC to DC and explains why the issue is still open. First, the function of the LE is shadowed by the action of the AS that produces a key pulling force during DC [16, 17]. Still, ablation of the AS does not prevent dorsal closure, suggesting that the AC compensates this action. Indeed, ablation of both the AS and the LE prevents closure, indicating that the LE can drive closure in the absence of the AS. A difficulty with the interpretation of these experiments is that ablating the LE affects both the cable and the filopodia[14, 18]. Using genetics to target cytoskeletal molecules also induced pleiotropic effects when the components mediate general cellular functions. For example, the dominant negative form of the rho GTPase led to a weaker AC but also to an over-production of filopodia[13]. In addition, embryos lacking components of the cable such as actin or myosin are also difficult to analyse since these components are broadly expressed in the embryo and affects other cell types. As far as we know, there is no report of a physical or genetic method that could target the AC in a specific manner and ascertain its function.

Here we report that the AC does not produce a major force during epithelial closure and has very limited effects on closure dynamics. We found that *Z band alternatively spliced PDZ-motif containing protein 52 (Zasp52)* is specifically required for the formation of the AC, and used Zasp52 mutants as a paradigm to understand the cable function. Zasp52 is a member of the Alp/Enigma family that associates with alpha-actinin in muscles both in vertebrates [19-21] and *Drosophila* [22, 23]. Mutations in Zasp lead to severe cardiac-vascular, congenital and adult myopathies in mice [20, 24],

humans [25-27] and in *Drosophila* [22]. These muscle-specific defects indicate that Zasp52 is dedicated to highly specialized cytoskeletal structures and our observations confirm that Zasp52 is not a general regulator of the cytoskeleton. During *Drosophila* embryogenesis, Zasp52 accumulates specifically at the level of the AC during DC [22, 28, 29] and here we show that Zasp52 acts as an upstream regulator of the AC formation. Surprisingly, embryos mutant for Zasp52 still close without a cable, even in the absence of AS: The cable does not participate in closure and does not act as a redundant mechanism to rescue closure when the AS is defective. Because the absence of the cable has limited impact on closure dynamics but allows other morphogenetic processes such as groove formation to interfere with DC, we propose that the cable acts as a static force field that protects LE cells. The cable preserves regular cell packing, maintains tissue organization and polarity and guarantees the integrity of a seamless epithelium at the end of the process. Perfect healing and the absence of scaring in embryos thus do not rely on enhanced dynamics but on the coherent integration of tissue and cell level forces by the cable.

RESULTS

The actin cable is a discontinuous structure

The actin cable (AC) has always been described as a continuous structure that surrounds the amnioserosa (AS) of wild-type embryos [10-13, 16]. Surprisingly, super-resolution analysis of the fixed actin cytoskeleton reveals that in all the WT embryos we imaged (*n > 10*), the AC is interrupted in multiple locations in one or two cells in a row (Fig. 1a-e). These breaches do not modify the leading edge (LE) structure and indicate that some LE cells can resist the longitudinal tension without being deformed even when they do not produce an AC. To test whether AC interruptions are fixation artifacts, we performed a live analysis of Zasp52::GFP embryos: This exon-trap GFP is inserted in the Zasp52 gene [30] and marks specifically the AC and the filopodia during dorsal closure [28, 29] (Fig. 1f-h'', Fig. S1). Live imaging shows that the AC is interrupted during dorsal closure and that our observations in wild-type embryos are not fixation artifacts (Fig. 1f-g, Video S1). Thus, the AC is dispensable for the mechanical continuity of the LE in WT embryos, at least on short distances. This contrasts with the high tension that is proposed to mediate the purse-string effect on DC.

Zasp52 is specifically required for actin cable formation

To address the function of the AC, we searched for a setting where the cable is missing. Zasp52 loss of function was a promising setting: First Zasp52::GFP and actin interruptions strictly correlate (Fig. 1f-h''). Second Zasp52 is crucial in *Drosophila* for muscle formation and attachment [22, 31]. We used Phalloidin to visualize actin in *ZaspΔ* embryos, a null allele of *Zasp52* [22]. Super-resolution imaging reveals

that the AC is absent in *ZaspΔ* embryos whereas the filopodia are still present (Fig. 2a-b'', Fig. S1). Thus, Zasp52 appears to be specifically required for AC formation. To confirm this finding, we analyzed the expression of Enabled (Ena), an actin-binding molecule that is enriched at the AC during dorsal closure [32]. In control embryos, Ena accumulates in tri-cellular junctions at the AS/LE interface and in most cells from the epidermis (Fig. 2c-c''). Conversely, in *ZaspΔ* embryos, Ena is lost specifically at the LE/AS cable interface but displays a wild-type pattern in the rest of the epidermis (Fig. 2d-d''). To verify that Zasp52 acts upstream of Ena, we tested whether Ena over-expression rescues AC formation in *ZaspΔ* embryos. First, we verified that ectopic Ena is correctly addressed to the AC by over-expressing Ena in the *paired* stripes (*prd>ena*) (Fig. 2e). Next, we over-expressed Ena in the dorsal epidermis of either WT or *ZaspΔ* embryos with the *pannier* driver (*pnr>ena*) and found that Ena does not accumulate at the level of the AC in *ZaspΔ* embryos (Fig. 2f,g). We conclude that Zasp52 is a specific regulator of the cable that acts upstream of Ena, whereas it is not required for Ena localization in other cell types. *ZaspΔ* mutants thus provide a unique setting to specifically study the function of the AC during DC.

The actin cable is dispensable for dorsal closure

To test the role of the AC during epithelial closure we analyzed *ZaspΔ* embryos. Surprisingly, closure proceeds with similar dynamics in both control and *ZaspΔ* embryos. *ZaspΔ* embryos only display a slight delay at the end of closure, indicating that the AC does not provide a major force (Fig. 3a-c, Video S2). One possibility is that putative forces generated by the cable are hidden by the action of the AS. We therefore tested whether the AC is required for closure when the AS is defective.

Strikingly, following laser ablation of the full AS, both WT and *ZaspΔ* embryos complete closure with similar dynamics (Fig. 3d-e). Thus, there is an additional force that is independent of both the AC and the AS that permits closure. Together these results indicate that the AC does not provide a major contractile force during DC.

The actin cable is dispensable for wound healing

As the AC is not necessary to produce critical forces to close the dorsal hole in the absence of the AS, we reasoned that the cable should be dispensable for wound closure. We observed that wounds close with a slight delay in *ZaspΔ* embryos: they close 20% slower than in wild type embryos (Fig. 4a-c). We found that whereas in a wild-type context both the AC and filopodia are visible around the wounds, the AC does not form around wounds in *ZaspΔ* and the actin is detected as focal points that produce filopodia (Fig. 4d-e, Video S3). We conclude that the AC has a limited contribution to wound closure dynamics.

The actin cable promotes LE straightness

Previous reports indicate that the integrity of the AC is important to maintain a taut LE [13, 33, 34]. We confirm this finding and show that *ZaspΔ* embryos display an irregular and misshapen LE (Fig. 5a-b'). While the LE straightness of control embryos increases over time, the LE straightness is strongly affected in *ZaspΔ* embryos regardless of the stage of closure (Fig. 5c-h). The quantification of the relative deviation of the LE straightness in live embryos confirms the data obtained on fixed embryos and indicates that the AC promotes straightness during most of dorsal closure (Fig. 5i-k, Video S4).

Zasp52 is required for correct leading edge tension

The foregoing observations prompted us to use laser-mediated microsurgery to test whether tensions at the leading are weaker in *ZaspΔ* than in WT embryos. Indeed, after a cut at the level of the AC, the neighboring vertices snap apart, indicating that the LE is under tension [14]. The vertices displacement after the cut fits an exponential recovery-type curve that we used to extract the initial recoil that is proportional to the tension present at that location before the cut [35-37] (Fig. 6a-e, Video S5, see methods). First, we assessed the initial recoil of LE cells in control embryos at the beginning of DC when the AC begins to form and in later embryos when the AC is robust. When the AC is present, there is a 3-fold increase in the initial recoil compared with similar embryos at the beginning of DC (Fig. 6f). This is consistent with previous findings [14, 15] that showed that the AC provides mechanical tensions. Next, we performed similar cell-junction cuts in *ZaspΔ* embryos after the first half of DC was completed. In these embryos, the initial recoil is comparable to control embryos at the beginning of dorsal closure, confirming that in *ZaspΔ* embryos, AC tension is defective (Fig. 6f). Thus the AC is important to establish the mechanical tensions present at the LE.

The actin cable homogenizes tensions along the leading edge

Interestingly, the *ZaspΔ* LE/AS interface is wavy, with a succession of “Hills” and “Valleys”. Importantly, “Valleys” often correspond to groove cells where Ena accumulates and that express the transcription factor *Odd skipped* [38] (Fig. 6c, g-i). By contrast, in stage 13-15 control embryos, the same groove cells do not form “Valleys” and the LE is straight. Thus, the AC maintains homogenous tensions at the AS/LE interface that overcome the other forces present in the epidermis. We reasoned that without the AC, these groove cells that form the “Valleys” might be stiffer that cells

forming the “Hills”, thus accounting for this defect in LE cell alignment. To test this assumption, we analyzed cuts performed either in “Hills” or “Valleys” and found that although recoil of both cell types is way slower that recoil in similar control embryos, the recoil is faster in “Valleys” than in “Hills” (Fig. 6j). This suggests that without the AC, tensions are stronger in groove cells that in other cells (Fig. 6i-j) and that the AC maintains homogenous, strong tensions along the antero-posterior axis of the LE.

To quantify the local effect of the cable on cell shape and avoid any possible interference from tensions generated at the canthi, we monitored cell shape changes in an interval of 15 LE cells: we performed two simultaneous laser cuts and monitored the size of the interval as a function of time. We find that LE cells contract 1.5 times more in wild-type than in *ZaspΔ* embryos, indicating that the cable has a significant effect on local cell shape (Fig 6k-m).

Altogether these results indicate that the cable applies a mechanical constraint that buffers local tensions, leading to a coordinated migration front.

The actin cable protects tissue organization

The absence of a taut LE AS interface has been reported in several mutants to impair the correct segment matching during the zippering step [13, 33, 34]. To monitor segment matching we marked the embryos with the segment polarity gene *patched* that is expressed in two independent stripes of cells in each segment. Surprisingly the matching between the right and left epidermis is correct in the absence of the AC (Fig. 7a-b”). Still, we noticed segmental fusion between stripes present on the same side of the embryo. Indeed, dynamic analysis reveals that the Valleys typical of *ZaspΔ* embryos sometimes initiate the formation of ectopic canthi, where cells from one LE get connected. Instead of keeping their rectangular shape the cells become

triangular and the tissue fuses abnormally (Fig. 7a-a''), leading to important deformations of the segmental pattern (Fig. 7b-c''). In addition, these abnormal fusions due to the absence of the AC are not resolved over time (Fig. S2). We conclude that the AC maintains the integrity of the segmental pattern during DC.

To analyze the effect of these deformations on cell geometry we labeled control and *ZaspΔ* embryos with E-Cadherin to mark cell junctions and puc-lacZ to indicate the nuclei of LE cells. We observed that in control embryos, LE nuclei are aligned, and closure is perfect (Fig. 7d-d''). By contrast, in *ZaspΔ* embryos, after the completion of DC, cell shapes are strongly affected compared to WT, and the dorsal midline of the embryo is asymmetric. Importantly the sites where ectopic canthi were present are not resolved in a flat epidermis but produce folds and stretches (Fig. 7e-e''). This phenotype is highly reminiscent of scaring, that is a long-term aberrant modification of the epidermis.

The hallmark of scaring in vertebrates is the absence of skin appendages such as hairs. To test whether the absence of cable leads to the formation of scar defects in the fly embryo, we marked dorsal hairs that are usually organized in segmental patterns. Actin staining reveals that hair polarity is affected in ZaspΔ embryos and that some areas are deprived of hairs at the level of the dorsal midline, where the right and left epidermis fused (Fig. 7f-g'). We conclude that the AC is important for the epidermis to keep its cellular geometry and to prevent scaring in the dorsal epidermis.

DISCUSSION

For several decades, the actin cable has been proposed to prevent scar formation by acting as a contractile purse string in embryos from invertebrates to vertebrates. For the first time, we demonstrate that targeting the cable selectively induces scar formation in embryos. Surprisingly, we found that the cable does not act as a contractile purse string. Using the power of fly genetics and 4D microscopy, we dissected the underlying mechanism that prevents scar formation in embryos.

The actin cable does not prevent scar formation by driving epithelial closure

Here we establish a paradigm to investigate the function of the AC. Zasp52 is a crucial component of highly specialized cytoskeleton structures, such as muscle fibers [22]. We show that Zasp52 is also required to build the AC during *Drosophila* dorsal closure. Importantly, in our model, filopodia length, distribution and number appear wild-type which differs from previous settings used to study cable loss of function, such as *rho* mutant embryos [13]. With this genetic tool that specifically and completely disrupts the AC without altering other structures we found that the AC does not provide a contractile force during epithelial closure. Even by destroying the AS, an action that is supposed to reveal the driving force produced by the AC, we show that closure occurs at a similar speed with or without the cable. Thus a third element must drive DC in the absence of both the AS and the AC, possibly the cellular extensions produced by LE cells. To extend our findings to a more general case of wound healing, we generated laser wounds in Zasp52 embryos and showed that wound closure is only slowed down by 20 percent. We conclude that the AC does not act as a purse string to drive epithelial closure and that the modest effects

we monitored on closure dynamics are unlikely to account for the difference between perfect healing and scaring.

The actin cable prevents scar formation by establishing a static force field

Previous studies reported that the cable is important to produce a taut front that enables the efficient zippering of the right and left epidermis [13, 33, 34]. Without the cable, the zippering process would be affected and results in segment mismatches. We tested whether the specific deletion of the cable causes the segment mismatches previously reported. We found that despite the wavy LE of *Zasp52* mutant embryos, the zippering produces perfectly matching segments between the right and left epidermis. Thus, the AC is not necessary for the coordination of the zippering between segments of the right and left epidermis. Importantly, we noticed a distinct phenotype where cells from a given side get matched together at the level of segmental grooves. Tensions exerted by segmental grooves appear to disrupt the organization of the LE, and our time-laps analysis shows the progressive matching of these cells that form ectopic canthi. Surprisingly, these ectopic canthi do not interfere with the matching between the right and left segments, showing that the zippering is a very robust process. Still, the interference of these ectopic canthi has deleterious consequences: cells located at the interface between grooves and LE are subjected to physical deformation. These cells do not display wild-type geometry, but are rather stretched or compressed. After closure, the planar cell polarity is highly disrupted in these regions, indicating that the tissue fails to heal perfectly and produces scars. The AC is therefore a structure that allows the integration of forces acting at different scales so that individual cells are protected from the forces that drive epithelia morphogenesis. Together, these results indicate that the tension present along the

LE neutralizes the forces produced by the segmental grooves, but does not pull the epidermis in the dorsal direction. As the cable does not generate motion but just counterbalances interference from other morphogenetic processes the tension forces along the cable are limited in intensity. Our model explains why the interruptions of the cable present in wild-type embryos are not deleterious and do not jeopardize the structure of the LE.

Interestingly, in other collective migration systems the position of the AC does not always correlate with the leading cells: during Madin-Darby canine kidney (MDCK) cell finger-like migration, the AC is present on the flanks of the "finger" structure but not at the level of the tip cells [39]. In MDCK cells the cable does not provide a migration force, but maintains the structure of the "finger". Together, data from MDCK cells and our results can be combined in a unique model where the cable keeps the integrity of the migrating structure. Thus, a specific requirement for collective migration compared to individual cell migration is that the migrating structure needs to be protected from the surrounding environmental constraints by a dedicated supracellular structure that is the AC.

Altogether we propose that the AC functions as a static force field that protects cells from the forces present at the tissue scale to prevent scar formation in embryonic tissues. As the AC is present in vertebrate embryos, it will be interesting to test whether it prevents scars there, and if ectopic cables in adult vertebrate tissues limits scarring.

REFERENCES

1. Martin, P. & Lewis, J. Actin cables and epidermal movement in embryonic wound healing. *Nature* **360**, 179-183 (1992).
2. Wood, W. *et al.* Wound healing recapitulates morphogenesis in Drosophila embryos. *Nat Cell Biol* **4**, 907-912 (2002).
3. Martin, P. & Parkhurst, S.M. Parallels between tissue repair and embryo morphogenesis. *Development* **131**, 3021-3034 (2004).
4. Belacortu, Y. & Paricio, N. Drosophila as a model of wound healing and tissue regeneration in vertebrates. *Dev Dyn* **240**, 2379-2404 (2011).
5. Brock, J., Midwinter, K., Lewis, J. & Martin, P. Healing of incisional wounds in the embryonic chick wing bud: characterization of the actin purse-string and demonstration of a requirement for Rho activation. *J Cell Biol* **135**, 1097-1107 (1996).
6. Davidson, L.A., Ezin, A.M. & Keller, R. Embryonic wound healing by apical contraction and ingression in Xenopus laevis. *Cell Motil Cytoskeleton* **53**, 163-176 (2002).
7. Mateus, R. *et al.* In vivo cell and tissue dynamics underlying zebrafish fin fold regeneration. *PLoS One* **7**, e51766 (2012).
8. Bement, W.M., Forscher, P. & Mooseker, M.S. A novel cytoskeletal structure involved in purse string wound closure and cell polarity maintenance. *J Cell Biol* **121**, 565-578 (1993).
9. Danjo, Y. & Gipson, I.K. Actin 'purse string' filaments are anchored by E-cadherin-mediated adherens junctions at the leading edge of the epithelial wound, providing coordinated cell movement. *J Cell Sci* **111 (Pt 22)**, 3323-3332 (1998).
10. Jacinto, A., Martinez-Arias, A. & Martin, P. Mechanisms of epithelial fusion and repair. *Nat Cell Biol* **3**, E117-123 (2001).
11. Young, P.E., Richman, A.M., Ketchum, A.S. & Kiehart, D.P. Morphogenesis in Drosophila requires nonmuscle myosin heavy chain function. *Genes Dev* **7**, 29-41 (1993).
12. Jacinto, A. *et al.* Dynamic actin-based epithelial adhesion and cell matching during Drosophila dorsal closure. *Curr Biol* **10**, 1420-1426 (2000).
13. Jacinto, A. *et al.* Dynamic analysis of actin cable function during Drosophila dorsal closure. *Curr Biol* **12**, 1245-1250 (2002).
14. Kiehart, D.P., Galbraith, C.G., Edwards, K.A., Rickoll, W.L. & Montague, R.A. Multiple forces contribute to cell sheet morphogenesis for dorsal closure in Drosophila. *J Cell Biol* **149**, 471-490 (2000).
15. Rodriguez-Diaz, A. *et al.* Actomyosin purse strings: renewable resources that make morphogenesis robust and resilient. *HFSP J* **2**, 220-237 (2008).
16. Solon, J., Kaya-Copur, A., Colombelli, J. & Brunner, D. Pulsed forces timed by a ratchet-like mechanism drive directed tissue movement during dorsal closure. *Cell* **137**, 1331-1342 (2009).
17. Toyama, Y., Peralta, X.G., Wells, A.R., Kiehart, D.P. & Edwards, G.S. Apoptotic force and tissue dynamics during Drosophila embryogenesis. *Science* **321**, 1683-1686 (2008).
18. Hutson, M.S. *et al.* Forces for morphogenesis investigated with laser microsurgery and quantitative modeling. *Science* **300**, 145-149 (2003).

19. Faulkner, G. *et al.* ZASP: a new Z-band alternatively spliced PDZ-motif protein. *J Cell Biol* **146**, 465-475 (1999).
20. Zhou, Q. *et al.* Ablation of Cypher, a PDZ-LIM domain Z-line protein, causes a severe form of congenital myopathy. *J Cell Biol* **155**, 605-612 (2001).
21. Zhou, Q., Ruiz-Lozano, P., Martone, M.E. & Chen, J. Cypher, a striated muscle-restricted PDZ and LIM domain-containing protein, binds to alpha-actinin-2 and protein kinase C. *J Biol Chem* **274**, 19807-19813 (1999).
22. Jani, K. & Schock, F. Zasp is required for the assembly of functional integrin adhesion sites. *J Cell Biol* **179**, 1583-1597 (2007).
23. Katzemich, A., Liao, K.A., Czerniecki, S. & Schock, F. Alp/Enigma family proteins cooperate in Z-disc formation and myofibril assembly. *PLoS Genet* **9**, e1003342 (2013).
24. Pashmforoush, M. *et al.* Adult mice deficient in actinin-associated LIM-domain protein reveal a developmental pathway for right ventricular cardiomyopathy. *Nat Med* **7**, 591-597 (2001).
25. Arimura, T. *et al.* A Cypher/ZASP mutation associated with dilated cardiomyopathy alters the binding affinity to protein kinase C. *J Biol Chem* **279**, 6746-6752 (2004).
26. Selcen, D. & Engel, A.G. Mutations in ZASP define a novel form of muscular dystrophy in humans. *Ann Neurol* **57**, 269-276 (2005).
27. Vatta, M. *et al.* Mutations in Cypher/ZASP in patients with dilated cardiomyopathy and left ventricular non-compaction. *J Am Coll Cardiol* **42**, 2014-2027 (2003).
28. Ducuing, A., Keeley, C., Mollereau, B. & Vincent, S. A DPP-mediated feed-forward loop canalizes morphogenesis during Drosophila dorsal closure. *J Cell Biol* **208**, 239-248 (2015).
29. Stronach, B. Extensive nonmuscle expression and epithelial apicobasal localization of the Drosophila ALP/Enigma family protein, Zasp52. *Gene Expr Patterns* **15**, 67-79 (2014).
30. Morin, X., Daneman, R., Zavortink, M. & Chia, W. A protein trap strategy to detect GFP-tagged proteins expressed from their endogenous loci in Drosophila. *Proc Natl Acad Sci U S A* **98**, 15050-15055 (2001).
31. Katzemich, A., Long, J.Y., Jani, K., Lee, B.R. & Schock, F. Muscle type-specific expression of Zasp52 isoforms in Drosophila. *Gene Expr Patterns* **11**, 484-490 (2011).
32. Gates, J. *et al.* Enabled plays key roles in embryonic epithelial morphogenesis in Drosophila. *Development* **134**, 2027-2039 (2007).
33. Grevengoed, E.E., Loureiro, J.J., Jesse, T.L. & Peifer, M. Abelson kinase regulates epithelial morphogenesis in Drosophila. *J Cell Biol* **155**, 1185-1198 (2001).
34. Laplante, C. & Nilson, L.A. Differential expression of the adhesion molecule Echinoid drives epithelial morphogenesis in Drosophila. *Development* **133**, 3255-3264 (2006).
35. Legoff, L., Rouault, H. & Lecuit, T. A global pattern of mechanical stress polarizes cell divisions and cell shape in the growing Drosophila wing disc. *Development* **140**, 4051-4059 (2013).
36. Peralta, X.G. *et al.* Upregulation of forces and morphogenic asymmetries in dorsal closure during Drosophila development. *Biophys J* **92**, 2583-2596 (2007).
37. Verma, S. *et al.* A WAVE2-Arp2/3 actin nucleator apparatus supports junctional tension at the epithelial zonula adherens. *Mol Biol Cell* **23**, 4601-4610 (2012).

38. Vincent, S., Perrimon, N. & Axelrod, J.D. Hedgehog and Wingless stabilize but do not induce cell fate during Drosophila dorsal embryonic epidermal patterning. *Development* **135**, 2767-2775 (2008).
39. Reffay, M. *et al.* Interplay of RhoA and mechanical forces in collective cell migration driven by leader cells. *Nat Cell Biol* **16**, 217-223 (2014).

Methods

Methods and any associated references are available in the online version of the paper.

Acknowledgements

We thank the ARTHRO-TOOLS and PLATIM facilities of the UMS3444, Bertrand Mollereau for laboratory space and the Bloomington and the DSHB for reagents. We thank Dali MA for the critical reading of this manuscript. The authors declare no conflict of interest. We thank the Centre National de la Recherche Scientifique for a “Chaire” to SV and the Fonds Recherche from the Ecole Normale Supérieure de Lyon for funding.

AUTHOR CONTRIBUTIONS. A.D performed experimental work. A.D and S.V performed data interpretation and preparation of the manuscript. All authors discussed the results and implications and commented on the manuscript at all stages.

COMPETING FINANCIAL INTERESTS

The authors declare no competing financial interests

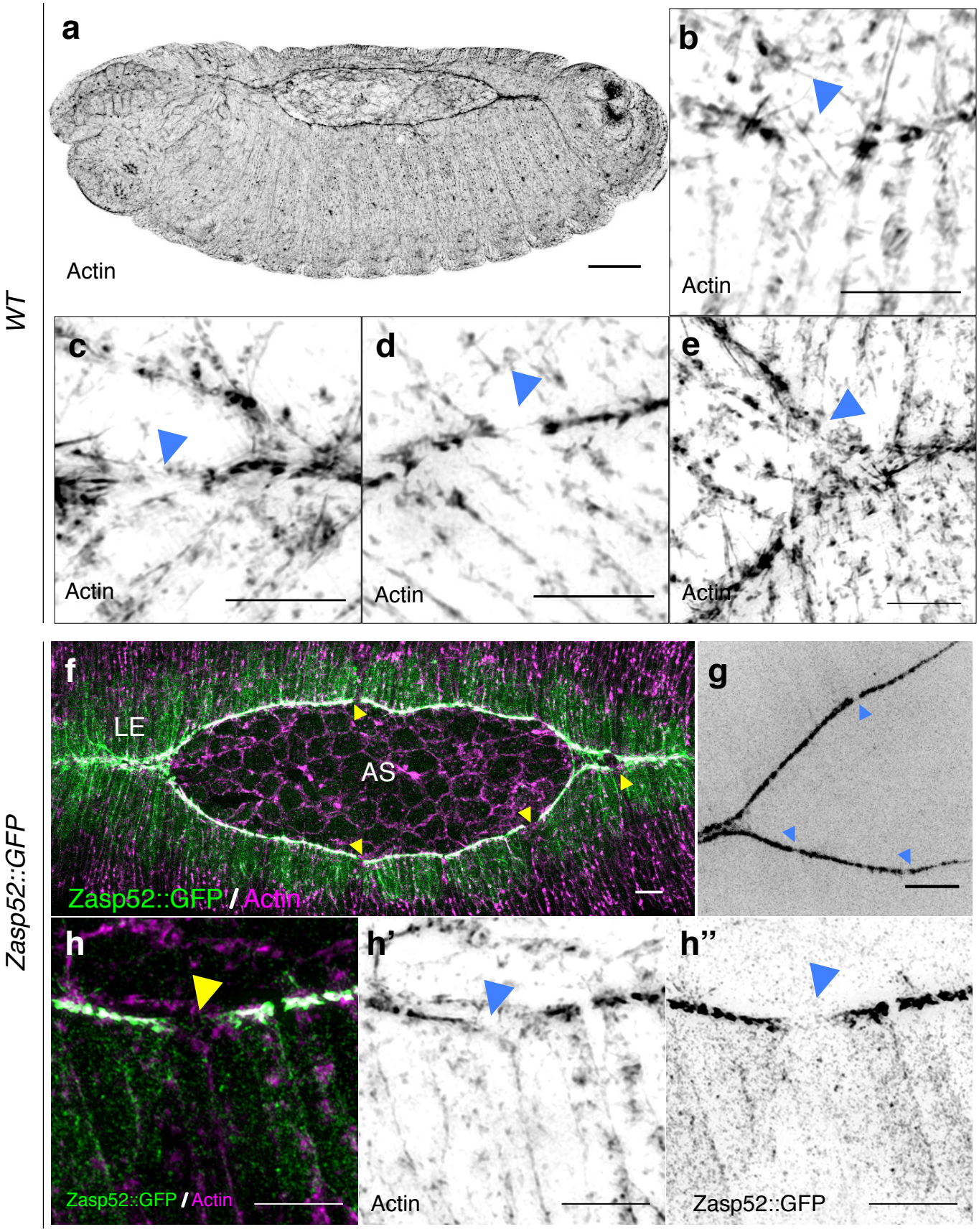

Figure 1 Ducuing and Vincent

Figure 1. The actin cable is a discontinuous structure.

(**a-e**) WT embryos marked with phalloidin to label actin. Scale bar: 50 *μ*m (**a**) or 10 *μ*m (**b-e**). Arrowheads indicate leading edge cell deprived of an actin cable.

(**f**) *Zasp52::GFP* embryo marked with GFP (green) and phalloidin (magenta). Scale bar: 10 *μ*m.

(**g**) Still image from a time-lapse movie of a *Zasp52::GFP* embryo. Scale bar: 10 *μ*m. See also Movie S1.

(**h-h''**) *Zasp52::GFP* embryo marked with GFP and phalloidin. Scale bar: 10 *μ*m. Arrowheads indicate leading edge cells where Zasp52::GFP and the actin cable are missing.

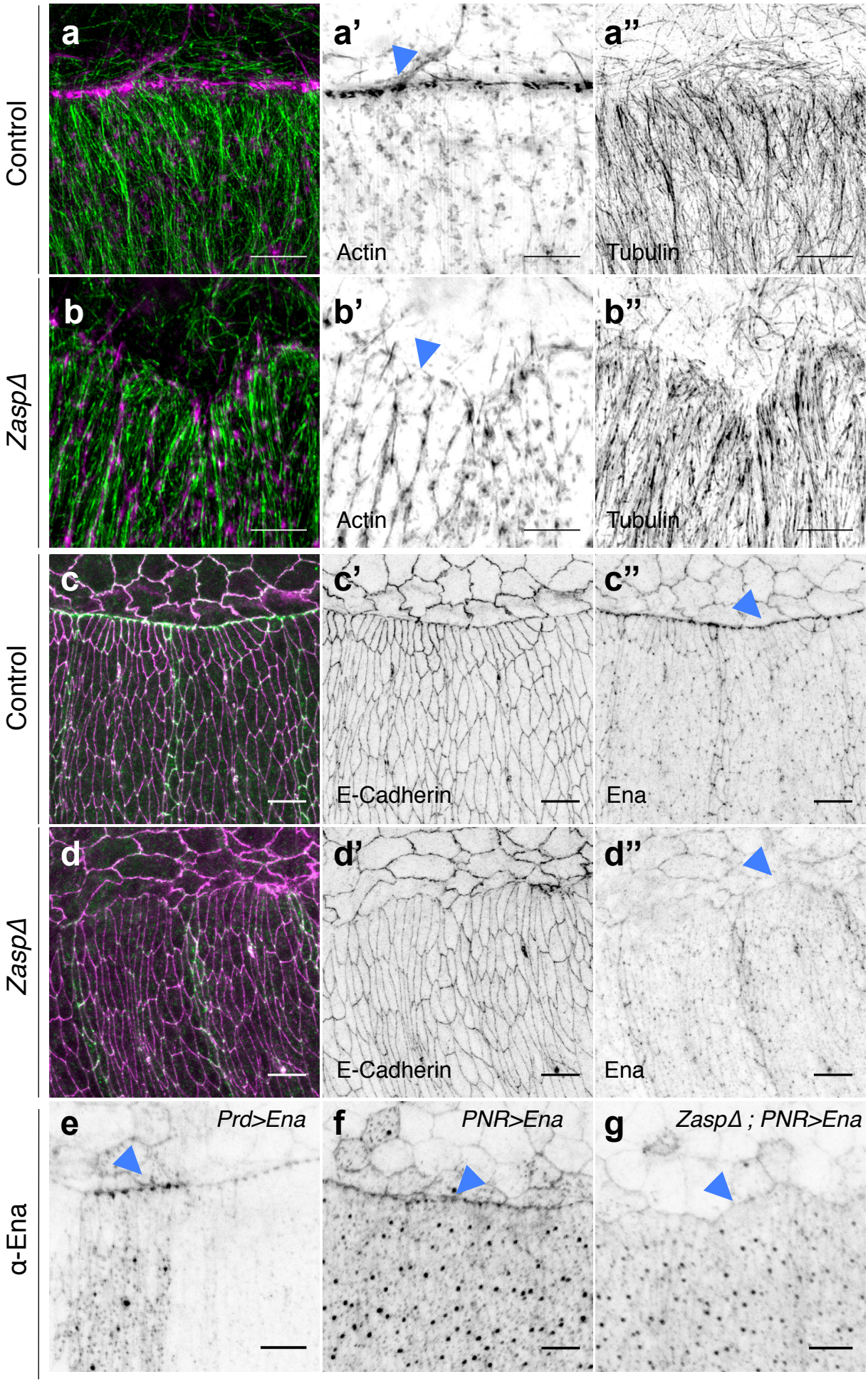

Figure 2 Ducuing and Vincent

Figure 2. Zasp52 in an upstream regulator of actin cable formation.

(**a-d**'') Control (**a-a'', c-c**'') and *ZaspΔ* (**b-b'', d-d''**) embryos marked with alpha-tubulin and phalloidin to label actin (**a, b**) or with Ena and E-Cadherin (**c, d**). Scale bar: 10 *μ*m. Both actin and Ena accumulation at the amnioserosa / leading edge interface are absent in ZaspΔ embryos (arrowheads).

(**e-g**), *Prd>Ena* (**e**), *Pnr>Ena* (**f**) and *ZaspΔ, Pnr>Ena* (**g**) embryos marked with Ena (grey). Scale bar: 10 *μ*m. Ena over-expression in leading edge cells leads to more Ena at the amnioserosa / leading edge interface in a *WT* (**e-f**, arrowheads) but not in a *ZaspΔ* mutant background (**g**, arrowheads).

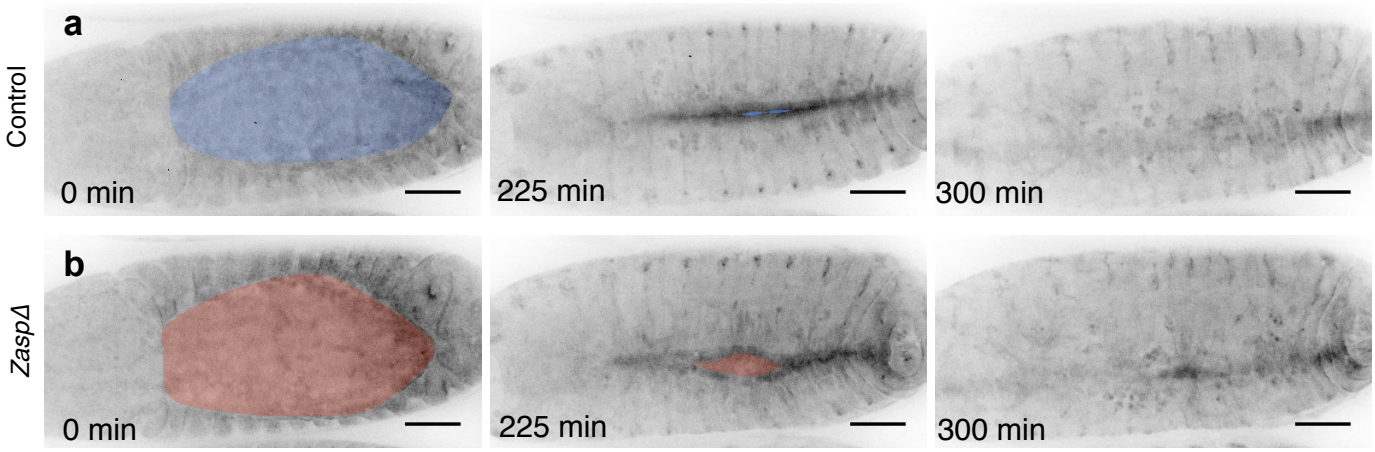
a
Control
0 min
225 min
300 min
b
ZaspΔ
0 min
225 min
300 min

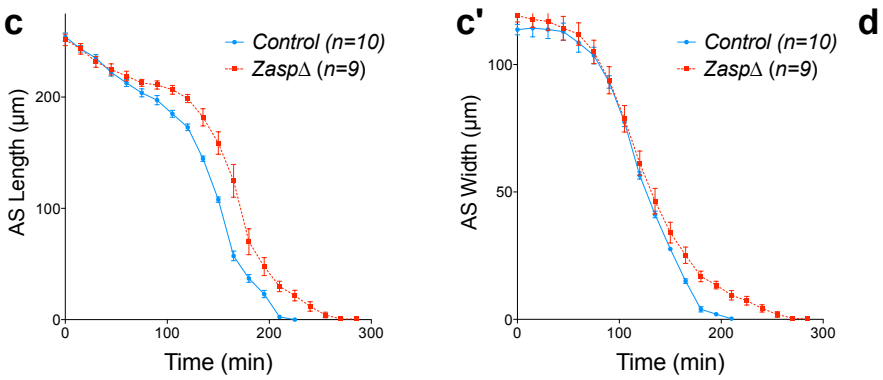
c
Control (n=10)
ZaspΔ (n=9)
AS Length (μm)
Time (min)
c'
Control (n=10)
ZaspΔ (n=9)
AS Width (μm)
Time (min)

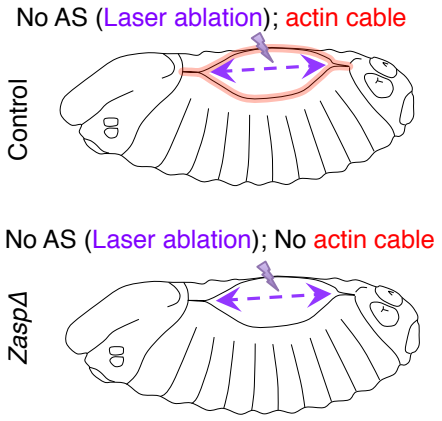
d
No AS (Laser ablation); actin cable
Control
No AS (Laser ablation); No actin cable
ZaspΔ

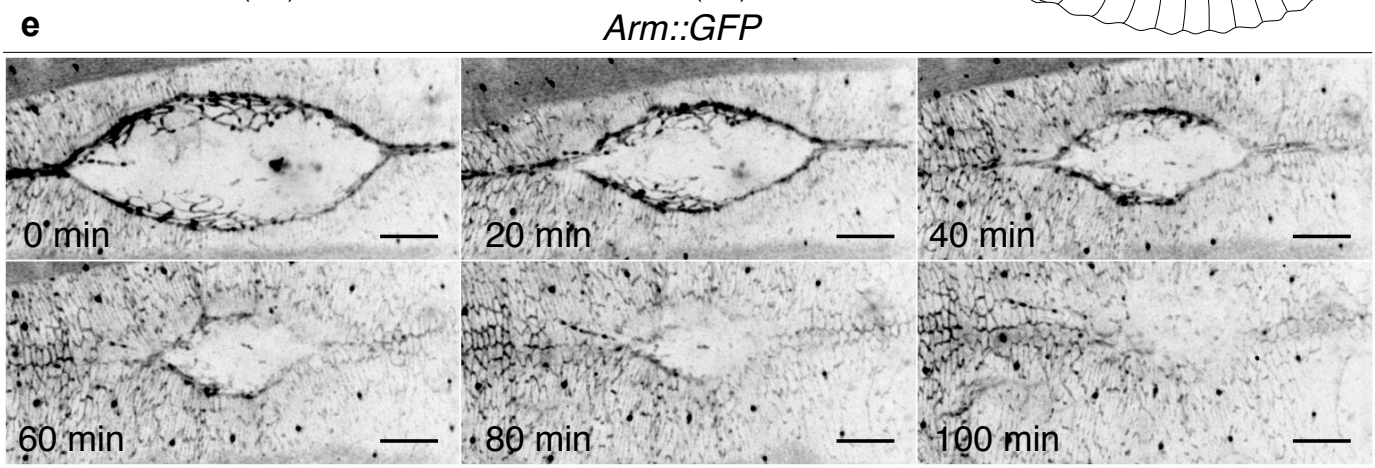
e
Arm::GFP
0 min
20 min
40 min
60 min
80 min
100 min

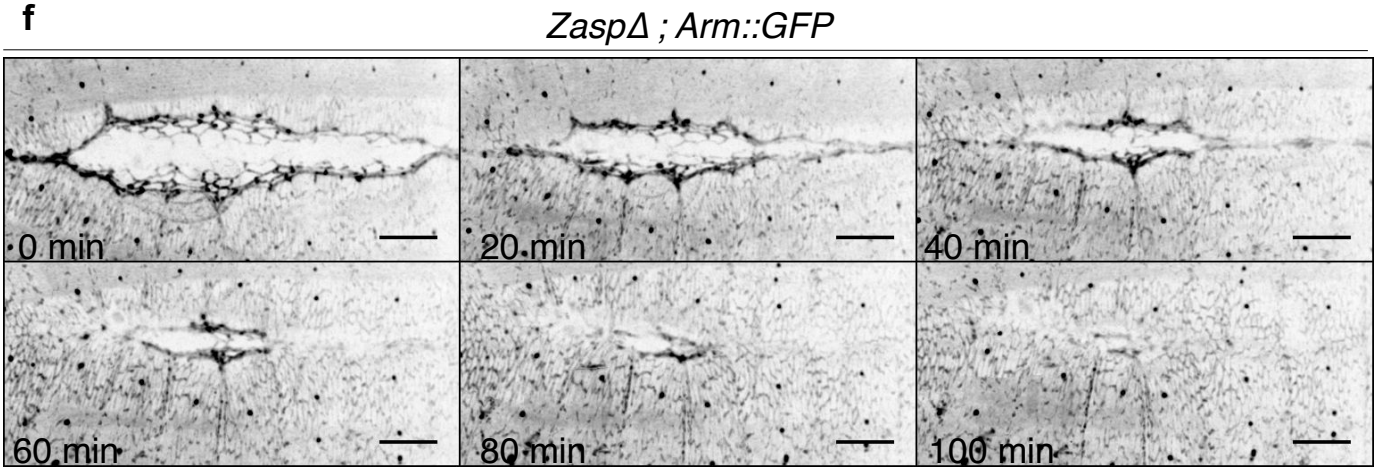
f
ZaspΔ ; Arm::GFP
0 min
20 min
40 min
60 min
80 min
100 min

Figure 3. The actin cable is dispensable and does not provide a major contractile force during dorsal closure.

(**a,b**) Still image of *Jupiter::GFP/+* (**a**) and *ZaspΔ, Jupiter::GFP/+* (**b**) embryos. Jupiter::GFP is is grey. Scale bar: 50 *μ*m. See also Movie S2. Closure is completed in *ZaspΔ* embryos.

(**c,c'**) Plot representing the normalized dorsal opening length and width over time of Jupiter::GFP and *ZaspΔ ; Jupiter::GFP* embryos *(n≥9)*. Dorsal closure proceeds slower at the end of the process in *ZaspΔ* embryos.

(**d**) Experimental strategy. Laser ablation of the amnioserosa has been performed on control and *ZaspΔ* embryos.

(**e, f**) Still images of *Arm::GFP* and ZaspΔ; Arm::GFP embryos after the laser ablation of their amnioserosa. Scale bar: 25 *μ*m. Both embryos without their amnioserosa complete closure in a similar dynamic with (**e**) or without (**f**) an actin cable.

a
Arm::GFP
b
ZaspΔ , Arm::GFP
d
Mosin::GFP
e
ZaspΔ , Mosin::GFP
0 min
35 min
70 min
102 min
143 min
18 min
53 min
70 min
c
Control (n=14)
ZaspΔ (n=9)
Wound diameter (µm)
Time (min)
0
10
20
0
50
100

Figure 4. The actin cable is dispensable for embryonic wound healing.

(a,b) Still images of *Arm::GFP* (**a**) and *ZaspΔ, Arm::GFP* (**b**) embryos wounded in the lateral epidermis. Scale bar: 10 *μ*m. Healing occurs in ZaspΔ embryos. See also Movie S3.

(**c**) Plot representing the wound diameter over time. Wound healing is slightly delayed in ZaspΔ embryo ($n \geq 9$).

(**d,e**) Still images of *Moesin::GFP* (**h**) and *ZaspΔ, Moesin::GFP* (**i**) embryos wounded in the lateral epidermis. Scale bar: 10 *μ*m. An actin cable forms in the *Moesin::GFP* embryos (**d**, arrowheads) but not in the *ZaspΔ, Moesin::GFP* embryos.

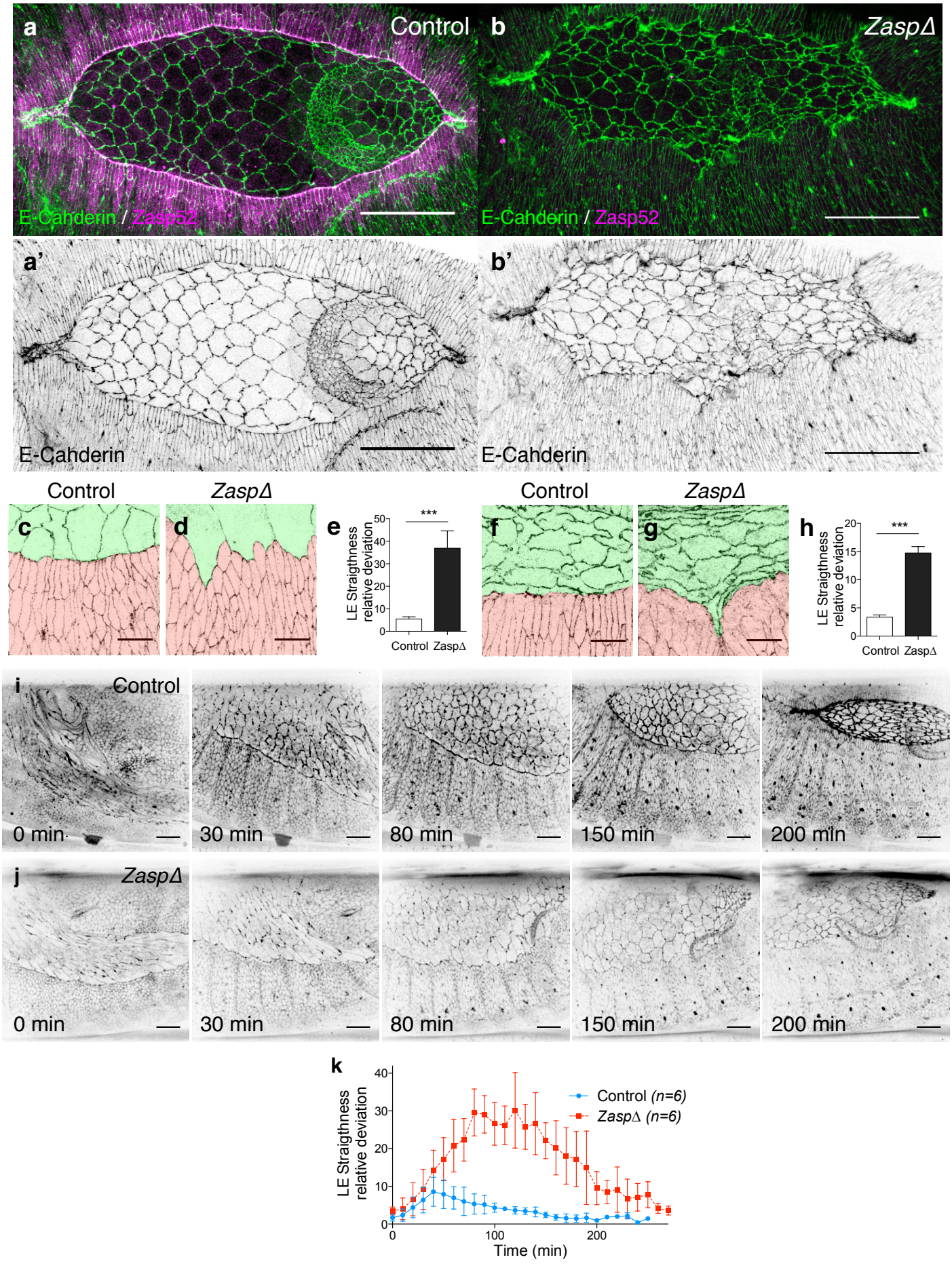
a
Control
E-Cahderin / Zasp52
b
ZaspΔ
E-Cahderin / Zasp52
a'
E-Cahderin
b'
E-Cahderin
Control
ZaspΔ
c
d
e
LE Straigthness relative deviation
***
Control
ZaspΔ
Control
ZaspΔ
f
g
h
LE Straigthness relative deviation
***
Control
ZaspΔ
i
Control
0 min
30 min
80 min
150 min
200 min
j
ZaspΔ
0 min
30 min
80 min
150 min
200 min
k
LE Straigthness relative deviation
Control (n=6)
ZaspΔ (n=6)
Time (min)

Figure 5. The actin cable is crucial for leading edge straightness.

(**a-b''**) Control (**a**) and *ZaspΔ* embryos (**b**) marked with E-Cadherin and Zasp52. Scale bar: 50 *μ*m. ZaspΔ embryos display a highly misshapen, wavy amnioserosa / leading edge interface.

(**c-d, f-g**) Control (**c, f**) or *ZaspΔ* (**d, g**) embryos at the beginning (**c, d**) or at the end of dorsal closure (**f, g**) marked with E-Cadherin (grey). The amnioserosa and the lateral epidermis have been color-coded in green and red respectively to enlight the amnioserosa / leading edge interface.

(**e, h**) Quantification of leading edge straightness defects of Control and *ZaspΔ* embryos at the beginning (**e**) or at the end (**h**) of dorsal closure. See also material and methods for quantifications. Error bars: ±s.e.m (For all panels: Mann–Whitney's *U* test, *n≥10*, ***: *P<0.001). ZaspΔ* embryos display straightness defects during dorsal closure.

(**i-j**) Still images of time-lapse movies of *Arm::GFP* (**i**) or *ZaspΔ, Arm::GFP* (**j**) embryos from germ band retraction. See also Movie S4. Scale bar: 25 *μ*m.

(**k**) Bar graph representing the mean leading edge straightness deviation over time. Defects in leading edge straightness are higher in *ZaspΔ* embryos, but these defects are reduced over time (*n=6*).

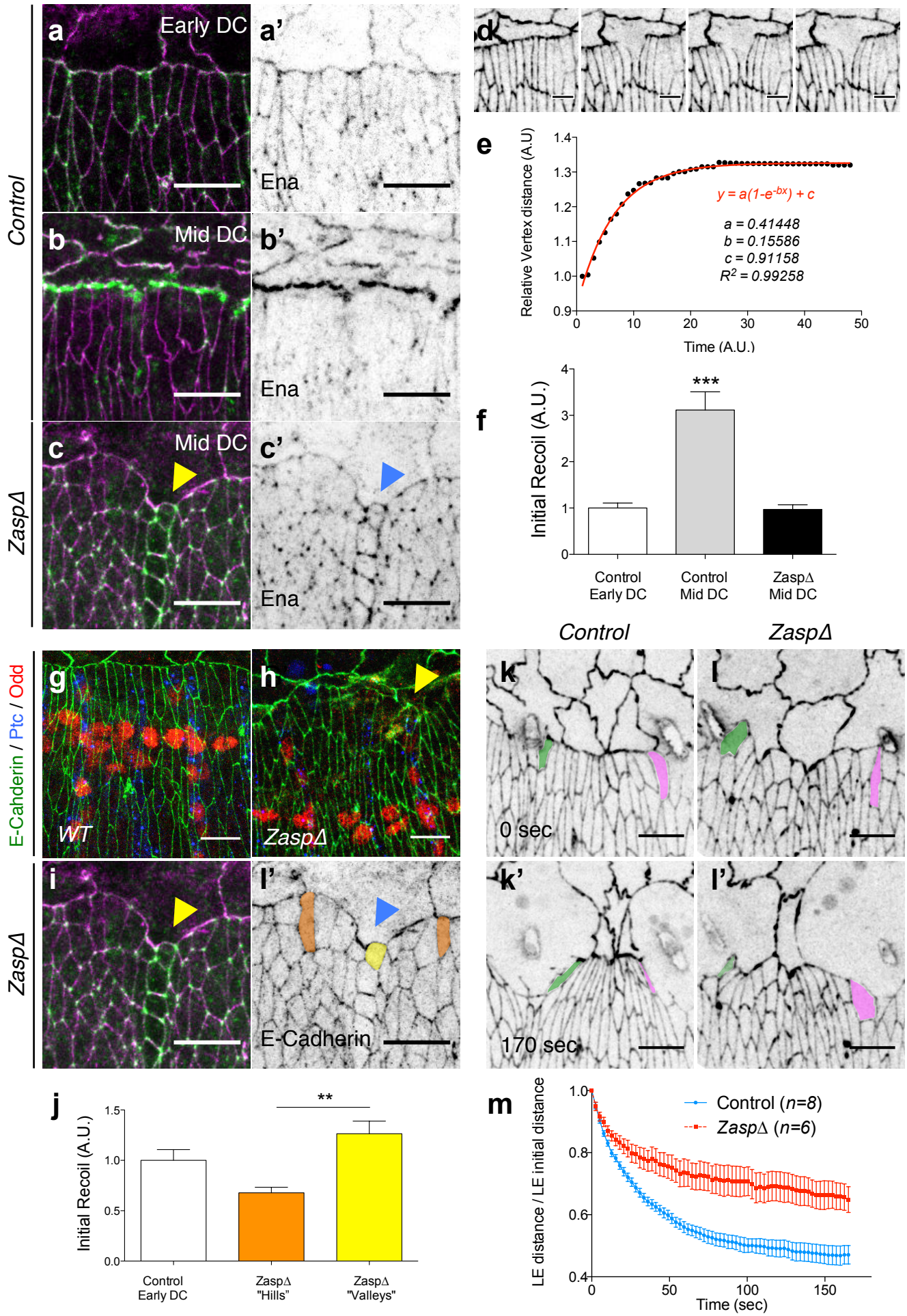
Control
ZaspΔ
a
Early DC
a'
Ena
b
Mid DC
b'
Ena
c
Mid DC
c'
Ena
d
e
Relative Vertex distance (A.U)
y = a(1-e^-bx) + c
a = 0.41448
b = 0.15586
c = 0.91158
R2 = 0.99258
Time (A.U.)
f
Initial Recoil (A.U.)
***
Control Early DC
Control Mid DC
ZaspΔ Mid DC
E-Cahderin / Ptc / Odd
g
WT
h
ZaspΔ
i
l'
E-Cadherin
Control
ZaspΔ
k
0 sec
l
k'
170 sec
l'
j
Initial Recoil (A.U.)
**
Control Early DC
ZaspΔ "Hills"
ZaspΔ "Valleys"
m
LE distance / LE initial distance
Control (n=8)
ZaspΔ (n=6)
Time (sec)

Figure 6. The actin cable maintains strong tensions to homogenize leading edge behavior.

(**a-c**) Control (**a, b**) and *ZaspΔ* embryo (**c**) marked with Ena (green in **a-c**, grey in **a'-c'**) and E-Cadherin (magenta in **a-c**). Scale bar: 10 *μ*m. Ena staining becomes stronger at the beginning of dorsal closure in Control control but not in *ZaspΔ* embryos. (**d**) Still images from a *shg::GFP* embryo after single-cell junction cut. See also Movie S5. E-Cadherin is in grey. Scale bar: 10 *μ*m.

(**e**) Graph representing the vertex displacement over time after the cut. The experimental curve fits an exponential-recovery type curve (red curve).

(**f**) Relative initial recoil of control embryos at the beginning or at the middle of dorsal closure and *ZaspΔ* embryos. Recoil is 3 times faster is control embryos at the middle of dorsal closure than control embryos at the beginning or *ZaspΔ* embryos (*n≥ 10*; One-way ANOVA and Tukey's *post-hoc* test, *** *P<0.001).*

(**g-i**) Control (**g**) and *ZaspΔ* (**h, i**) embryos marked with E-Cadherin (green), Odd Skipped (red) and Ptc (blue) or with Ena (green in **i**) and E-Cadherin (magenta in **i**, grey in **i'**). Scale bar: 10 *μ*m. Arrowheads indicate groove cells that express Odd Skipped that constitute the "Valleys" and accumulate Ena.

(**j**) Relative initial recoil of control embryos at the beginning or at the middle of dorsal closure and in *ZaspΔ* embryos performed in "Hills" or "Valleys". Recoil is faster is cells that constitute the "Valleys" compared with cells that constitue the "Hills". (*n≥ 8* ; One-way ANOVA and Tukey's *post-hoc* test, ** *P<0.01).*

(**k-l'**) Still images from *Arm::GFP* (**k, k'**) or *ZaspΔ, Arm::GFP* (**l, l'**) embryos subjected to a double, simultaneous laser cut. Arm::GFP is in grey. See also Movie S6. Scale bar: 10 *μ*m.

(**m**) Plot showing the mean ± s.e.m relative leading edge distance after the cut (*n ≥ 6*). The leading edge of *Arm::GFP* embryos retracts faster and in a grater extent compared with *ZaspΔ, Arm::GFP* ones.

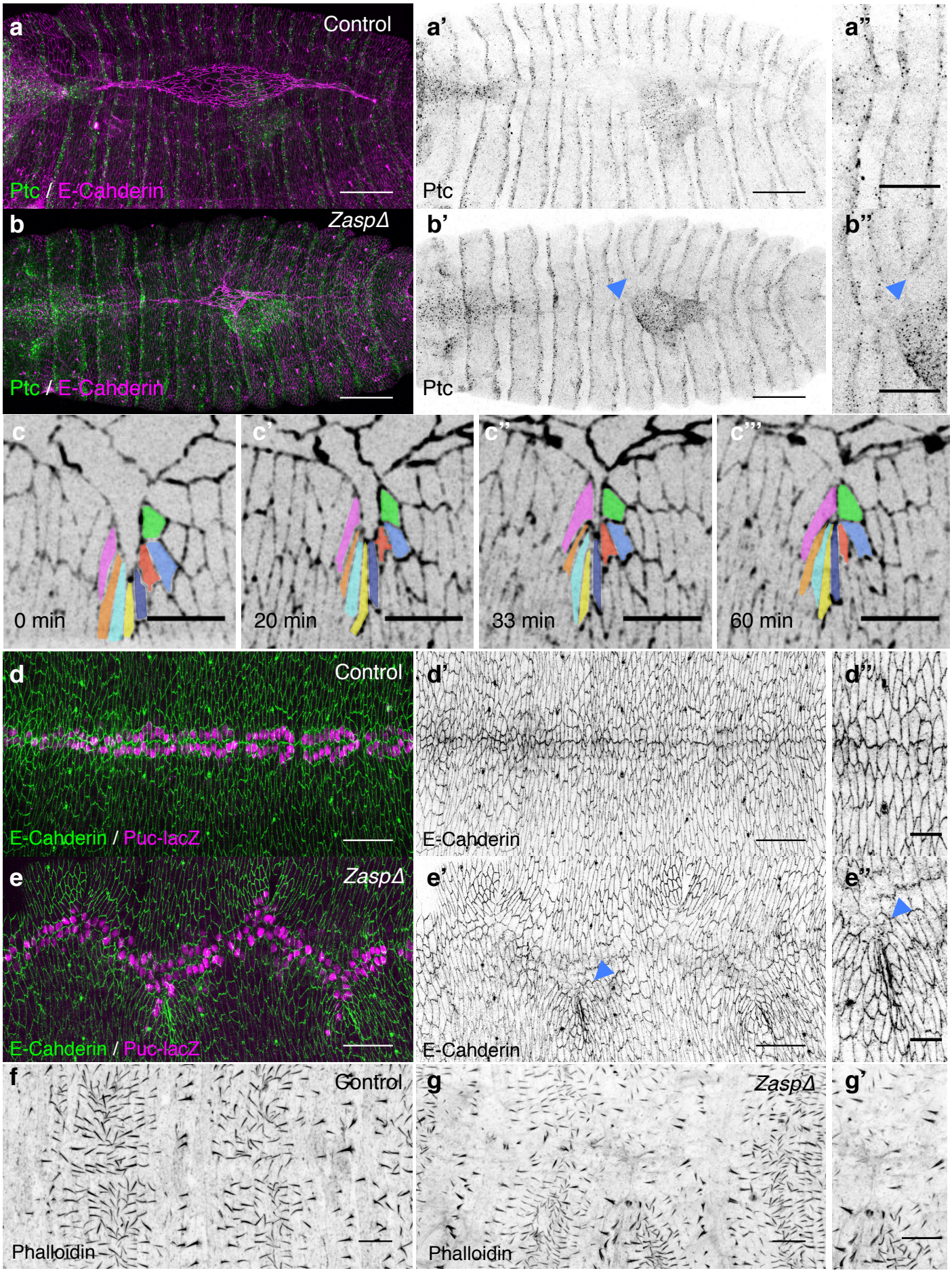
a
Control
Ptc / E-Cahderin
a'
Ptc
a''
b
ZaspΔ
Ptc / E-Cahderin
b'
Ptc
b''
c
0 min
c'
20 min
c''
33 min
c'''
60 min
d
Control
E-Cahderin / Puc-lacZ
d'
E-Cahderin
d''
e
ZaspΔ
E-Cahderin / Puc-lacZ
e'
E-Cahderin
e''
f
Control
Phalloidin
g
ZaspΔ
Phalloidin
g'

Figure 7. The actin cable prevents ectopic canthi formation to promote a perfect closure.

(**a-b’’**) Control (**a-a’’**) and *ZaspΔ* (**b-b’’**) embryos marked for Ptc and E-Cadherin. Scale bar : 50 *µ*m for **a, a’, b, b’** and 30 *µ*m for **a’’** and **b’’**. Arrowheads indicate Ptc-positive cells where an ectopic canthus has been closed.

(**c-c’’’**) Still images of a *ZaspΔ, Arm::GFP* embryo. Scale bar: 10 *µ*m. Over time, the ectopic canthus is suturated. See also Movie S7.

(**d-e’’**) *puc-lacZ/+* (**d-d’’**) and *ZaspΔ ; puc-lacZ/+* (**e-e’’**) stage 15 embryos marked for Puc-lacZ (magenta) and E-Cadherin (green or grey). Scale bar: 30 *µ*m for **d, d’, e, e’,** and 10 *µ*m for **d’’** and **e’’**. In *puc-lacZ/+* embryos closure is perfect (no scar visible), and puc-lacZ nuclei are aligned. In *ZaspΔ ; puc-lacZ/+* embryos, closure is not perfect with puckering of cells, puc-lacZ nuclei are not correctly aligned.

(**f-g’**) Control (**f**) and *ZaspΔ* (**g,g’**) stage 16 embryos marked with phalloidin to label actin. Scale bar: 10 *µ*m. ZaspΔ embryos show after closure defects in cuticle organization.

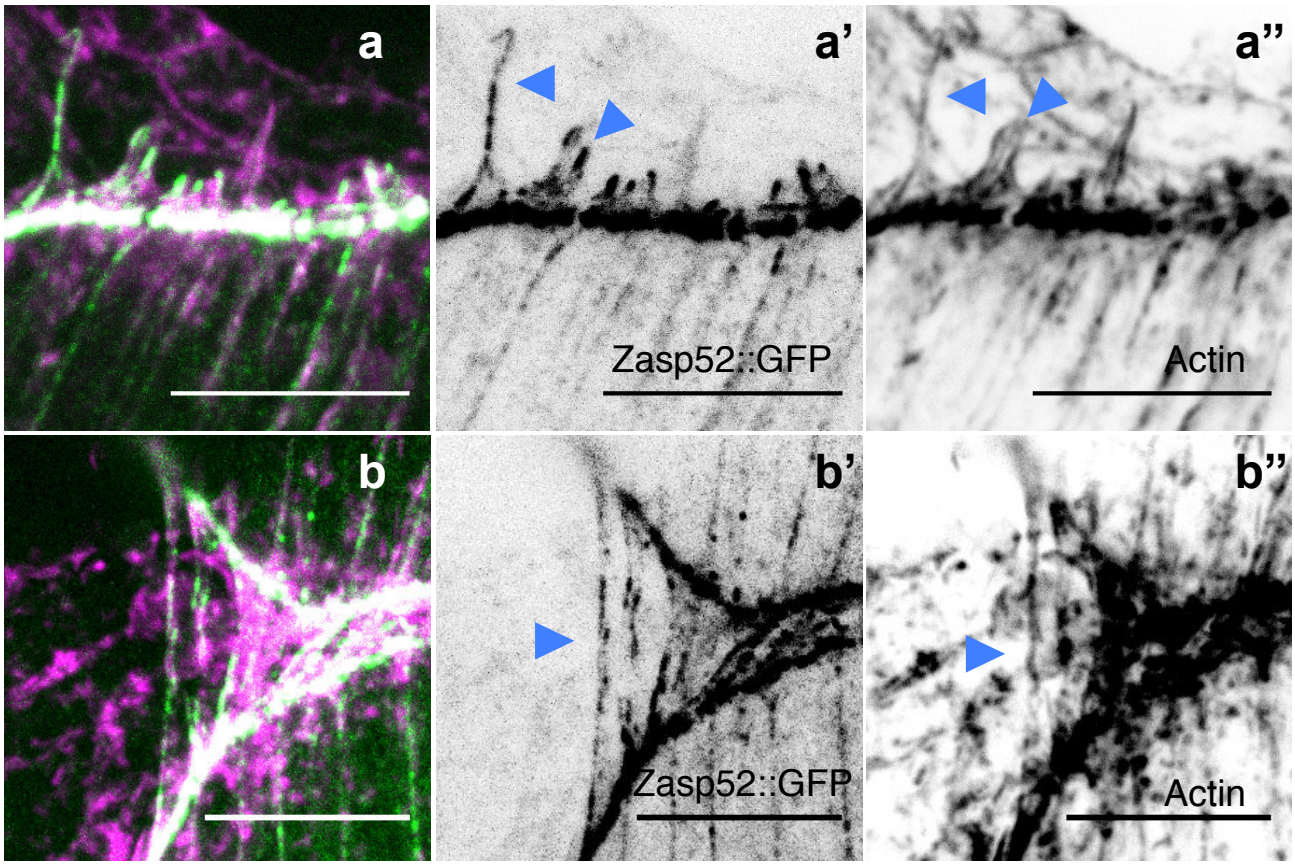

Control

ZaspΔ

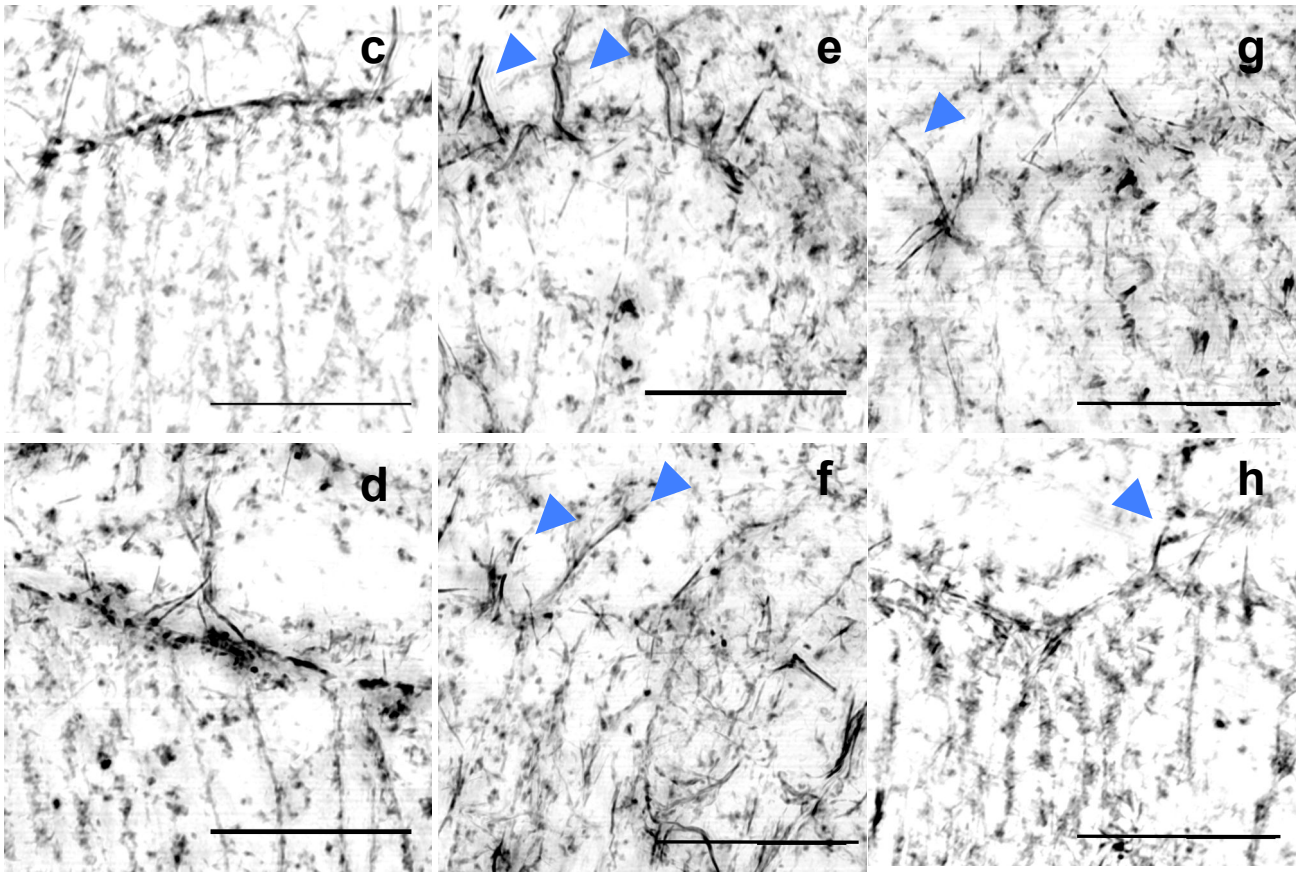

Supplementary Figure 1. Filopodia distribution in control and ZaspΔ embryos.

(**a, b**) Zasp52::GFP embryos marked with GFP (green) and Phalloidin (magenta). Arrowheads indicate filopodia where Zasp52::GFP is detected. Scale bar: 10 μm.

(**c-h**) Super-resolution images of control (**c, d**) and *ZaspΔ* (**e-h**) embryos marked with Phalloidin (grey). Scale bar: 10 μm. Filopodia are still present in *ZaspΔ* embryos.

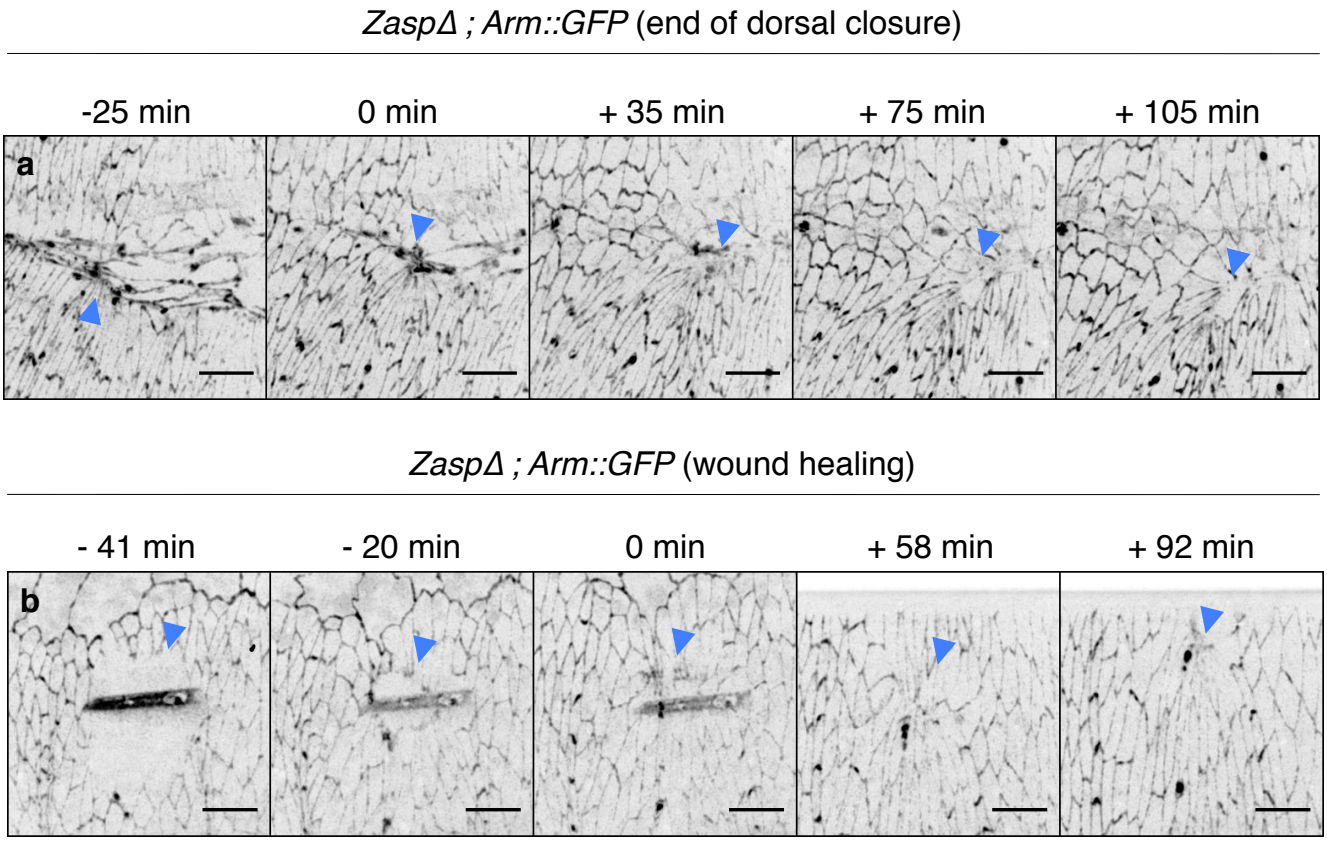

Supplementary Figure 2. Stable epithelial defects in ZaspΔ embryos.

(**a, b**) *ZaspΔ, Arm::GFP* embryos marked at the end of dorsal closure (**a**) or after a wound (**b**). Arm::GFP is in grey. Scale bar: 10 μm. In both cases, epithelial defects are still visible over time.

3. Stress-induced JNK story

While working on the Jupiter::GFP, we noticed that whereas Jupiter::GFP was lost in early *tkv*^{8} mutant embryos, in the late ones that display the so-called 'dorsal open phenotype' some leading edge cells accumulated Jupiter::GFP. This was intriguing and we found that Jupiter::GFP as well as Jaguar were accumulated over time in cells that are subjected to high mechanical stress. Using a JNK reporter called TRE-GFP we analysed the putative role of JNK in response to mechanical stress and wound healing.

JNK acts as a mechanical stress mediator and is crucial for *Drosophila* embryonic wound healing.

Antoine Ducuing[1] and Stéphane Vincent[1,*]

[1] LBMC, UMR5239 CNRS/Ecole Normale Supérieure de Lyon, SFR 128 Biosciences Lyon Gerland, Université de Lyon, Lyon, France

* Corresponding author: stephane.vincent11@ens-lyon.fr

LBMC, Ecole Normale Supérieure de Lyon

46 Allée d'Italie

69007 Lyon

France

Phone: +33 (0)4 72 72 85 74

Keywords : JNK ; *Drosophila* ; Stress ; Wound Healing ;

Words: 2721

ABSTRACT

The Jun N-terminal Kinase pathway (JNK) is an evolutionary conserved signalling pathway that acts as a stress-mediator but that also controls various developmental processes. In *Drosophila,* JNK induces in response to stress an array of mechanisms including apoptosis, compensatory proliferation or regeneration. Importantly, JNK is also crucial for larval and adult wound healing. By contrast, in the *Drosophila* embryo, JNK acts predominantly during dorsal closure, a key developmental process that is reminiscent of wound healing. Here we show that during embryonic development, JNK can act as stress mediator. Using embryos where epidermal cells are under abonormal mechanical stress, we showed that JNK is at work is cells with abnormal tensions. Second, we showed that during embryonic wound healing JNK is ectopically triggered by the surrounding epidermal cells and is crucial for the healing process. Altogether, we propose that JNK responds to mechanical stress during embryogenesis.

INTRODUCTION

The Jun N-terminal Kinase pathway (JNK) is an eukaryotic evolutionary conserved stress-response pathway that also controls several developmental processes both in vertebrates and in flies. The JNK pathway is a conserved type of Mitogen-Activated Protein Kinase pathway (MAPK), with a core pathway composed of three kinases where each kinase phosphorylates and subsequently activates its downstream partner to eventually activate the AP-1 transcription factor complex. In *Drosophila*, the JNKK *hemipetrous* (*hep*) phosphorylates the JNK *basket* (*bsk*) that in turn phosphorylates at its N-termini Jun-related-antigen (Jra or D-Jun), the *Drosophila* c-Jun homolog (Rios-Barrera and Riesgo-Escovar, 2013). Phosphorylated Jra eventually associates with Kayak (Kay, D-Fos) to form the AP-1 complex that controls specific gene expression. Since a single gene (*bsk*) encodes the *Drosophila* Jun kinase while mammalian Jun Kinase comprises three partially redundant isoforms, *Drosophila* is a powerful model organism to assess the contribution of the JNK pathway during developmental and homeostatic processes.

In *Drosophila*, the JNK pathway acts a stress mediator in a variety of cellular and homeostatic mechanisms. For instance, JNK induces apoptosis in response to UV or gamma-irradiation in larva and adults (Leppa and Bohmann, 1999; McEwen and Peifer, 2005; Igaki, 2009). The JNK pathway is also involved in the healing of larval and adult wounds (Ramet et al., 2002; Galko and Krasnow, 2004; Belacortu and Paricio, 2011), as well as triggering compensatory proliferation (Ryoo et al., 2004) or regeneration following an injury (Bosch et al., 2005).

However, in the *Drosophila* embryo, JNK acts predominantly to control development. Indeed, JNK, together with the TGF-ß homologue Decapentaplegic (DPP) controls dorsal closure, an embryonic process during which a transient dorsal gap covered by the amnioserosa is progressively closed by the fusion of the two dorsal-most epidermal row of cells that constitue the leading edge cells (Glise et al., 1995; Glise and Noselli, 1997; Hou et al., 1997; Kockel et

al., 1997; Riesgo-Escovar and Hafen, 1997). Leading edge cells during dorsal closure and epidermal cells around a wound have common cytoskeleton properties since they both accumulate a trans-cellular acto-myosin cable as well as actin-based protrusions called filopodia (Young et al., 1993; Jacinto et al., 2000; Wood et al., 2002; Martin and Parkhurst, 2004; Belacortu and Paricio, 2011). Thus, the JNK pathway could be involved in embryonic wound healing, but this remains unproved. In addition, little is known about the putative stress-mediator roles of JNK during embryogenesis. A recent study suggested that the developmental JNK at the leading edge could trigger apoptosis in DPP signalling mutant embryos (Beira et al., 2014). However, whether JNK can be ectopically activated in response to stress in the embryos remains elusive.

Here we report that JNK acts as a stress-mediator in the *Drosophila* embryo. Using embryos mutant for the DPP receptor *thickveins* (*tkv*) where abnormal tensions are generated at the amnioserosa / leading edge interface we showed that JNK responds to mechanical stress and activates the dorsal closure targets Jupiter and Jaguar (Jar). Second we tested whether JNK pathway is triggered during wound healing. We found that JNK is induced in epidermal cells around the wound. In addition, we showed that this JNK pathway activation is crucial for embryonic wound healing, since embryos deprived of JNK activity failed to heal their wounds. Taken together, our results suggest that JNK can acts as a mechanical stress mediator and is crucial for embryonic wound healing.

RESULTS AND DISCUSSION

Jupiter and Jar are expressed in late DPP signalling mutant embryos

Jupiter and Jaguar (Jar) are two proteins associated with the cytoskeleton of leading edge cells during dorsal closure. Jupiter and Jar are regulated by the JNK/DPP feed-forward loop where JNK induces DPP and both signals are absolutely required for accumulation of Jupiter and Jar as well as proper leading edge cell differentiation (Ducuing et al., 2015). Importantly, Jupiter::GFP and Jar fail to accumulate at the leading edge in embryos mutant for the DPP receptor *thickveins* (*tkv*) at stage 12, when morphological defects are not visible (Fig. 1A-B'', arrowheads and (Ducuing et al., 2015)). However, we observed that in stage 15 tkv^{8} embryos that exhibit a dorsal open phenotype, Jupiter::GFP and Jar are together detected in groups of leading edge and lateral epidermal cells (Fig. 1C-D'', arrowheads). We also observed a similar accumulation of the Jupiter::GFP and Jar in other DPP signalling mutant embryos, indicating that this is not an allele-specific effect (Fig. S1). Since neither Jupiter::GFP nor Jar are expressed at the leading edge of stage 12 tkv^{8} embryos, we wondered whether they accumulate over time. To address this question, we performed time-lapse movies of embryos expressing Jupiter::GFP either in a WT or a tkv^{8} mutant background. In control embryos, Jupiter::GFP is detected from the end of the germ band retraction. As closure proceeds, Jupiter::GFP accumulates in all the leading edge cells (Fig. 1E-E''', see also Supplemental Movie S1). In tkv^{8} mutant embryos, Jupiter::GFP does not accumulate at the leading edge during germ-band retraction. However, some leading edge cells gradually accumulate Jupiter::GFP while the amnioserosa / leading edge interface progressively disrupts, leading to the dorsal open phenotype (Fig. 1F-F''', blue arrowheads, see also Supplemental Movie S2). Importantly, we observed that not all the leading edge cells accumulated Jupiter::GFP. Indeed, Jupiter::GFP predominantly accumulates in the last epidermal cells that were in contact with the amnioserosa. Interestingly, the amnioserosa cell that was in contact with

these leading edge cells also accumulated Jupiter::GFP (Fig. 1F-F''', orange arrowheads). Taken together, our results suggest that both Jar and Jupiter can accumulate in the absence of DPP signalling in cells that are likely to be subjected to excessive tensions. Since the JNK pathway is the instructive signal that controls leading edge accumulation of Jupiter and Jar during dorsal closure (Ducuing et al., 2015) and since JNK is also a stress-induced pathway in *Drosophila*, we wondered whether differences in JNK signalling could explain the late accumulation of Jupiter and Jar in late tkv^{8} mutant embryos.

JNK controls late accumulation of Jupiter and Jar in response to mechanical stress

To test whether stress induces we first monitored JNK activity in tkv^{8} mutant embryos. We recombined the tkv^{8} allele with the JNK sensor TRE-GFP (a GFP under the control of four AP-1 binding sites downstream of an hsp70 promoter, see (Chatterjee and Bohmann, 2012). This way, we can simultaneously impair DPP signalling and monitor JNK activity as the dorsal open phenotype progresses. Time-lapse movie revealed that TRE-GFP dramatically accumulates in leading edge and amnioserosa cells that were last in contact before the dorsal open phenotype (Fig. 2A, blue and orange arrowheads, see also Supplemental Movie 3). This indicates that JNK signal becomes stronger over time in cells that are subjected to mechanical stress.

Next, we analyzed whether cells where JNK is induced and cells where Jar accumulate are the same. We found that increased TRE-GFP expression and Jar accumulation correlate in tkv^{8} mutant embryos (Fig. 2B-B', dotted lines). Importantly, leading edge cells with a basal level of TRE-GFP failed to accumulate Jar (Fig. 2B-B', arrowheads), indicating that only cells with high JNK activity accumulate Jar in the absence of DPP signalling.

To test that JNK signalling is causal is the late accumulation of the targets, we over-expressed a dominant negative form of the Jun kinase *basket (bsk)* to impair JNK signalling in the dorsal and lateral epidermis with the *pannier* driver. *pannier-gal4, UAS-*bsk^{DN} embryos

exhibit a dorsal open phenotype with abnormal tensions at the amnioserosa / leading edge interface (See supplemental Movie 4). Interestingly, in leading edge cells subjected to mechanical stress, Jar does not accumulate (Fig. 2C-C'), confirming that JNK signalling is causal in the late accumulation of Jupiter and Jar in mechanically stressed cells. Altogether, we found that in response to mechanical stress, JNK is active and induces its targets. Our work therefore provides a striking example where mechanical stress can trigger activation of the JNK pathway. Another situation where JNK acts as a stress mediator is during wound healing (reviewed in (Belacortu and Paricio, 2011). We next wondered whether JNK is involved during embryonic wound healing.

JNK controls embryonic wound healing

In *Drosophila,* several studies suggested that the JNK pathway is at work during wound healing (Belacortu and Paricio, 2011). Indeed, lacZ reporters of the JNK target *puckered* (*puc*) as well as the JNKKKK *misshapen* (*msn*) accumulate around wounds in larvae or in adults (Ramet et al., 2002; Galko and Krasnow, 2004). However, there is no evidence that JNK signalling is involved in embryonic wound healing: only the developmental function of JNK has been reported during dorsal closure to our knowledge. To test whether JNK is induced during embryonic wound healing, we wounded *TRE::GFP, Moesin::mCherry* embryos. We reasoned that if JNK is upregulated during embryonic wound healing, TRE::GFP should accumulate around the wounds. A difficulty is that, because of the maturation time of the GFP, TRE::GFP should light up after a delay, e.g. after the wound has been healed. We therefore performed large wounds to let the GFP accumulate in the lateral epidermis of stage 14/15 embryos. During the first 60 minutes post-injury, an actin cable forms around the wound that is progressively healed (Fig. 3 A-C'', arrowheads, see also Supplemental Movie 5). After 80 minutes post-injury, TRE::GFP is detected around the wound, albeit at lower levels compared with TRE::GFP levels at the leading edge (Fig. 3 D-D''', arrowheads). Over

time, epidermal cells around the wound display a strong GFP fluorescence (Fig. 3 E-J’’’, arrowheads, see also Supplemental Movie 5), that becomes even stronger than the GFP intensity at the leading edge at the end of dorsal closure (Compare TRE::GFP intensity in Fig. 3A and A’’ with Fig. 3J and J’’). This confirms that during embryonic wound healing, the JNK pathway is ectopically activated.

Next, we tested whether JNK targets during dorsal closure such as Jupiter accumulate after a wound. We wounded embryos *Jupiter::GFP, TRE-dsRed* embryos to simultaneously monitor JNK activity with the TRE-dsRed reporter and Jupiter::GFP accumulation. We observed that in the cells around the wound that accumulate the JNK reporter TRE-dsRed, Jupiter::GFP also accumulates (Fig. S2, see also Supplemental Movie 6). Thus, targets such as Jupiter involved during dorsal closure are likely to be involved during wound healing.

Next, we tested whether JNK is required for embryonic wound healing. We wounded embryos expressing the Moesin::GFP reporter either in a WT or in a background mutant for the JNK transcription factor Jra (Jun-related antigen). In WT embryos, the wound is healind within the 140 minutes. In these embryos, JNK signalling is impaired, and the process of wound healing is aborted: after 184 minutes, the wound is still not healed (Fig. 4, see also Supplemental Movie 7).

In conclusion, we provide evidence that JNK signalling is crucial for embryonic wound healing. Our results are in line with previous reports showing that JNK is at work during larval and adult wound healing (Ramet et al., 2002; Galko and Krasnow, 2004; Bosch et al., 2005).

Altogether, we found that JNK is activated in response to stress in the *Drosophila* embryo. These stress functions are distinct from the well-established developmental role of JNK during dorsal closure.

MATERIALS AND METHODS

Fly strains and genetics

We used the following lines: *tkv*^{8} (amorphic allele, # BL 34509), *shn*^{1} (amorphic allele, #BL 3008), *UAS-bsk*^{DN} (# BL6409), *UAS-ActinRFP* (# BL), *Jupiter::GFP* (GFP knock-in, # BL 6836), *TRE-GFP* (# BL 59010), *TRE-dsRed* (# BL 59012), *Moesin::mCherry* (#BL), *Moesin::GFP* (Kiehart et al., 2000), *pnr-Gal4* (#BL 3039). All crosses were performed at 25°C.

Immunofluorescence and quantification

We used standard techniques of immunohistofluorescence as described in (Ducuing et al., 2013). Embryos were dechorionated with bleach, fixed in a 1:1 mix of 4% PFA–Heptane. Embryos were subsequently devitellinized by replacing the 4% PFA with methanol. Samples were incubated with primary antibodies, with fluorescent-coupled secondary antibodies and mounted in VectaShield. We used the following primary antibodies: rat anti DE-Cadherin (DSHB, 1:333), Rabbit anti-GFP (1:400; Invitrogen), mouse anti Jar 3C7 (1:100, (Kellerman and Miller, 1992). Secondary antibodies are from Invitrogen and were used at 1:500.

Image processing

Images were acquired on the Confocal Leica SP5 microscope at the PLATIM facility and analysed with ImageJ. Unless otherwise indicated, all images are projections of confocal sections.

Live imaging

Live imaging was performed at 25°C. Embryos were staged and aligned in Halocarbon oil 27 (Sigma-Aldrich) and then imaged with a spinning disk (Leica), with a 40X oil objective (numerical aperture: 1.25), and a 100X oil (numerical aperture 1.4). We used an iXon3 (Andor Technology) camera with the acquisition software MetaMorph (Molecular Devices). *tkv*^{8} mutant embryos were identified with the dorsal open phenotype.

Laser ablation experiments. Embryos were prepared as described above. We used a UV laser (SFV-08E-0S0-BETA, teem photonics™, frequency of repetition: 8 KHz) controlled by the iLas2 module. For all the cuts we used a set ROI, a set number of Z-sections and a set exposure for Control and *jra*^{7619} embryos. We ablated with 5 laser repetitions with 100% of power.

Acknowledgements

We thank the DROSO-TOOLS and PLATIM facilities of the UMS3444, Bloomington and the DSHB for reagents. The authors declare no conflict of interest.

Author contributions

A.D and S.V designed the experiments, A.D performed the experiments, A.D and S.V analyzed the data and wrote the manuscript.

REFERENCES

Beira, J. V., Springhorn, A., Gunther, S., Hufnagel, L., Pyrowolakis, G. and Vincent, J. P. (2014). The Dpp/TGFbeta-Dependent Corepressor Schnurri Protects Epithelial Cells from JNK-Induced Apoptosis in Drosophila Embryos. *Dev Cell* **31**, 240-247.

Belacortu, Y. and Paricio, N. (2011). Drosophila as a model of wound healing and tissue regeneration in vertebrates. *Dev Dyn* **240**, 2379-2404.

Bosch, M., Serras, F., Martin-Blanco, E. and Baguna, J. (2005). JNK signalling pathway required for wound healing in regenerating Drosophila wing imaginal discs. *Dev Biol* **280**, 73-86.

Chatterjee, N. and Bohmann, D. (2012). A versatile PhiC31 based reporter system for measuring AP-1 and Nrf2 signalling in Drosophila and in tissue culture. *PLoS One* **7**, e34063.

Ducuing, A., Mollereau, B., Axelrod, J. D. and Vincent, S. (2013). Absolute requirement of cholesterol binding for Hedgehog gradient formation in Drosophila. *Biol Open* **2**, 596-604.

Ducuing, A., Keeley, C., Mollereau, B. and Vincent, S. (2015). A DPP-mediated feed-forward loop canalizes morphogenesis during Drosophila dorsal closure. *J Cell Biol* **208**, 239-248.

Galko, M. J. and Krasnow, M. A. (2004). Cellular and genetic analysis of wound healing in Drosophila larvae. *PLoS Biol* **2**, E239.

Glise, B. and Noselli, S. (1997). Coupling of Jun amino-terminal kinase and Decapentaplegic signalling pathways in Drosophila morphogenesis. *Genes Dev* **11**, 1738-1747.

Glise, B., Bourbon, H. and Noselli, S. (1995). hemipterous encodes a novel Drosophila MAP kinase kinase, required for epithelial cell sheet movement. *Cell* **83**, 451-461.

Hou, X. S., Goldstein, E. S. and Perrimon, N. (1997). Drosophila Jun relays the Jun amino-terminal kinase signal transduction pathway to the Decapentaplegic signal transduction pathway in regulating epithelial cell sheet movement. *Genes Dev* **11**, 1728-1737.

Igaki, T. (2009). Correcting developmental errors by apoptosis: lessons from Drosophila JNK signalling. *Apoptosis* **14**, 1021-1028.

Jacinto, A., Wood, W., Balayo, T., Turmaine, M., Martinez-Arias, A. and Martin, P. (2000). Dynamic actin-based epithelial adhesion and cell matching during Drosophila dorsal closure. *Curr Biol* **10**, 1420-1426.

Kellerman, K. A. and Miller, K. G. (1992). An unconventional myosin heavy chain gene from Drosophila melanogaster. *J Cell Biol* **119**, 823-834.

Kiehart, D. P., Galbraith, C. G., Edwards, K. A., Rickoll, W. L. and Montague, R. A. (2000). Multiple forces contribute to cell sheet morphogenesis for dorsal closure in Drosophila. *J Cell Biol* **149**, 471-490.

Kockel, L., Zeitlinger, J., Staszewski, L. M., Mlodzik, M. and Bohmann, D. (1997). Jun in Drosophila development: redundant and nonredundant functions and regulation by two MAPK signal transduction pathways. *Genes Dev* **11**, 1748-1758.

Leppa, S. and Bohmann, D. (1999). Diverse functions of JNK signalling and c-Jun in stress response and apoptosis. *Oncogene* **18**, 6158-6162.

Martin, P. and Parkhurst, S. M. (2004). Parallels between tissue repair and embryo morphogenesis. *Development* **131**, 3021-3034.

McEwen, D. G. and Peifer, M. (2005). Puckered, a Drosophila MAPK phosphatase, ensures cell viability by antagonizing JNK-induced apoptosis. *Development* **132**, 3935-3946.

Ramet, M., Lanot, R., Zachary, D. and Manfruelli, P. (2002). JNK signalling pathway is required for efficient wound healing in Drosophila. *Dev Biol* **241**, 145-156.
Riesgo-Escovar, J. R. and Hafen, E. (1997). Drosophila Jun kinase regulates expression of decapentaplegic via the ETS-domain protein Aop and the AP-1 transcription factor DJun during dorsal closure. *Genes Dev* **11**, 1717-1727.
Rios-Barrera, L. D. and Riesgo-Escovar, J. R. (2013). Regulating cell morphogenesis: the Drosophila Jun N-terminal kinase pathway. *Genesis* **51**, 147-162.
Ryoo, H. D., Gorenc, T. and Steller, H. (2004). Apoptotic cells can induce compensatory cell proliferation through the JNK and the Wingless signalling pathways. *Dev Cell* **7**, 491-501.
Wood, W., Jacinto, A., Grose, R., Woolner, S., Gale, J., Wilson, C. and Martin, P. (2002). Wound healing recapitulates morphogenesis in Drosophila embryos. *Nat Cell Biol* **4**, 907-912.
Young, P. E., Richman, A. M., Ketchum, A. S. and Kiehart, D. P. (1993). Morphogenesis in Drosophila requires nonmuscle myosin heavy chain function. *Genes Dev* **7**, 29-41.

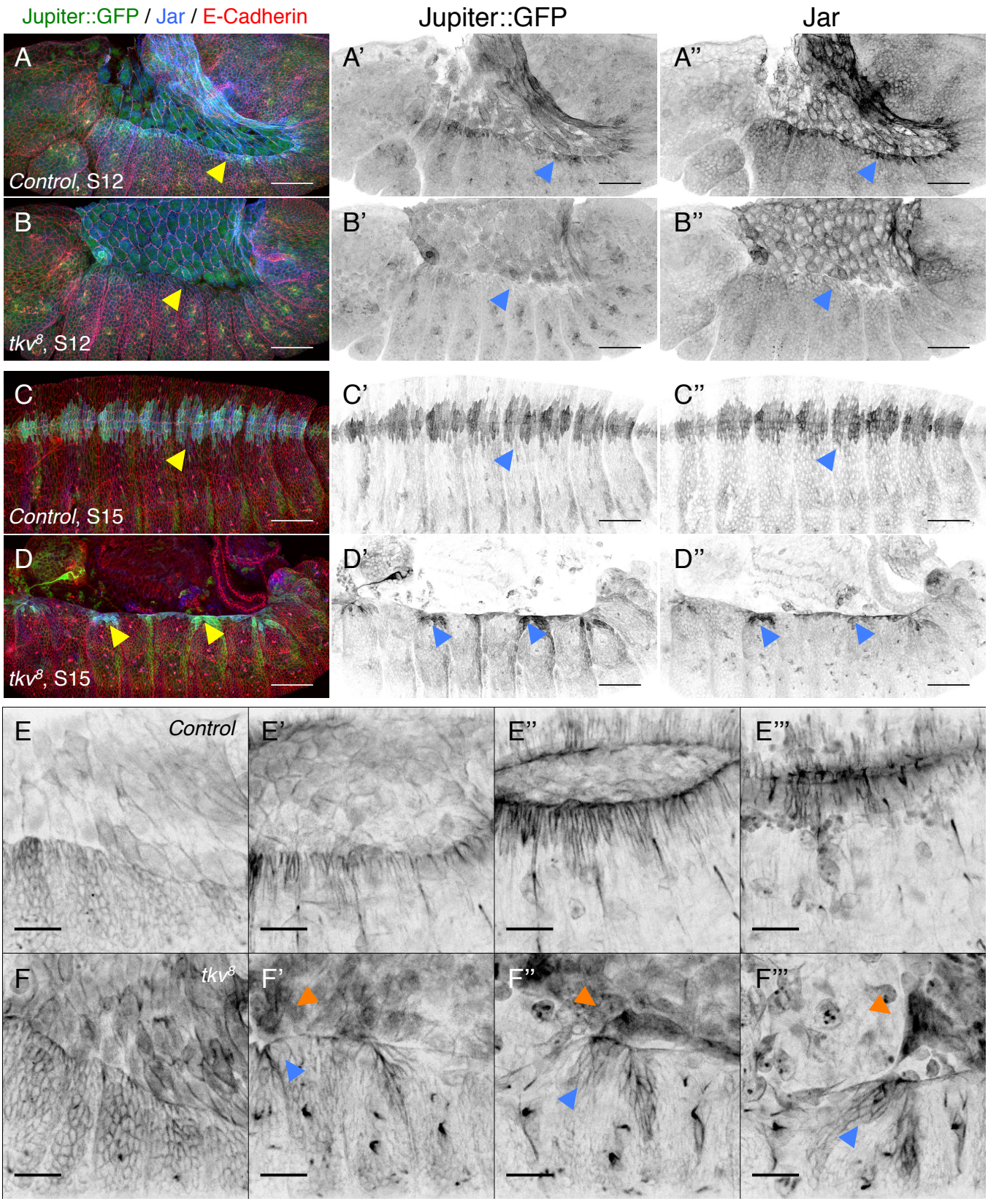

Figure 1. Late accumulation of Jupiter::GFP and Jaguar in *tkv* mutant embryos. (A-D) Control (A-A", C-C") and *tkv*^{8} mutant (B-B", D-D") at stage 12 (A-B") or stage 15 (C-D") marked for E-Cadherin, Jupiter::GFP and Jar. Scale bar: 50 μm. (A-B) At stage 12, Jupiter::GFP and Jar fail to accumulate at the leading edge of *tkv*^{8} embryos (arrowheads), whereas they accumulate in groups of leading edge and lateral epidermal cells in stage 15 *tkv*^{8} embryos (arrowheads). (E-F) Still images of a time-lapse movie of a representative Jupiter::GFP and *tkv*^{8}*, Jupiter::GFP* embryo. Scale bar: 25 μm. Jupiter::GFP accumulates over time in *tkv*^{8} mutant embryos in leading edge and amnioserosa cells. These cells are the last one in contact.

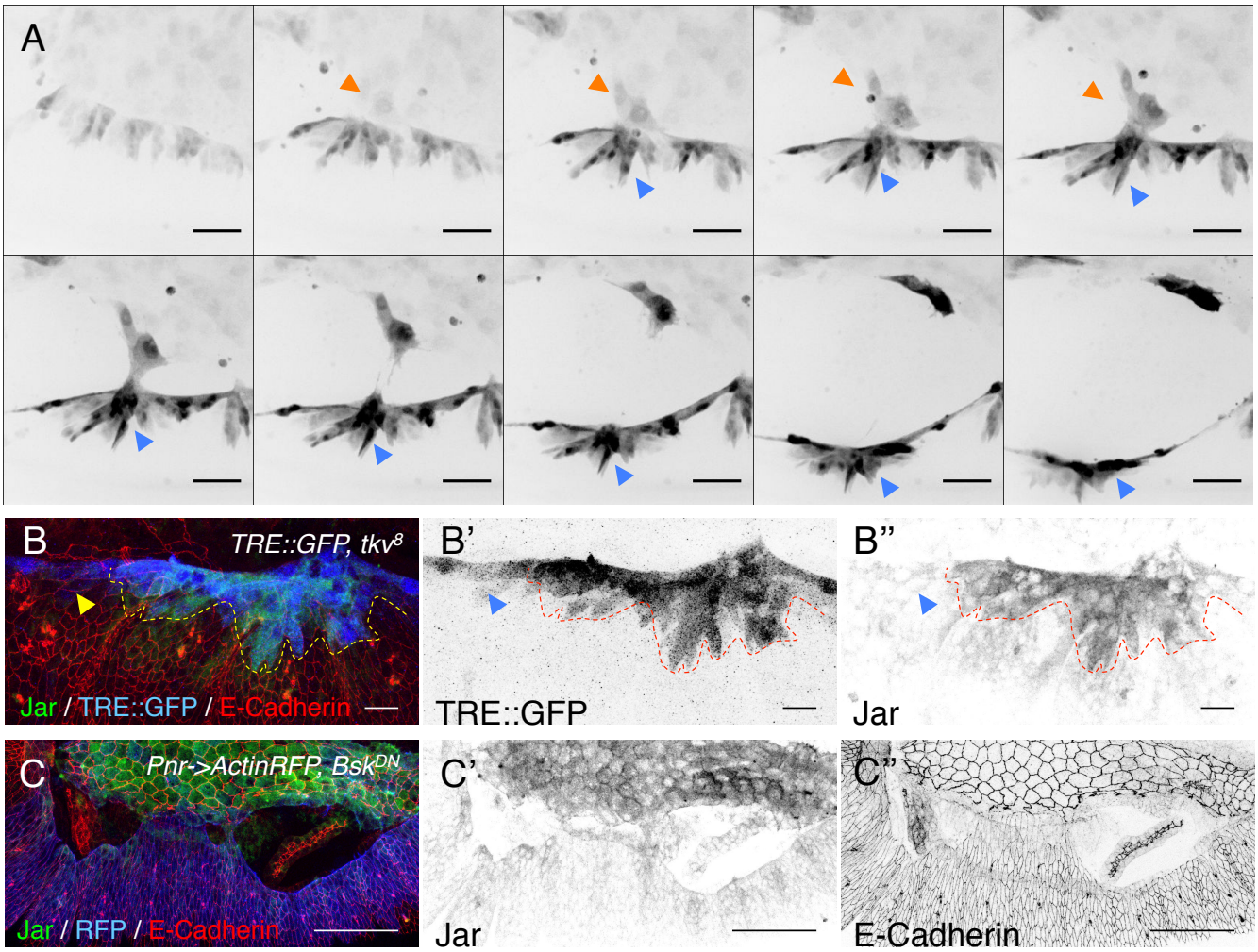

Figure 2. Stress-induced JNK controls the late accumulation of Jupiter and Jar.

(A) Still images of a time-lapse movie of a representative *tkv^{8}, TRE::GFP* embryo. Scale bar: 40 μm. TRE::GFP fluorescence becomes stronger over time in both leading edge and amnioserosa cells that are disrupting.

(B, B'). Closeup of a stage 15 *tkv^{8}, TRE::GFP* marked with GFP, E-Cadherin and Jar. Jar and intense accumulation of TRE correlate (dotted lines). In leading edge cells where TRE level is basal, Jar does not accumulate (arrowheads). Scale bar: 25 μm.

(C,C') *pannier-Gal4, UAS-ActinRFP, UAS-bsk^{DN}* embryo marked with E-Cadherin, RFP and Jar. Scale bar: 10 μm. Jar does not accumulate in the leading edge cells.

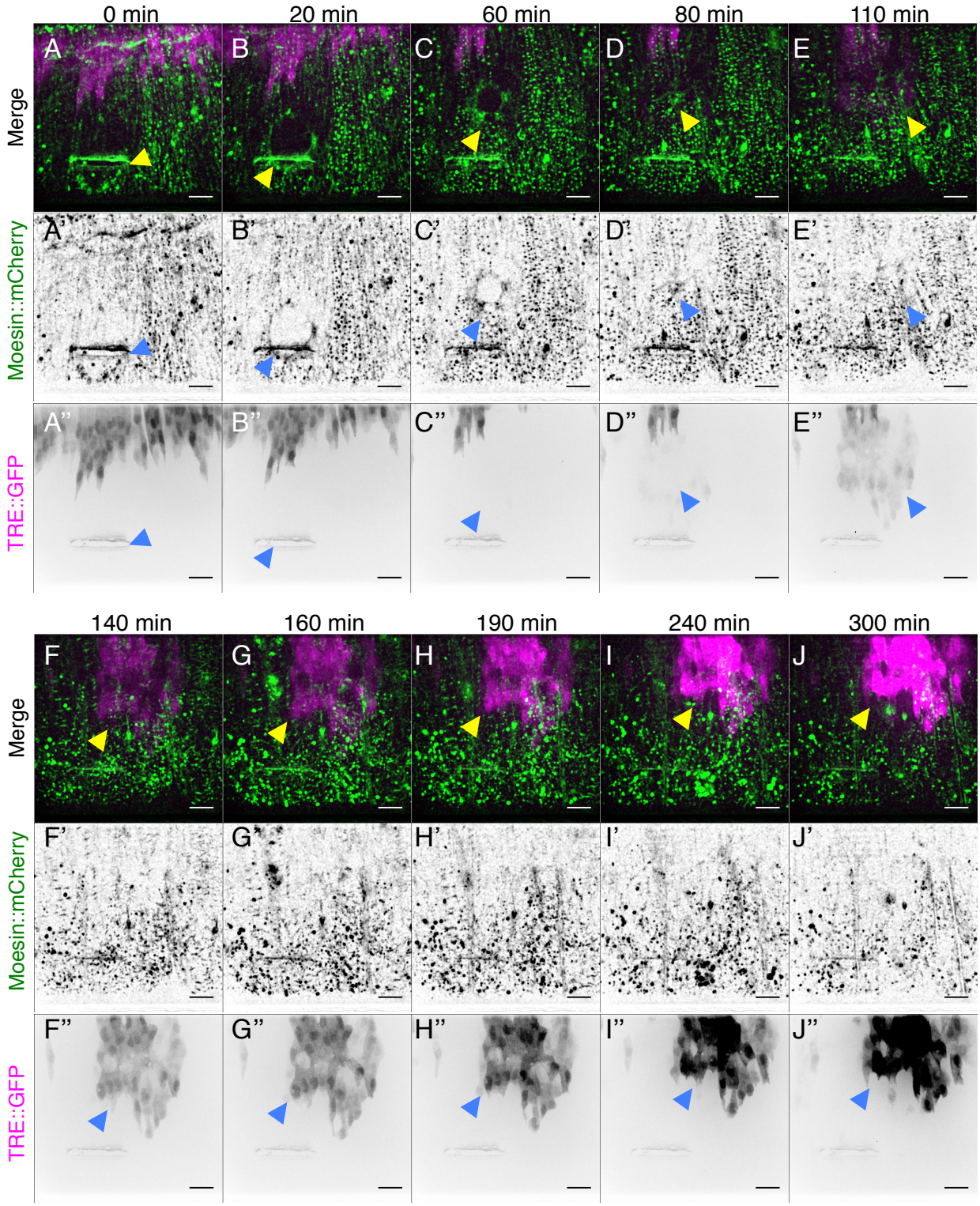

Figure 3. JNK signaling is activated during embryonic wound healing. (A-J''') Still images of a *TRE-GFP, Moesin::mCherry* embryo after a wound. TRE-GFP is in magenta (A-J) or grey (A''-J''), Moesin::mCherry is in green (A-J) or in grey (A'-J'). Scale bar: 10 μm. An actin cable forms around the wound that is progressively healed. Cells around the wound accumulate the JNK reporter TRE:GFP that becomes more intense over time. Note that the temporal delay between the healing process and the accumulation of the GFP is likely due to the folding time of the GFP that is *de novo* synthesized.

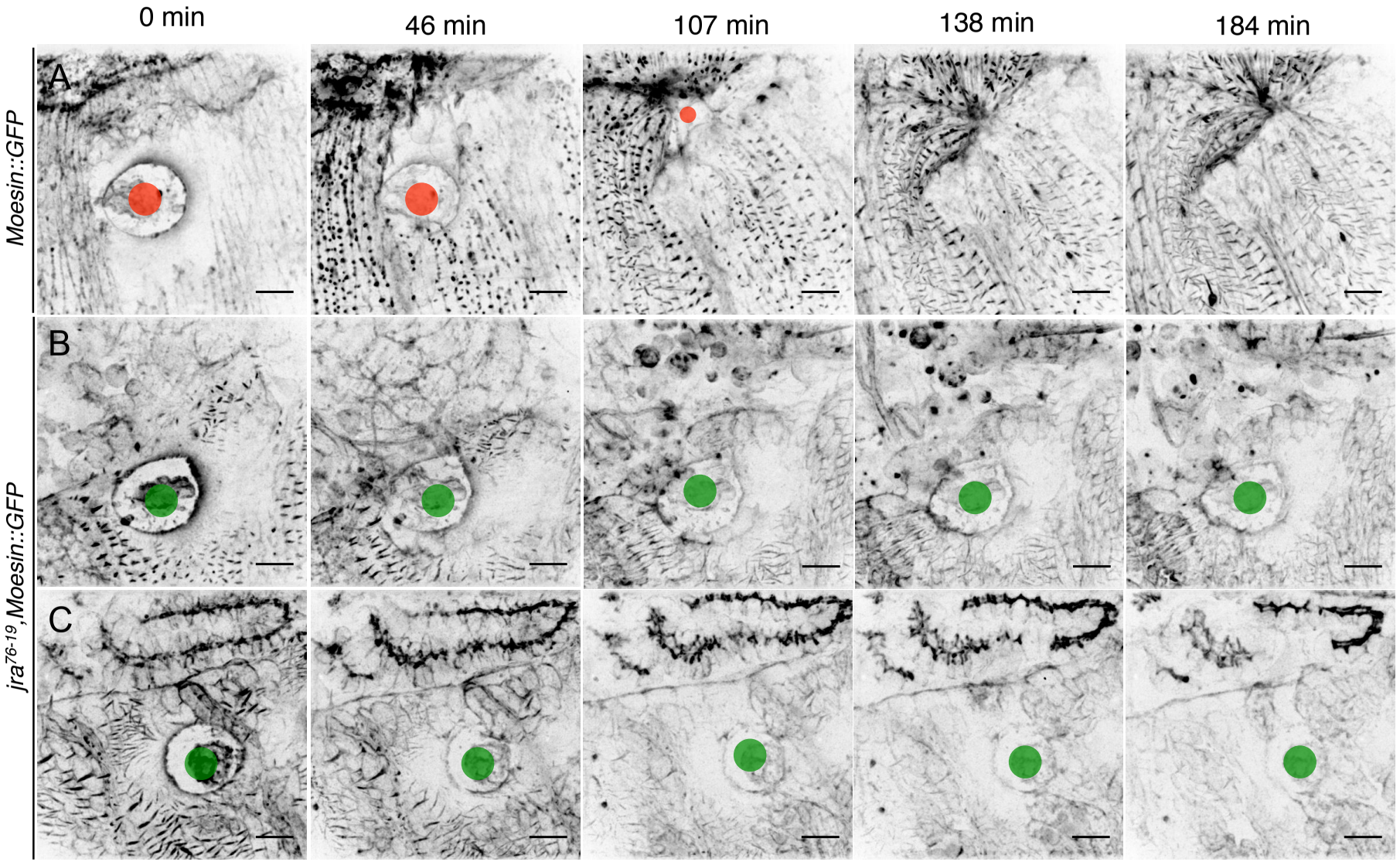

Figure 4. Stress-induced JNK is crucial for embryonic wound healing.
(A, C) Still images of a time-lapse movie of a representative *Moesin::GFP* (A) and *jra*$^{76\text{-}19}$*, Moesin::GFP* (B, C) embryos after a wound. Scale bar: 10 μm. The wound is healed within the next 138 in *Moesin::GFP* embryos. In *jra*$^{76\text{-}19}$ embryos, the healing process failed.

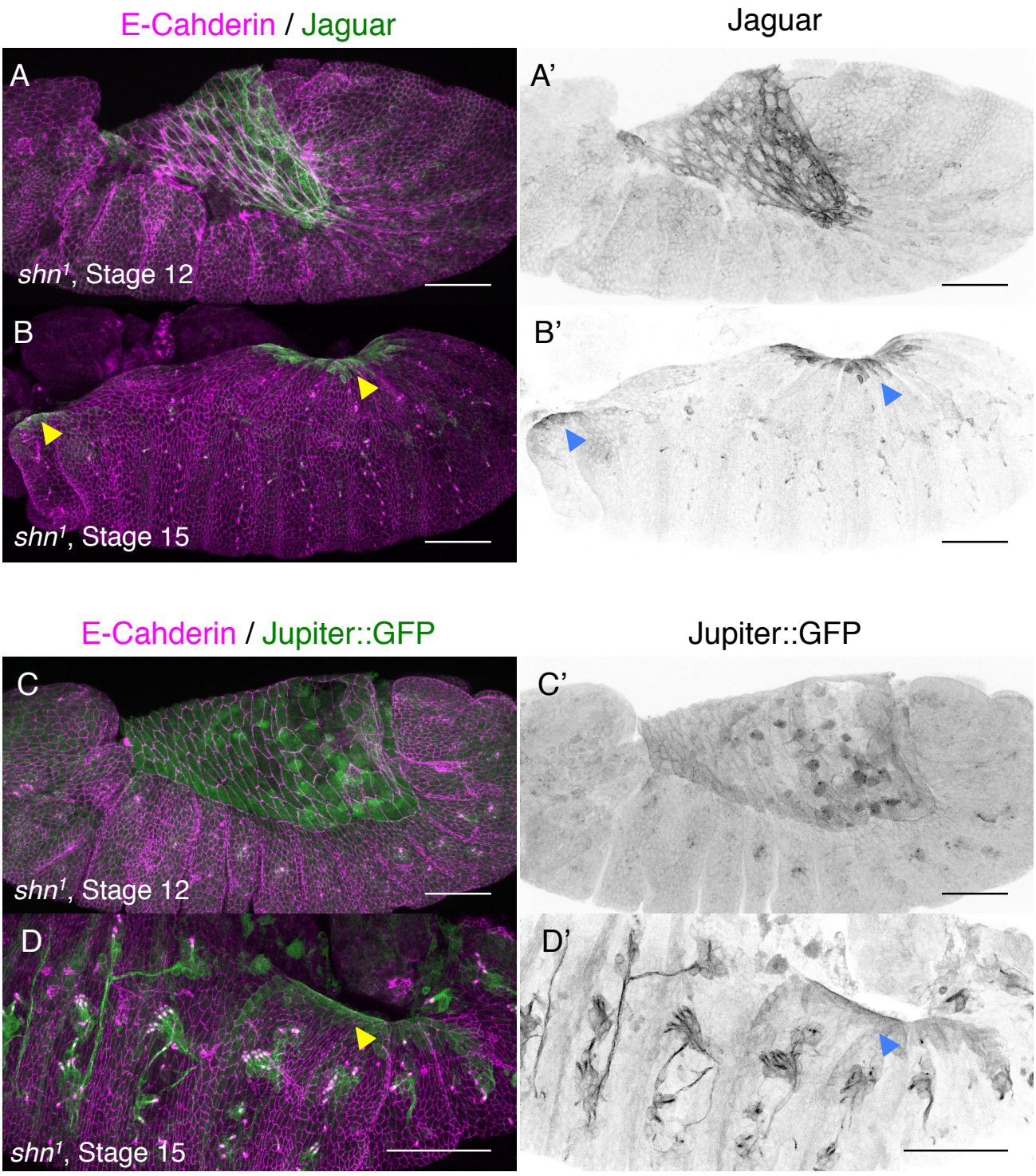

Figure S1. Late accumulation of Jupiter::GFP and Jaguar in *shn* mutant embryos.
(A-D) *shn¹* mutant embryos at stage 12 (A-A", C-C") or stage 15 (B-B", D-D") marked for E-Cadherin and Jar (A-B") or E-Cadherin and Jupiter::GFP (C-D"). Scale bar: 50 μm.
(A-B) At stage 12, Jupiter::GFP and Jar fail to accumulate at the leading edge of *shn¹* embryos, whereas they accumulate in groups of leading edge and lateral epidermal cells at stage 15 (arrowheads).

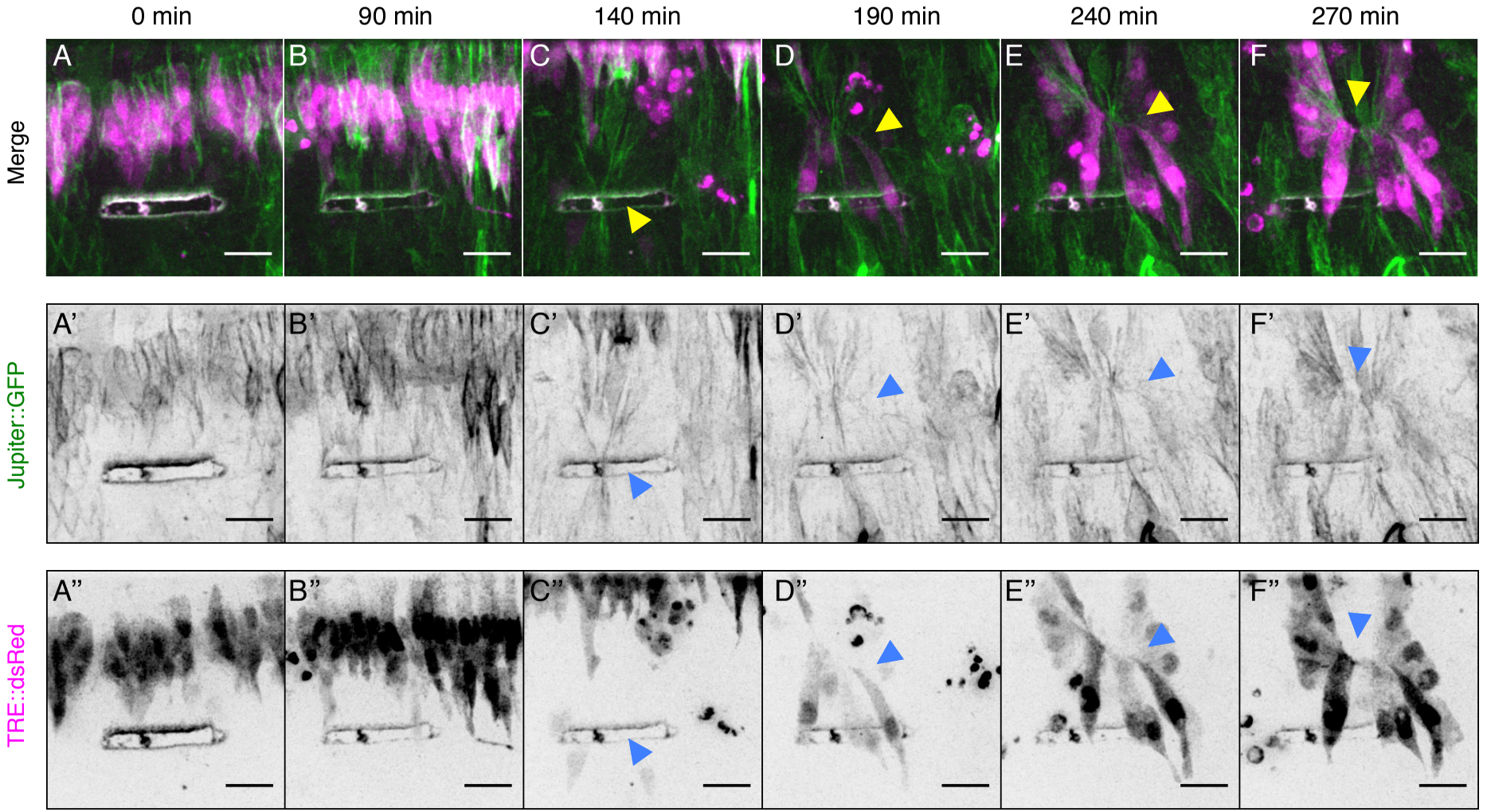

Figure S2. Jupiter::GFP acculmulates around wounds.

(A-F") Still images of a *Jupiter::GFP, TRE-dsRED* embryo after a wound. TRE-dsRed is in magenta (A-F) or grey (A"-F"), Jupiter::GFP is in green (A-F) or in grey (A'-F'). Scale bar: 10 μm.

Cells around the wound accumulate the JNK reporter TRE-dsRed that becomes more intense over time. Cells around the wound also accumulate Jupiter::GFP.

4. Cell death paper

While under the revision process of our JNK/DPP feed-forward paper, two of the three reviewers wanted us to comment on an article published after our initial submission in JCB. In this paper, Beira and colleagues showed that in DPP signalling mutant embryos, the pro-apoptotic gene reaper is expressed at the leading edge in a JNK dependant manner. According to them, the dorsal open phenotype would also be due to cell death at the leading edge. Therefore they set up a model where DPP via its co-repressor Shn prevents the JNK-induced apoptosis at the leading edge (Beira et al., 2014). I had the same idea and I tested this hypothesis one year before this paper was published: I marked *tkv* mutant embryos with cleaved caspase 3, an antibody that labels aopoptotic cells. I never detected any mark of cell death at the leading edge. Still, the Jean-Paul Vincent lab published the contrary, although they did not show a single caspase 3 staining in the article (some are provided in the supplemental information, but are not very convincing). I thus assessed precisely whether DPP signalling mutant embryos undergo JNK-dependent apoptosis at the leading edge.

Drosophila dorsal epidermis is refractory to JNK-induced apoptosis independently of DPP input

Antoine Ducuing[1] Bertrand Mollereau[1] and Stéphane Vincent[1*].

[1] LBMC, UMR5239 CNRS/Ecole Normale Supérieure de Lyon, SFR 128 Biosciences Lyon Gerland, Université de Lyon, Lyon, France

* Corresponding author: stephane.vincent11@ens-lyon.fr

Stéphane Vincent, Ph.D

LBMC, Ecole Normale Supérieure de Lyon

46 Allée d'Italie

69007 Lyon

France

Phone: +33 (0)4 72 72 85 74

Fax: +33 (0)4 72 72 86 74

Abstract

During development, JNK is a key signalling pathway that plays a dual role: it responds to stress and triggers apoptosis, or induces cell differentiation during patterning. A recent study in the *Drosophila* embryo by Beira and colleagues analyzed the regulation of the pro-apoptotic gene *reaper* and proposed that DPP signalling prevents JNK-induced *reaper* expression, thus blocks cell death and promotes leading edge cell differentiation. Here we question these conclusions and show that cells in the dorsal epidermis do not die when DPP signalling is impaired, even upon ectopic JNK activation. We further demonstrate that the cell death that contributes to the dorsal open phenotype of DPP signalling mutants does not occur in the dorsal epidermis, but in an extra-embryonic tissue, the amnioserosa. We conclude that DPP does not prevent cell death in this setting, and that the driving force of dorsal closure is JNK and DPP independent.

Introduction

Programmed cell death, or apoptosis, is a key cellular process during animal development, and the onset of this irreversible process is tightly controlled (Arya and White, 2015). During *Drosophila* development, cell death takes place in various processes such as the removal of unwanted cells from the central nervous system (Bergmann et al., 2002). By the same token, physiological cell death shapes future organs. For example, the elimination of amnioserosa cells generates tension forces that promote dorsal closure in the embryo (Toyama et al., 2008) and the elimination of cells in the pupal leg joints induces leg joint formation during metamorphosis (Monier et al., 2015). Apoptosis is regulated by the RHG family of proapoptotic genes that include *reaper (rpr)*, *head involution defective* (*hid*), *grim* and *sickle*. Specifically, these gene products antagonize the *Drosophila* inhibitor of apoptosis protein (DIAP1) and thus activate caspases (DRONC, DCP-1 and DRICE) (Mollereau, 2009). Apoptosis is induced in response to environmental stress such as irradiations to eliminate damaged cells in a JNK-dependent manner (Leppa and Bohmann, 1999; Igaki, 2009; Perez-Garijo et al., 2009; Dhanasekaran, 2013). Latent JNK activity is modulated by the *puckered* (*puc*) phosphatase that prevents unbridled apoptosis in both the fly embryo and imaginal discs (McEwen and Peifer, 2005). Interestingly, during dorsal closure JNK activates the expression of the BMP homologue DPP and patterns the dorsal-most epidermal cells so that they differentiate into leading edge cells (Glise and Noselli, 1997; Hou et al., 1997; Kockel et al., 1997; Riesgo-Escovar and Hafen, 1997; Riesgo-Escovar et al., 1997). Leading edge cells display a specific cytoskeletal configuration that leads to the accumulation and the polarization of microtubules (Kaltschmidt et al., 2002) as well as the formation of a transcellular

actomyosin cable and filopodia (Jacinto et al., 2000; Jacinto et al., 2002). In fact, the integrity of the actin cable can only be maintained in a way that no cell death occurs at the leading edge. Indeed, the dorsal epidermis is refractory to cell death as shown by the analysis of mutants deficient for the apical determinant *crumbs* (*crb*): In the *crb* mutant epidermis, most lateral and ventral cells undergo apoptosis but the dorsal epidermal cells, and thereby the future leading edge cells are spared (Kolahgar et al., 2011). What then is the factor that provides the competence to leading edge cells to interpret JNK as a differentiation factor and not a cell death inducer?

Recently, Beira and colleagues proposed an elegant model in which DPP signalling provides a survival signal that prevents the expression of the pro-apoptotic gene *reaper* (*rpr*), so that JNK can only be interpreted as a differentiation cue instead of a death signal in the dorsal epidermis (Beira et al., 2014). In addition to providing a conceptual framework to understand cell competence towards death or differentiation, this explanation also offers a re-interpretation of the "dorsal open" phenotype: in the absence of the DPP pathway components such as *thick veins (tkv)* or *shnurri (shn)* not only dorsal closure is aborted but the amnioserosa is also ripped away from the leading edge, resulting in gut extrusion and the so-called "dorsal open" phenotype. Beira and colleagues therefore highlight that unwanted apoptosis would be an important factor in the deleterious chain of events that leads to the dorsal open phenotype.

In order to understand the implication of apoptosis at the leading edge in the dorsal open phenotype, we analyzed cell dynamics during the failed dorsal closure process in *tkv* and *shn* mutants. In *Drosophila,* active cell death can be clearly visualized and tracked as dying cells exude on the basal side of the monolayered

epithelia in imaginal discs or embryos (Gibson and Perrimon, 2005; Toyama et al., 2008). Surprisingly, we did not identify any cell loss nor any sign of apoptosis in the dorsal epidermis in mutants defective for DPP signalling. We further found that JNK over-activation does not lead to apoptosis at the leading edge, whether or not DPP signalling is intact. Our data confirm that a singularly important determining factor of the dorsal open phenotype is the apoptotic force emanating from the amnioserosa as described by Toyama and colleagues, since there is no apoptosis in the dorsal epidermis. Our data strongly dispute the claim that DPP protects leading edge cells against apoptosis and rule out that the dorsal open phenotype of DPP signalling deficient embryos originates from cell death in the dorsal epidermis.

Results

Dorsal epidermal cells do not disappear in *tkv*^{4} *or shn*^{1} embryos

To verify the contribution of apoptosis to the dorsal open phenotype in the embryos deficient in DPP signalling, we closely monitored the dorsal epidermal cell behavior in live *tkv* or *shn* mutants before and during the dorsal closure process. We analyzed stage-13 *tkv* and *shn* mutant embryos, where apoptosis is reported to occur (Beira et al., 2014). We tracked individual cells marked by GFP-tagged junctional markers: Cadherin GFP-fusion (*shg::GFP)* expressed in *tkv* mutants, and Beta-catenin GFP fusion (Arm::GFP) expressed in *shn* embryos. We started tracking individual cells 90 minutes before the first sign of the dorsal open phenotype, and continued to image the epidermis for an additional 30 minutes. In this two-hour interval, every cell in the dorsal epidermal within the field of view, which sums to approximately 50 cells, stays alive and is accounted for (Fig. 1A-P, see also Movie S1 and S2 with color-coded cell

tracking). In other words, we did not observe a single event of cell delamination during this time interval. Therefore, contrary to what Beira and colleagues suggest, we conclude that epidermal cell disappearance does not occur and is hence unlikely to contribute to the dorsal open phenotype of *tkv* and *shn* mutants.

Leading edge cells in *tkv* or *shn* embryos do not display Caspase activity

Even though we failed in our attempt to identify and pinpoint dying cells in the dorsal epidermis, we admit the possibility that dorsal cells in the *tkv* or *shn* embryos may undergo slow cell death while remaining at their location. Beira and colleagues have detected activated caspase 3 staining in stage 12 *shn* mutants. The activated caspase-3 antibody recognizes cleavage products by Dronc (Fan and Bergmann, 2010), but it is now recognized that the sensitivity of this antibody may vary depending on the tissue and the batches of antibody production (K. Yacobi-Sharon and E. Arama, personal communication). We therefore analyzed tkv^{4} and shn^{1} mutant embryos with an antibody that recognizes the cleaved and active form of Death caspase-1 (DCP-1), but not the full length and hence inactive DCP-1 precursor (Song et al., 1997). We first verified that the anti cleaved DCP-1 specifically marks regions where apoptosis is known to take place in the embryo, but fails to light up in the *H99* embryos where apoptosis is impaired (Fig. S1). We then analyzed DCP-1 staining pattern in the dorsal epidermis of control and mutant embryos, first at stage 12 during germ band retraction, then at stage 13 during the early onset of the dorsal open phenotype, and finally at stage 14 where the dorsal open phenotype is fully manifested. We did not detect cleaved DCP-1 in the epidermis of either control, *shn* or *tkv* embryos (Fig. 2) in any of these stages. We have however detected cleaved DCP-1 in macrophages that can phagocytose dead amnioserosa cells during these

stages (Fig. 2I-L'). In addition, in the stage-12 control, *tkv* and *shn* mutant embryos, DCP-1 positive cells were present in the deeper confocal sections in the vicinity of Cut-positive neurons (Fig. 2B, D, F, Fig. S2). We carefully examined these DCP-1 positive cells and determined that they were in fact a subset of the Cut-positive neurons undergoing apoptosis (Fig. 3A-C''). Based on this observation, we assessed whether these cells marked by cleaved DCP-1 were neuroblasts by studying Numb expression in these cells. We found that a number of Numb-positive neuroblasts do undergo cell death in both DPP deficient embryos and control embryos (Fig. 3D-F''), yet we still failed to detect any cleaved DCP-1 in the dorsal epidermis. In sum, we conclude that not only the epidermal cells do not delaminate in *tkv* and *shn* embryos, but that they do not display caspase activity. Therefore, leading edge cells appear healthy in the absence of *tkv* or *shn*, indicating that during dorsal closure DPP signalling does not protect dorsal epidermal cells from cell death that is apparently non-existent. **Last, we extended our findings by marking *shn*^{TDS} embryos with DCP-1, E-Cahderin and Cut (Figure TDS_1). This way we used the very same allele as the one used by Jean-Paul Vincent. We NEVER detected cell death in the dorsal epidermis, but in lower sections that are corresponding to Cut-positive neurons or around trachea.**

JNK over-expression does no kill leading edge cells in *tkv* mutant embryos

The work by Beira and colleagues predicted that robust JNK activity could induce cell death at the leading edge in the absence of DPP signalling, which is detrimental to the dorsal closure process. Even though so far neither did we find delaminating cells in the dorsal epidermis, nor did we detect any caspase activity, one could argue that

perhaps the strength of JNK signalling is compromised in *tkv* or *shn* embryos compared to wild type embryos. This could potentially account for our failure to detect any apoptosis in different stages in different genetic backgrounds. We therefore determined to boost JNK signalling at the leading edge in the absence of DPP signalling, and examine if robust JNK signalling alone can induce apoptosis in the dorsal epidermis. First, as a positive control, we over-expressed Rpr in *paired* stripes in the epidermis and observed massive apoptosis across both the dorsal and lateral epidermis (Fig. 4A-A'''). We next over-activated JNK signalling by over-expressing an activated form of the JNK kinase *hemipterous* (*hep*^{ACT}) that induces apoptosis when over-expressed in wing imaginal discs (Perez-Garijo et al., 2009). We reasoned that ectopic JNK should lead to *rpr* mRNA upregulation and therefore to cell death. We monitored ectopic JNK territory with the JNK target Jaguar (Jar) (Ducuing et al., 2015). Although Jaguar was strongly induced by *hep*^{ACT} in the leading edge cells, we found no trace of DCP-1 staining in this region. Interestingly, the ectopic Jar territory became narrower in the lateral epidermis, the only region where concomitant DCP-1 staining was present (Fig. 4B-B'). Therefore, ectopic JNK activity induces DCP-1 cleavage in the lateral epidermis but not in the dorsal epidermis, which is refractory to JNK induced cell death.

Next, we focused on the dorsal cells that receive JNK signalling and differentiate as leading edge cells in the wild type embryo. We tested whether strong JNK over-activation can kill these cells in the absence of DPP signalling. We marked the ectopic JNK activity with the reporter DPP-lacZ (Blackman et al., 1991). Importantly no DCP-1 was detected in lacZ-positive nuclei, suggesting that even though these cells correctly activate the target Dpp-lacZ as a response to JNK over-

activation, they do not undergo apoptosis. (Fig. 4C-D'', arrowheads, Fig. S3). Thus, we conclude that even robust and continuous JNK activity in the absence of DPP signalling fails to induce cell-death at the leading edge. Altogether, our data show that the cells in the dorsal epidermis are competent to undergo apoptosis when Rpr is over-activated, but not when JNK is activated in the absence of Dpp.

Inhibition of apoptosis in the amnioserosa, but not in the dorsal epidermis rescues *tkv* dorsal open phenotype

Beria and colleagues provided genetic evidence that apoptosis takes place in the dorsal epidermis and must play an important role in the dorsal closure phenotype: they observed that in *shn* mutant embryos, the dorsal open phenotype is rescued in the background of the *Df(3L)X38* deficiency that spans *rpr, sickle* and the regulatory region of *grim* (Tan et al., 2011). However, as we did not find any evidence that suggests cell death in the dorsal epidermis, we reasoned that the apoptosis inferred from this particular experiment originates from an entirely different tissue: the neighboring amnioserosa. During dorsal closure, about 10 to 30% of the amnioserosa cells undergo apoptosis and delaminate in a stochastic fashion (Kiehart et al., 2000; Toyama et al., 2008). In addition, enhancing or reducing apoptosis in the amnioserosa accelerates or slows dorsal closure respectively, indicating that cell death in the amnioserosa fine-tunes the speed of closure (Toyama et al., 2008; Muliyil et al., 2011). We reasoned that physiological amnioserosa cell death and cell delamination must generate a tension that disrupts the amnioserosa-epidermis contact in DPP signalling mutant embryos. To test this hypothesis, we inactivated cell death specifically in the lateral epidermis or in the amnioserosa of tkv^4 mutant embryos by over-expressing the caspase inhibitor p35. Blocking apoptosis by p35 in

the lateral epidermis with the *pannier* (*pnr*) driver does not rescue the dorsal-open phenotype: The amnioserosa is ripped away, and the gut is extruded (Fig 5 A-D"). However, blocking apoptosis specifically in the amnioserosa rescues of the dorsal open phenotype, similar to what Beria and colleagues observed with *shn, Df(3L)X38* embryos (Fig 5E-F'). Specifically, In the presence of p35 driven by amnioserosa-specific GAL4, the amnioserosa is fully present and remains attached to the lateral epidermis and the gut does not protrude. In these embryos, closure proceeds slowly since leading edge cell differentiation is impaired, but the dorsal open phenotype is rescued. Thus, blocking apoptosis in the amnioserosa prevents its apical reduction, and therefore protects embryos against the dorsal open phenotype.

Discussion

DPP does not protect leading edge cells against apoptosis.

In a recent study, Beira and colleagues proposed that DPP signalling is the source of the competence that grants the dorsal epidermal cells of the *Drosophila* embryo to interpret JNK as a differentiation signal rather than a pro-apoptotic stimulus. In this context, JNK and DPP would form an incoherent feed-forward loop that controls the expression of the proapoptotic gene *reaper*: JNK induces *dpp* and *rpr*, but DPP represses *rpr*. Our data argue against this model. First, we show that in the absence of Dpp signalling, as a result of *tkv* or *shn* mutation, the cells in the dorsal epidermis remain alive and intact, and do not display caspase activity. Encompassing all the stages that we examined, the only cells that potentially undergo apoptosis are a subset of neurons beneath the epidermis, whether in a wild-type or a Dpp signalling

mutant embryo. Therefore, there is no apoptosis in the dorsal epidermis per se to protect from.

Furthermore, leading edge cells do not die either upon robust induction of JNK alone or in the absence of DPP signalling. In fact, the only condition where we detected apoptosis in the dorsal epidermis was upon Rpr induction. Beira and colleagues have also shown that *rpr* transcript is up-regulated in *shn* and *tkv* homozygous embryos. We firmly believe the validity of this observation and thus assume that in our *shn* and *thv* embryos, *rpr* transcript level must be similarly elevated. However, such elevation in rpr transcript fails to translate into the classic cell death behavior such as delamination and extrusion, or elicit caspase activity in the dorsal epidermis. If not for inducing apoptosis, the explanation of such up-regulation of rpr may be intriguing, but it is beyond the scope of this study to find it mechanistically. It can also suggest that a DPP-independent post-transcriptional regulation limits Rpr activity. Nevertheless, in the leading edge cells, the JNK activation and Rpr induction are unexpectedly uncoupled. The dorsal epidermal cells are competent to undergo apoptosis, but the identity of the factor(s) that protect these dorsal epidermal cells against apoptosis is not DPP.

The dorsal open phenotype does not stem from apoptosis in the dorsal epidermis

Beira and colleagues proposed that apoptosis in the dorsal epidermis is contributing to the dorsal open phenotype of embryos deficient in Dpp signalling. We tested this hypothesis by expressing the apoptosis inhibitor P35 at the leading edge of *tkv* mutants and showed that there is no rescue of the dorsal open phenotype. On the other hand, preventing cell death specifically in the amnioserosa rescues the dorsal

open phenotype, as the amnioserosa remains attached to the leading edge. Therefore, our data indicate that the well-described apoptotic force originating from the amnioserosa is the major culprit that ruptures the tissue, which consequently leads to the dorsal open phenotype (Toyama et al., 2008).

In addition of its role at the leading edge, DPP controls graded *U-shaped* (*Ush*) expression in the amnioserosa (Lada et al., 2012). *Ush* may in turn regulate the cytoskeleton or cell adhesion in order to potentiate dorsal closure. Whether DPP regulates the contractile activity of the amnioserosa is still intensely debated. Indeed, the dynamics within the amnioserosa is the main driver of tissue movement during dorsal closure (Wells et al., 2014). As we show that the apoptotic force in the amnioserosa generates a tension that eventually leads to the dorsal open phenotype in mutants where Dpp signalling is disrupted, we propose that the apoptotic force exerted by the amnioserosa is mostly DPP independent.

DPP function during dorsal closure

We recently described a coherent feed forward loop (FFL) integrating the action of JNK and DPP signalling. In this FFL, JNK induces DPP expression and both signals are simultaneously required for the differentiation of leading edge cells (Ducuing et al., 2015). Furthermore, we demonstrated that DPP robustly filters out aberrant short bursts of JNK signals so that cells do not mistake them as cues for differentiation. Our model implies that in order for leading edge cells to differentiate, JNK activity must be stable and long-lasting enough for DPP to be produced, to accumulate in the extracellular space, reach its activity threshold and prevent the repressive action of the transcription factor Brinker. Here we demonstrate that DPP is

not involved in protection against cell death and is not required in the amnioserosa to generate the driving force of the amnioserosa, therefore the main function of DPP during dorsal closure is dedicated to filter JNK signalling so that morphogenesis is robust and faithful.

Experimental procedures

Fly strains and genetics

We used the following lines: *CantonS (WT)*, *tkv*^{4} (amorphic allele, point mutation), *shn*^{1} */ Cyo, Wg::lacZ* (amorphic allele, # BL 3008)*, Prd-Gal4* (# BL 1947), *Pnr-Gal4* (# BL 3039), *c381-Gal4* (# BL 3734), *UAS-hep*^{ACT} (# BL 9306), *UAS-GFP*^{NLS} (# BL 4776), *UAS-APC2::GFP* (# BL 8815), *UAS-rpr* (*rpr* coding sequence under the control of a promoter containing UAS sequence, Kind gift from Véronique Morel), *UAS-p35* (# BL 5073), *shg::GFP* (*shg::GFP* construct replacing the endogenous *shg* gene via targeted site-specific DNA integration, see (Huang et al., 2009)), *Arm::GFP* (# BL 8555), *DPP-lacZ*^{NUCLEAR} (lacZ-NLS coding sequence cloned after the BS 3.0 promoter of DPP, see (Blackman et al., 1991)). All crosses were performed at 25°C.

Immunofluorescence

We used standard techniques of immunofluorescence as described in Ducuing et al., 2014. Embryos were bleached for 3 minutes, fixed in a 1:1 mix of 4% PFA–Heptane. Embryos were devitellinized by replacing the PFA phase with methanol and then vigorously shaken for 15 seconds. Samples were washed with Methanol, then 1X PBS-0.1% Triton. Samples were then incubated with primary antibodies for 1h30, then with fluorescent-coupled secondary antibodies for 1h30 and eventually mounted in VectaShield with or without DAPI.

We used the following primary antibodies: rabbit anti cleaved DCP-1 (Cell Signalling, 1:500), mouse anti-lacZ (Sigma G4644, 1:250), rabbit anti-lacZ (Cappel, 1:100), mouse anti-Jar 3C7 (Kellerman and Miller, 1992)(1:100), rat anti DE-Cadherin (DSHB, 1:333), mouse anti Cut (DSHB, 1:250), Goat anti Numb (Santa Cruz Biotechnology, 1:250). Secondary antibodies are from Invitrogen and were used at 1:500. We used the following secondary antibodies: Alexa Donkey anti-Mouse 488, Alexa Goat anti-Mouse 633, Alexa Donkey anti-Rat 488, Alexa Goat anti-Rat 633, Alexa Donkey anti-Rabbit 488, Alexa Goat anti-Rabbit 546, Alexa Donkey anti-Guinea Pig 546. For Fig. 4D and 4E, samples were incubated with Rabbit anti-lacZ in addition of the Rabbit anti-DCP-1 in order to identify the embryos carrying the wg-lacZ balancer.

Image processing

Images were acquired on the Confocal Leica SP5 AOBS CLSM microscope with the following objectives: MULTI IMMERSION 20X Oil (numerical aperture: 0.7), HCX PL APO 40X Oil (numerical aperture: 1.25) and HCX PL APO 63X 1.4-0.6 Oil (numerical aperture: 1.4) using the acquisition software LASAF at the PLATIM facility and analyzed with ImageJ.

Live imaging

Unless otherwise indicated, all crosses were performed at 25°C. Stage 12 embryos were dechorionated, staged and aligned in Halocarbon oil 27 (Sigma, H8773) and then imaged at 25°C with a Leica spinning disk, with a 100X immersion objective (numerical aperture: 1.4) with a Andor iXon3 camera using the acquisition software

Metamorph. For Figure 2, *tkv^{4},shg::GFP / CKG (Cyo, Kr>GFP)* embryos where aligned and selected against the green fluorescent balancer. For Figure 3, w ; *shn^{1}/ CyO ; +* females where crossed with *w ; + ; Arm-GFP* males. *shn^{1}/+ ; Arm-GFP/+* males and females where crossed together to analyze the progeny. The correct genotype was confirmed by the dorsal open phenotype.

Supplemental online information

Fig. S1 shows DCP-1 staining in stage 11, 12 and 13/14 WT embryos and in Control and *H99* stage 14 embryos. Fig. S2 is an extended version of Fig. 2 with individual sections used for Fig. 2A-E'' panels. Fig. S3 is an extended version of Fig. 4 with individual sections used for Fig. 4C-D''''. Video 1 is a live recording of a *tkv^{4}, shg ::GFP* embryo at 25°C. Video 2 is a live recording of a *shn^{1}, Arm ::GFP/+* embryo at 25°C.

Acknowledgement

We thank the ARTHRO-TOOLS and PLATIM facilities of the UMS3444 and Bloomington and the Developmental Studies Hybridoma Bank for reagents.

We thank Dali MA for the critical reading of this manuscript.

This work was supported by a Chair from the Centre National de la Recherche Scientifique to S. Vincent.

The authors declare no competing financial interests.

References

Arya, R., and White, K. (2015). Cell death in development: Signalling pathways and core mechanisms. Seminars in cell & developmental biology.

Beira, J.V., Springhorn, A., Gunther, S., Hufnagel, L., Pyrowolakis, G., and Vincent, J.P. (2014). The Dpp/TGFbeta-Dependent Corepressor Schnurri Protects Epithelial Cells from JNK-Induced Apoptosis in Drosophila Embryos. Developmental cell *31*, 240-247.

Bergmann, A., Tugentman, M., Shilo, B.Z., and Steller, H. (2002). Regulation of cell number by MAPK-dependent control of apoptosis: a mechanism for trophic survival signalling. Developmental cell *2*, 159-170.

Blackman, R.K., Sanicola, M., Raftery, L.A., Gillevet, T., and Gelbart, W.M. (1991). An extensive 3' cis-regulatory region directs the imaginal disk expression of decapentaplegic, a member of the TGF-beta family in Drosophila. Development *111*, 657-666.

Dhanasekaran, D.N. (2013). JNK Signalling Network and Cancer. Genes Cancer *4*, 332-333.

Ducuing, A., Keeley, C., Mollereau, B., and Vincent, S. (2015). A DPP-mediated feed-forward loop canalizes morphogenesis during Drosophila dorsal closure. The Journal of cell biology *208*, 239-248.

Fan, Y., and Bergmann, A. (2010). The cleaved-Caspase-3 antibody is a marker of Caspase-9-like DRONC activity in Drosophila. Cell death and differentiation *17*, 534-539.

Gibson, M.C., and Perrimon, N. (2005). Extrusion and death of DPP/BMP-compromised epithelial cells in the developing Drosophila wing. Science *307*, 1785-1789.

Glise, B., and Noselli, S. (1997). Coupling of Jun amino-terminal kinase and Decapentaplegic signalling pathways in Drosophila morphogenesis. Genes Dev *11*, 1738-1747.

Hou, X.S., Goldstein, E.S., and Perrimon, N. (1997). Drosophila Jun relays the Jun amino-terminal kinase signal transduction pathway to the Decapentaplegic signal transduction pathway in regulating epithelial cell sheet movement. Genes & development *11*, 1728-1737.

Huang, J., Zhou, W., Dong, W., Watson, A.M., and Hong, Y. (2009). From the Cover: Directed, efficient, and versatile modifications of the Drosophila genome by genomic engineering. Proc Natl Acad Sci U S A *106*, 8284-8289.

Igaki, T. (2009). Correcting developmental errors by apoptosis: lessons from Drosophila JNK signalling. Apoptosis *14*, 1021-1028.

Jacinto, A., Wood, W., Balayo, T., Turmaine, M., Martinez-Arias, A., and Martin, P. (2000). Dynamic actin-based epithelial adhesion and cell matching during Drosophila dorsal closure. Current biology : CB *10*, 1420-1426.

Jacinto, A., Wood, W., Woolner, S., Hiley, C., Turner, L., Wilson, C., Martinez-Arias, A., and Martin, P. (2002). Dynamic analysis of actin cable function during Drosophila dorsal closure. Current biology : CB *12*, 1245-1250.

Kaltschmidt, J.A., Lawrence, N., Morel, V., Balayo, T., Fernandez, B.G., Pelissier, A., Jacinto, A., and Martinez Arias, A. (2002). Planar polarity and actin dynamics in the epidermis of Drosophila. Nature cell biology *4*, 937-944.

Kellerman, K.A., and Miller, K.G. (1992). An unconventional myosin heavy chain gene from Drosophila melanogaster. The Journal of cell biology *119*, 823-834.

Kiehart, D.P., Galbraith, C.G., Edwards, K.A., Rickoll, W.L., and Montague, R.A. (2000). Multiple forces contribute to cell sheet morphogenesis for dorsal closure in Drosophila. The Journal of cell biology *149*, 471-490.
Kockel, L., Zeitlinger, J., Staszewski, L.M., Mlodzik, M., and Bohmann, D. (1997). Jun in Drosophila development: redundant and nonredundant functions and regulation by two MAPK signal transduction pathways. Genes & development *11*, 1748-1758.
Kolahgar, G., Bardet, P.L., Langton, P.F., Alexandre, C., and Vincent, J.P. (2011). Apical deficiency triggers JNK-dependent apoptosis in the embryonic epidermis of Drosophila. Development *138*, 3021-3031.
Lada, K., Gorfinkiel, N., and Martinez Arias, A. (2012). Interactions between the amnioserosa and the epidermis revealed by the function of the u-shaped gene. Biology open *1*, 353-361.
Leppa, S., and Bohmann, D. (1999). Diverse functions of JNK signalling and c-Jun in stress response and apoptosis. Oncogene *18*, 6158-6162.
McEwen, D.G., and Peifer, M. (2005). Puckered, a Drosophila MAPK phosphatase, ensures cell viability by antagonizing JNK-induced apoptosis. Development *132*, 3935-3946.
Mollereau, B. (2009). Cell death: what can we learn from flies? Editorial for the special review issue on Drosophila apoptosis. Apoptosis : an international journal on programmed cell death *14*, 929-934.
Monier, B., Gettings, M., Gay, G., Mangeat, T., Schott, S., Guarner, A., and Suzanne, M. (2015). Apico-basal forces exerted by apoptotic cells drive epithelium folding. Nature *518*, 245-248.
Muliyil, S., Krishnakumar, P., and Narasimha, M. (2011). Spatial, temporal and molecular hierarchies in the link between death, delamination and dorsal closure. Development *138*, 3043-3054.
Perez-Garijo, A., Shlevkov, E., and Morata, G. (2009). The role of Dpp and Wg in compensatory proliferation and in the formation of hyperplastic overgrowths caused by apoptotic cells in the Drosophila wing disc. Development *136*, 1169-1177.
Riesgo-Escovar, J.R., and Hafen, E. (1997). Drosophila Jun kinase regulates expression of decapentaplegic via the ETS-domain protein Aop and the AP-1 transcription factor DJun during dorsal closure. Genes & development *11*, 1717-1727.
Riesgo-Escovar, J.R., Hafen, E., Hou, X.S., Goldstein, E.S., Perrimon, N., Glise, B., Noselli, S., Kockel, L., Zeitlinger, J., Staszewski, L.M*., et al.* (1997). Connecting up the pathways in Drosophila development. Trends Cell Biol *7*, 421-422.
Song, Z., McCall, K., and Steller, H. (1997). DCP-1, a Drosophila cell death protease essential for development. Science *275*, 536-540.
Tan, Y., Yamada-Mabuchi, M., Arya, R., St Pierre, S., Tang, W., Tosa, M., Brachmann, C., and White, K. (2011). Coordinated expression of cell death genes regulates neuroblast apoptosis. Development *138*, 2197-2206.
Toyama, Y., Peralta, X.G., Wells, A.R., Kiehart, D.P., and Edwards, G.S. (2008). Apoptotic force and tissue dynamics during Drosophila embryogenesis. Science *321*, 1683-1686.
Wells, A.R., Zou, R.S., Tulu, U.S., Sokolow, A.C., Crawford, J.M., Edwards, G.S., and Kiehart, D.P. (2014). Complete canthi removal reveals that forces from the amnioserosa alone are sufficient to drive dorsal closure in Drosophila. Molecular biology of the cell *25*, 3552-3568.

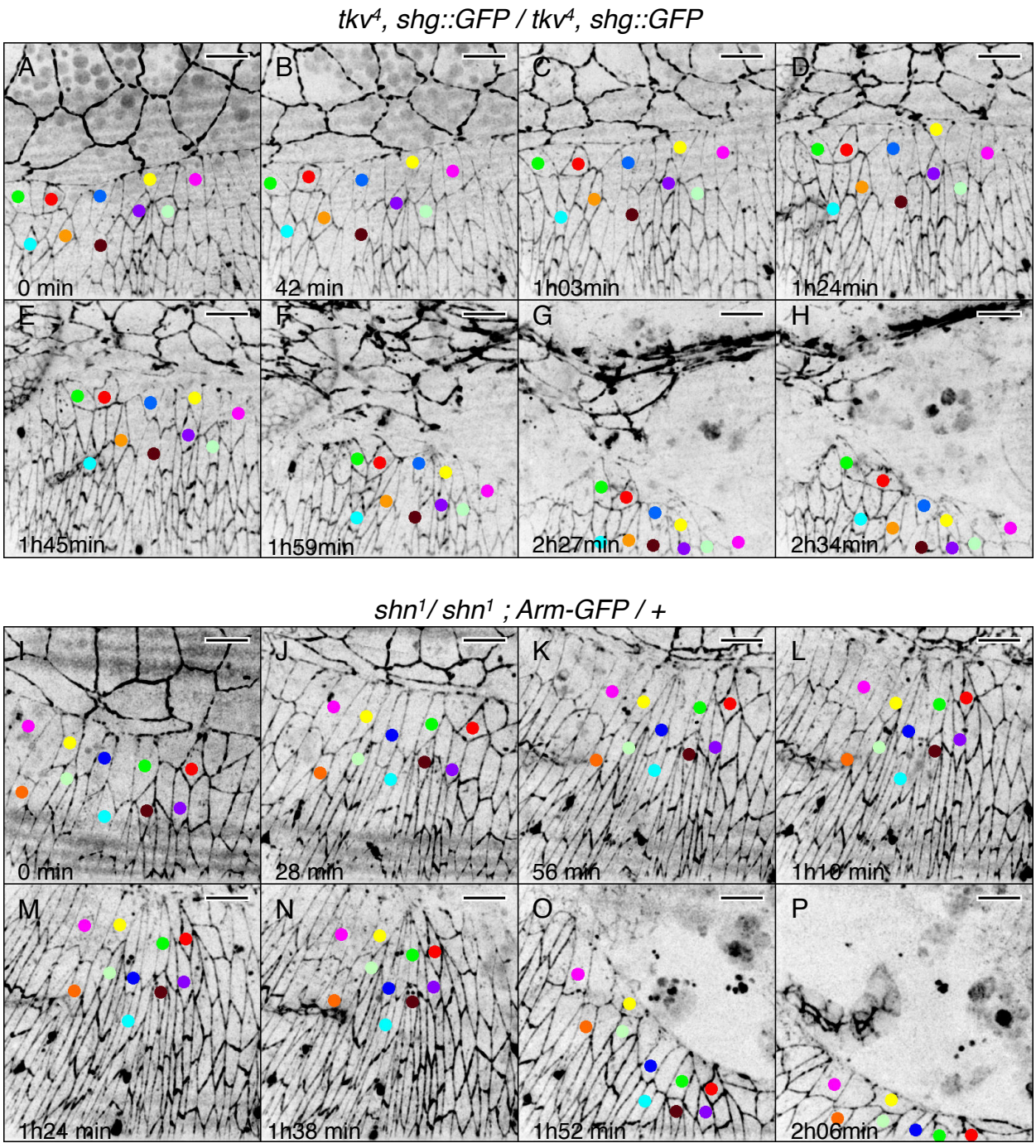

Figure 1 (Ducuing *et al.*)

Figure 1. Dorsal epidermal cells do not disappear in *tkv*^{4} *or shn*^{1} embryos

(A-P) Still images from time lapse movie of a *tkv*^{4}*, shg::GFP* embryo (A-H) and a *shn*^{1} *; Arm::GFP/+* embryo (I-P). All images are projections of confocal sections. Scale bar: 10 μm. About 5 leading edge and 5 dorsal epidermal cells have been tracked during the process. All the tracked cells and the cells in between tracked cells are present at the end of the process, even when the AS/LE junction breaks. See also Movie S1 and S2.

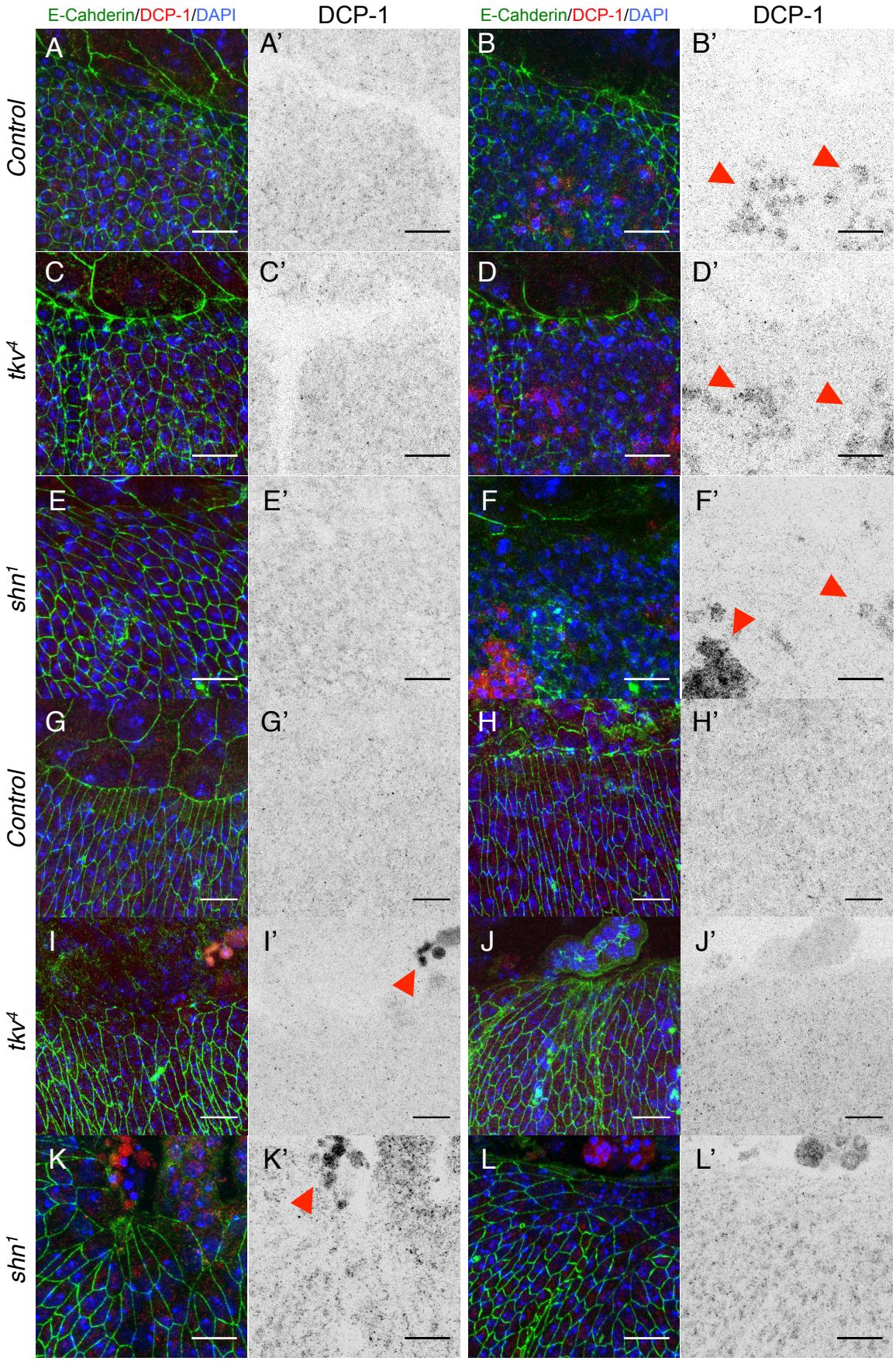

Figure 2 (Ducuing *et al.*)

Figure 2. Cleaved DCP-1 is not detected in the dorsal epidermis of DPP signalling mutant embryos.

Control (A, B, G and H), *tkv*^{4} (C, D, I and J) or *shn*^{1} (E, F, K and L) mutant embryos at stage 12 (A-F'), stage 13 (G, I and K) or stage 14 (H, J and L) stained for DAPI (blue), E-cadherin (green) and DCP-1 (red). All images are projections of confocal sections. Scale bar: 10 μm.

(A-F') No DCP-1 staining is detected in the dorsal epidermis of both control, *tkv*^{4} and *shn*^{1} mutant embryos at stage 12. DCP-1 is detected in lower sections of the same embryos (B, D, F). See also Figure S1.

(G-L') No DCP-1 staining is detected in the lateral epidermis of control, *tkv*^{4} and *shn*^{1} mutant embryos at stage 13 (G, I and K) and stage 14 (H, J and L).

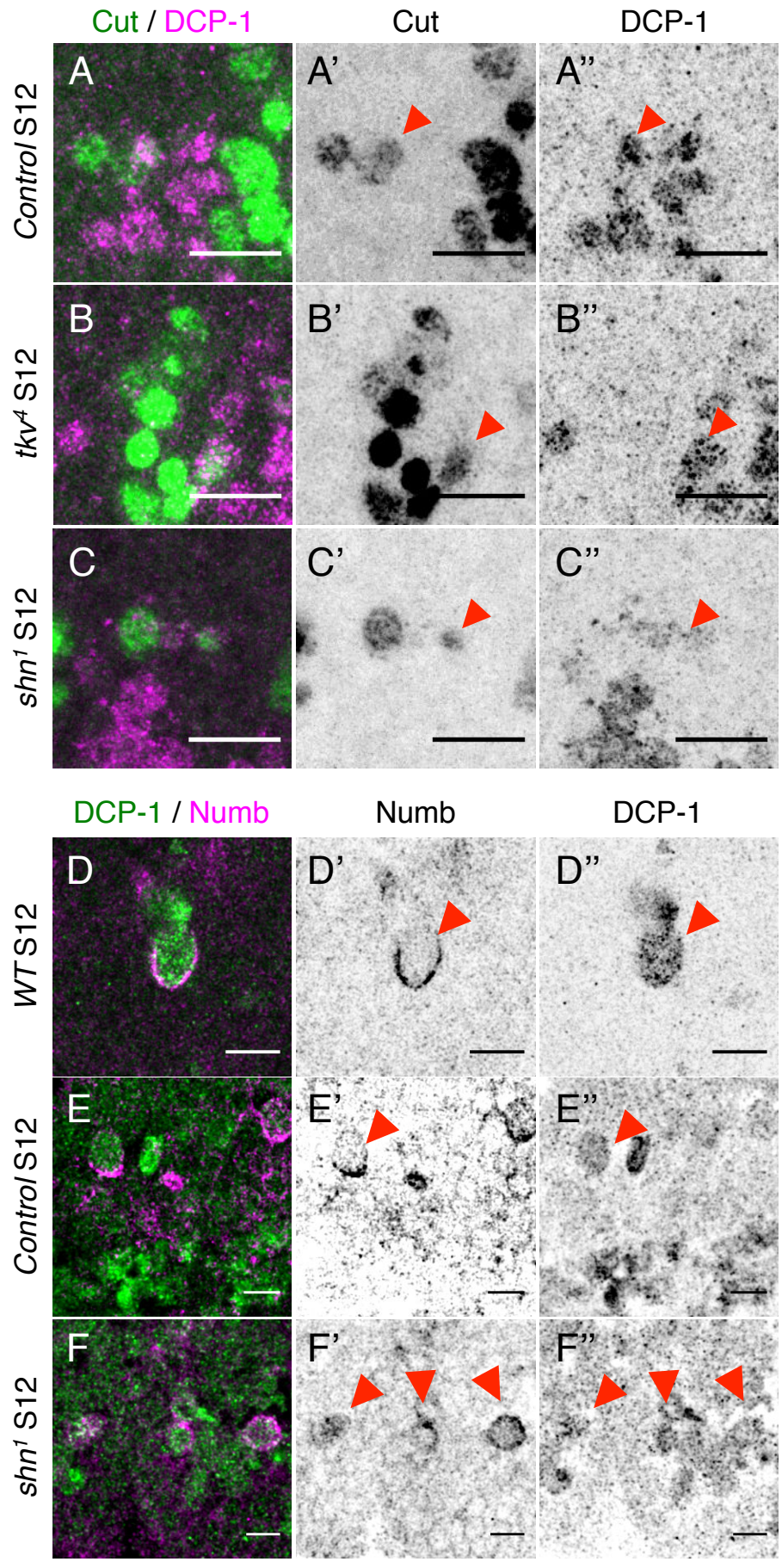
Cut / DCP-1
Cut
DCP-1
A
A'
A''
Control S12
B
B'
B''
tkv4 S12
C
C'
C''
shn1 S12
DCP-1 / Numb
Numb
DCP-1
D
D'
D''
WT S12
E
E'
E''
Control S12
F
F'
F''
shn1 S12

Figure 3. Neuroblasts and Cut-positive neurons display DCP-1 staining in stage 12 embryos.

(A-C) Control (A-A"), *tkv*^{4} (B-B") and *shn*^{1} (C-C") stage 12 embryos marked for Cut (green in A-C, grey in A'-C') and DCP-1 (magenta in A-C, grey in A''-C''). All images are projections of confocal sections. Scale bar: 10 μm. Cut-positive neurons are DCP-1-positive, indicating that they undergo apoptosis (arrowheads). Please note that Cut-levels are reduced in these apoptotic neurons.

(D-F) *WT* (D-D"), Control (E-E") and *shn1* (F-F") stage 12 embryos marked for DCP-1 (green in D-F, grey in D''-F'') and Numb (magenta in D-F, grey in D'-F'). All images are single confocal sections. Scale bar: 10 μm. DCP-1 can be detected in Numb-positive Neuroblasts (arrowheads).

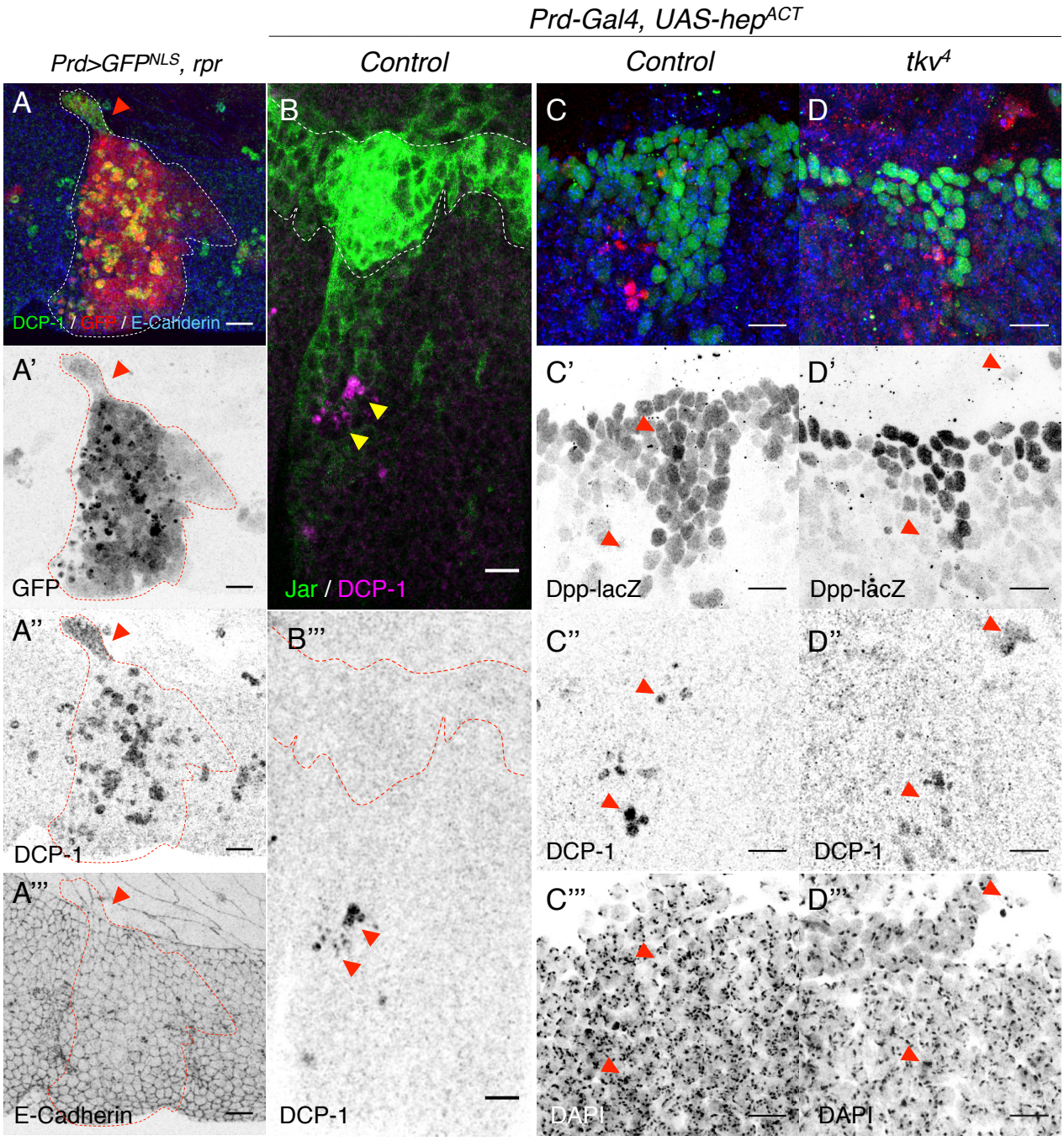

Figure 4 (Ducuing *et al.*)

Fig. 4 JNK over-expression does no kill leading edge cells even in the absence of DPP signalling.

(A) *Prd-Gal4, UAS-GFP^{NLS}, UAS-rpr* embryos marked for GFP (red in E, grey in E'), DCP-1 (green in E, grey in E") and E-Cadherin (blue in E, grey in E''). All images are projections of confocal sections. Scale bar: 10 μm. The dashed lines delineate *paired* expressing cells. *rpr* ectopic expression leads to cell death in the dorsal epidermis and in the amnioserosa (arrowhead).

(B-B') Single section of a *Prd-Gal4, UAS-hep^{ACT}* embryo stained for Jar (green) and DCP-1 (magenta in B, grey in B'). Scale bar: 10 μm. In the lateral epidermis where ectopic Jar gets narrower DCP-1 positive cells are detected (arrowheads).

(C-D) *Prd-Gal4, UAS-hep^{ACT}, Dpp-lacZ* (C) and *tkv^{4}, Prd-Gal4, UAS-hep^{ACT}, Dpp-lacZ* (D) embryos marked for DPP-lacZ (green in C and D, grey in C' and D'), DCP-1 (red in C and D, grey in C" and D") and DAPI (blue in C and D, grey in C''' and D''') The ectopic JNK territory is marked with nuclear lacZ. All images are projections of confocal sections. Scale bar: 10 μm. The arrowheads indicate DCP-1 positive cells (see also Figure S2). DCP-1 is never detected at the leading edge, even in the absence of DPP signalling.

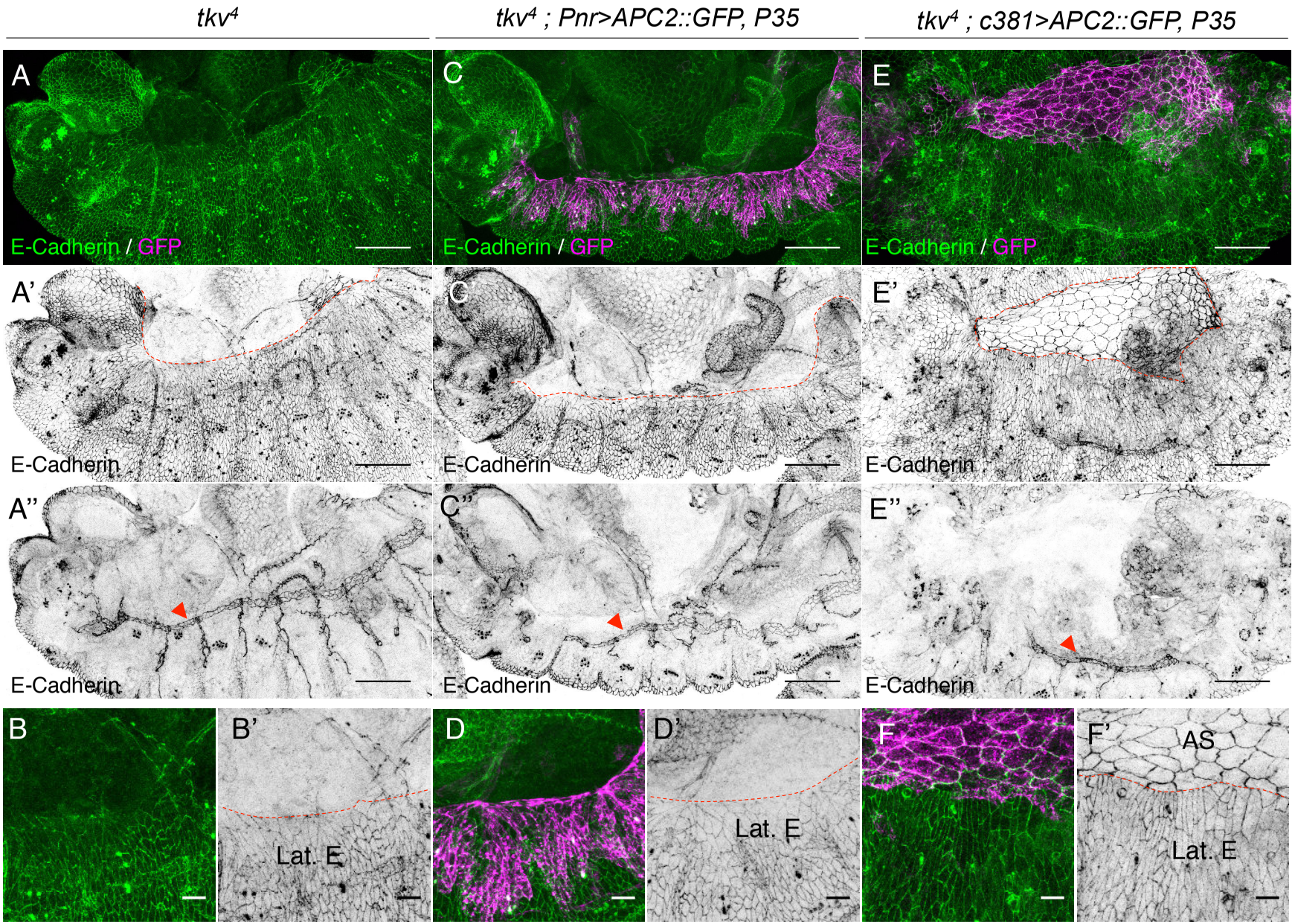

Figure 5 (Ducuing *et al.*)

Fig. 5 Blocking apoptosis selectively in the aminoserosa but not in the lateral epidermis rescues the "dorsal open" phenotype of *tkv*^{4} mutant embryos.

(A-F) *tkv*^{4} (A-B'), *tkv*^{4}*, Pnr-Gal4, UAS-APC2::GFP, UAS-P35* (C-D') and *tkv*^{4}*, c381-Gal4, UAS-APC2::GFP, UAS-p35* (E-F') embryos marked for E-Cadherin (green or grey in all panels) and GFP (magenta in all panels). All panels are projections of confocal sections. Scare bar is 50 μm for A-A", C-C" and E-E" panels, 10 μm for B-B', D-D', F-F' panels. The dashed lines delineate the leading edge. *tkv*^{4} homozygous embryos were determined by the absence of dorsal tracheal branches (A", C", E", arrowheads). (A-D') P35 overexpression in the dorsal epidermis of *tkv*^{4} embryos leads to a similar "dorsal open" phenotype as *tkv*^{4} embryos. The amnioserosa (AS) is ripped away, and the digestives organs are dorsally extruded. P35 over expression in the amniosrrosa of *tkv*^{4} embryos rescues the dorsal open phenotype. The amnioserosa (AS), labeled with GFP in E and F is intact and still attached to the lateral epidermis (F-F', Lat. E). The digestive organs are still present under the amnioserosa.

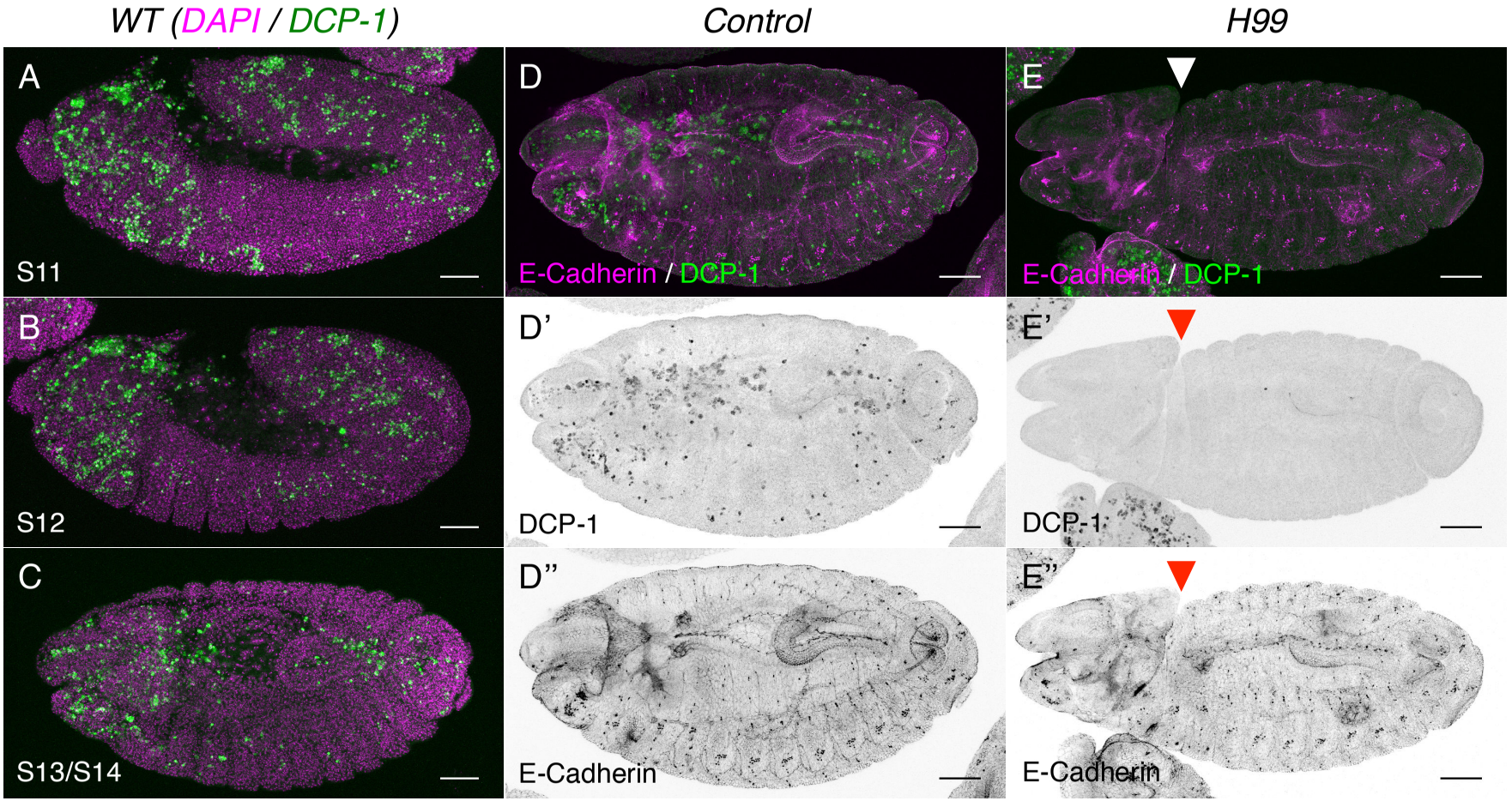

Figure S1
(Ducuing *et al.*)

Fig. S1 DCP-1 staining in *WT* and *H99* embryos.

(A-C) Stage 11 (A), Stage 12 (B) and Stage 13/14 (C) WT embryos marked for DCP-1 (green) and DAPI (magenta). All images projections of confocal sections. Scale bar: 50 μm. DCP-1 is detected in various locations in WT embryos.

(D-E) Control (D-D'') and *H99* (E-E'') embryos marked for DCP-1 (green in D and E, grey in D' and E') and E-Cadherin (magenta in D and E, grey in D'' and E''). All images are projections of confocal sections. Scale bar: 50 μm. DCP-1 staining is absent in *H99* embryos, recognized by the head involution defects (arrowheads).

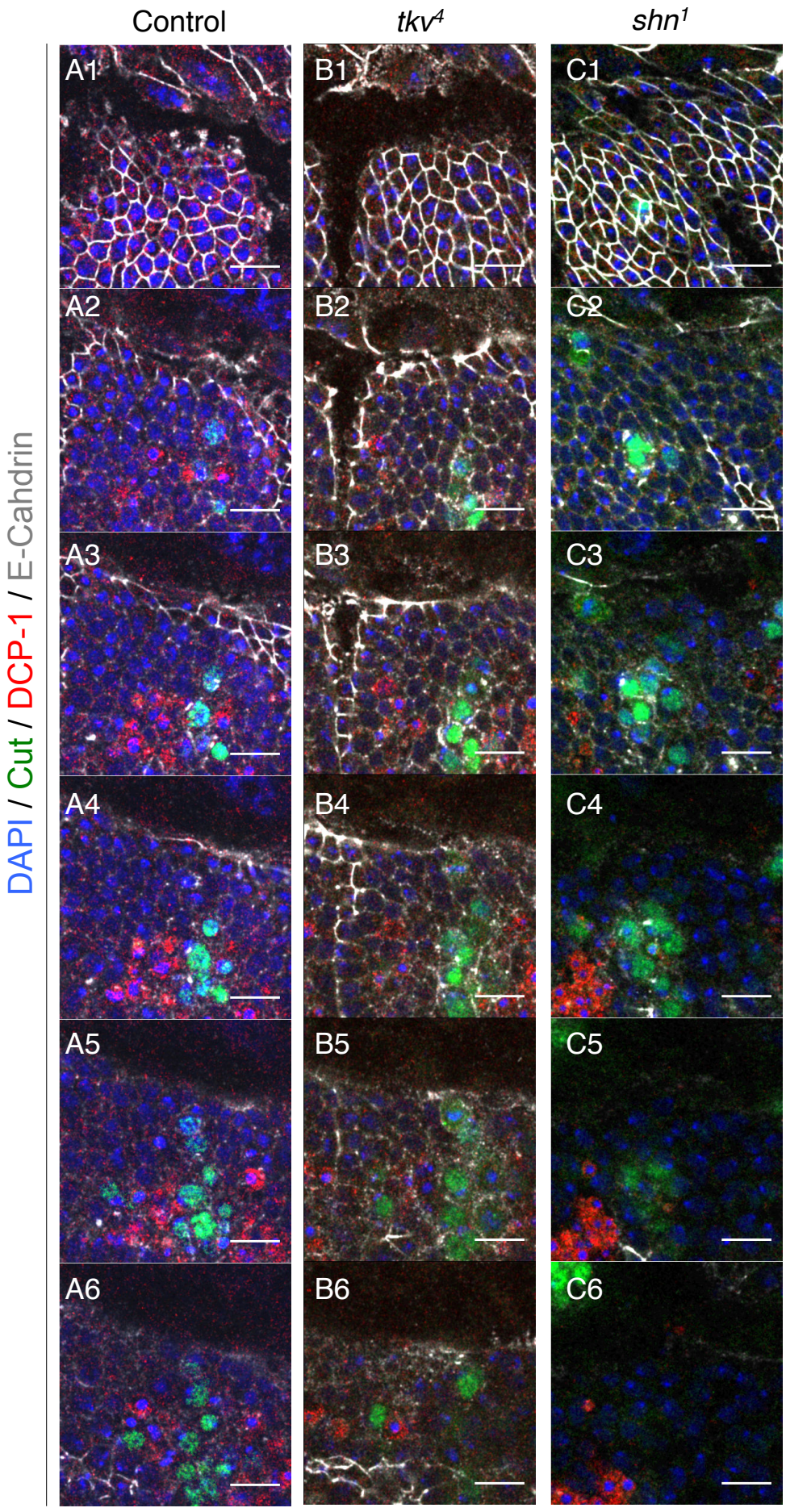

Figure S2
(Ducuing *et al.*)

Fig. S2 Extended data of Figure 2.

(A-C) Control (A), *tkv*^{4} (B) and *shn*^{1} (C) stage 12 embryos marked for E-Cadherin (grey), DAPI (blue), DCP-1 (red) and Cut (green). All images are single confocal sections. A1, B1 and C1 are most apical sections with visible E-Cadherin whereas A6, B6 and C6 are deepest sections of the stack. Scale bar: 10 μm. DCP-1 staining is not visible in epidermal cells, but is detected in the vicinity of Cut-positive neurons in both control and DPP signalling mutant embryos.

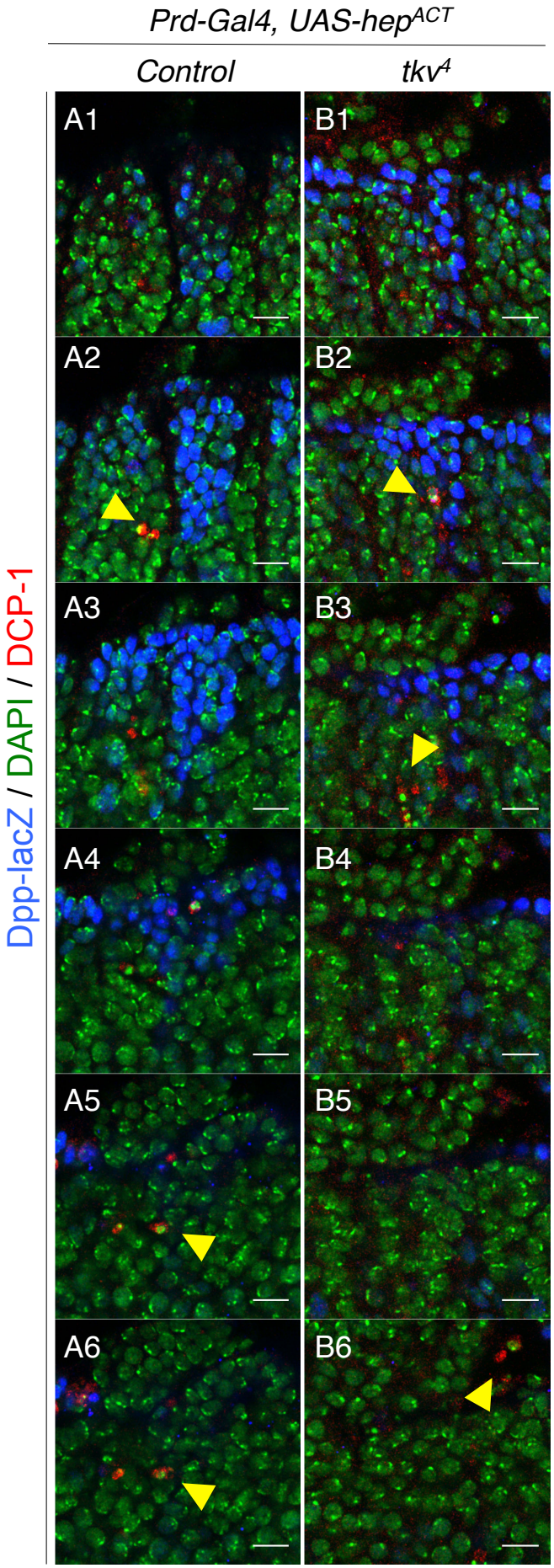

Figure S3
(Ducuing *et al.*)

Fig. S3 Extended data of Figure 4.

(A-B) *Prd-Gal4, UAS-hep^{ACT}, Dpp-lacZ* (A), *tkv^{4}, Prd-Gal4, UAS-hep^{ACT}, Dpp-lacZ* (B) embryos marked for DPP-lacZ (blue), DCP-1 (red) and DAPI (green). The ectopic JNK territory is marked with nuclear lacZ. All images are single confocal sections. A1 and B1 display the most apical sections whereas A6 and B6 are the deepest sections of the stack. Scale bar: 10 μm. The arrowheads indicate DCP-1 positive cells in lower sections that are neither visible in the epidermal layer, nor in the ectopic JNK territory

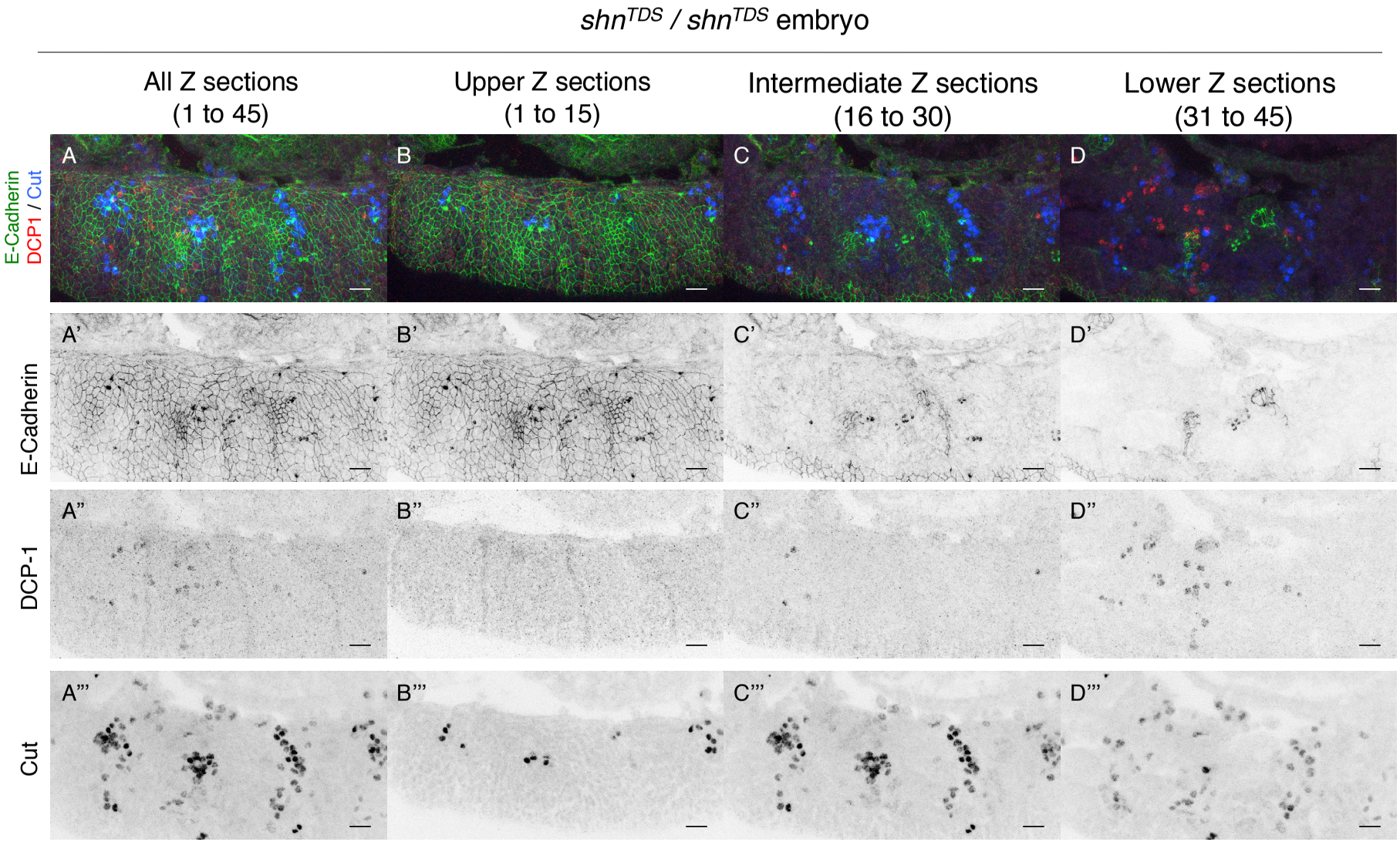

Figure TDS_1. Cleaved DCP-1 is not detected in the dorsal epidermis of *shn^{TDS}* embryos.
(A-D) closeup of the *shn^{TDS}* stage 14 mutant embryo in Fig. 1 A stained for E-Cadherin (green in A-D, grey in A'-D') and DCP-1 (red in A-D, grey in A''-D'') and Cut (bleu in A-D, grey in A'''-D'''). All images are projections of confocal sections. Scale bar: 10 μm. Please note that DCP-1 is detected in lower sections under the Cut-positive neurons and in the vicinity of tracheas. No DCP1 is detected in the epidermal sections.

ADDITIONAL PAPERS

1. Absolute requirement of cholesterol binding for Hedgehog gradient formation in *Drosophila*.

I officially started my Ph.D in September 2012. During this first year as a Ph.D student, in parallel to the dorsal closure work, I finished a story that we initiated with Stéphane when I made a rotation as an undergraduate student (L3) for seven weeks during summer 2009. This work is about Hedgehog (Hh) and the role of the cholesterol adduct on Hh range of action. In short, Hh is a key signalling ligand than is bound to two lipid adducts, the palmitate at its C-terminus and the cholesterol at its N-terminus. The role of the cholesterol moiety was controversial: it was either increasing, or decreasing Hh range of action depending on the experimental settings. To assess the role of the cholesterol moiety on Hh range of action, we decided to over-express either the cholesterol-bound or the cholesterol-free form of Hh perpendicular to the endogenous Hh expression pattern and analyse the targets where Hh signalling is not active. I showed that cholesterol-free Hh diffuses and activates its targets at a greater ranger than the wild-type, cholesterol bound form of Hh, showing that the cholesterol adduct restricts Hh diffusion both in the *Drosophila* embryo and the wing imaginal disc. Importantly, we showed that without cholesterol, Hh fails to adopt a graded distribution (the gradient becomes plateau), showing that the cholesterol adduct is also crucial for the **establishment** of Hh gradient. The data are published in the *Biology Open* paper (Ducuing et al., 2013).

Absolute requirement of cholesterol binding for Hedgehog gradient formation in *Drosophila*

Antoine Ducuing[1], Bertrand Mollereau[1], Jeffrey D. Axelrod[2] and Stephane Vincent[1,*]

[1]LBMC, UMR5239 CNRS/Ecole Normale Supérieure de Lyon, SFR 128 Biosciences Lyon Gerland, Université de Lyon, 69364 Lyon Cedex 07, France
[2]Pathology Department, Stanford School of Medicine, Palo Alto, CA 94304, USA
*Author for correspondence (stephane.vincent11@ens-lyon.fr)

Biology Open 2, 596–604
doi: 10.1242/bio.20134952
Received 3rd April 2013
Accepted 12th April 2013

Summary

How morphogen gradients are shaped is a major question in developmental biology, but remains poorly understood. Hedgehog (Hh) is a locally secreted ligand that reaches cells at a distance and acts as a morphogen to pattern the *Drosophila* wing and the vertebrate neural tube. The proper patterning of both structures relies on the precise control over the slope of Hh activity gradient. A number of hypotheses have been proposed to explain Hh movement and hence graded activity of Hh. A crux to all these models is that the covalent binding of cholesterol to Hh N-terminus is essential to achieve the correct slope of the activity gradient. Still, the behavior of cholesterol-free Hh (Hh-N) remains controversial: cholesterol has been shown to either increase or restrict Hh range depending on the experimental setting. Here, in fly embryos and wing imaginal discs, we show that cholesterol-free Hh diffuses at a long-range. This unrestricted diffusion of cholesterol-free Hh leads to an absence of gradient while Hh signaling strength remains uncompromised. These data support a model where cholesterol addition restricts Hh diffusion and can transform a leveled signaling activity into a gradient. In addition, our data indicate that the receptor Patched is not able to sequester cholesterol-free Hh. We propose that a morphogen gradient does not necessarily stem from the active transfer of a poorly diffusing molecule, but can be achieved by the restriction of a highly diffusible ligand.

© 2013. Published by The Company of Biologists Ltd. This is an Open Access article distributed under the terms of the Creative Commons Attribution License (http://creativecommons.org/licenses/by/3.0), which permits unrestricted use, distribution and reproduction in any medium provided that the original work is properly attributed.

Key words: *Drosophila*, Hedgehog, Cholesterol, Gradient, Patterning

Introduction

The Hedgehog (Hh) gene family encodes secreted ligands that regulate patterning in both vertebrates and invertebrates (Ingham and McMahon, 2001; Ingham et al., 2011). The range of action of Hh ligands determines patterns of prominent body structures such as the segments in the fly embryo, the appendages in both the adult fly and vertebrates (Riddle et al., 1993; Tabata and Kornberg, 1994) and the ventral neural tube in vertebrates (Jessell, 2000). Hh regulates its targets in a concentration-dependent manner, and thus acts as a morphogen in the *Drosophila* wing imaginal disc and the vertebrate neural tube: Hh is secreted locally and its range of action patterns distinct territories (Briscoe et al., 2001; McMahon et al., 2003). Hh differential activity must therefore be carefully controlled.

Two opposing views may explain how the slope of a morphogen gradient is generated: First, a freely diffusible molecule can encounter a restrictive mechanism, leading to its accumulation near the source of secretion. Up to now, such hypothesis has received little support. Second, a poorly diffusible molecule could be transferred upon interaction with a carrier in order to reach the cells that need to be patterned. Distinct transfer mechanisms have been proposed to explain gradient formation in the *Drosophila* wing imaginal disc (Kornberg and Guha, 2007): First, during serial transfer also known as trancytosis, secreted Hh would be endocytosed by the neighboring cell in a receptor-dependent manner, and then secreted again. Repeating this scenario in the rest of the cells in the epithelium will lead to the formation of the gradient. Second, lipoprotein particle transfer would involve the binding of Hh to lipophorin. The Hh–lipophorin complex would move across the tissue, allowing long-range signaling (Panáková et al., 2005; Eugster et al., 2007). Third, Hh may be transferred by long cellular protrusions called cytonemes (Ramírez-Weber and Kornberg, 1999). Cells interpreting a ligand would send specific cytonemes bearing a receptor to pick up the ligand at the secretion site (Roy et al., 2011). Another possibility is that the cytonemes originate from the Hh producing cells as shown in the niche of the *Drosophila* female germline stem cells (Rojas-Ríos et al., 2012). Recently, cytonemes have also been shown to originate from the Hh producing cells in the wing imaginal disc (Bilioni et al., 2013). The question of how Hh activity gradient is established is therefore highly controversial and remains open. The underlying idea behind these models is that a transfer mechanism carries local Hh in order to generate an activity gradient with a precise slope.

Hh protein biosynthesis includes the addition of palmitic acid and cholesterol to the N moiety (Hh-N) (reviewed by Mann and Beachy, 2004). Hh is palmitoylated at its N-terminus by the

Biology Open

acetyl transferase *skinny hedgehog* and is required for Hh secretion (Chamoun et al., 2001; Micchelli et al., 2002). The second lipid modification is the covalent addition of a cholesterol moiety. Cholesterol addition requires the autocatalytic Hh C-terminal domain that gets cleaved during the reaction (Porter et al., 1996a; Bürglin, 2008). Cholesterol covalent binding is crucial for Hh release mediated by the transmembrane protein Dispatched (Disp) that contains a sterol-sensing domain (Burke et al., 1999). Still, expressing the Hh N-terminal domain alone produces a form of Hh not bound to cholesterol that is efficiently secreted in a *disp* independent manner (Porter et al., 1996b; Burke et al., 1999). Hh-N was used to show that cholesterol addition enhances membrane association (Porter et al., 1996b). The more striking behavior of Hh-N is its range of action that is different from the one of the wild-type, cholesterol bound form of Hh. The problem is that depending on experimental conditions, the cholesterol adduct would increase (Gallet et al., 2003; Panáková et al., 2005; Gallet et al., 2006; Eugster et al., 2007) or decrease (Porter et al., 1996b; Burke et al., 1999; Dawber et al., 2005; Callejo et al., 2006; Su et al., 2007) Hh range of action (reviewed by Wendler et al., 2006).

It was first found that cholesterol addition limits Hh diffusion, as predicted from its biochemical properties (Porter et al., 1996b; Burke et al., 1999). In wing imaginal discs, Hh-N would diffuse further than the wild-type tending to decrease the slope of its gradient and thus reducing peak levels while elevating low levels at a distance. In this case, the domains of the high-threshold targets *patched (ptc)* and *engrailed (en)* would decrease in size or may even get lost (Dawber et al., 2005; Callejo et al., 2006; Gallet et al., 2006). On the other hand, Hh-N can activate the low-threshold targets *Collier* and *Iroquoi* over a greater range than Hh-WT (Dawber et al., 2005; Callejo et al., 2006). Besides, the direct analysis of the spreading of Hh GFP fusions showed that the Hh-N-GFP would diffuse twice further than Hh-GFP (Su et al., 2007). Therefore this model suggests that the cholesterol moiety concentrates Hh in a given domain above the activation threshold of the pathway and defines the effective range of Hh (Guerrero and Chiang, 2007).

Still, other data indicated that cholesterol binding could be used to increase Hh range of action: wing imaginal disc clones overexpressing Hh-N induced the expression of the target reporter *dpp-lacZ* at a range of 3 to 4 cells whereas similar clones overexpressing Hh-WT induce *dpp-lacZ* at a range of 5 to 6 cells (Gallet et al., 2006). In the embryo, whereas it was first shown that Hh-N diffuses more than Hh-WT (Burke et al., 1999), it was later proposed that cholesterol binding is necessary for Hh movement (Gallet et al., 2003; Gallet et al., 2006). The hydrophobic nature of cholesterol and the longer range observed were reconciled by the observation that the cholesterol adduct promotes the association of Hh into lipoparticles able to travel in the extracellular matrix (Greco et al., 2001; Panáková et al., 2005; Eugster et al., 2007). Indeed, Hh copurifies with lipophorin, and Hh range of action decreases when lipophorin levels were reduced with RNAi in *Drosophila* larvae. As a result, *dpp-lacZ* expression decreased from 11 to 6 rows of cells at the anteroposterior boundary of wing imaginal disc (Panáková et al., 2005). Hence, the cholesterol adduct appeared to increase Hh range by a factor of 2. Inexplicably, the expression range of the other Hh target *Collier (Col)* was unaffected. Another difficulty with this model is that lipoparticles are known to carry GPI-anchored proteins, but GPI-anchored Hh does not diffuse (Burke et al., 1999). Cholesterol binding would therefore provide a way by which a poorly diffusing molecule could get transferred to the neighboring cells.

Altogether the control of Hh range of action by cholesterol modification is unclear: in the *Drosophila* embryo it is admitted that cholesterol modification increases Hh range of action. In discs, Hh-N range of action was either described as decreasing by a factor of 2 (Gallet et al., 2003; Gallet et al., 2006) or increasing by a factor of 2 although only for low-threshold targets (Dawber et al., 2005; Callejo et al., 2006; Su et al., 2007). Most of all, the wider implication of these studies is that cholesterol binding does not change Hh behavior in a drastic manner, but only tunes the shape of the gradient. The process of cholesterol binding would therefore be dispensable to the formation of the gradient itself.

Our data in both the *Drosophila* embryo and the wing imaginal disc show a dramatic increase in the range of Hh-N. Cholesterol-bound or unbound Hh was expressed in the embryonic dorsal epidermis and the activity of Hh pathway was monitored along an axis perpendicular to the direction of endogenous Hh diffusion. This setting allowed us to demonstrate that Hh-N can act at a long range in the *Drosophila* embryo, as far as 25 cells away. Second, we show that cholesterol-free Hh displays unrestricted diffusion in the wing disc by using *ptc* expression as a readout. This unrestricted diffusion leads to an absence of activity gradient. This plateau of Hh activity is still able to induce high threshold targets such as En, indicating that Hh-N is potent enough to induce full Hh pathway activation, implying that the longer range is not obtained at the expanse of the strength of the signal. We conclude that cholesterol modification is essential for Hh gradient formation.

Materials and Methods

Fly strains and genetics

We used the hh^{ts2} (# BL 1684), a temperature sensitive allele with restrictive temperature at 29°C. To drive ectopic expression with the UAS/Gal4 system (Brand et al., 1994), we used the following Gal4 lines: *pnr-Gal4* (pnr^{MD237}, # BL 3039) which drives expression in the dorsal epidermis of the embryo, and *ap-Gal4* (ap^{MD544}, # BL 3041) which drives expression in the dorsal domain of the wing disc. We used the following UAS lines: *UAS-ActinRFP, UAS-hh-WT* (Gallet et al., 2003), *UAS-hh-N* (Gallet et al., 2003), *UAS-hh::GPI*, a fusion of FasI C-terminal residues that include a GPI anchoring signal with the Hh-N moiety (Burke et al., 1999) and *UAS-Hh::CD2*, a fusion of the rat membrane protein CD2 with the Hh-N moiety (Strigini and Cohen, 1997). We also used the *Dpp-lacZ* line BS3.0 (Blackman et al., 1991). pnr^{MD237}, ap^{MD544}, *UAS-RFP* and hh^{ts2} lines are from the Bloomington *Drosophila* stock centre. *UAS-hh-WT*, *UAS-hh-N*, *UAS-hh::GPI*, *UAS-hh::CD2* are a kind gift from Armel Gallet. The *Dpp-lacZ* reporter is a kind gift from L.S. Shashidhara. Crosses were performed at 25°C. For the hh^{ts2} experiment, larvae were incubated at restrictive temperature (29°C) 19 hours before dissection.

Immunofluorescence and quantification

We used standard techniques of immunohistofluorescence: embryos were dechorionated with bleach, fixed in a 1:1 mix of 4% PFA–Heptane. Embryos were subsequently devitellinized by replacing the 4% PFA with methanol. Discs were fixed in 4% PFA on ice for 1 hour. Samples were then incubated with primary antibodies, later fluorescent-coupled secondary antibodies. Samples were eventually mounted in VectaShield. We used the following primary antibodies: anti-Odd (kind gift from J. Skeath), anti-Ci, anti-En, anti-Ptc, anti-DCadherin, anti-Wg, developed respectively by R. Holmgren, C. Goodman, I. Guerrero, T. Uemura, S. Cohen, were obtained from the Developmental Studies Hybridoma Bank developed under the auspices of the NICHD and maintained by the University of Iowa, Department of Biology, Iowa City, IA 52242. Anti-β-Gal is from Cappel. We used the following secondary antibodies: Alexa Donkey anti-Mouse 488 (Invitrogen), Alexa Goat anti-Mouse 633 (Invitrogen), Alexa Goat anti-Rat 633 (Invitrogen), Alexa anti-Rabbit 633 (Invitrogen). Images were acquired on the Confocal Leica SP5 microscope and analysed with ImageJ. Unless otherwise indicated, all images are projections of confocal sections. For all panels,

scale bar is 10 µm. ImageJ plot profile function was used to quantify Ptc intensity for Figs 4 and 5.

Western blot

We used the same protocol as previously described (Dourlen et al., 2012). 100 embryos or 20 wing imaginal discs for each genotype were homogenized in Laemmli buffer (10% glycerol, pH 6.8 0.5M Tris, 10% SDS, 1% bromophenol blue, 1% β-mercaptoethanol, 100 mM DTT). Samples were then boiled and loaded onto a 12% acrylamide gel (Biorad), transferred and incubated overnight at 4℃ with a primary antibody. Samples were then incubated with HRP-coupled secondary antibodies, and eventually detected with a chemoluminescent kit (GE Healthcare Life Sciences). The following antibodies were used: "Calvados" Anti-Hh (kind gift from P. Thérond) and Anti-Tubulin (Sigma). We used the following secondary antibodies: Anti-mouse HRP and Anti-rabbit HRP antibodies (Biorad). We used the ImageJ software to quantify protein bands.

Statistical analyses

We used the Prism software to generate graphs. Bar graphs represent mean±s.e.m. Mann–Whitney's *U* test was used to determine significant differences for Figs 1, 2. Student *t*-test was used to determine significant differences for Fig. 4.

Results

Unrestricted diffusion of cholesterol-free Hh in the *Drosophila* embryo

hh is a segment polarity gene (Nüsslein-Volhard and Wieschaus, 1980) that regulates patterning within each segment of the *Drosophila* embryo. Hh is secreted by the *en*-expressing cells (Kornberg et al., 1985) and induces *ptc* expression in the *Ci*-expressing domain. Ptc expression is detected in all Ci positive cells at early stage 10 (Taylor et al., 1993) and is refined to single stripes of cells abutting the En domain at stage 13 (Fig. 1A–A″). We therefore characterized the range achieved by different Hh variants by monitoring ectopic Ptc expression in stage 13 embryos. We used the *pannier-Gal4* (*pnr-Gal4*) driver to overexpress Hh variants in the dorsal domain, marked with Actin-RFP (Calleja et al., 1996) (supplementary material Fig. S1A). Whereas previous experiments had tested Hh range of action across few cell diameters, this setup enabled us to test the range of Hh over 25 cells.

We first overexpressed Hh::GPI and Hh::CD2, two membrane-anchored forms of Hh (Strigini and Cohen, 1997; Burke et al., 1999) as controls and showed that they induce Ptc only within the Pnr domain (Fig. 1B–C″). We next overexpressed cholesterol-bound and cholesterol-free Hh. Ptc staining indicated that wild-type Hh diffuses 1 to 4 cells away (Fig. 1D–D″) whereas cholesterol-free Hh (Hh-N) diffuses throughout the dorsoventral axis (Fig. 1E–E″), which is about 25 cells away (Fig. 1F). Western blot analysis indicates that the greater range of Hh-N is not due to a stronger expression of the Hh-N transgene (supplementary material Fig. S2A,B). Therefore, without cholesterol, Hh diffuses much further than wild-type Hh.

Next, we verified that the activation of the Hh pathway is sufficient to regulate cell identity. In cells posterior to the En cells, *hh* maintains *odd skipped* (*odd*) expression and segmental groove identity (Vincent et al., 2008). In *pnr-Gal4, UAS-RFP* embryos, endogenous Odd expression is wild-type and consists of a single stripe of cells abutting the En domain (Fig. 2A–A″). Hh-WT maintains Odd to about 3 to 4 cells away, correlating perfectly with Ptc expression (Fig. 2B–B″; supplementary material Fig. S3). By contrast, Hh-N maintains Odd throughout the dorsolateral axis (Fig. 2C–C″; supplementary material Fig. S3), which is about 20 cells away (Fig. 2D). This correlation between Ptc expression and Odd maintenance shows that the dose

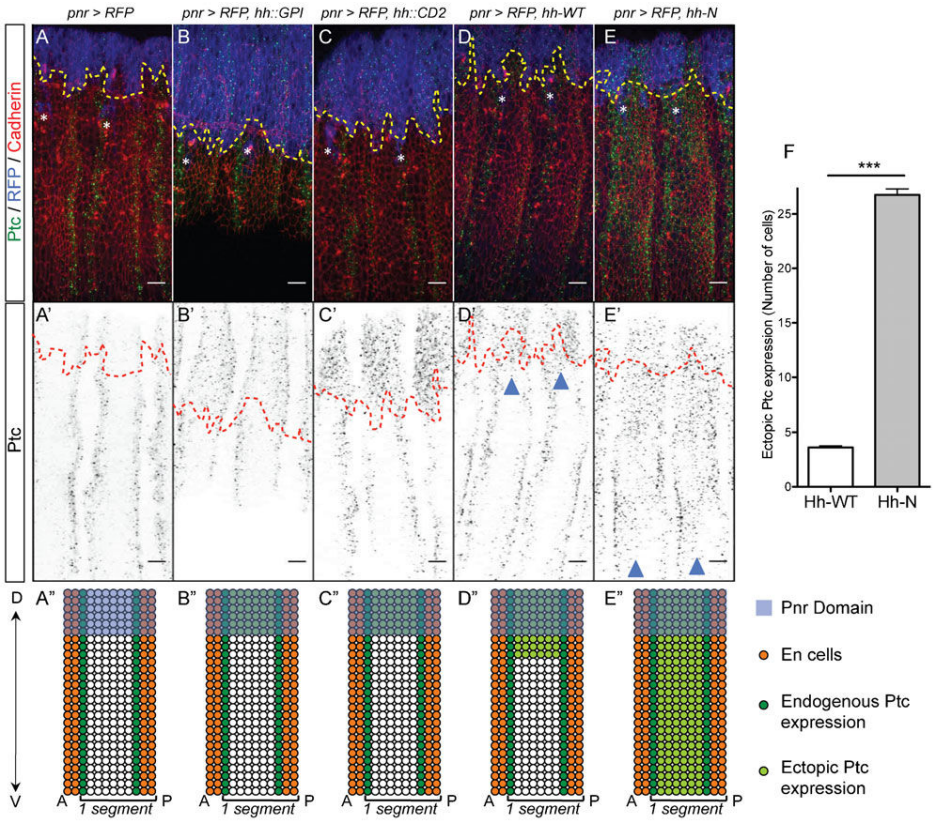

Fig. 1. Hh-N activates Ptc expression ten times further than Hh-WT in the *Drosophila* embryo. (**A–E′**) Ptc, Cadherin and RFP expression in stage 13 embryos. The ectopic expression domain is located above the dashed lines. Asterisks indicate underlying Pnr-positive PNS neurons. (A–C′) Control embryos. Endogenous Ptc is detected in 1-cell wide stripes abutting the En domain (A,A′). Both Hh:GPI, and Hh::CD2 induce Ptc cell-autonomously (B′–C′). (D–E′) In *pnr-Gal4, UAS-RFP, UAS-hh-WT* embryos, Ptc is induced at a 3-cell range inside the lateral epidermis whereas in *pnr-Gal4, UAS-RFP, UAS-hh-N* embryos, Ptc is induced throughout the epidermis (D–E′, arrowheads). (**A″–E″**) Schematics representing segments of the above genotypes. Ectopic Ptc is in light green. (**F**) Quantification of ectopic Ptc expression range ($n \geq 8$, $P\text{-value} = 0.0003$). Scale bars: 10 µm.

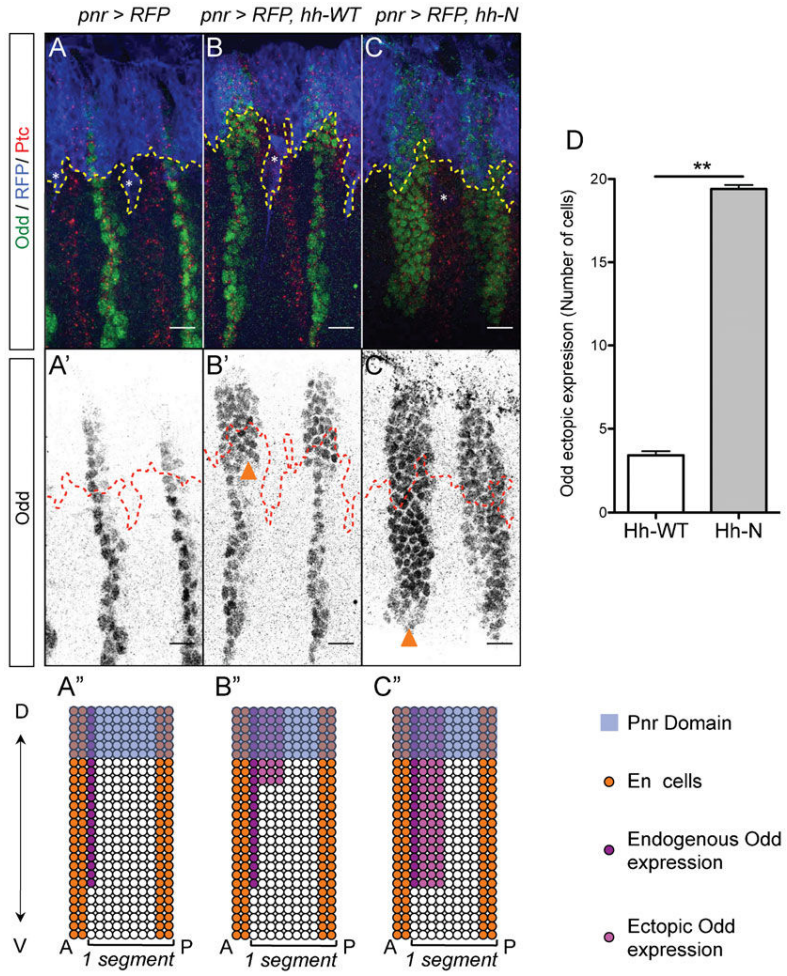

Fig. 2. Hh-N maintains Odd expression at a long-range in the *Drosophila* embryo. (**A–C′**) Odd, Ptc and RFP expression in stage 13 embryos. The ectopic expression domain is located above the dashed lines. Asterisks indicate underlying Pnr-positive PNS neurons. (A,A′) Endogenous Odd is detected in a 1-cell wide stripe in the dorsal and the lateral epidermis. (B,B′) Hh-WT maintains Odd only 3 cells away from the pnr domain, whereas Hh-N maintains a 4-cell wide stripe of Odd cells all through the lateral epidermis. (**A″–C″**) Schematics representing segments of the above genotypes. Ectopic Odd is in magenta. (**D**) Quantification of ectopic Odd expression range ($n \geq 5$, *P-value=0.0097*). Scale bars: 10 µm.

of Hh received by distant cells is strong enough to modify segmental patterning. At this stage, *odd* is not expressed in the ventral epidermis of wild-type embryos (Vincent et al., 2008) and cannot indicate whether Hh-N is active in this region. In order to address whether Hh-N diffuses all the way to the ventral epidermis, we next monitored the pattern of *wg*-expressing cells.

In the dorsal and the ventral epidermis of the embryo, *hh* maintains *wg* expression in cells anterior to the En stripe (Baker, 1987; Alexandre et al., 1999) (Fig. 3A–A″). In *pnr-Gal4, UAS-hh-WT* embryos, supernumerary Wg-expressing cells are detected in the dorsal epidermis but not in the ventral epidermis (Fig. 3B,B′). By contrast, in *pnr-Gal4, UAS-hh-N* embryos, additional rows of Wg-expressing cells are maintained in both the dorsal epidermis and the ventral epidermis (Fig. 3C–C″). Thus Hh-N produced in the dorsal domain diffuses as far as the midline of the ventral epidermis, about 25 cells away. Hence, we conclude that cholesterol-free Hh can diffuse and modify patterning at least ten times further than cholesterol-bound Hh.

Unrestricted diffusion and absence of gradient with cholesterol-free Hh in the wing imaginal disc

We next adopted a similar strategy in the wing imaginal disc and tested Hh-N range of action. In the wing imaginal disc, Hh is produced by the posterior *en* cells and activates Ptc in a 10-cell stripe bordering the *en* domain (Fig. 4A–A″). In order to avoid the influence of endogenous Hh activity, we ectopically expressed Hh variants in the dorsal domain with *ap-Gal4* and analyzed their range of action in the anteroventral domain (Calleja et al., 1996; Glise et al., 2005; Ranieri et al., 2012) (supplementary material Fig. S1B). In *ap-Gal4, UAS-RFP, UAS-hh-WT* discs, ectopic Ptc is detected in a stripe of 10 cells along the dorsoventral border (Fig. 4B–B″). In *ap-Gal4, UAS-RFP, UAS-hh-N* discs, ectopic Ptc is detected throughout the anteroventral quadrant of the wing pouch (Fig. 4C–C″). Thus, cholesterol-free Hh induces Ptc expression at least ten times further than cholesterol-bound Hh. Western blot analysis indicates that Hh-N greater range is not due to a stronger expression of the Hh-N transgene (supplementary material Fig. S2C,D). To verify that endogenous Hh does not interfere with these results, we overexpressed Hh-N in a hh^{ts2} background raised at restrictive temperature during the 19 hours preceding dissection. We observed a similar broad Ptc ectopic expression and an absence of the endogenous Ptc expression (Fig. 5A–D′). Quantitative analysis of Ptc expression reveals that no gradient forms in response to Hh-N (Fig. 4D, Fig. 5E). This is striking as Ptc is a high-threshold Hh target and was strictly detected in a cell-autonomous manner during clonal ectopic expression of Hh-N (Callejo et al., 2006).

We therefore decided to analyze the response of the target that requires the highest Hh activity, Engrailed (Blair, 1992). En was

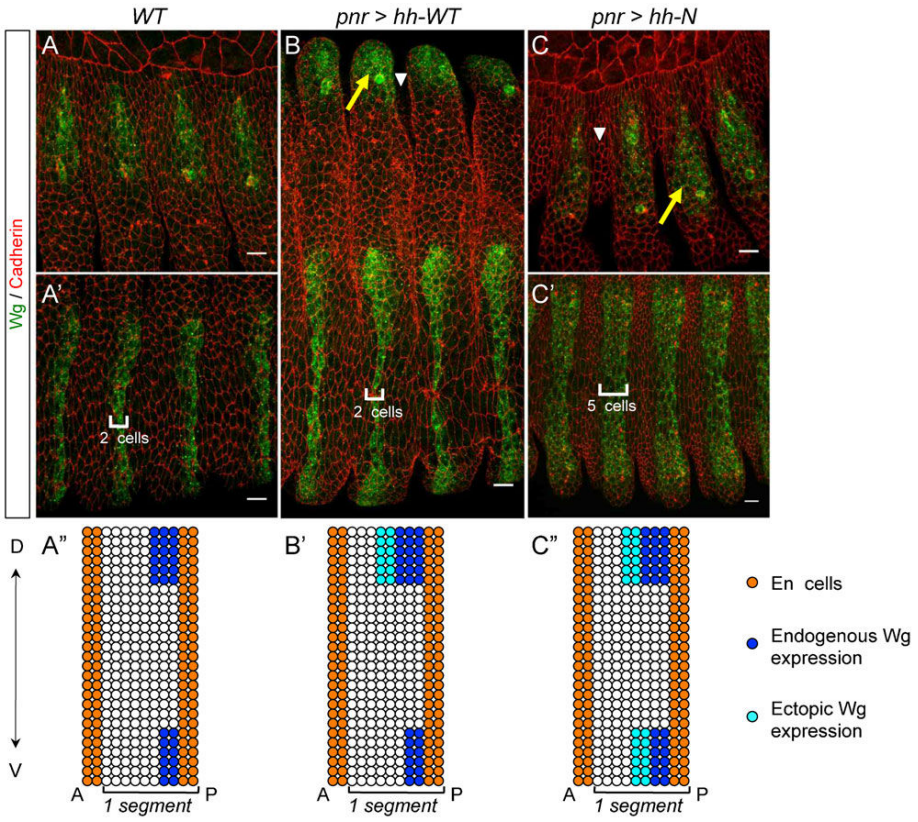

Fig. 3. Hh-N maintains Wg expression at a long-range in the *Drosophila* embryo. (**A,A′,B,C,C′**) Stage 13 embryos stained for Wg and Cadherin. (A,A′) *WT* embryos. Wg is expressed in anterior cells of the dorsal epidermis, and in a 2-cell wide stripe in the ventral epidermis. (B,C,C′) Embryos overexpressing Hh-WT or Hh-N exhibit a wider Wg domain (arrows) and wider grooves (arrowheads) in the dorsal epidermis. Only embryos overexpressing Hh-N exhibit ectopic Wg in the ventral epidermis. (**A″,B′,C″**) Schematics representing a segment of the above genotypes. Ectopic Wg is in cyan. Scale bars: 10 µm.

also confined to Hh-N expressing clones (Dawber et al., 2005; Callejo et al., 2006; Gallet et al., 2006). In *ap-Gal4, UAS-RFP, UAS-hh-WT* discs, ectopic En is detected in a stripe of 4 cells along the dorsoventral border (Fig. 6B–B″). In *ap-Gal4, UAS-RFP, UAS-hh-N* discs, ectopic En is detected throughout the anteroventral quadrant of the wing pouch (Fig. 6C–C″), albeit at a weaker level compared to Hh-WT discs. Another target of Hh is *cubitus interruptus* (*ci*): *ci* marks the anterior cells, and is

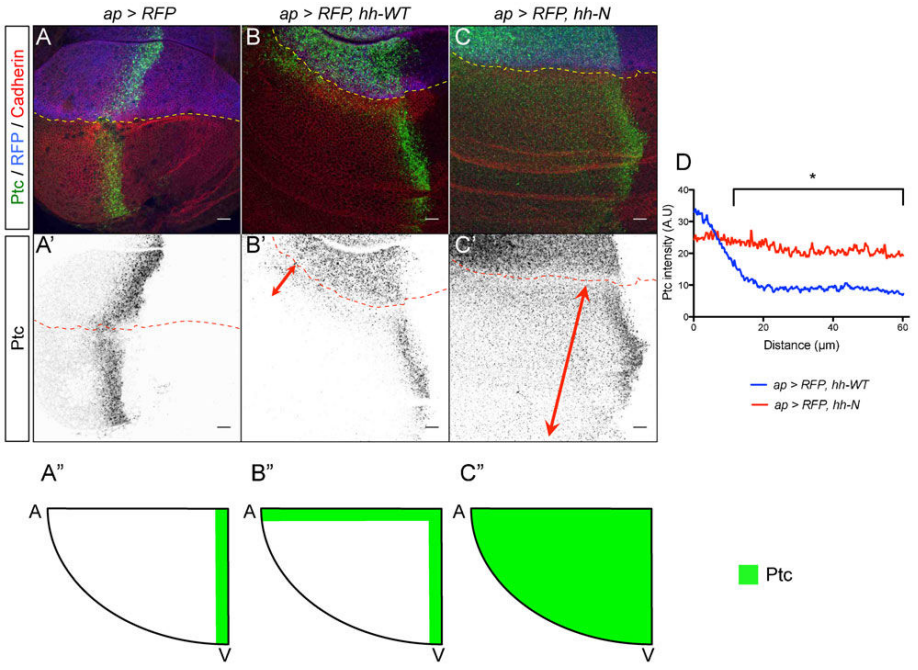

Fig. 4. Hh-N induces a long-range plateau of Ptc expression in the *Drosophila* wing disc. (**A–C′**) Ptc, Cadherin and RFP expression in wing imaginal discs. The expression domain is located above the dashed lines. (A,A′) Control discs: a 10-cell stripe abutting the A/P border expresses Ptc. (B–C′) In *ap-Gal4, UAS-RFP, UAS-hh-WT* discs, ectopic Ptc is detected at a 10-cell range whereas in *ap-Gal4, UAS-RFP, UAS-hh-N* Ptc expression expends all throughout the anteroventral quadrant (arrows). (**A″–C″**) Schematics representing anteroventral quadrants of the above genotypes. Ectopic Ptc is in green. (**D**) Quantification of ectopic Ptc expression revealing Hh-WT activity gradient and Hh-N longrange plateau ($n \geq 6$, for distances >12 µm $P\text{-value} < 0.05$). Scale bars: 10 µm.

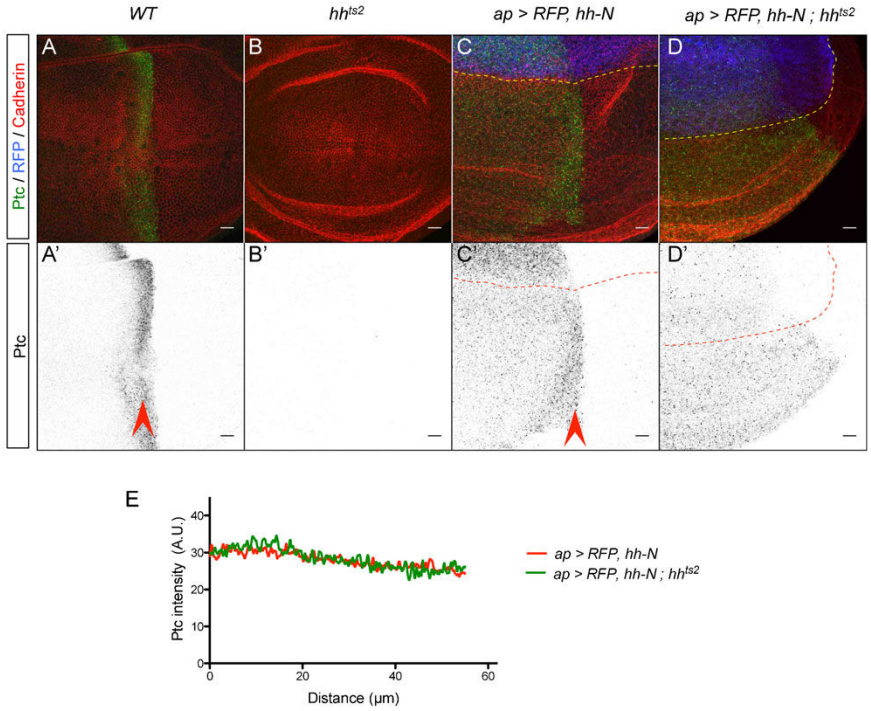

Fig. 5. The plateau of Ptc expression induced by Hh-N is independent from endogenous Hh. (**A–D′**) Ptc, Cadherin and RFP expression in wing imaginal discs raised for 19 hours at restrictive temperature (29°C). (A–B′) Control discs. The endogenous Ptc stripe is visible in WT discs (arrowheads) and absent in hh^{ts2} discs. (C–D′) In both *ap-Gal4, UAS-RFP, UAS-hh-N* and *ap-Gal4, UAS-RFP, UAS-hh-N ; hh^{ts2}* discs, ectopic Ptc is detected throughout the anteroventral quadrant. (**E**) Quantification of ectopic Ptc expression revealing homogenous Hh-N activity ($n \geq 4$). Scale bars: 10 µm.

upregulated by Hh. Ci is considered a low-threshold target (Dawber et al., 2005). Interestingly, Ci expression is inversely correlated with En expression: The stripe of 4 En cells induced by Hh-WT expresses minimal Ci levels, followed by an area of strong Ci staining that is about 10-cell wide (Fig. 7B–B″). This weaker Ci expression may be due to En-mediated repression. Conversely, Hh-N induces Ci upregulation throughout the anteroventral quadrant (Fig. 7C–C″). Thus the activity plateau generated by Hh-N is strong enough to modify En and Ci patterns, indicating that the longer range of Hh-N does not form at the expense of the activity of the molecule.

Last, we checked whether Hh-N can induce the low-threshold target *dpp* over a greater range than Hh-WT by analyzing the expression of a *dpp-lacZ* reporter construct (Blackman et al.,

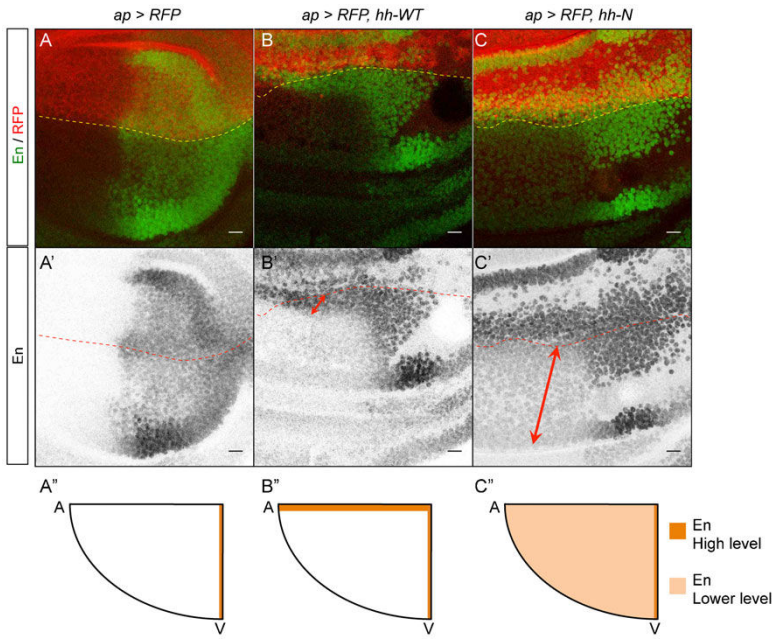

Fig. 6. Hh-N influences En patterning at a long-range in the wing *Drosophila* disc. (**A–C′**) Confocal sections presenting En and RFP expression in wing imaginal discs. The expression domain is located above the dashed lines. (A,A′) Control discs. Hh induces En in a 2-cell stripe abutting the A/P border. (B,B′) *ap-Gal4, UAS-RFP, UAS-hh-WT* discs. Ectopic En is detected at a 4-cell range (red arrow). In the rest of the quadrant, En is not detected. (C,C′) *ap-Gal4, UAS-RFP, UAS-hh-N* discs. Ectopic En is detected throughout the anteroventral quadrant (red arrow). (**A″–C″**) Schematics representing anteroventral quadrants of the above genotypes. Ectopic En is in orange. Scale bars: 10 µm.

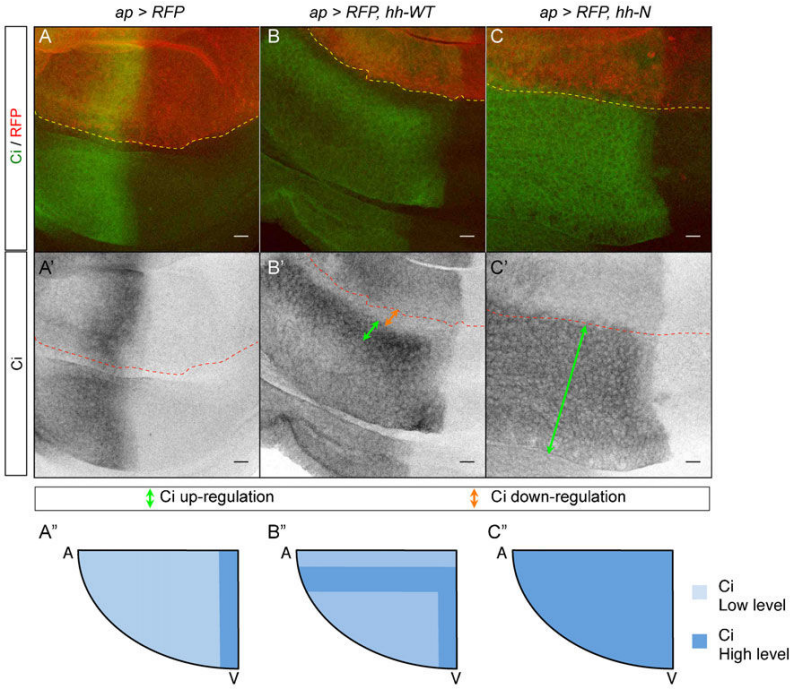

Fig. 7. Hh-N influences Ci patterning at a long-range in the wing *Drosophila* disc. (**A–C′**) Ci and RFP expression in wing imaginal discs. The expression domain is located above the dashed lines. (A,A′) Control discs. Hh induces Ci in a 15-cell stripe abutting the A/P border. (B,B′) *ap-Gal4, UAS-RFP, UAS-hh-WT* discs. Ci expression is weak at a 4-cell range where En levels are high, upregulated in the following 10 rows where En is not detected (orange and green arrows respectively). In the rest of the quadrant, Ci level is basal. The endogenous Ci stripe is visible. (C,C′) *ap-Gal4, UAS-RFP, UAS-hh-N* discs. Ci expression is upregulated throughout the quadrant (green arrow), and the endogenous stripe is no more visible. (**A″–C″**) Schematics representing anteroventral quadrants of the above genotypes. Ectopic Ci is in blue. Scale bars: 10 µm.

1991). Indeed, there is a clear disagreement on whether Hh-N induces dpp-lacZ over a greater range (Callejo et al., 2006) or a reduced range (Gallet et al., 2006) compared with Hh-WT. Our data indicate that whereas Hh-WT induces dpp-lacZ expression in a stripe of about 15 cells along the dorsoventral border, Hh-N induces dpp-lacZ throughout the anterioventral quadrant of the wing pouch (Fig. 8A–C″). As controls, we verified that membrane-anchored Hh induces its targets in a cell-autonomous manner (supplementary material Fig. S4). All the Hh targets we analyzed indicate that cholesterol prevents the formation of a high Hh activity plateau that would cover the full wing pouch. Cholesterol addition is therefore crucial to Hh gradient formation.

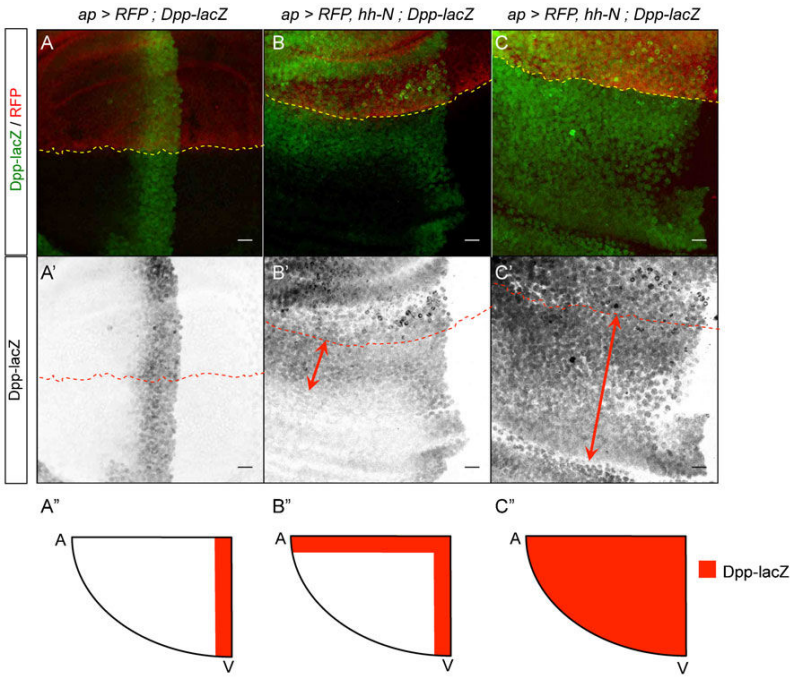

Fig. 8. Hh-N induces Dpp-lacZ at a long-range in the *Drosophila* wing disc. (**A–C′**) Dpp-lacZ and RFP expression in wing imaginal discs. The expression domain is located above the dashed lines. (A,A′) Control discs. Hh induces Dpp-lacZ in a 15-cell stripe abutting the A/P border. (B,B′) *ap-Gal4, UAS-RFP, UAS-hh-WT* discs. Ectopic Dpp-lacZ is detected at a 15-cell range (arrows). (C,C′) *ap-Gal4, UAS-RFP, UAS-hh-N* discs. Dpp-lacZ is detected throughout the anteroventral quadrant (arrows). (**A″–C″**) Schematics representing anteroventral quadrants of the above genotypes. Ectopic Dpp-lacZ is in red. Scale bars: 10 µm.

Discussion

Cholesterol-free Hh acts at long range in both the embryo and the wing imaginal disc

Our data show that cholesterol-free Hh signals at long range. In the embryo, cholesterol-free Hh diffuses and influences patterning at least ten times further than Hh-WT. This clearly contrasts with the generally admitted view that the cholesterol is necessary to send Hh away in the *Drosophila* embryo (Gallet et al., 2003; Gallet et al., 2006) and agrees with pioneer data (Burke et al., 1999). Results showing that cholesterol is necessary to send Hh away may be explained by the fact that Hh does not induce but maintains cell identity in the embryo (Vincent et al., 2008). In experiments performed in Hh null background, target cell identity may have been lost with any delay in Hh-N production, explaining why in these experiments Hh-N would not even act on the very first neighboring cell. Still the novelty of our results resides in the detection of a range that has not been appreciated before: until now, Hh variants were expressed in a striped-pattern and Hh activity was monitored along a maximum range of about 5 cells within each segment (Burke et al., 1999; Gallet et al., 2003; Gallet et al., 2006). Here we show that Hh-N travels at least 25 cells away from its source of secretion and demonstrate for the first time a long-range activity for Hh-N in the *Drosophila* embryo.

In the wing imaginal disc, our data show that cholesterol-free Hh activates at a long range the low-threshold targets such as Dpp, which confirms previous data (Callejo et al., 2006), but also the high-threshold targets such as Ptc and En, which has never been shown before. It has been proposed that the long-range activation of Dpp by Hh-N initially observed by Burke and colleagues would result from ectopic expression of Hh-N in the cells of the peripodial membrane (Gallet et al., 2006). The peripodial cells would secrete Hh-N in the disc lumen, where it would diffuse in a Ptc-independent manner (Callejo et al., 2006). This argument cannot apply against our data: Ap, that drives the Gal4, is the dorsal determinant and is never expressed in the peripodial cells, that are of ventral origin. Thus, Hh-N produced by the dorsal cells of the disc proper is able to travel freely throughout the Ptc expressing epithelium.

Cholesterol-free Hh can travel through a Ptc expressing territory both in the embryo and the wing imaginal disc

This movement through a Ptc expressing territory in both the embryo and the wing imaginal disc is unexpected. Indeed, Hh-WT moves freely through Ptc minus clones in the wing imaginal disc, indicating that Ptc sequesters Hh-WT (Chen and Struhl, 1996). As both Hh-WT and Hh-N activate signaling, it is assume that both contact Ptc in order to activate the pathway. The movement of Hh-N through a Ptc expressing tissue suggests that Hh and Ptc may undergo several types of interactions: First, a cholesterol-independent interaction would promote signaling. Second, a cholesterol-dependent interaction would promote tethering. Such cholesterol-mediated retention of Hh provides an attractive hypothesis to explain how cholesterol shapes the Hh morphogen gradient.

Cholesterol binding is required for gradient formation

Still, the most striking result of this analysis is that cholesterol-free Hh leads to the formation of a high Hh activity plateau that extends through the wing pouch. Previous studies concluded that both Hh-N and Hh-WT could establish a gradient and that the function of cholesterol modification is to tune the slope of the gradient (Dawber et al., 2005; Callejo et al., 2006; Gallet et al., 2006; Su et al., 2007). In contrast, our data suggest that cholesterol is not important to refine the gradient as previously believed, but rather is crucial to generate the gradient.

Robustness as a possible pitfall for morphogen analysis

The vertebrate field provides us with an attractive hypothesis to explain the discrepancy observed in the range of action of Hh-N: Elegant studies about the Sonic Hh (SHh) gradient during the patterning of the neural tube have shown that SHh concentration at a given time is not sufficient to provide spatial information: Aberrant variations in SHh signalling can be ignored, and the memory of the system prevails through a transcription factor feedback loop, a property called hysteresis (Balaskas et al., 2012). The drawback of this robustness is that an experimentally triggered variation in signalling may not give the same result as the same variation performed at steady state. The prediction is that if hysteresis is involved in the fly system, overexpression clones will show different results compared with a steady state overexpression. Several lines of evidence suggest that hysteresis plays an important role in *Drosophila*. First, in the embryo, we have previously shown that Hh does not induce, but maintains groove identity, indicating that memory is crucial to embryonic development (Vincent et al., 2008). Second, the correspondence that we observe between En and Ci expression in the wing imaginal disc indicates that here also a transcription factor loop is at work downstream of Hh signaling. Altogether, steady state analysis appears to be a more appropriate tool than clonal analysis in order to avoid caveats linked to hysteresis.

Compatibility with the cytoneme model

Cholesterol covalent binding may guide Hh through a specific path to generate an activity gradient (Kornberg, 2011). In this view, cholesterol would function as a barcode in secreting cells to route Hh from the apical membrane to the basal side where cytonemes are produced (Bilioni et al., 2013). In contrast, Hh-N would fail to be targeted basally and would accumulate at the apical surface to be eventually released when the accumulation is too important. This byproduct of Hh synthesis was predicted to generate weakened signaling (Kornberg, 2011). Conversely, our data indicate that Hh-N induces robust levels of high-threshold targets at long distance, arguing against an accidental release. On the other hand, our data may provide a testable hypothesis in order to assess the relevance of cytonemes in Hh gradient formation: As Ptc appears to be specifically required to sequester the cholesterol-bound form, the mechanism that distributes Hh as a gradient should enable Ptc tethering activity: If cytonemes are implicated in Hh movement, they should allow the traveling of Hh through Ptc minus clones and a shift in the position of the gradient. In order to cross Ptc minus clones, cytonemes should either expand or carry a higher number of Hh molecules and resume their wild-type behavior once wild-type tissue is reached. Whereas targeting Hh to cytonemes with cholesterol is an interesting possibility, further experiments need to be performed in order to favor this hypothesis.

Altogether, our data demonstrate unambiguously that Hh without cholesterol diffuses further than Hh-WT in both the embryonic epidermis and the wing imaginal disc. In the embryo, cholesterol binding ensures short-range signaling and in the wing imaginal disc it allows gradient formation. This opens the

possibility that a morphogen gradient may not form by the active transfer of a poorly diffusible ligand, but could be generated from the restriction of a highly diffusible ligand.

Acknowledgements

We thank the DROSO-TOOLS and PLATIM facilities of the UMS3444, Armel Gallet, Pascal Thérond, L.S. Shashidara, James Skeath, Bloomington and the Developmental Studies Hybridoma Bank for reagents. This work was supported by the Chaire d'excellence Program from the CNRS to S.V., the FRM and ATIP from CNRS to B.M.

Competing Interests

The authors have no competing interests to declare.

References

Alexandre, C., Lecourtois, M. and Vincent, J. (1999). Wingless and Hedgehog pattern Drosophila denticle belts by regulating the production of short-range signals. *Development* **126**, 5689-5698.

Baker, N. E. (1987). Molecular cloning of sequences from wingless, a segment polarity gene in Drosophila: the spatial distribution of a transcript in embryos. *EMBO J.* **6**, 1765-1773.

Balaskas, N., Ribeiro, A., Panovska, J., Dessaud, E., Sasai, N., Page, K. M., Briscoe, J. and Ribes, V. (2012). Gene regulatory logic for reading the Sonic Hedgehog signaling gradient in the vertebrate neural tube. *Cell* **148**, 273-284.

Bilioni, A., Sánchez-Hernández, D., Callejo, A., Gradilla, A. C., Ibáñez, C., Mollica, E., Carmen Rodríguez-Navas, M., Simon, E. and Guerrero, I. (2013). Balancing Hedgehog, a retention and release equilibrium given by Dally, Ihog, Boi and shifted/DmWif. *Dev. Biol.* **376**, 198-212.

Blackman, R. K., Sanicola, M., Raftery, L. A., Gillevet, T. and Gelbart, W. M. (1991). An extensive 3′ cis-regulatory region directs the imaginal disk expression of decapentaplegic, a member of the TGF-beta family in Drosophila. *Development* **111**, 657-666.

Blair, S. S. (1992). Engrailed expression in the anterior lineage compartment of the developing wing blade of Drosophila. *Development* **115**, 21-33.

Brand, A. H., Manoukian, A. S. and Perrimon, N. (1994). Ectopic expression in Drosophila. *Methods Cell Biol.* **44**, 635-654.

Briscoe, J., Chen, Y., Jessell, T. M. and Struhl, G. (2001). A hedgehog-insensitive form of patched provides evidence for direct long-range morphogen activity of sonic hedgehog in the neural tube. *Mol. Cell* **7**, 1279-1291.

Bürglin, T. R. (2008). The Hedgehog protein family. *Genome Biol.* **9**, 241.

Burke, R., Nellen, D., Bellotto, M., Hafen, E., Senti, K. A., Dickson, B. J. and Basler, K. (1999). Dispatched, a novel sterol-sensing domain protein dedicated to the release of cholesterol-modified hedgehog from signaling cells. *Cell* **99**, 803-815.

Calleja, M., Moreno, E., Pelaz, S. and Morata, G. (1996). Visualization of gene expression in living adult Drosophila. *Science* **274**, 252-255.

Callejo, A., Torroja, C., Quijada, L. and Guerrero, I. (2006). Hedgehog lipid modifications are required for Hedgehog stabilization in the extracellular matrix. *Development* **133**, 471-483.

Chamoun, Z., Mann, R. K., Nellen, D., von Kessler, D. P., Bellotto, M., Beachy, P. A. and Basler, K. (2001). Skinny hedgehog, an acyltransferase required for palmitoylation and activity of the hedgehog signal. *Science* **293**, 2080-2084.

Chen, Y. and Struhl, G. (1996). Dual roles for patched in sequestering and transducing Hedgehog. *Cell* **87**, 553-563.

Dawber, R. J., Hebbes, S., Herpers, B., Docquier, F. and van den Heuvel, M. (2005). Differential range and activity of various forms of the Hedgehog protein. *BMC Dev. Biol.* **5**, 21.

Dourlen, P., Bertin, B., Chatelain, G., Robin, M., Napoletano, F., Roux, M. J. and Mollereau, B. (2012). Drosophila fatty acid transport protein regulates rhodopsin-1 metabolism and is required for photoreceptor neuron survival. *PLoS Genet.* **8**, e1002833.

Eugster, C., Panáková, D., Mahmoud, A. and Eaton, S. (2007). Lipoprotein-heparan sulfate interactions in the Hh pathway. *Dev. Cell* **13**, 57-71.

Gallet, A., Rodriguez, R., Ruel, L. and Therond, P. P. (2003). Cholesterol modification of hedgehog is required for trafficking and movement, revealing an asymmetric cellular response to hedgehog. *Dev. Cell* **4**, 191-204.

Gallet, A., Ruel, L., Staccini-Lavenant, L. and Thérond, P. P. (2006). Cholesterol modification is necessary for controlled planar long-range activity of Hedgehog in Drosophila epithelia. *Development* **133**, 407-418.

Glise, B., Miller, C. A., Crozatier, M., Halbisen, M. A., Wise, S., Olson, D. J., Vincent, A. and Blair, S. S. (2005). Shifted, the Drosophila ortholog of Wnt inhibitory factor-1, controls the distribution and movement of Hedgehog. *Dev. Cell* **8**, 255-266.

Greco, V., Hannus, M. and Eaton, S. (2001). Argosomes: a potential vehicle for the spread of morphogens through epithelia. *Cell* **106**, 633-645.

Guerrero, I. and Chiang, C. (2007). A conserved mechanism of Hedgehog gradient formation by lipid modifications. *Trends Cell Biol.* **17**, 1-5.

Ingham, P. W. and McMahon, A. P. (2001). Hedgehog signaling in animal development: paradigms and principles. *Genes Dev.* **15**, 3059-3087.

Ingham, P. W., Nakano, Y. and Seger, C. (2011). Mechanisms and functions of Hedgehog signalling across the metazoa. *Nat. Rev. Genet.* **12**, 393-406.

Jessell, T. M. (2000). Neuronal specification in the spinal cord: inductive signals and transcriptional codes. *Nat. Rev. Genet.* **1**, 20-29.

Kornberg, T. B. (2011). Barcoding Hedgehog for intracellular transport. *Sci. Signal.* **4**, pe44.

Kornberg, T. B. and Guha, A. (2007). Understanding morphogen gradients: a problem of dispersion and containment. *Curr. Opin. Genet. Dev.* **17**, 264-271.

Kornberg, T., Sidén, I., O'Farrell, P. and Simon, M. (1985). The engrailed locus of Drosophila: in situ localization of transcripts reveals compartment-specific expression. *Cell* **40**, 45-53.

Mann, R. K. and Beachy, P. A. (2004). Novel lipid modifications of secreted protein signals. *Annu. Rev. Biochem.* **73**, 891-923.

McMahon, A. P., Ingham, P. W. and Tabin, C. J. (2003). Developmental roles and clinical significance of hedgehog signaling. *Curr. Top. Dev. Biol.* **53**, 1-114.

Micchelli, C. A., The, I., Selva, E., Mogila, V. and Perrimon, N. (2002). Rasp, a putative transmembrane acyltransferase, is required for Hedgehog signaling. *Development* **129**, 843-851.

Nüsslein-Volhard, C. and Wieschaus, E. (1980). Mutations affecting segment number and polarity in Drosophila. *Nature* **287**, 795-801.

Panáková, D., Sprong, H., Marois, E., Thiele, C. and Eaton, S. (2005). Lipoprotein particles are required for Hedgehog and Wingless signalling. *Nature* **435**, 58-65.

Porter, J. A., Young, K. E. and Beachy, P. A. (1996a). Cholesterol modification of hedgehog signaling proteins in animal development. *Science* **274**, 255-259.

Porter, J. A., Ekker, S. C., Park, W. J., von Kessler, D. P., Young, K. E., Chen, C. H., Ma, Y., Woods, A. S., Cotter, R. J., Koonin, E. V. et al. (1996b). Hedgehog patterning activity: role of a lipophilic modification mediated by the carboxy-terminal autoprocessing domain. *Cell* **86**, 21-34.

Ramírez-Weber, F. A. and Kornberg, T. B. (1999). Cytonemes: cellular processes that project to the principal signaling center in Drosophila imaginal discs. *Cell* **97**, 599-607.

Ranieri, N., Ruel, L., Gallet, A., Raisin, S. and Thérond, P. P. (2012). Distinct phosphorylations on kinesin costal-2 mediate differential hedgehog signaling strength. *Dev. Cell* **22**, 279-294.

Riddle, R. D., Johnson, R. L., Laufer, E. and Tabin, C. (1993). Sonic hedgehog mediates the polarizing activity of the ZPA. *Cell* **75**, 1401-1416.

Rojas-Ríos, P., Guerrero, I. and González-Reyes, A. (2012). Cytoneme-mediated delivery of hedgehog regulates the expression of bone morphogenetic proteins to maintain germline stem cells in Drosophila. *PLoS Biol.* **10**, e1001298.

Roy, S., Hsiung, F. and Kornberg, T. B. (2011). Specificity of Drosophila cytonemes for distinct signaling pathways. *Science* **332**, 354-358.

Strigini, M. and Cohen, S. M. (1997). A Hedgehog activity gradient contributes to AP axial patterning of the Drosophila wing. *Development* **124**, 4697-4705.

Su, V. F., Jones, K. A., Brodsky, M. and The, I. (2007). Quantitative analysis of Hedgehog gradient formation using an inducible expression system. *BMC Dev. Biol.* **7**, 43.

Tabata, T. and Kornberg, T. B. (1994). Hedgehog is a signaling protein with a key role in patterning Drosophila imaginal discs. *Cell* **76**, 89-102.

Taylor, A. M., Nakano, Y., Mohler, J. and Ingham, P. W. (1993). Contrasting distributions of patched and hedgehog proteins in the Drosophila embryo. *Mech. Dev.* **42**, 89-96.

Vincent, S., Perrimon, N. and Axelrod, J. D. (2008). Hedgehog and Wingless stabilize but do not induce cell fate during Drosophila dorsal embryonic epidermal patterning. *Development* **135**, 2767-2775.

Wendler, F., Franch-Marro, X. and Vincent, J. P. (2006). How does cholesterol affect the way Hedgehog works? *Development* **133**, 3055-3061.

Supplementary Material
Antoine Ducuing et al. doi: 10.1242/bio.20134952

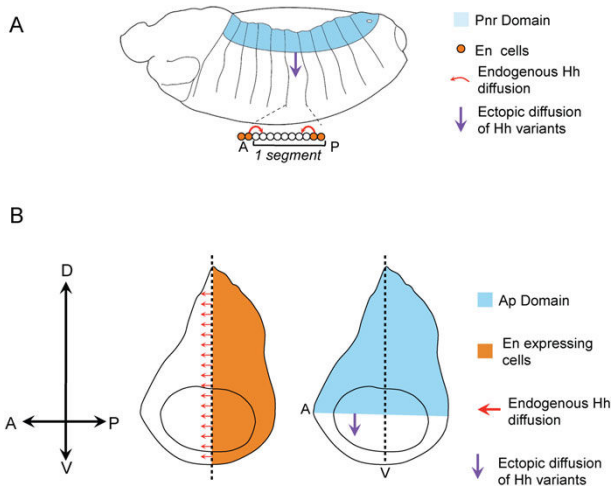

Fig. S1. Cholesterol-free Hh activates Hh targets at a long-range in the *Drosophila* embryo. (**A**) Experimental strategy in the *Drosophila* embryo. Hh is secreted by En cells and diffuses in the *Ci* domain along the anteroposterior axis. In order to monitor Hh diffusion across a higher number of cells, *UAS-hh* variants were expressed in the dorsal epidermis with the *pnr-Gal4* driver and the diffusion was monitored in the lateral and the ventral epidermis (purple arrow). (**B**) Experimental strategy in the *Drosophila* wing imaginal disc. Hh is secreted by En cells (orange) in the posterior compartment and diffuses in the anterior compartment. In order to be independent of endogenous Hh activity and to avoid peripodial membrane expression, *UAS-hh* variants were expressed in dorsal cells (blue) with the *ap-Gal4* driver and the diffusion was monitored along the anteroventral quadrant (purple arrow).

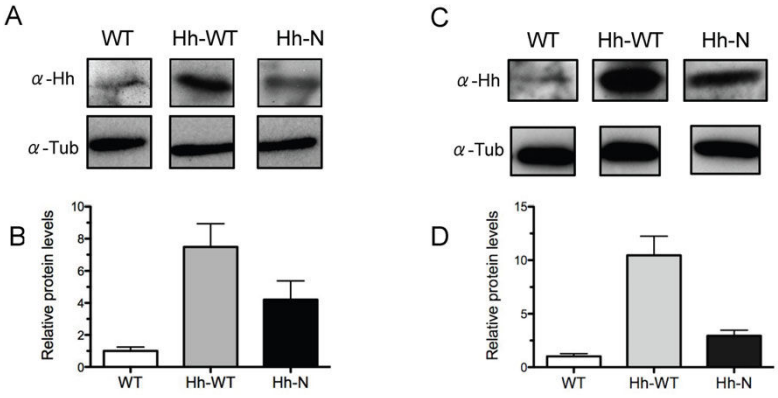

Fig. S2. Quantification of Hh-WT and Hh-N protein levels. (**A**) Western blot analysis of *WT*, *pnr-Gal4, UAS-RFP, UAS-hh-WT* and *pnr-Gal4, UAS-RFP, UAS-hh-N* embryos. Tubulin was used as a loading control. (**B**) Quantification of protein levels. In this system, Hh-WT is expressed at higher level than Hh-N. (**C**) Western blot analysis of *WT*, a*p-Gal4, UAS-RFP, UAS-hh-WT* and *ap-Gal4, UAS-RFP, UAS-hh-N* wing imaginal discs. Tubulin was used as a loading control. (**D**) Quantification of protein levels. In this system, Hh-WT is expressed at higher level than Hh-N.

Biology Open

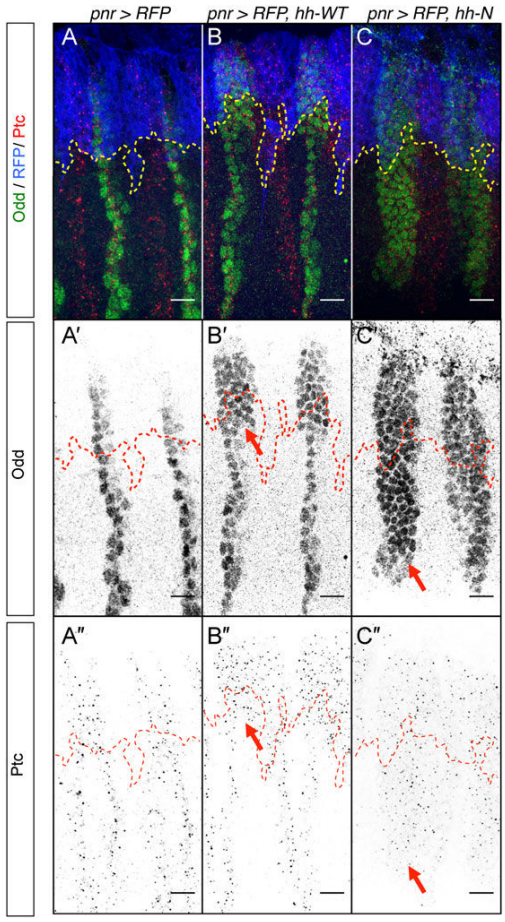

Fig. S3. Expended version of Fig. 2A–C′ showing individual images of Ptc. (**A–A″**) *pnr-Gal4, UAS-RFP*, (**B–B″**) *pnr-Gal4, UAS-RFP, UAS-hh-WT* (**C–C″**) and *pnr-Gal4, UAS-RFP, UAS-hh-N* stage 13 embryos stained for Odd and Ptc. RFP is in blue. Note that in embryos overexpressing Hh-WT Ptc and Odd are detected at a 4-cell range inside the lateral epidermis (arrows). In embryos overexpressing Hh-N, the ectopic Ptc and Odd are detected throughout the lateral epidermis (arrows). Scale bars: 10 µm.

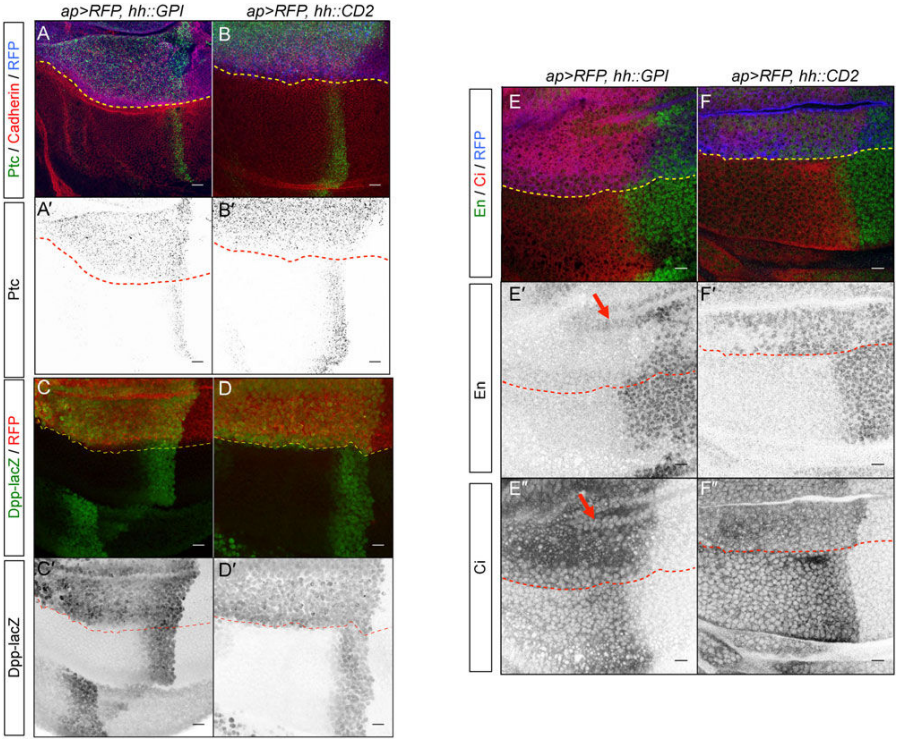

Fig. S4. Hh::GPI and Hh::CD2 activate Ptc, En, Ci and Dpp-lacZ expression in a cellautonomous manner. (**A–B′**) Ptc, Cadherin and RFP, (**C–D′**) Dpp-lacZ and RFP and (**E–F″**) En, Ci and RFP expression in wing imaginal discs. The Apterous domain is located above the dashed lines. Hh::GPI produced in the dorsal domain induces Ptc, dpp-lacZ and Ci upregulation in a cellautonomous manner only. In some cells within the expression domain, (arrows) En is expressed and Ci expression is decreased. Hh::CD2 produced in the dorsal domain induces Ptc, dpp-lacZ and En ectopic expression in a cell-autonomous manner only. Ci is also slightly upregulated in the expression domain only. Scale bars: 10 µm.

2. Cholesterol-free and cholesterol-bound Hedgehog: Two sparring-partners working hand in hand in the Drosophila wing disc?

Following up the publication of our first manuscript in *Biology Open*, I decided to write a journal club to comment an article published by Suzanne Eaton (Palm et al., 2013) that I found to be puzzling. I decided to involve Matthieu Querenet, another Ph.D student in the lab, working on a different topic, but enthusiastic about the idea of writing a commentary. Together we published our journal club in *Fly* (Ducuing and Querenet, 2013). After that, I focused on dorsal closure.

Fly 7:4, 213–215; October/November/December 2013; © 2013 Landes Bioscience

Cholesterol-free and cholesterol-bound Hedgehog

Two sparring-partners working hand in hand in the *Drosophila* wing disc?

Antoine Ducuing* and Matthieu Querenet
LBMC; UMR5239 CNRS/Ecole Normale Supérieure de Lyon; Université de Lyon; Lyon, France

Downloaded by [Bibliotheque Diderot de Lyon] at 01:48 20 August 2015

Keywords: *Drosophila*, Hedgehog, cholesterol, morphogen, patterning

*Corresepondence to: Antoine Ducuing; Email: antoine.ducuing@ens-lyon.fr

Submitted: 06/12/2013

Accepted: 07/08/2013

http://dx.doi.org/10.4161/fly.26279

Exra View to: W Palm, MM Swierczynska, V Kumari, M Ehrhart-Bornstein, SR Bornstein, S Eaton. Secretion and signaling activities of lipoprotein-associated hedgehog and non-sterol-modified hedgehog in flies and mammals. PLoS Biol 2013; 11: e1001505;PMID: 23554573; http://dx.doi.org/10.1371/journal.pbio.1001505

Hedgehog (Hh) is a signaling ligand conserved from flies to humans that is covalently bound to both palmitate and cholesterol moieties. These lipid modifications are crucial for Hh signaling. A recent article reports that in both flies and human-cultured cells a cholesterol-free form of Hh (SHh-N*/Hh-N*) is produced and secreted. In the *Drosophila* wing disc, Hh associated with Lipoproteins-lipophorin complexes (Lpp) would lead to the accumulation of *Cubitus interruptus* (*Ci*), the transcription factor in the Hh pathway but this would be insufficient to activate Hh target genes. On the other hand, Lpp-free Hh-N* would act in synergy with Lpp-associated Hh to eventually activate target gene expression. This suggests that Hh can be secreted in 2 different forms that would have distinct and synergic functions.

The Hedgehog (Hh) gene family encodes secreted ligands that regulate patterning in both vertebrates and invertebrates. Hh graded distribution is tightly controlled to ensure correct patterning. Hh is a double lipid-modified molecule with addition of palmitate at its N-terminus and cholesterol at its C-terminus (for review, see ref. 1). In both flies and vertebrates, Hh palmitoylation is required for Hh secretion.[2-4] Cholesterol addition at its C-terminus[5,6] is crucial for Hh signaling range, but its role remains controversial: it has been reported in *Drosophila* to either increase or decrease Hh range of action (for review, see ref. 7). In the *Drosophila* wing disc, lipid modifications would enable Hh to reach target cells at a distance. The Eaton laboratory proposed that Hh would be boarded on lipoprotein-lipophorin complex (Lpp) that originate from the fat body. Hh-Lpp would move across the tissue, thus allowing Hh long-range signaling.[8,9] These Lpp also contains lipids that would repress the Hh pathway in the absence of Hh.[10] Palm et al. raised the possibility that in the wing disc Hh can be secreted in 2 forms that would have complementary functions and would synergize to activate Hh target genes.[11] First, cholesterol-modified Hh would be secreted in a Lpp-associated manner and would lead to the accumulation of the transcription factor Ci in a full-length, but inactive form. Second, cholesterol-free Hh (Hh-N*) would be secreted in a Lpp-free manner and would not be able to activate Hh target genes by itself either. However, when both Hh and Hh-N* are present together, they could act in synergy to eventually trigger Hh target gene expression.

Palm et al. first showed that Hh proteins can be secreted in a lipoparticle-associated-manner but also in a lipoprotein-free manner when overexpressed in both human cultured cells and in the *Drosophila* hemolymph. The lipoparticle-associated SHh/Hh secretion would require either palmitate or cholesterol since cholesterol-free and palmitate-free SHh/Hh can still associate with lipoparticles. Conversely, a form of SHh/Hh that lacks both palmitate and cholesterol cannot associate with lipoparticles. Therefore, any lipid moiety is sufficient to promote Hh association to a broad diversity of lipoparticles.

The authors next investigated the molecular characteristics of lipoparticle-free Hh. They showed that Lpp-free Hh is cholesterol-free. Indeed, when *Drosophila*

Downloaded by [Bibliotheque Diderot de Lyon] at 01:48 20 August 2015

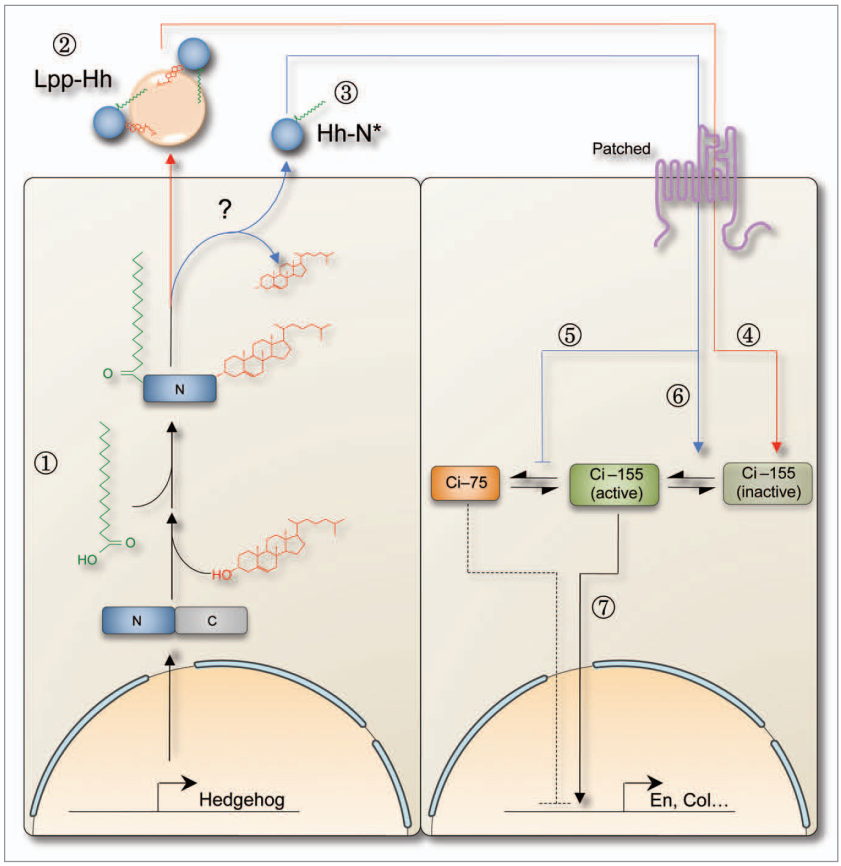

Figure 1. Proposed model of Hh and Hh-N* secretions and actions in the *Drosophila* wing imaginal disc. The left cell is producing Hh, the right one is receiving Hh through its receptor Patched (purple). Hh is first covalently bound to cholesterol and palmitate moieties (**1**). Processed Hh would be secreted in a Lpp-associated manner (Lpp-Hh, red lines) (**2**). A putative unknown esterase would lead to the formation of a cholesterol-free pool of Hh that is secreted in a Lpp-free manner (Hh-N*, blue lines) (**3**). Lpp-Hh would stabilize the inactive form of full-length Ci (**4**). Hh-N* would decrease the amount of cleaved Ci (**5**), but importantly would promote the switch from inactive to active full-length Ci (**6**). Thus, when present together, Hh and Hh-N* would act in synergy to eventually trigger the transcription of the Hh target genes (**7**).

S2 cells are transfected with ^{3}H-cholesterol, the soluble pool of Hh that is Lpp-free is also free from cholesterol. It is worth noting that reducing Lpp levels leads to an accumulation of Lpp-free Hh. Since the authors suggest that Lpp-free Hh is cholesterol-free, it implies that one of the pleiotropic effects of Lpp knockdown is to somehow promote the formation of cholesterol-free Hh, which should be further investigated.

Next, Palm et al. analyzed whether cholesterol-free Hh is produced in vivo. First, reducing Lpp levels in the disc leads to a slight decrease of Patched expression range. Palm et al. hypothesized that the secretion of a cholesterol-free form of Hh would account for the remaining Patched expression. Using Triton X-114 phase separation, they showed that the soluble Hh pool is detected exclusively in the aqueous phase, suggesting that this pool of Hh is cholesterol-free (Hh-N*). This contradicts pioneer studies that used the Triton X-114 protocol and showed that cholesterol-free Hh is detected both in the aqueous and the detergent phase.[5] Therefore further biochemical evidence is required to definitely prove the in vivo existence of Hh-N*.

The authors then investigated the signaling properties of Lpp-associated Hh and Hh-N* in the wing disc. They found that by overexpressing Hh in the hemolymph, ectopic Hh is detected in the anterior compartment of wing discs. In these discs, Ci accumulates in its full-length form, which is the one able to activate Hh target genes. Surprisingly, the Hh target genes are not expressed, which suggests that Lpp-associated Hh promotes the stabilization of full-length Ci in an inactive form. To investigate whether Hh-N* could have additional effects on Hh target gene expression when co-expressed with Hh, Palm et al. overexpressed Hh in the fat body in Lpp-RNAi larvae. With these settings, Hh-N* is produced at moderate levels with some Lpp-associated Hh in the hemolymph. Palm et al. suggest that Hh-N* can activate target genes when full-length Ci is stabilized by remaining Lpp-Hh as an anterior overgrowth is observed in these discs. However, one can notice that the expression range of the Hh target Dpp-lacZ appears to be unaffected, although an extra Dpp-lacZ stripe perpendicular to the endogenous one is detected. The origin of this extra-stripe is not discussed but still can account for the anterior compartment overgrowth

Downloaded by [Bibliotheque Diderot de Lyon] at 01:48 20 August 2015

observed in these discs. Besides, the analysis of the other Hh targets is required to confirm that Hh-N* with remaining Hh-Lpp can activate the transcription of Hh target genes. Still, to confirm that Hh-N* can synergize with Hh-Lpp to activate Hh target genes, Palm et al. expressed in the fat body either Hh, Hh-N (cholesterol-free Hh variant genetically engineered) or both and subsequently analyzed Hh target gene expression in the wing disc. Strikingly, combination of low levels of Hh-N and Hh-WT in the fat body leads to a broad expression of Collier and Engrailed in the anterior compartment, suggesting that Hh and Hh-N can synergize to activate Hh targets. However, moderate levels of Hh-N in the fat body leads to a similar broad expression of Collier and Engrailed. Thus, Hh-N by itself is capable to induce target genes at a distance, which contradicts the model of Palm et al. in which Hh-N* alone is not able to induce Hh target genes. Still, the authors propose that the Hh-N genetically engineered would have the feature of both Lpp-associated Hh and Hh-N*, thus explaining why Hh-N is able to induce Hh target genes. However, a much simpler hypothesis is that cholesterol-free Hh can signal by itself at a long-range independently of endogenous Hh, as reported in several instances.[12-14] Besides, Palm et al. proposed that Hh-N* and Hh would have complementary functions as Hh-N overexpression decreases the amount of cleaved-Ci without changing the amount of full-length Ci. However, since the amount of cleaved-Ci is not documented for Hh-N* and since the authors report that Hh-N may have different features from Hh-N*, it is hard to state that Hh-N* and Hh have complementary functions.

Altogether, Palm et al. brought evidence that both mammals and flies can release Lpp-associated Hh and Lpp-free Hh-N*. Particularly, Palm et al. raised the possibility that wing imaginal discs produce Hh-N*. These data support a model in which Hh-N* and Hh could synergize to activate Hh target genes in the wing disc (**Fig. 1**). However, further investigations are required to confirm the consistency of this model. Most of all, it is crucial to understand how 2 distinct Hh variants that bind to the same receptor Patched could trigger differential responses. Also, biochemical and genetic experiments are needed to understand how cholesterol-free Hh is produced. Indeed, since cholesterol is required for the correct processing of Hh, it implies that a putative esterase should remove the cholesterol moiety to generate a pool of Hh-N*.

Still, a crux of the different current models is that cholesterol would enable a long-range signaling of Hh, although Hh activates its targets at a shorter distance compared with other ligands such as Decapentaplegic or Wingless. Based on this assumption a number of mechanisms have been proposed. A first model is that Hh could board on cytonemes originating from receiving cells.[15] Alternatively, Hh would be secreted apically and then released basolaterally with a complex choreography to board cytonemes that originate from the Hh-producing cells.[16,17] A third model proposed by Palm et al. is that both cholesterol-bound Hh and cholesterol-free Hh could be secreted, and act in synergy although the putative mechanism that generate cholesterol-free Hh is unknown.[11] Thus, how can we reconcile all these mutually exclusive mechanisms to explain how Hh gradient is generated in the wing disc? A clue may come from a simple but still instructive experiment: overexpressing cholesterol-free Hh leads to ectopic activation of Hh targets at a long-range that is never encountered in vivo.[12,14] Furthermore, it has been shown that cholesterol-free Hh induces a long-range plateau of Hh targets, suggesting that the cholesterol adduct is required for the establishment of a short-range Hh gradient.[14] Therefore, the role of the cholesterol moiety is to ensure a short-range Hh spread, rather than enabling a "long-range" signaling. Most importantly, one should conclude that the mechanism that truly accounts for Hh short-range gradient formation should specifically involve the cholesterol moiety.

Disclosure of Potential Conflicts of Interest

No potential conflicts of interest were disclosed.

References

1. Mann RK, Beachy PA. Novel lipid modifications of secreted protein signals. Annu Rev Biochem 2004; 73:891-923; PMID:15189162
2. Pepinsky RB, Zeng C, Wen D, Rayhorn P, Baker DP, Williams KP, et al. Identification of a palmitic acid-modified form of human Sonic hedgehog. J Biol Chem 1998; 273:14037-45; PMID:9593755; http://dx.doi.org/10.1074/jbc.273.22.14037
3. Chamoun Z, Mann RK, Nellen D, von Kessler DP, Bellotto M, Beachy PA, et al. Skinny hedgehog, an acyltransferase required for palmitoylation and activity of the hedgehog signal. Science 2001; 293:2080-4;PMID:11486055;http://dx.doi.org/10.1126/science.1064437
4. Micchelli C, The I, Selva E, Mogila V, Perrimon N. Rasp, a putative transmembrane acyltransferase, is required for Hedgehog signaling. Development 2002; 123:843-51; PMID:11861468.
5. Porter JA., Ekker SC, Park WJ, von Kessler DP, Young KE, Chen CH, Ma Y., Woods AS, Cotter RJ, Koonin EV et al. Hedgehog patterning activity: role of a lipophilic modification. Cell 1996; 86:21-34. PMID: 8689684; http://dx.doi.org/10.1016/S0092-8674(00)80074-46. Porter JA, Young KE, Beachy PA. Cholesterol modification of hedgehog signaling proteins in animal development. Science 1996a; 274:255-9; PMID:8824192; http://dx.doi.org/10.1126/science.274.5285.255
7. Wendler F, Franch-Marro X, Vincent JP. How does cholesterol affect the way Hedgehog works? Development 2006; 133:3055-61; PMID:16873581; http://dx.doi.org/10.1242/dev.02472
8. Panáková D, Sprong H, Marois E, Thiele C, Eaton S. Lipoprotein particles are required for Hedgehog and Wingless signalling. Nature 2005; 435:58-65; PMID:15875013; http://dx.doi.org/10.1038/nature03504
9. Eugster C, Panáková D, Mahmoud A, Eaton S. Lipoprotein-heparan sulfate interactions in the Hh pathway. Dev Cell 2007; 13:57-71; PMID:17609110; http://dx.doi.org/10.1016/j.devcel.2007.04.019
10. Khaliullina H, Panáková D, Eugster C, Riedel F, Carvalho M, Eaton S. Patched regulates Smoothened trafficking using lipoprotein-derived lipids. Development 2009; 136:4111-21; PMID:19906846; http://dx.doi.org/10.1242/dev.041392
11. Palm W, Swierczynska MM, Kumari V, Ehrhart-Bornstein M, Bornstein SR, Eaton S. Secretion and signaling activities of lipoprotein-associated hedgehog and non-sterol-modified hedgehog in flies and mammals. PLoS Biol 2013; 11:e1001505; PMID:23554573; http://dx.doi.org/10.1371/journal.pbio.1001505
12. Burke R, Nellen D, Bellotto M, Hafen E, Senti KA, Dickson BJ, et al. Dispatched, a novel sterol-sensing domain protein dedicated to the release of cholesterol-modified hedgehog from signaling cells. Cell 1999; 99:803-15; PMID:10619433; http://dx.doi.org/10.1016/S0092-8674(00)81677-3
13. Callejo A, Torroja C, Quijada L, Guerrero I. Hedgehog lipid modifications are required for Hedgehog stabilization in the extracellular matrix. Development 2006; 133:471-83; PMID:16396909; http://dx.doi.org/10.1242/dev.02217
14. Ducuing A, Mollereau B, Axelrod JD, Vincent S. Absolute requirement of cholesterol binding for Hedgehog gradient formation in Drosophila. Biol Open 2013; 2:596-604; PMID:23789110; http://dx.doi.org/10.1242/bio.20134952
15. Roy S, Hsiung F, Kornberg TB. Specificity of Drosophila cytonemes for distinct signaling pathways. Science 2011; 332:354-8; PMID:21493861; http://dx.doi.org/10.1126/science.1198949
16. Rojas-Ríos P, Guerrero I, González-Reyes A. Cytoneme-mediated delivery of hedgehog regulates the expression of bone morphogenetic proteins to maintain germline stem cells in Drosophila. PLoS Biol 2012; 10:e1001298; PMID:22509132; http://dx.doi.org/10.1371/journal.pbio.1001298
17. Bilioni A, Sánchez-Hernández D, Callejo A, Gradilla AC, Ibáñez C, Mollica E, et al. Balancing Hedgehog, a retention and release equilibrium given by Dally, Ihog, Boi and shifted/DmWif. Dev Biol 2013; 376:198-212; PMID:23276604; http://dx.doi.org/10.1016/j.ydbio.2012.12.013

DISCUSSION

During my thesis, I investigated the signalling and morphogenesis during *Drosophila* dorsal closure.

1. JNK and DPP form a coherent feed-forward loop during dorsal closure.

It was known for a long time that JNK and DPP signal in the leading edge cells during dorsal closure. Both signalling pathways are required for dorsal closure since closure fails in embryos mutant for JNK or DPP pathway components. Because DPP is downstream of JNK and since DPP is a diffusible ligand, it was proposed that DPP could act as a relay to induce a wide ranger of targets. Still, JNK was also shown to regulate the cytoskeleton. Thus, how the leading edge cells integrate these signals remained unclear. We showed that at the leading edge, JNK and DPP form a coherent feed-forward loop, where JNK induces DPP and both JNK and DPP signals are absolutely required for leading edge identity. This feed-forward loop is coherent "and-type FLL" as both JNK and DPP act positively, as either signal alone does not trigger a response. The general function of the indirect branch of a coherent feed-forward loop is to filter the input received by the direct branch (Mangan and Alon, 2003). During dorsal closure, JNK is therefore the instructive signal, while the DPP branch filters this spatial information. Interestingly, under normal laboratory conditions, at 25°C, the JNK/DPP feed-forward loop is dispensable for dorsal closure. Conversely, when embryos are subjected to thermal stress, the DPP/Brk branch of the feed-forward loop is crucial to restrict the interpretation of JNK signal only in the leading edge cells to ensure correct closure. DPP here buffers against environmental challenges and canalizes cell identity, which is a novel function from its

well-established ability to act as a morphogene. Our data are coherent with other evidence that taken together suggest that JNK signals "has to be" restricted to leading edge cells during dorsal closure. First, JNK pathway possesses numerous inhibitors including *puc, scaf, row* and *aop.* Therefore multiple components dampen JNK signalling. In addition, it has been shown that *acal* is a non-coding RNAi that is expressed in the lateral epidermis and that is required to inhibit JNK signalling in these lateral epidermal cells (Rios-Barrera et al., 2015). Ectopic JNK signalling is deleterious for dorsal closure since in *puc* mutant embryos that display ectopic JNK activity in the lateral epidermis closure completes but resulting in a puckering of the epidermis toward the dorsal midline (Martin-Blanco et al., 1998). Thus, JNK is tightly restricted to the leading edge during dorsal closure and our data provide another evidence that unwanted JNK signal can be filtered out to ensure robust, canalized dorsal closure.

Interestingly, our data also suggest that Scaf and Puc are both under the control of the JNK / DPP feed-forward loop. Therefore, the signalling network at the leading edge is more complex than what was initially described. We do not understand yet what are the consequences of *Scaf* and *puc* being under the control of solely JNK or under the control of the JNK/DPP feed-forward loop. We propose that if Puc and Scaf were solely under the control of JNK, in case of a short burst of unwanted JNK signal, the immediate transcription of Puc and Scaf would dampen both the short burst and the "real" developmental JNK signal. In this scenario, Puc and Scaf early action would be deleterious for dorsal closure. Conversely, by being under the control of the JNK/DPP feed-forward loop, short bursts of JNK do not elicit a transcription of Scaf and Puc, leaving the "real" developmental JNK signal unaffected. This is a hypothesis, and experimental evidence to confirm its consistency are lacking. Mostly, we are reaching the limit of the conventional biology and *in silico*

modelling constitutes the next logical step toward a better understanding of these network motifs.

2. What is the leading edge?

To decipher this JNK/DPP feed-forward loop, we used 3 markers of the leading edge identity: Jupiter, Jaguar and Zasp52. We noticed that these three markers are not only expressed in the dorsal-most row of epidermal cells, but also in the second row of dorsal epidermal cells. This is consistent with the JNK reporter TRE::GFP that is expressed in the first two rows of dorsal epidermal cells. In most of - if not all - the literature, the leading edge is considered as the very first row of epidermal cells in contact with the amnioserosa (Harden, 2002; Rios-Barrera and Riesgo-Escovar, 2013). This is largely based on the "historical" observation that the *puc-lacZ* reporter is only expressed in the first row of dorsal epidermal cells (Glise and Noselli, 1997; Hou et al., 1997; Kockel et al., 1997; Riesgo-Escovar and Hafen, 1997). However, based on our observations, from a signalling point of view, the leading edge should be considered as the first two rows of dorsal epidermal cells. In addition, I (and likely others) observed that homozygous *puc-lacZ* embryos display lacZ staining in the first two rows of dorsal epidermal cells. Therefore, the *puc-lacZ* line at heterozygous state is likely to reflect only the maximal JNK levels (and should be used with caution).

Still, whereas the first two rows of dorsal epidermal cells accumulate Jupiter, Zasp52, Jaguar and Scarface, only the first row of cells in contact with the amnioserosa accumulate microtubules, actin cable and filopodia. In the second row of dorsal epidermal cells, Echinoid (Ed) distribution is homogenous (Laplante and Nilson, 2011). Therefore, it is possible that the second row of cells is not able to produce an actin cable, filopodia, or to accumulate microtubules because of Ed symmetric distribution. Why, then, JNK is at work in this second row of dorsal epidermal cells? Interestingly, after ablation of leading edge cells in contact with the amnioserosa, the new row of cells are likely to become the new "leading edge". This is based on the observation that following repeated wounds, leading edge cells are able

to form a secondary or a tertiary purse-string (Rodriguez-Diaz et al., 2008). It still remains to be verified whether these cells in addition of forming an actomyosin cable also accumulate markers of the leading edge identity. If it were the case, this would indicate that epidermal cells are competent to become leading edge cells in case of unexpected events. Therefore, a possibility is that the second row of leading edge cells is in a "ready-to-go" state and is therefore quickly able to accumulate microtubules, produce an actin cable as well as filopodia. The next logical step would be to wound the first row of leading edge cells and observe if the second row of leading edge cells that were positive for Jupiter, Jaguar, Zasp52 and Scaf quickly form an actin cable, produce filopodia and accumulate microtubules. The dynamic of such putative changes should be compared with similar embryos where the two first rows of leading edge cells are wounded. In this case, the new leading edge would be formed by epidermal cells that where never positive for the JNK pathway and where the targets where not expressed. This should provide a clue to better understand of the function of this second row of leading edge cells.

3. Zasp52 is an upstream regulator of the actin cable

While deciphering the JNK/DPP feed-forward loop, we focused on Zasp52, an actin-associated protein enriched at the level of the actin cable. Since we observed that Zasp52 is enriched at the actin cable, and since interruptions of the actin cable correlates with lack of Zasp52, we hypothesised that Zasp52 could be an upstream regulator of the actin cable. Indeed, in Zasp52 embryos, the actin cable does not form. Interestingly, Ena staining at the leading edge / amnioserosa interface is lost in Zasp52 mutant embryos. However, when ectopically expressed in the leading edge cells of Zasp52 mutant embryos, Ena fails to accumulate at the leading edge / amnioserosa interface. In addition, we observed that in Zasp52 mutant embryos, actin is present but disorganized at the leading edge / amnioserosa interface. Taken together, our data suggests that Zasp52 controls the correct organisation and / or assembly of the diverse components of the actin cable. This is consistent with the observation that in *Drosophila* muscles, Zasp52 physically controls the recruitment of alpha actinin (Jani and Schock, 2007). However, we do not know yet how Zasp52 acts at the molecular level during dorsal closure, and whether it acts *via* alpha actinin. First, Zasp52 has fourteen predicted isoforms. Recently, Beth Stronach identified that the GFP insertion in the Zasp52::GFP line matches with a specific isoform (Stronach, 2014). Thus, creating a UAS-Zasp52 line with this specific isoform will constitute the next logical step towards a better understanding of Zasp52 molecular action. In parallel, since Zasp52 contains a PDZ that is known to interact with alpha actinin, creating a version of Zasp52 lacking with PDZ domain may produce a dominant negative effect, or may fail to rescue the Zasp52 mutant phenotype.

Last, we observed that both Zasp52 and the actin cable are interrupted in several instances in wild-type embryos. Time-lapse movies indicate that the interruptions are quite stable over time. We do not fully understand yet the origin

and the consequences of such functions. It has been shown that during dorsal closure, two cells from the second row of dorsal epidermal cells intercalate between the groove cells and the cell posterior to the groove cells (Gettings et al., 2010). It is therefore possible that the intercalated cells called the 'mixer cells' do not produce an actin cable, or with a delay, thus mechanically creating interruptions in the actin cable. To test this hypothesis, it would be interesting to track the mixer cells that express Engrailed *de novo*. In this scenario, the interruption of the actin cable would be a consequence of the cell mixing.

4. The actin cable: do not call me purse string.

Overall, our data show that in Zasp52 mutant embryos, the actin cable is specifically affected. We therefore set up a unique model to examine the function of the actin cable during dorsal closure and wound healing. Indeed, a powerful experimental setting to assess the function of the actin cable during dorsal closure was lacking so far. Laser ablation experiments have the disadvantage that they do not only affect the actin cable but also the integrity of the leading edge cells and possibly also filopodia. Therefore in all these experiments, the leading edge AND the actin cable were affected but not the actin cable alone (Kiehart et al., 2000; Hutson et al., 2003; Rodriguez-Diaz et al., 2008). Alternatively, in embryos where the actin network is affected other actin-related structures such as the amnioserosa or the filopodia are also affected (Grevengoed et al., 2001; Jacinto et al., 2002; Hutson et al., 2003; Laplante and Nilson, 2006; Houssin et al., 2015). Last, the use of JNK or DPP signalling mutant embryos is dangerous since in these mutant have numerous cytoskeletal defects and not only actin cable defects.

With the Zasp52 mutant embryos, we set up a unique model where the actin cable is specifically affected. Our data suggest that the actin cable is dispensable for both dorsal closure and wound healing. It has been suggested that in the absence of a functional or continuous cable, the amnioserosa is able to compensate this absence and enables a correct closure. However, after the ablation of the amnioserosa, Zasp52 mutant embryos still complete closure with a similar dynamic compared to wild-type embryos with similar ablation of their amnioserosa. This raises two important possibilities. First, the actin cable does not provide a major contractile force during dorsal closure, and is unlikely to act as a contractile purse string. Second, it indicates that another factor can drive closure in the absence of the amnioserosa and the actin cable. This could be the filopodia. Indeed, when making the zippering effective,

filopodia "secure" the dorsal progression of the two edges. The filopodia are possibly a – not to say the – key driving force of dorsal closure and wound healing.

This raises the following question: if the cable does not provide a major contractile force, what then is its function?

Overall, we observed that the leading edge / amnioserosa interface is not straight at all stages of dorsal closure, as previously reported (Grevengoed et al., 2001; Laplante and Nilson, 2006). The interface is highly misshapen with successions of "Hills" and "Valleys". We further showed that in embryos lacking the actin cable, tension at the leading edge is lacking. This is consistent with laser ablation experiments that showed that the tensions are present at the level of the cable (Kiehart et al., 2000; Rodriguez-Diaz et al., 2008). Interestingly we noticed that the leading edge / amnioserosa interface was not randomly disorganized: the cells forming the 'Valleys' often correspond to groove cells. These cells are highly different from their neighbours in the lateral epidermis since they accumulate specific proteins such as aPKC, Crumbs or Ena (Vincent et al., 2008). We found that the groove cells that form the "Valleys" are stiffer that cells forming the "Hills", thus accounting for this anisotropy in leading edge cell alignment. Under normal conditions, the physical properties of groove or non-groove cells are overcome by the presence of the actin cable and the leading edge remains straight. Our data thus reconciles the previous observation in the purse-string model that the cable generates tension: when the cable is present, we propose that it imposes strong tensions that go along leading edge to homogenize the leading edge cell behaviour.

Interestingly, we noticed that in some cases, the "Valleys" rather constitute an ectopic canthus that gets closed overtime with unwanted, ectopic zippering. This probably greatly contributes to increase the leading edge straightness in Zasp52 mutant embryos as closure proceeds. Importantly, these ectopic canthi due to the absence of the actin cable leave visible marks after the completion of closure, that is

similar to a scar. Indeed, the patterning is affected and the tissue is stretched with many cells remaining misshapen. Thus, we propose that the actin cable prevents scar formation. This is in agreement with pioneer studies that suggested that the actin cable present during embryonic wound healing prevents scar formation, while its absence leads to scaring in adult wound healing (Martin and Lewis, 1992). However, while it has been hypothesised that the cable would leave no scar by reducing the timing of closure, we rather believe that this is rather because the cable maintains cell integrity regarding the major forces that accumulate at the leading edge.

Altogether, the actin cable allows a perfect epithelial closure by stabilizing the mechanical forces required for healing. The actin cable is therefore a structure that allows the combination of forces acting at different scales and protects individual cells from the forces that drive epithelium reorganization. Since we believe that the actin cable prevents "scar" formation, the next logical step would be to ectopically express Zasp52 in adults and observe if an actin cable forms after a wound. If it were the case it would be of interest to compare the scar left after a wound in WT *versus* Zasp52 overexpressing adults.

5. Is JNK acting as a stress-mediator pathway in the embryo?

The JNK pathway is a stress response pathway that also controls developmental processes such as dorsal closure. While in other tissues JNK can trigger apoptosis in response to stress, leading edge JNK does not activate apoptosis but rather controls leading edge cell identity during dorsal closure. This raises the question of how a single pathway can either kill or pattern.

Beira and colleagues showed during dorsal closure that JNK-induced apoptosis is prevented at the leading edge by the DPP co-repressor Shn (Beira et al., 2014). Thus, JNK and DPP would form an incoherent feed-forward loop that controls the expression of the proapoptotic gene *rpr*: JNK induces *dpp* and *rpr*, but DPP represses *rpr*. This is based on the observation that in *shn* and *tkv* mutant embryos, the *rpr* mRNA is up regulated at the leading edge in a JNK-dependent manner. Second, Beira and colleagues reported that epidermal cells are apoptosed in *shn* mutant embryos, indicating that DPP protects against JNK-induced cell death.

Our data argue against this model and indicate that leading edge cells do not die in DPP signalling mutant embryos. First, we showed using live imaging that leading edge cells do not undergo apoptosis. Second, we showed that in fixed embryos, leading edge cells do not display any sign of caspase activity in the absence of DPP signalling. Second, blocking the putative cell death in the lateral epidermis with the apoptosis inhibitor P35 in *tkv* mutants does not rescue of the dorsal open phenotype. Third, strong ectopic activation of the JNK pathway in the absence of DPP does cause leading edge cell death. Altogether, our data suggest that DPP does not protect against JNK-induced apoptosis. Thus, how can we explain the discrepancies between our results and Beira and colleague results?

First, Beira and colleagues never showed a caspase 3 or DCP-1 staining to label cell death. In our study, we used these markers as well as precise live imaging to

precisely labels cells undergoing apoptosis. Using only *rpr* mRNA is a surprising approach since *rpr* mRNA accumulation is not the last step that triggers apoptosis. Rather, the use of antibodies recognizing cleaved caspases is a more relevant tool. If *rpr* mRNA accumulation at the leading edge of DPP signalling mutant embryos is true, this suggests that another factor that is DPP-independent may prevent *rpr* mRNA from being active. Such putative factor may act on *rpr* mRNA maturation, protein stability or on downstream components.

Second, Beira and colleagues quantified neuronal loss in *shn* mutant embryos with the Cut antibody to prove that epidermal cells where undergoing cells death. When we analyzed *shn* or *tkv* embryos, we were able to detect cell death in lower tissues in the vicinity of Cut-positive neurons, but not in the epidermis. Therefore, I believe that quantifying neuronal cell death to assess epidermal cell death is not the most rigorous approach.

Last, but not least, Beria and colleagues provided genetic evidence that cell death is involved in the dorsal closure phenotype: in *shn* mutant embryos, the dorsal open phenotype is partially rescued by removing *rpr* and *skl* using the Df(3L)X38 deficiency. We showed that preventing cell death in the leading edge cells does not rescue the dorsal open phenotype. However, blocking apoptosis specifically in the amnioserosa leads to a rescue of the dorsal open phenotype, similar to what Beria and colleagues observed with *shn*^{1}*, Df(3L)X38* embryos. This is consistent with the observations that 10 to 30% of amnioserosa cells undergo cell death and that apoptosis rate in the amnioserosa tunes the speed of closure (Toyama et al., 2008; Muliyil et al., 2011). Therefore, the apoptotic force of the amnioserosa is DPP-independent and is likely to be a major contributor to the dorsal open phenotype. We thus believe that blocking specifically cell death in one tissue or another is a more accurate approach to understand the contribution of cell death in DPP signalling mutant embryos.

Altogether, we propose that DPP is unlikely to protect against JNK-induced apoptosis. However, we found that JNK can act as a stress-mediator pathway in other context.

Indeed, we found that JNK may respond to mechanical stress. Using embryos mutant for the DPP receptor *thickveins* (*tkv*) where abnormal tensions are generated at the amnioserosa / leading edge interface I showed that JNK respond to mechanical stress and activate the dorsal closure targets Jupiter and Jaguar (Jar). Second, I tested whether JNK pathway is at work during wound healing. I found that epidermal cells around trigger activation of the JNK pathway. Third, I showed that this JNK pathway activation is crucial for embryonic wound healing, since embryos deprived of JNK activity failed to heal their wounds. This is in line with other studies that suggested that the JNK pathway is at work during larval and adult wound healing (Ramet et al., 2002; Galko and Krasnow, 2004; Belacortu and Paricio, 2011).

Taken together, our results suggest that JNK can act as a mechanical stress mediator and is crucial for embryonic wound healing.

At the moment, we are currently looking for a way to generate sustained mechanical stress without killing cells. This will constitute an interesting tool to strengthen the idea that JNK can respond to abnormal tensions.

6. Conclusion

During my Ph.D, I tried to better understand dorsal closure from a signalling and morphogenetic point of view. I found that at the leading edge JNK and DPP form a coherent feed-forward loop, where JNK is the instructive signal, and DPP filters out unwanted JNK signals to ensure robust and canalized dorsal closure. Second, I found that the actin cable produced by leading edge cells is dispensable for dorsal closure. Specifically, I showed that the actin cable does not provide a major contractile force but rather imposes strong tensions to balance forces and to stabilize cell geometry so that closure resolves in a perfectly structured and scar-free tissue. I also showed that JNK can respond to mechanical tensions and acts during embryonic wound healing. However, DPP is unlikely to protect cells from JNK induced apoptosis.

To end up this thesis, I would like to give a synthetic view of how dorsal closure could *simply* work, taking into account all the data I generated (this is strictly my opinion and may not reflect the reality). During dorsal closure, the amnioserosa is pulsing and cells are delaminating. This is undeniably the key driving force of dorsal closure. The filopodia play a role of primed importance since they secure the dorsal-ward progression of leading edge cells. They can act in lieu of the amnioserosa, as it is the case during wound healing. The actin cable does not produce a driving force during dorsal closure. It is not a contractile purse string. Rather, it maintains a straight leading edge to make a perfect closure. This also may help the filopodia to zip at each extremity by limiting the angle of each canthus. From a signalling point of view, the cytoskeleton of leading edge cells is controlled by the JNK / DPP feed-forward loop. The main purpose of such a sophisticated network motif is likely to filters out unwanted JNK inputs. Indeed, ectopic JNK activity is deleterious for dorsal closure (see the *puc* mutant phenotype for instance). I found that at least temperature and mechanical stress can lead to ectopic JNK activity,

and I believe that other stresses could trigger JNK activation. Therefore, this JNK / DPP feed forward ensures that only the developmentally programmed JNK signal is interpreted by the leading edge cells.

Dorsal closure is therefore a striking example of how signalling pathways and cytoskeletal components act in concert to promote a perfect, robust and coordinated action of hundreds of cells.

MATERIALS AND METHODS

The section aims at describing the different methods I used and their improvement over my Ph.D. It contains all the tips that are NEVER FOUND in the Material and Methods sections of articles.

1. Embryo collection

For setting up the cages, I used the following bottles that where perforated with a needle to let the flies breath. For agar plates, use 1 g of agar in 100 mL of tap water (no need for distilled water). Make it boil twice. Once it is hot, add blackcurrant syrup, agitate your flash and pour. Keep your plates at 4°C.

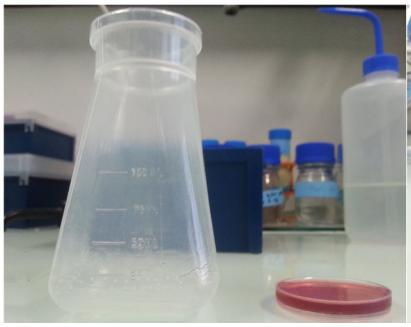
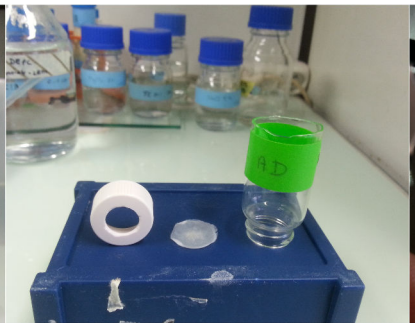


For embryo collection, put dried yeast at the middle of the agar plate and add a bit of water. Change your laying pots before leaving the lab and collect your embryos the day after. The next day, the first step is to put bleach on the plate to remove the chorion (100% bleach, 5 minutes) and collect them (usually with a basket and a brush). We use home-made collection vials. We ordered scintillation vials. We made a hole in the lead with a drill and we cut the bottom of the glass vial with a diamond grinding wheel (put some tape where you plan to cut to avoid fracturation of the glass). Last, we stuck a filter between the lead and the vial. This way, when we poor bleached embryos onto our vials, all the embryos are stuck on the filter Then, we just

have to unplug the lead and collect the filter with a forceps, thus avoiding any loss of embryos.

2. Fly stocks

In addition of the traditional balancers, here are the special balencer I used.

CDY: *Cyo, Dfd::YFP*. CyO balancer carrying Sb, Hu and Tb markers. Expresses YFP under the control of the Dfd promoter. Visible in the embryo from stage 13, onwards. Visible in the larvae.

TDY: *TM6, Sb, Tb, Hu, Dfd::YFP*. TM6 balancer carrying Sb, Hu and Tb markers. Expresses YFP under the control of the Dfd promoter. Visible in the embryo from stage 13. Visible in the larvae.

CKG: *Cyo, Kruppel-Gal4, UAS-GFP.* Cyo balancer with GFP expressed in the Kruppel[+] pattern. Visible in embryos from Stage 10 onwards, in larvae, pupae and adults.

CWZ: *Cyo, Wg::lacZ*. Cyo balencer with lacZ expressed in Wingless[+] stripes in the embryo that is visible from stage 8/9, onwards.

TUZ: *TM3, Sb, Ubx::lacZ*. TM3 balancer carrying Sb marker. Express lacZ in the Ubx[+] pattern that is visible in the embryo from Stage 13, onwards.

En-Gal4	*yw ; en-Gal4 ; +*	Drives expression in epidermal stripes in the embryo. Strong Gal4.
Prd-Gal4	*w ; + ; Prd-Gal4 / TDY*	Drives expression in epidermal stripes in the embryo. Strong Gal4.
Pnr-Gal4	*w ; + ; Pnr-Gal4 / TDY*	Drives expression in the first 10 rows of dorsal epidermal cells.
c381-Gal4	*w ; + ; + ; c381-Gal4*	On the 4th chromosome. Drives expression in the amnioserosa.

UAS-ActinRFP	*w ; + ; UAS-ActinRFP*	UAS sequences control expression of RFP-tagged Actin.
UAS-APC2::GFP	*w ; + ; UAS-APC2::GFP*	GFP fused with APC2 (labels actin). Brightest reporter ever used.
UAS-Brk	*w ; UAS-Brk / TUZ*	UAS sequences control expression of Brk. Escapers visible.
UAS-bsk^{DN}	*yw, UAS-bsk^{DN} ; + ; +*	On X. Dominant negative forme of the JNK *basket*.
UAS-Ed::GFP	*w ; + ; UAS-Ed::GFP*	Gift from L. Neilson. UAS sequences control expression of GFP-tagged Echinoid.
UAS-Ena	*w ; + ; UAS-Ena*	UAS sequences control expression of ena tagged with six histidines.
UAS-GFP^{NLS}	*w ; + ; UAS-GFP^{NLS}*	UAS sequences control expression of nuclear GFP. Visible in the cytoplasm too.
UAS-hep^{ACT}	*w ; UAS-hep^{ACT} ; +*	Dominant active form of the JNKK *hemipterous*.
UAS-p35	*w + ; UAS-p35 / TM6B*	UAS sequences control expression of the caspase inhibitor p35.
UAS-rpr	*w ; + ; UAS-rpr / TM6B*	UAS sequences control expression of rpr.
UAS-tkv^{ACT}	*w ; UAS-tkv^{ACT} ; +*	Dominant active form of the DPP receptor tkv.
Brk^{M68}	*yw, brkM68 / FM7, Ftz::lacZ*	On X, loss-of-function allele, see (Jazwinska et al., 1999).
jra$^{76\text{-}19}$	*w ; jra$^{76\text{-}19}$ / CWZ*	Amorphic allele, see (Hou et al., 1997)
puc^{E69}	*w ; + ; puc^{E69} / TDY*	Known as Puc-lacZ. Homozygous embryos have a salt and pepper JNK signalling. See (Martin-Blanco et al., 1998).
shn^{1}	*w ; shn^{1} / CWZ*	Amorphic allelle, see (Grieder et al., 1995)
shn^{TDS}	*w ; shn^{TDS}/CWZ*	Known as *shn^{3}*, amorphic allele, see (Grieder et al., 1995)
tkv^{4}	*yw ; tkv^{4} / Cyo,w+*	Known as *tkv^{a12}*, amorphic allele, point mutation. See (Affolter et al., 1994)
tkv^{8}	*w ; tkv^{8} / CWZ*	Loss-of-function allele. See (Affolter et al., 1994)
ZaspΔ	*ZaspΔ / CKG*	Loss-of-function allele, see (Jani and Schock, 2007).

Arm::GFP	*w ; + ; Arm::GFP*	Ubiquitous expression of GFP-tagged Armadillo.
DPP-lacZ	*w^+ ; Dpp-lacZ^{NUC} / CyO ; +*	lacZ is [ry+] and not w+. lacZ-NLS coding sequence cloned after the BS 3.0 promoter of DPP, see (Blackman et al., 1991).
Jupiter::GFP	*w ; + ; Jupiter::GFP*	GFP knock-in, see (Morin et al., 2001).
Moesin::GFP	*w ; + ; Moesin::GFP*	sGCMA, where the sqh promoter drives expression of a fragment of Moe tagged with GFP, see (Kiehart et al., 2000).
Moesin::mCherry	*w ; + ; Moesin::mCherry*	The Moesin actin binding domain fused to Cherry driven constitutively with the sqh promoter, see (Abreu-Blanco et al., 2011).
shg::GFP	*yw; shg::GFP ; +*	shg::GFP construct replacing the endogenous shg gene via targeted site-specific DNA integration, see (Huang et al., 2009).
TRE::GFP	*w ; TRE::GFP ; +*	Contains four AP-1 binding sites downstream of an hsp70 promoter, see (Chatterjee and Bohmann, 2012)
TRE::RFP	*w ; TRE::RFP ; +*	
Zasp52::GFP	*w ; Zasp52::GFP ; +*	GFP knock-in, see (Morin et al., 2001).

I also generated the following recombinants and/or multiple lines:

#R1 Prd-Gal4, UAS-GFP^{NLS} / TDY

#R2 Prd-Gal4, Jupiter::GFP / TDY

#R3 Prd-Gal4, UAS-ActinRFP

#R4 Pnr-Gal4,UAS-APC2::GFP / TDY

#R5 Pnr-Gal4, UAS-ActinRFP / TDY

#R6 Pnr-Gal4, UAS-GFP^{NLS} / TDY

#R7 Zasp52::GFP, TRE::RFP

#R8 UAS-hep^{ACT}, Dpp-lacZ / CDY

#R9 tkv^{4}, UAS-hep^{ACT} / CDY

#R10 tkv^{4}, Dpp-lacZ / CDY

#R11 tkv^{4}, shg::GFP / CKG

#R12 tkv^{8}, TRE::GFP / CKG

#M1 *shg::GFP ; Prd-Gal4 / TDY*

#M2 tkv^{8} / CDY ; Jupiter::GFP

#M3 ZaspΔ / CKG ; Arm::GFP

#M4 ZaspΔ / CKG ; Moesin::GFP

#M5 ZaspΔ / CKG ; Jupiter::GFP

#M6 Zasp52::GFP ; Prd-Gal4 / ST

#M7 tkv^{4} ; UAS-p35 / ST

#M8 TRE::GFP ; Moesin::mCherry

3. Immunofluorescence

3.1 Regular immunofluorescence

Although this protocol looks trivial at a glance, we optimized it to avoid excessive time consumption and we identified the critical steps to make capricious stainings (such as E-Cadherin, Brinker or Phospho-Mad) working perfectly.

DECHORIONATION

1. Add bleach in the laying pots during 5 minutes
2. Pour the liquid in the filter box
3. Wash the filter (where the embryos are) to get rid of yeasts and bleach
4. Check that embryos have been COMPLETELY dechorionated.
5. Dry the filter. **This is a critical step. If the filter has not been perfectly dried at this stage, some staining, including the E-Cadherin staining will NOT be optimal.**

FIXATION

6. Add 500 µL of heptane and 500 µL of 4% PFA in an eppendorf tube.
7. Add the filter up and down in the eppendorf tube to let the embryos in the filter sink into the eppendorf tube.
8. Put the tube under strong agitation during 20 minutes.

PRIMARY ANTIBODIES

9. Remove the lower phase that contains PFA and add 500µL of methanol
10. Shake vigorously by hand the tube during 15 true seconds (you do not need more).
11. Remove methanol and heptane and add methanol.
12. Let sedimentate the embryos. At this stage, embryos can be stored at -20°C for months. **Keeping embryos at 20°C for couple of days can be beneficial, especially for phospho-mad or E-Cadherin staining. However, keeping them too long (> 1 month) will ruin your staining.**
13. Remove methanol and rinse quickly with PBT.
14. Incubate primary antibodies 1h30 at room temperature with a rotative shaker.

Secondary antibodies

16. Rinse quickly with PBT and then wash with PBT (2 x 10min).
17. Incubate secondary antibodies 1h30 at room temperature.

Final steps

18. Rinse quickly with PBT and then wash with PBT (2 x 10min).
19. Add 2 or 3 droplets of vectashield in the eppendorf.
20. Keep overnight at 4°C or at room temperature until the embryos have sedimented before mounting the slide.

3.2. Phalloidin stainings

This is an optimised protocol for outstanding Phalloidin stainings. This protocol is very sensitive and requires patience and adjustment. Please read the entire protocol before attempting to use it. All the GFP lines I tested never required a GFP antibody with this protocol.

1. Follow the exact same seven steps than for regular immunofluorescence.
2. Fix your embryos for 22 minutes **exactly**. Note that if the PFA is not warm enough, this can cause trouble shooting for hand devitellinisation.

3. Remove the PFA.

It is important at this step to remove the entire PFA, including the remaining small bubbles that are at the interface between the embryos and the heptane. It is preferable to loose some embryos while removing all the PFA than leaving all the embryos intact with some bubbles.

4. Once the embryos are in heptane, prepare a small petri dish with double-side tape on it. Pipet the embryos (P 1000 tip cut at its extremity), and spread them homogenously in the entire tape (do it under a binocular glass to control this step).

It is important to minimize the quantity of heptane taken while pipeting your embryos form the eppendorf tube. The less heptane you take, the more concentrated the embryos will be in your P 1000 tip, but the easier it will be for you later. If you have groups of embryos on the tape, separate them gently with the P 1000 tip.

5. Now starts the critical phase. Let your embryos dry on the double side tape (the heptane evaporates). They have to look glossy and you should be able to see the vitelline membrane that is getting flattened on the embryo (the membrane should look like a membrane of a agarose gel left by mistake for too long at room temperature). Once you have decided that this is the good moment, put 2 mL of 0.1 % Triton PBS (PBT), an 4 µL of Rhodamin-Phalloidin.

6. Remove the vitelline membrane with a thin needle. If you let your embryos dry and rehydrate correctly, you should see a space between the embryo and the vitelline membrane. Take your needle at the posterior pole of the embryo, and create a hole. Extract the embryo by pushing its head with the needle towards the posterior hole you created.

Note that at this step, you may encounter several issues that are listed below.

- If you did not let them dry enough, they will be too soft, and they will be smashed and split if different pieces while trying to extract them from their vitelline membrane.
- If you had too much heptane on your tape, the evaporation will never be efficient, and embryos will be too soft.
- If you did not spread your embryos correctly, the lonely ones will dry too much while the ones in clusters will not be dried enough (so spread them correctly). If you have only clusters, it means that you fixed and spread too much embryos at once. It is preferable to make two correct laying pots and repeat twice this protocol, rather than doing one big, unique laying pot.

- If embryos are not correctly stuck on the double side tape, it might be due to residual PFA bubbles that are on the tape.

Fixing these issue can take a little bit of time, and requires some fine tuning. **Always remember that it is better to let embryos dry too long than not long enough.**

7. Once all the embryos of the correct stage are hand devitellinized, collect them with a P 1000 and transfer them in an eppendorf tube. Let sedimentate your embryos. Pipette the liquid and put it back on your plate to take the last embryos. Do it several times to collect all your embryos.

8. Rinse quickly twice with PBT (invert the tube 3-4 times and let sediment your embryos).

9. If you just needed phalloidin, put them in VectaShield. If you want to add other antibodies, continue the staining as if you were at stage 13 of a regular immunofluorescence protocol.

3.3 Antibodies list

Commercial primary antibodies:

Mouse anti alpha-Tubulin (1:1 000, Sigma-Aldrich T6199)

Mouse anti Armadillo (1:250, DSHB)

Mouse anti Cut (1:250, DSHB)

Mouse anti Enabled (1:500, DSHB)

Mouse anti Patched (1:250, DSHB)

Mouse anti lacZ (1:250, Sigma G464,)

Rat anti DE-Cadherin (1:333, DSHB)

Rabbit anti DCP1 (1:500, Cell Signalling)

Rabbit anti-GFP (1:400, Invitrogen)

Rabbit anti Jun (1:10, Santa-Cruz)

Goat anti Numb (1:250, Santa Cruz Biotechnology)

Other primary antibodies:

Mouse anti Jar 3C7 (1,100, Kellerman and Miller, 1992)

Rabbit anti-PMad (1:1500)

Rabbit anti–Odd Skipped (1:400, gift from J. Skeath)

Rabbit anti-Zasp52 (1:400, gift from F. Schöck)

Guinea-pig anti Brk (1:500, gift from G. Morata)

Secondary antibodies:

Secondary antibodies are from Invitrogen and were used at 1:500. I used the following secondary antibodies: Alexa Donkey anti-Mouse 488, Alexa Goat anti-Mouse 633, Alexa Donkey anti-Rat 488, Alexa Fluor goat anti–rat 546, Alexa Goat anti-Rat

633, Alexa Donkey anti-Rabbit 488, Alexa Goat anti-Rabbit 546, Alexa Donkey anti-Guinea Pig 546, Alexa Donkey anti-Guinea Pig 488.

4. Live imaging and in vivo techniques

4.1. Aligning embryos for the Spinning disc

For live imaging, embryos are dechorionated except for Jupiter::GFP expressing embryos where the fluorescence is strong enough to overcome the auto fluorescence of the chorion.

Embryos are bleached (100% Bleach, 5 minutes), and then immerged on Halocarbon Oil 27 (Sigma, the 27 one works better than the 700 one).

When imaging a mutant, because of the CKG balancer, the Arm::GFP is not visible. Therefore, one need to use Arm::GFP strain alone as a control, instead of taking heterozygous flies as controls. This is true if you set up a recombinant or a stable line with your mutation (e.g. *Zasp*Δ */ CKG ; Arm::GFP*).

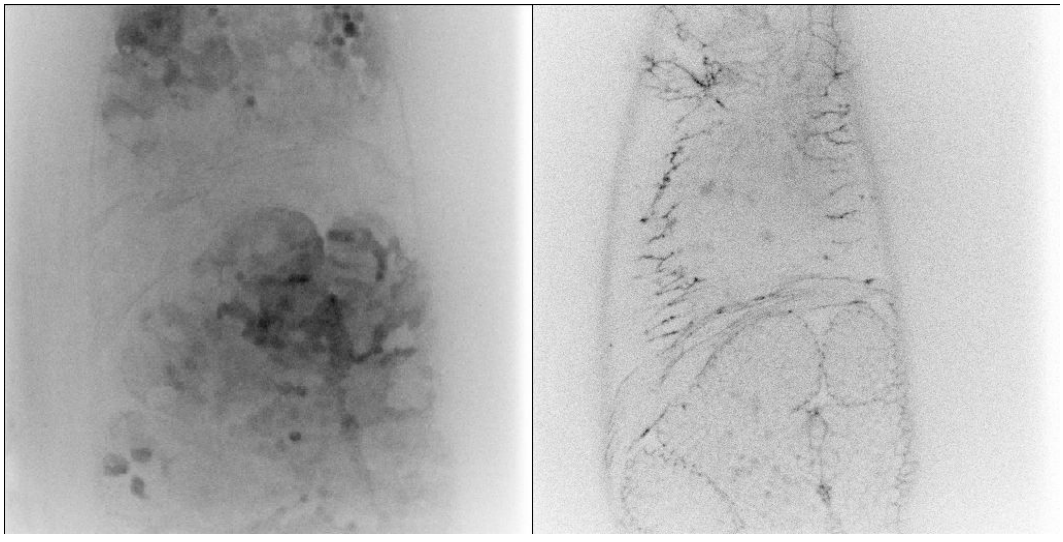

Left: single section of an embryo with the CKG balancer and Arm::GFP. Membranes are not visible because of the balancer.

Right: single section of a mutant embryo without the CKG balancer. Arm::GFP and the membrane are visible.

The idea is to align on the same coverslip control and mutant embryos, with 75% of embryos from the mutant laying pot and 25% from the control laying pot. Indeed, among the embryos form the "mutant" laying pot, only 25% will be homozygous mutants.

I usually start with the mutant line. I put all the embryos in the upper part of the coverslip. I then extract embryos with the correct stage one by one, and start aligning them, parallel to the slide, the head pointing to the top of the slide. I make two lines, with one line composed of mutants only, and one line with half mutants.

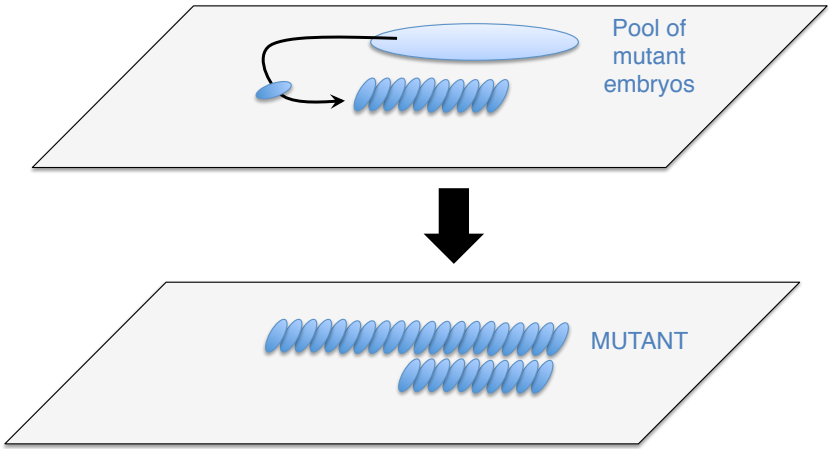

Once the mutants are done, I remove the pool of non-aligned mutant embryos and I repeat the same process with the control ones. It is important to leave a gap between the control and the mutants. It should look like this:

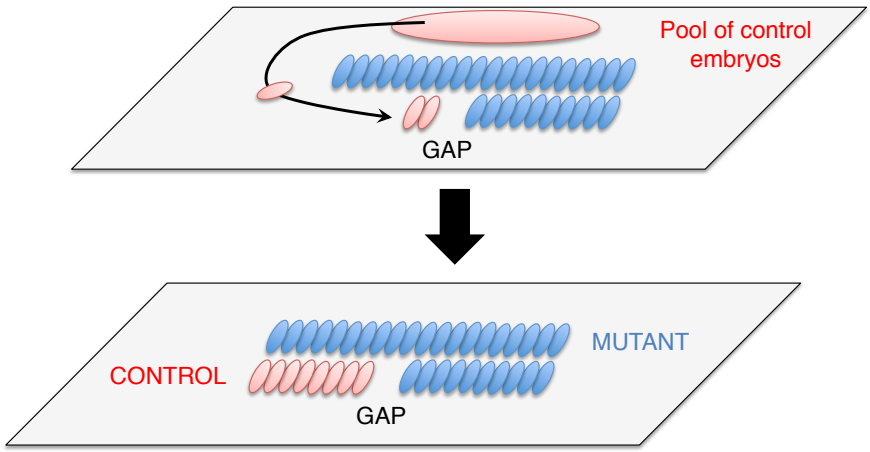

Although all embryos look identical, it is now impossible to confuse the different genotypes on the coverslip. The preferential orientation of the embryo is dorsal. This is perfect for monitoring closure dynamics at 20X or zippering dynamics at 100X. For wound healing experiments, it is preferable to put embryos in a lateral configuration. For other live imaging / single-cell junction cut experiments, a dorso-lateral orientation is the best suited (half of amnioserosa visible, and 6/7 rows of dorsal epidermal cells).

Before going to the confocal, I form a ring of wet tissue around a small plate. This will be put in top of the coverslip to prevent the excessive drying of the embryos.

4.2 Setting up the Spining disc

During my Ph.D, I used the Metamorph software. Here are some tips to ensure a perfect live imaging session.

1. Make sure that the current objective is the 10X one. Put the coverslip, and the plate with wet tissue on top of it.
2. Start Metamorph software (opening the software will change the focus of the microscope, that is why you do not need to do the focus at Step 1.)
3. Create a folder for the imaging session. Here is an example: 15-03-25 Zasp and Arm 100X. The reverse format of the date is convenient: once the data are stored on a hard drive the alphabetic order will reflect the anti-chronologic order (most recent data at the top of the list).
4. Start the MultiDimensionnal acquisition.
5. Tick the Time Lapse, Multiple Stages Position, Z series, Stream. Tick the Run Journals boxes **only if you use the FRAP module like for recoil experiments**.

6. On the Saving tab, choose the correct folder for saving the data. I use the following type of title 15-03-25 Zasp and Arm 100X, X WT then mutants. I will modify the title at the very end.

7. Set up the saving, duration and period of the time lapse. Note: when doing multiple stages, the software is not able to determine the time required to image all your stage positions. It is up to you to find the limits (e.g. X embryos, with Y sections, with a Z exposure time takes overall less than W minutes). If the specified frequency it too low, the acquisition will proceed as fast as possible, in a continuous manner. This is DANGEROUS for your data! For instance, I determined that imaging 10 embryos with 71 Z sections with a 300 ms exposure time takes less than 10 minutes. Once finishing the imaging of my 10 embryos, the microscope waits for 40 seconds before starting to image the next time point. Therefore all my embryos will be imaged with a frequency of 10 exact minutes. By keeping the same settings, tomorrow, the day after, in one month, all my embryos will have the same frequency of acquisition. If I want to quantify something over time I can pool ALL my data. Now, if I have been too greedy, and decided to image 13 embryos, the frequency of acquisition might be 12.325 min. One month after I decided to image 15 embryos, now the frequency of acquisition might be 14.765 sec. I am now UNABLE to pool the two sets of data, and I need to use mathematical artifices to create intermediary time points that were NEVER recorded (interpolation).

8. Make sure that the wavelength is appropriate. My favourite settings are GFP-spinning-single, 14 MHz, 1 EM Gain.

9. On the Stream Tab, tick the Stream Z box. The exposure has to be set in this section. I use 300 as Gain and 250 to 300 ms as Exposure Time.

10. Make the focus to localise the embryos, and centre the focus to the control embryos.

11. Change the focus to make the objective go down. Change the objective (100X) and turn the objective wheel half as if you wanted to switch from the 100X to the 40X. The 100X objective is now visible, and you can put the immersion oil on it (see below).

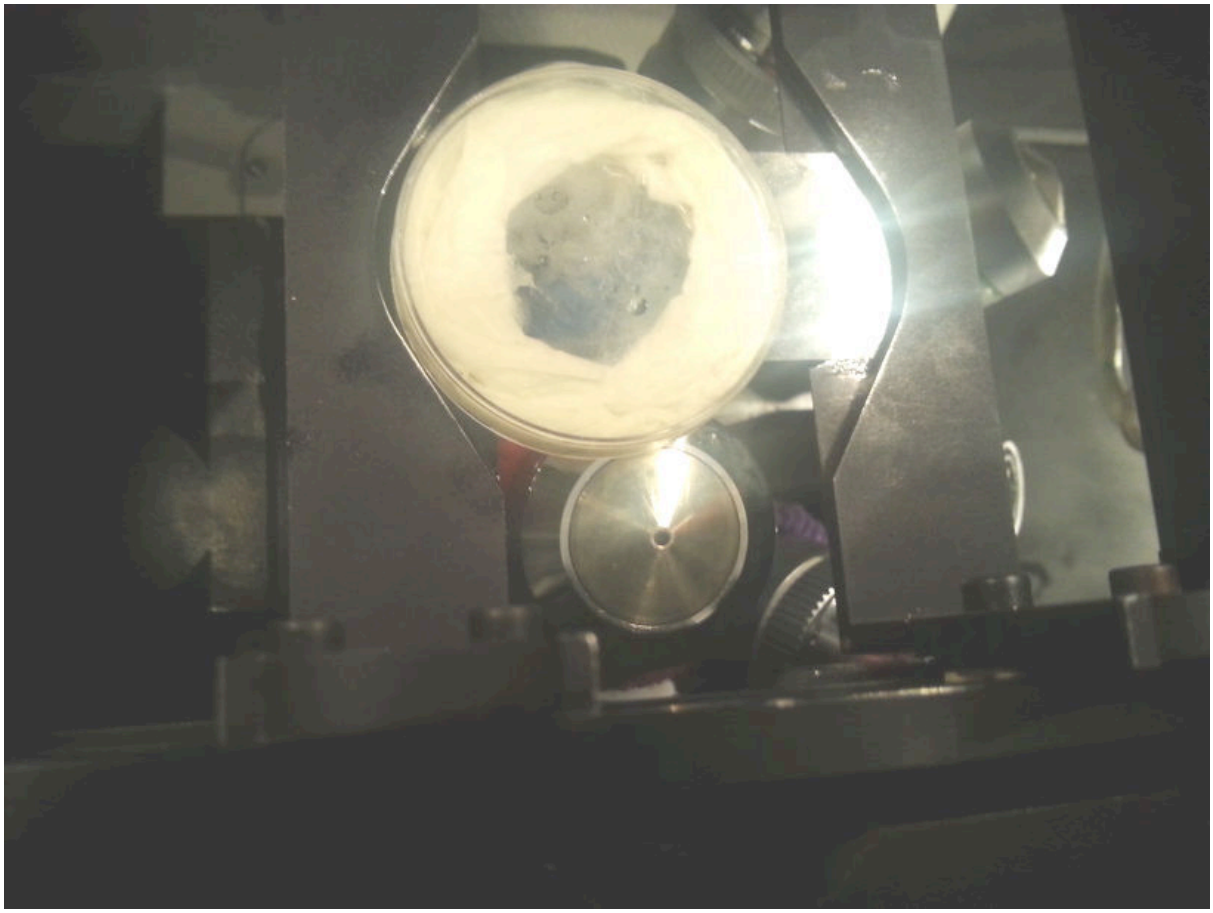

12. Put back the 100X objective under your samples. Make again the focus. This way the immersion oil will spread perfectly. If you forgot to change the focus at Step 11, the oil will likely spread incorrectly while putting the 100X under your samples.

13. Make the focus on the bottom left control embryo.

14. Switch from binocular to live mode. Switch the shutter, and press the "SPI" button. Go to the Multiple Stage position, and rename position 1 to "Control 1". Now, for each embryo, add a position if the orientation and/or stage is correct. Once you found the gap stop.

15. Count the number of control embryos you imaged. Then modify the title of your files 15-03-25 Zasp and Arm 100X, X WT then mutants → 15-03-25 Zasp and Arm 100X, 5 WT then mutants. Change in the multiple stage position tab "Control 6' by "Mutant 1".

16. Cross the gap, and tick all the mutant embryos you want. Once arriving at the end of the first (mixed) line, go to the upper line (mutant only), starting from the right. Go to the left.

17. Each position is defined by X, Y and Z coordinates. Z coordinate should be 0 for all sections.

18. You have two ways to change the focus. The first way is manual (with the scroll) and the second way is via the software in the Z-series section. The two systems do not communicate. If the electronic Z is 0, by changing the focus manually, it will not change dynamically this value (and this is PERFECT). My policy is to do a large number of sections for an embryo. This is based on the observation that over time embryos change their focus to usually go to (very) negative Z-values. I usually do 70 sections with a 1 µm step. With the multiple stage position, only the "Range around current" option is taken into account by the software. Therefore, I specify a 70 µm range around current.

19. Now go back to the first embryo and do manually the focus in a section just under the membranes (new 0). Electronically move to +30 µm. Your embryo should be out of focus. Manually change the focus until reaching the apical-most section of your embryo, and then go slightly out of focus. What you have done is that you specified that the +30 µm electronic value corresponds to the top limit of your first embryo.

20. Go to the second embryo and check that at +30 µm, the embryo is out-of-focus. If it is not the case, readjust manually the focus to have now +30 µm corresponding to the top-most sections of the second embryo. If the second embryo is entirely

imaged, the first one will be entirely imaged too. Repeat this for all your stages. At the end of this step, all your embryos will be imaged between +35 and -35 µm.
21. Start the acquisition.

4.3. Laser ablation experiments.

Embryos were prepared as described above. I used a UV laser (SFV-08E-0S0-BETA, teem photonicsTM, frequency of repetition: 8 KHz) controlled by the iLas2 module. For all the cuts I used a set ROI, a set number of Z-sections and a set exposure for Control and ZaspΔ embryos. I ablated with 5 laser repetitions with 100% of power. For recoil experiments I monitored the recoil with a frequency of ~ 0.7 s per frame for about 30 seconds.

For double simultaneous cell-junction cut, I ablated with 5 laser repetitions with 100% of power and monitored the recoil with a frequency of ~ 5.8 s per frame for about 2 min 30 seconds. I monitored the distance between the vertices over time using the MtrackJ plugin, with the initial distance normalized to 1.

5. Quantifications

5.1. Closure dynamics

For closure dynamics, I measured the length and the width over time of each embryo using ImageJ. I normalized the data for each embryo with the initial length and width respectively. With the 20X magnification, I determined the first time point of closure when I noticed closure occurring at the posterior canthi.

5.2. Recoil experiments

For recoil experiments, I collected with the Mtrack J plugins the coordinates of the vertices over time. The distance between two vertices is given by the very simple formula :

$$D(A-B)=\sqrt{\left(x_A-x_B\right)^2+\left(y_A-y_B\right)^2} \quad (1)$$

I plotted the resulting values on imageJ and used the exponential-recovery curve fitting tool to generate the following equation linking the distance y to the time t:

$$y(t)=a\left(1-e^{-bt}\right)+c \quad (2)$$

I then calculated the Initial Recoil as the slope of tangent at the origin, which corresponds to the derivate of equation (2) at t = 0.

$$Initial\,\mathrm{Re}coil=\left(\frac{dy(t)}{dt}\right)_{t=0}=\left(abe^{-bt}\right)_{t=0}=ab \quad (3)$$

5.3. Leading edge straightness.

For the leading edge straightness, I imaged control and ZaspΔ embryos at the same magnification. For each image, I measured the length of the interface between the amnioserosa and the leading edge (L_{real}), and the shortest distance between the two canthi (L_{th}). Sometimes, I used a segmented line to take into account the natural curvature of the embryo. Therefore the leading edge straightness reflects only differences in perimeter. I then calculated the leading edge straightness relative deviation (Δ) as:

$$\Delta = \left(\frac{L_{real} - L_{th}}{L_{th}} \right) \times 100 \quad (4).$$

5.4 Quantification and statistical analyses.

I used the Prism software (GraphPad Software) to generate graphs. I used Mann–Whitney's U test to determine significant differences between two conditions, and a one-way analysis of variance (ANOVA) followed by a Tukey's Multi Comparison *post-hoc* test for three or more conditions.

6. Image processing

6.1 Live imaging

Live imaging was performed on a confocal spinning disc (Leica). For all live imaging (except with Jupiter::GFP), I used the following procedure:

1. Open all the time points on Image J.
2. Make an hyperstack using Image > Stack > Tool > Concatenate (tick All open windows, and Open as a 4D Image).
3. Go to Process > Filter > Gaussian Blur = 1.00 to all sections
4. Go to Process > Subtract Background and (50.0 pixels) to all sections (make sure that "Light Background" box is not ticked)
5. Go to Image > Stack > Z-projection (Max intensity).

The purpose of the Gaussian blur is to homogenize the background to make the subtract background step more efficient. It is critical to do this on each and single section, and do the Z projection at the end.

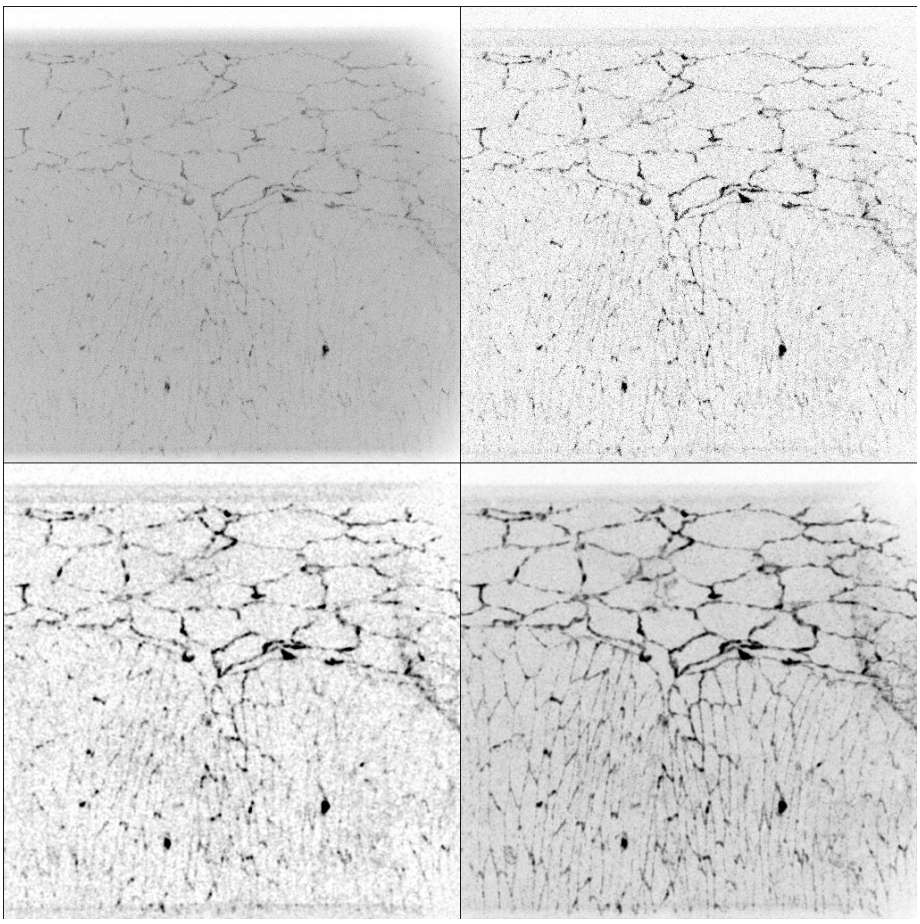

Here is an illustration. The top-left panel is a simple Z projection. The top-right panel is a Z projection and then subtract background. The bottom-left panel is a Z projection, then Gaussian Blur, then subtract background. The bottom-right panel is the Gaussian blur then subtract background on all sections and EVENTUALLY, the Z projection (best image!).

6.2 Immunofluorescence

Almost all the images were acquired on the spectral confocal laser-scanning microscope (SP5; Leica) with the following objectives: HCX Plan Apochromat 40× 1.25–0.75 oil (numerical aperture: 1.25), and HCX Plan Apochromat 63× 1.4–0.6 oil (numerical aperture: 1.4) using the acquisition software LAS AF (Leica) at the PLATIM imaging facility and analysed with ImageJ (National Institutes of Health).

For high-resolution images I used a super-resolution ELYRA SIM microscope Zeiss with HCX Plan Apochromat 100× oil (numerical aperture: 1.46) with the sCMOS Edge camera (PCO) using the ZEN acquisition software, with 5 rotations and 5 translations. I used the ZEN structure illumination reconstruction tool to generate the high-resolution images.

Unless otherwise indicated, all images are projections of confocal sections.

REFERENCES

Abreu-Blanco, M. T., Verboon, J. M. and Parkhurst, S. M. (2011). Cell wound repair in Drosophila occurs through three distinct phases of membrane and cytoskeletal remodeling. *J Cell Biol* **193**, 455-464.

Adelman, K. and Lis, J. T. (2012). Promoter-proximal pausing of RNA polymerase II: emerging roles in metazoans. *Nat Rev Genet* **13**, 720-731.

Affolter, M. and Basler, K. (2007). The Decapentaplegic morphogen gradient: from pattern formation to growth regulation. *Nat Rev Genet* **8**, 663-674.

Affolter, M., Nellen, D., Nussbaumer, U. and Basler, K. (1994). Multiple requirements for the receptor serine/threonine kinase thick veins reveal novel functions of TGF beta homologs during Drosophila embryogenesis. *Development* **120**, 3105-3117.

Alexandre, C., Lecourtois, M. and Vincent, J. (1999). Wingless and Hedgehog pattern Drosophila denticle belts by regulating the production of short-range signals. *Development* **126**, 5689-5698.

Arimura, T., Hayashi, T., Terada, H., Lee, S. Y., Zhou, Q., Takahashi, M., Ueda, K., Nouchi, T., Hohda, S., Shibutani, M. et al. (2004). A Cypher/ZASP mutation associated with dilated cardiomyopathy alters the binding affinity to protein kinase C. *J Biol Chem* **279**, 6746-6752.

Arora, K., Dai, H., Kazuko, S. G., Jamal, J., O'Connor, M. B., Letsou, A. and Warrior, R. (1995). The Drosophila schnurri gene acts in the Dpp/TGF beta signalling pathway and encodes a transcription factor homologous to the human MBP family. *Cell* **81**, 781-790.

Arya, R. and White, K. (2015). Cell death in development: Signalling pathways and core mechanisms. *Seminars in cell & developmental biology*.

Ashe, H. L., Mannervik, M. and Levine, M. (2000). Dpp signalling thresholds in the dorsal ectoderm of the Drosophila embryo. *Development* **127**, 3305-3312.

Avraham, K. B., Hasson, T., Steel, K. P., Kingsley, D. M., Russell, L. B., Mooseker, M. S., Copeland, N. G. and Jenkins, N. A. (1995). The mouse Snell's waltzer deafness gene encodes an unconventional myosin required for structural integrity of inner ear hair cells. *Nat Genet* **11**, 369-375.

Avraham, K. B., Hasson, T., Sobe, T., Balsara, B., Testa, J. R., Skvorak, A. B., Morton, C. C., Copeland, N. G. and Jenkins, N. A. (1997). Characterization of unconventional MYO6, the human homologue of the gene responsible for deafness in Snell's waltzer mice. *Hum Mol Genet* **6**, 1225-1231.

Aza-Blanc, P., Ramirez-Weber, F. A., Laget, M. P., Schwartz, C. and Kornberg, T. B. (1997). Proteolysis that is inhibited by hedgehog targets Cubitus interruptus protein to the nucleus and converts it to a repressor. *Cell* **89**, 1043-1053.

Baker, N. E. (1987). Molecular cloning of sequences from wingless, a segment polarity gene in Drosophila: the spatial distribution of a transcript in embryos. *EMBO J* **6**, 1765-1773.

Bardet, P. L., Guirao, B., Paoletti, C., Serman, F., Leopold, V., Bosveld, F., Goya, Y., Mirouse, V., Graner, F. and Bellaiche, Y. (2013). PTEN controls junction lengthening and stability during cell rearrangement in epithelial tissue. *Dev Cell* **25**, 534-546.

Bates, K. L., Higley, M. and Letsou, A. (2008). Raw mediates antagonism of AP-1 activity in Drosophila. *Genetics* **178**, 1989-2002.

Beira, J. V., Springhorn, A., Gunther, S., Hufnagel, L., Pyrowolakis, G. and Vincent, J. P. (2014). The Dpp/TGFbeta-Dependent Corepressor Schnurri Protects Epithelial Cells from JNK-Induced Apoptosis in Drosophila Embryos. *Dev Cell* **31**, 240-247.

Belacortu, Y. and Paricio, N. (2011). Drosophila as a model of wound healing and tissue regeneration in vertebrates. *Dev Dyn* **240**, 2379-2404.

Bement, W. M., Forscher, P. and Mooseker, M. S. (1993). A novel cytoskeletal structure involved in purse string wound closure and cell polarity maintenance. *J Cell Biol* **121**, 565-578.

Bergmann, A., Tugentman, M., Shilo, B. Z. and Steller, H. (2002). Regulation of cell number by MAPK-dependent control of apoptosis: a mechanism for trophic survival signalling. *Developmental cell* **2**, 159-170.

Bertet, C., Sulak, L. and Lecuit, T. (2004). Myosin-dependent junction remodelling controls planar cell intercalation and axis elongation. *Nature* **429**, 667-671.

Biswas, R., Stein, D. and Stanley, E. R. (2006). Drosophila Dok is required for embryonic dorsal closure. *Development* **133**, 217-227.

Blackman, R. K., Sanicola, M., Raftery, L. A., Gillevet, T. and Gelbart, W. M. (1991). An extensive 3' cis-regulatory region directs the imaginal disk expression of decapentaplegic, a member of the TGF-beta family in Drosophila. *Development* **111**, 657-666.

Blanchard, G. B., Murugesu, S., Adams, R. J., Martinez-Arias, A. and Gorfinkiel, N. (2010). Cytoskeletal dynamics and supracellular organisation of cell shape fluctuations during dorsal closure. *Development* **137**, 2743-2752.

Bosch, M., Serras, F., Martin-Blanco, E. and Baguna, J. (2005). JNK signalling pathway required for wound healing in regenerating Drosophila wing imaginal discs. *Dev Biol* **280**, 73-86.

Brand, A. H., Manoukian, A. S. and Perrimon, N. (1994). Ectopic expression in Drosophila. *Methods Cell Biol* **44**, 635-654.

Brigaud, I., Duteyrat, J. L., Chlasta, J., Le Bail, S., Couderc, J. L. and Grammont, M. (2015). Transforming Growth Factor beta/activin signalling induces epithelial cell flattening during Drosophila oogenesis. *Biol Open* **4**, 345-354.

Brock, J., Midwinter, K., Lewis, J. and Martin, P. (1996). Healing of incisional wounds in the embryonic chick wing bud: characterization of the actin purse-string and demonstration of a requirement for Rho activation. *J Cell Biol* **135**, 1097-1107.

Brummel, T. J., Twombly, V., Marques, G., Wrana, J. L., Newfeld, S. J., Attisano, L., Massague, J., O'Connor, M. B. and Gelbart, W. M. (1994). Characterization and relationship of Dpp receptors encoded by the saxophone and thick veins genes in Drosophila. *Cell* **78**, 251-261.

Byars, C. L., Bates, K. L. and Letsou, A. (1999). The dorsal-open group gene raw is required for restricted DJNK signalling during closure. *Development* **126**, 4913-4923.

Campbell, G. and Tomlinson, A. (1999). Transducing the Dpp morphogen gradient in the wing of Drosophila: regulation of Dpp targets by brinker. *Cell* **96**, 553-562.

Campos-Ortega, J. A. and Hartenstein, V. (1985). The Embryonic Development of Drosophila melanogaster. *Berlin: Springer Verlag*, 9-84.

Capdevila, J. and Guerrero, I. (1994). Targeted expression of the signalling molecule decapentaplegic induces pattern duplications and growth alterations in Drosophila wings. *EMBO J* **13**, 4459-4468.

Castrillon, D. H., Gonczy, P., Alexander, S., Rawson, R., Eberhart, C. G., Viswanathan, S., DiNardo, S. and Wasserman, S. A. (1993). Toward a molecular genetic analysis of spermatogenesis in Drosophila melanogaster: characterization of male-sterile mutants generated by single P element mutagenesis. *Genetics* **135**, 489-505.

Chalfie, M., Tu, Y., Euskirchen, G., Ward, W. W. and Prasher, D. C. (1994). Green fluorescent protein as a marker for gene expression. *Science* **263**, 802-805.

Chatterjee, N. and Bohmann, D. (2012). A versatile PhiC31 based reporter system for measuring AP-1 and Nrf2 signalling in Drosophila and in tissue culture. *PLoS One* **7**, e34063.

da Silva, S. M. and Vincent, J. P. (2007). Oriented cell divisions in the extending germband of Drosophila. *Development* **134**, 3049-3054.

Danjo, Y. and Gipson, I. K. (1998). Actin 'purse string' filaments are anchored by E-cadherin-mediated adherens junctions at the leading edge of the epithelial wound, providing coordinated cell movement. *J Cell Sci* **111 (Pt 22)**, 3323-3332.

David, D. J., Tishkina, A. and Harris, T. J. (2010). The PAR complex regulates pulsed actomyosin contractions during amnioserosa apical constriction in Drosophila. *Development* **137**, 1645-1655.

David, D. J., Wang, Q., Feng, J. J. and Harris, T. J. (2013). Bazooka inhibits aPKC to limit antagonism of actomyosin networks during amnioserosa apical constriction. *Development* **140**, 4719-4729.

Davidson, L. A., Ezin, A. M. and Keller, R. (2002). Embryonic wound healing by apical contraction and ingression in Xenopus laevis. *Cell Motil Cytoskeleton* **53**, 163-176.

Dawes-Hoang, R. E., Parmar, K. M., Christiansen, A. E., Phelps, C. B., Brand, A. H. and Wieschaus, E. F. (2005). folded gastrulation, cell shape change and the control of myosin localization. *Development* **132**, 4165-4178.

Deng, W., Leaper, K. and Bownes, M. (1999). A targeted gene silencing technique shows that Drosophila myosin VI is required for egg chamber and imaginal disc morphogenesis. *J Cell Sci* **112 (Pt 21)**, 3677-3690.

Dhanasekaran, D. N. (2013). JNK Signalling Network and Cancer. *Genes Cancer* **4**, 332-333.

Doyle, H. J., Harding, K., Hoey, T. and Levine, M. (1986). Transcripts encoded by a homoeo box gene are restricted to dorsal tissues of Drosophila embryos. *Nature* **323**, 76-79.

Driever, W. and Nusslein-Volhard, C. (1988). The bicoid protein determines position in the Drosophila embryo in a concentration-dependent manner. *Cell* **54**, 95-104.

Ducuing, A. and Querenet, M. (2013). Cholesterol-free and cholesterol-bound Hedgehog: Two sparring-partners working hand in hand in the Drosophila wing disc? *Fly (Austin)* **7**, 213-215.

Ducuing, A., Mollereau, B., Axelrod, J. D. and Vincent, S. (2013). Absolute requirement of cholesterol binding for Hedgehog gradient formation in Drosophila. *Biol Open* **2**, 596-604.

Ducuing, A., Keeley, C., Mollereau, B. and Vincent, S. (2015). A DPP-mediated feed-forward loop canalizes morphogenesis during Drosophila dorsal closure. *J Cell Biol* **208**, 239-248.

Eltsov, M., Dube, N., Yu, Z., Pasakarnis, L., Haselmann-Weiss, U., Brunner, D. and Frangakis, A. S. (2015). Quantitative analysis of cytoskeletal reorganization during epithelial tissue sealing by large-volume electron tomography. *Nat Cell Biol* **17**, 605-614.

Fan, Y. and Bergmann, A. (2010). The cleaved-Caspase-3 antibody is a marker of Caspase-9-like DRONC activity in Drosophila. *Cell death and differentiation* **17**, 534-539.

Faulkner, G., Pallavicini, A., Formentin, E., Comelli, A., Ievolella, C., Trevisan, S., Bortoletto, G., Scannapieco, P., Salamon, M., Mouly, V. et

al. (1999). ZASP: a new Z-band alternatively spliced PDZ-motif protein. *J Cell Biol* **146**, 465-475.

Fernandez, B. G., Arias, A. M. and Jacinto, A. (2007). Dpp signalling orchestrates dorsal closure by regulating cell shape changes both in the amnioserosa and in the epidermis. *Mech Dev* **124**, 884-897.

Fernandez, R., Takahashi, F., Liu, Z., Steward, R., Stein, D. and Stanley, E. R. (2000). The Drosophila shark tyrosine kinase is required for embryonic dorsal closure. *Genes Dev* **14**, 604-614.

Fernandez-Gonzalez, R., Simoes Sde, M., Roper, J. C., Eaton, S. and Zallen, J. A. (2009). Myosin II dynamics are regulated by tension in intercalating cells. *Dev Cell* **17**, 736-743.

Fjose, A., McGinnis, W. J. and Gehring, W. J. (1985). Isolation of a homoeo box-containing gene from the engrailed region of Drosophila and the spatial distribution of its transcripts. *Nature* **313**, 284-289.

Foe, V. E. (1989). Mitotic domains reveal early commitment of cells in Drosophila embryos. *Development* **107**, 1-22.

Foo, S. M., Sun, Y., Lim, B., Ziukaite, R., O'Brien, K., Nien, C. Y., Kirov, N., Shvartsman, S. Y. and Rushlow, C. A. (2014). Zelda potentiates morphogen activity by increasing chromatin accessibility. *Curr Biol* **24**, 1341-1346.

Frank, L. H. and Rushlow, C. (1996). A group of genes required for maintenance of the amnioserosa tissue in Drosophila. *Development* **122**, 1343-1352.

Franke, J. D., Montague, R. A. and Kiehart, D. P. (2005). Nonmuscle myosin II generates forces that transmit tension and drive contraction in multiple tissues during dorsal closure. *Curr Biol* **15**, 2208-2221.

Galko, M. J. and Krasnow, M. A. (2004). Cellular and genetic analysis of wound healing in Drosophila larvae. *PLoS Biol* **2**, E239.

Garcia-Bellido, A., Ripoll, P. and Morata, G. (1973). Developmental compartmentalisation of the wing disk of Drosophila. *Nat New Biol* **245**, 251-253.

Gates, J., Mahaffey, J. P., Rogers, S. L., Emerson, M., Rogers, E. M., Sottile, S. L., Van Vactor, D., Gertler, F. B. and Peifer, M. (2007). Enabled plays key roles in embryonic epithelial morphogenesis in Drosophila. *Development* **134**, 2027-2039.

Geisbrecht, E. R. and Montell, D. J. (2002). Myosin VI is required for E-cadherin-mediated border cell migration. *Nat Cell Biol* **4**, 616-620.

Gettings, M., Serman, F., Rousset, R., Bagnerini, P., Almeida, L. and Noselli, S. (2010). JNK signalling controls remodelling of the segment boundary through cell reprogramming during Drosophila morphogenesis. *PLoS Biol* **8**, e1000390.

Gibson, M. C. and Perrimon, N. (2005). Extrusion and death of DPP/BMP-compromised epithelial cells in the developing Drosophila wing. *Science* **307**, 1785-1789.

Glise, B. and Noselli, S. (1997). Coupling of Jun amino-terminal kinase and Decapentaplegic signalling pathways in Drosophila morphogenesis. *Genes Dev* **11**, 1738-1747.

Glise, B., Bourbon, H. and Noselli, S. (1995). hemipterous encodes a novel Drosophila MAP kinase kinase, required for epithelial cell sheet movement. *Cell* **83**, 451-461.

Goldman-Levi, R., Miller, C., Greenberg, G., Gabai, E. and Zak, N. B. (1996). Cellular pathways acting along the germband and in the amnioserosa may participate in germband retraction of the Drosophila melanogaster embryo. *Int J Dev Biol* **40**, 1043-1051.

Gorfinkiel, N., Blanchard, G. B., Adams, R. J. and Martinez Arias, A. (2009). Mechanical control of global cell behaviour during dorsal closure in Drosophila. *Development* **136**, 1889-1898.

Grevengoed, E. E., Loureiro, J. J., Jesse, T. L. and Peifer, M. (2001). Abelson kinase regulates epithelial morphogenesis in Drosophila. *J Cell Biol* **155**, 1185-1198.

Grieder, N. C., Nellen, D., Burke, R., Basler, K. and Affolter, M. (1995). Schnurri is required for Drosophila Dpp signalling and encodes a zinc finger protein similar to the mammalian transcription factor PRDII-BF1. *Cell* **81**, 791-800.

Grose, R. (2003). Epithelial migration: open your eyes to c-Jun. *Curr Biol* **13**, R678-680.

Harden, N. (2002). Signalling pathways directing the movement and fusion of epithelial sheets: lessons from dorsal closure in Drosophila. *Differentiation* **70**, 181-203.

Heitzler, P., Haenlin, M., Ramain, P., Calleja, M. and Simpson, P. (1996). A genetic analysis of pannier, a gene necessary for viability of dorsal tissues and bristle positioning in Drosophila. *Genetics* **143**, 1271-1286.

Herranz, H. and Morata, G. (2001). The functions of pannier during Drosophila embryogenesis. *Development* **128**, 4837-4846.

Hicks, J. L., Deng, W. M., Rogat, A. D., Miller, K. G. and Bownes, M. (1999). Class VI unconventional myosin is required for spermatogenesis in Drosophila. *Mol Biol Cell* **10**, 4341-4353.

Homem, C. C. and Peifer, M. (2009). Exploring the roles of diaphanous and enabled activity in shaping the balance between filopodia and lamellipodia. *Mol Biol Cell* **20**, 5138-5155.

Hou, X. S., Goldstein, E. S. and Perrimon, N. (1997). Drosophila Jun relays the Jun amino-terminal kinase signal transduction pathway to the Decapentaplegic

signal transduction pathway in regulating epithelial cell sheet movement. *Genes Dev* **11**, 1728-1737.

Houssin, E., Tepass, U. and Laprise, P. (2015). Girdin-mediated interactions between cadherin and the actin cytoskeleton are required for epithelial morphogenesis in Drosophila. *Development* **142**, 1777-1784.

Huang, J., Zhou, W., Dong, W., Watson, A. M. and Hong, Y. (2009). From the Cover: Directed, efficient, and versatile modifications of the Drosophila genome by genomic engineering. *Proc Natl Acad Sci U S A* **106**, 8284-8289.

Hunter, G. L., Crawford, J. M., Genkins, J. Z. and Kiehart, D. P. (2014). Ion channels contribute to the regulation of cell sheet forces during Drosophila dorsal closure. *Development* **141**, 325-334.

Hutson, M. S., Tokutake, Y., Chang, M. S., Bloor, J. W., Venakides, S., Kiehart, D. P. and Edwards, G. S. (2003). Forces for morphogenesis investigated with laser microsurgery and quantitative modeling. *Science* **300**, 145-149.

Igaki, T. (2009). Correcting developmental errors by apoptosis: lessons from Drosophila JNK signalling. *Apoptosis* **14**, 1021-1028.

Inaba, M., Buszczak, M. and Yamashita, Y. M. (2015). Nanotubes mediate niche-stem-cell signalling in the Drosophila testis. *Nature* **523**, 329-332.

Inoue, H., Imamura, T., Ishidou, Y., Takase, M., Udagawa, Y., Oka, Y., Tsuneizumi, K., Tabata, T., Miyazono, K. and Kawabata, M. (1998). Interplay of signal mediators of decapentaplegic (Dpp): molecular characterization of mothers against dpp, Medea, and daughters against dpp. *Mol Biol Cell* **9**, 2145-2156.

Irish, V. F. and Gelbart, W. M. (1987). The decapentaplegic gene is required for dorsal-ventral patterning of the Drosophila embryo. *Genes Dev* **1**, 868-879.

Irvine, K. D. and Wieschaus, E. (1994). Cell intercalation during Drosophila germband extension and its regulation by pair-rule segmentation genes. *Development* **120**, 827-841.

Jacinto, A., Martinez-Arias, A. and Martin, P. (2001). Mechanisms of epithelial fusion and repair. *Nat Cell Biol* **3**, E117-123.

Jacinto, A., Wood, W., Balayo, T., Turmaine, M., Martinez-Arias, A. and Martin, P. (2000). Dynamic actin-based epithelial adhesion and cell matching during Drosophila dorsal closure. *Curr Biol* **10**, 1420-1426.

Jacinto, A., Wood, W., Woolner, S., Hiley, C., Turner, L., Wilson, C., Martinez-Arias, A. and Martin, P. (2002). Dynamic analysis of actin cable function during Drosophila dorsal closure. *Curr Biol* **12**, 1245-1250.

Jani, K. and Schock, F. (2007). Zasp is required for the assembly of functional integrin adhesion sites. *J Cell Biol* **179**, 1583-1597.

Jankovics, F. and Brunner, D. (2006). Transiently reorganized microtubules are essential for zippering during dorsal closure in Drosophila melanogaster. *Dev Cell* **11**, 375-385.

Jasper, H., Benes, V., Schwager, C., Sauer, S., Clauder-Munster, S., Ansorge, W. and Bohmann, D. (2001). The genomic response of the Drosophila embryo to JNK signalling. *Dev Cell* **1**, 579-586.

Javelaud, D., Laboureau, J., Gabison, E., Verrecchia, F. and Mauviel, A. (2003). Disruption of basal JNK activity differentially affects key fibroblast functions important for wound healing. *J Biol Chem* **278**, 24624-24628.

Jazwinska, A., Kirov, N., Wieschaus, E., Roth, S. and Rushlow, C. (1999). The Drosophila gene brinker reveals a novel mechanism of Dpp target gene regulation. *Cell* **96**, 563-573.

Kaltschmidt, J. A., Lawrence, N., Morel, V., Balayo, T., Fernandez, B. G., Pelissier, A., Jacinto, A. and Martinez Arias, A. (2002). Planar polarity and actin dynamics in the epidermis of Drosophila. *Nat Cell Biol* **4**, 937-944.

Kankel, M. W., Duncan, D. M. and Duncan, I. (2004). A screen for genes that interact with the Drosophila pair-rule segmentation gene fushi tarazu. *Genetics* **168**, 161-180.

Karpova, N., Bobinnec, Y., Fouix, S., Huitorel, P. and Debec, A. (2006). Jupiter, a new Drosophila protein associated with microtubules. *Cell Motil Cytoskeleton* **63**, 301-312.

Kasza, K. E., Farrell, D. L. and Zallen, J. A. (2014). Spatiotemporal control of epithelial remodeling by regulated myosin phosphorylation. *Proc Natl Acad Sci U S A* **111**, 11732-11737.

Katzemich, A., Liao, K. A., Czerniecki, S. and Schock, F. (2013). Alp/Enigma family proteins cooperate in Z-disc formation and myofibril assembly. *PLoS Genet* **9**, e1003342.

Katzemich, A., Long, J. Y., Jani, K., Lee, B. R. and Schock, F. (2011). Muscle type-specific expression of Zasp52 isoforms in Drosophila. *Gene Expr Patterns* **11**, 484-490.

Kawakami, A. (2010). Stem cell system in tissue regeneration in fish. *Dev Growth Differ* **52**, 77-87.

Kellerman, K. A. and Miller, K. G. (1992). An unconventional myosin heavy chain gene from Drosophila melanogaster. *J Cell Biol* **119**, 823-834.

Kiehart, D. P., Galbraith, C. G., Edwards, K. A., Rickoll, W. L. and Montague, R. A. (2000). Multiple forces contribute to cell sheet morphogenesis for dorsal closure in Drosophila. *The Journal of cell biology* **149**, 471-490.

Kockel, L., Zeitlinger, J., Staszewski, L. M., Mlodzik, M. and Bohmann, D. (1997). Jun in Drosophila development: redundant and nonredundant functions and regulation by two MAPK signal transduction pathways. *Genes Dev* **11**, 1748-1758.

Kolahgar, G., Bardet, P. L., Langton, P. F., Alexandre, C. and Vincent, J. P. (2011). Apical deficiency triggers JNK-dependent apoptosis in the embryonic epidermis of Drosophila. *Development* **138**, 3021-3031.

Kornberg, T., Siden, I., O'Farrell, P. and Simon, M. (1985). The engrailed locus of Drosophila: in situ localization of transcripts reveals compartment-specific expression. *Cell* **40**, 45-53.

Krcmery, J., Camarata, T., Kulisz, A. and Simon, H. G. (2010). Nucleocytoplasmic functions of the PDZ-LIM protein family: new insights into organ development. *Bioessays* **32**, 100-108.

Lada, K., Gorfinkiel, N. and Martinez Arias, A. (2012). Interactions between the amnioserosa and the epidermis revealed by the function of the u-shaped gene. *Biology open* **1**, 353-361.

Lagha, M., Bothma, J. P., Esposito, E., Ng, S., Stefanik, L., Tsui, C., Johnston, J., Chen, K., Gilmour, D. S., Zeitlinger, J. et al. (2013). Paused Pol II coordinates tissue morphogenesis in the Drosophila embryo. *Cell* **153**, 976-987.

Laplante, C. and Nilson, L. A. (2006). Differential expression of the adhesion molecule Echinoid drives epithelial morphogenesis in Drosophila. *Development* **133**, 3255-3264.

Laplante, C. and Nilson, L. A. (2011). Asymmetric distribution of Echinoid defines the epidermal leading edge during Drosophila dorsal closure. *J Cell Biol* **192**, 335-348.

Le, T., Liang, Z., Patel, H., Yu, M. H., Sivasubramaniam, G., Slovitt, M., Tanentzapf, G., Mohanty, N., Paul, S. M., Wu, V. M. et al. (2006). A new family of Drosophila balancer chromosomes with a w- dfd-GMR yellow fluorescent protein marker. *Genetics* **174**, 2255-2257.

Lecuit, T., Brook, W. J., Ng, M., Calleja, M., Sun, H. and Cohen, S. M. (1996). Two distinct mechanisms for long-range patterning by Decapentaplegic in the Drosophila wing. *Nature* **381**, 387-393.

Legoff, L., Rouault, H. and Lecuit, T. (2013). A global pattern of mechanical stress polarizes cell divisions and cell shape in the growing Drosophila wing disc. *Development* **140**, 4051-4059.

Leppa, S. and Bohmann, D. (1999). Diverse functions of JNK signalling and c-Jun in stress response and apoptosis. *Oncogene* **18**, 6158-6162.

Leptin, M. (1999). Gastrulation in Drosophila: the logic and the cellular mechanisms. *EMBO J* **18**, 3187-3192.

Letsou, A., Arora, K., Wrana, J. L., Simin, K., Twombly, V., Jamal, J., Staehling-Hampton, K., Hoffmann, F. M., Gelbart, W. M., Massague, J. et al. (1995). Drosophila Dpp signalling is mediated by the punt gene product: a dual ligand-binding type II receptor of the TGF beta receptor family. *Cell* **80**, 899-908.

Levayer, R., Hauert, B. and Moreno, E. (2015). Cell mixing induced by myc is required for competitive tissue invasion and destruction. *Nature*.

Li, G., Gustafson-Brown, C., Hanks, S. K., Nason, K., Arbeit, J. M., Pogliano, K., Wisdom, R. M. and Johnson, R. S. (2003). c-Jun is essential for organization of the epidermal leading edge. *Dev Cell* **4**, 865-877.

Lin, X., Ruiz, J., Bajraktari, I., Ohman, R., Banerjee, S., Gribble, K., Kaufman, J. D., Wingfield, P. T., Griggs, R. C., Fischbeck, K. H. et al. (2014). Z-disc-associated, alternatively spliced, PDZ motif-containing protein (ZASP) mutations in the actin-binding domain cause disruption of skeletal muscle actin filaments in myofibrillar myopathy. *J Biol Chem* **289**, 13615-13626.

Loughran, G., Healy, N. C., Kiely, P. A., Huigsloot, M., Kedersha, N. L. and O'Connor, R. (2005). Mystique is a new insulin-like growth factor-I-regulated

PDZ-LIM domain protein that promotes cell attachment and migration and suppresses Anchorage-independent growth. *Mol Biol Cell* **16**, 1811-1822.

Macdonald, P. M. and Struhl, G. (1986). A molecular gradient in early Drosophila embryos and its role in specifying the body pattern. *Nature* **324**, 537-545.

Mangan, S. and Alon, U. (2003). Structure and function of the feed-forward loop network motif. *Proc Natl Acad Sci U S A* **100**, 11980-11985.

Martin, P. and Lewis, J. (1992). Actin cables and epidermal movement in embryonic wound healing. *Nature* **360**, 179-183.

Martin, P. and Parkhurst, S. M. (2004). Parallels between tissue repair and embryo morphogenesis. *Development* **131**, 3021-3034.

Martin-Blanco, E., Gampel, A., Ring, J., Virdee, K., Kirov, N., Tolkovsky, A. M. and Martinez-Arias, A. (1998). puckered encodes a phosphatase that mediates a feedback loop regulating JNK activity during dorsal closure in Drosophila. *Genes Dev* **12**, 557-570.

Martinez-Arias, A. and Lawrence, P. A. (1985). Parasegments and compartments in the Drosophila embryo. *Nature* **313**, 639-642.

Marty, T., Muller, B., Basler, K. and Affolter, M. (2000). Schnurri mediates Dpp-dependent repression of brinker transcription. *Nat Cell Biol* **2**, 745-749.

McClure, K. D. and Schubiger, G. (2005). Developmental analysis and squamous morphogenesis of the peripodial epithelium in Drosophila imaginal discs. *Development* **132**, 5033-5042.

McEwen, D. G. and Peifer, M. (2005). Puckered, a Drosophila MAPK phosphatase, ensures cell viability by antagonizing JNK-induced apoptosis. *Development* **132**, 3935-3946.

Michelsen, J. W., Schmeichel, K. L., Beckerle, M. C. and Winge, D. R. (1993). The LIM motif defines a specific zinc-binding protein domain. *Proc Natl Acad Sci U S A* **90**, 4404-4408.

Mihaly, J., Kockel, L., Gaengel, K., Weber, U., Bohmann, D. and Mlodzik, M. (2001). The role of the Drosophila TAK homologue dTAK during development. *Mech Dev* **102**, 67-79.

Millard, T. H. and Martin, P. (2008). Dynamic analysis of filopodial interactions during the zippering phase of Drosophila dorsal closure. *Development* **135**, 621-626.

Millo, H., Leaper, K., Lazou, V. and Bownes, M. (2004). Myosin VI plays a role in cell-cell adhesion during epithelial morphogenesis. *Mech Dev* **121**, 1335-1351.

Minami, M., Kinoshita, N., Kamoshida, Y., Tanimoto, H. and Tabata, T. (1999). brinker is a target of Dpp in Drosophila that negatively regulates Dpp-dependent genes. *Nature* **398**, 242-246.

Mollereau, B. (2009). Cell death: what can we learn from flies? Editorial for the special review issue on Drosophila apoptosis. *Apoptosis : an international journal on programmed cell death* **14**, 929-934.

Monier, B., Gettings, M., Gay, G., Mangeat, T., Schott, S., Guarner, A. and Suzanne, M. (2015). Apico-basal forces exerted by apoptotic cells drive epithelium folding. *Nature* **518**, 245-248.

Morgan, T. H., Sturtevant, A. H., Muller, H. J. and Bridges, C. B. (1915). The Mechanism of Mendelian Heredity *New York: Holt Rinehart & Winston.*

Morin, X., Daneman, R., Zavortink, M. and Chia, W. (2001). A protein trap strategy to detect GFP-tagged proteins expressed from their endogenous loci in Drosophila. *Proc Natl Acad Sci U S A* **98**, 15050-15055.

Morrison, J. K. and Miller, K. G. (2008). Genetic characterization of the Drosophila jaguar322 mutant reveals that complete myosin VI loss of function is not lethal. *Genetics* **179**, 711-716.

Muliyil, S. and Narasimha, M. (2014). Mitochondrial ROS regulates cytoskeletal and mitochondrial remodeling to tune cell and tissue dynamics in a model for wound healing. *Dev Cell* **28**, 239-252.

Muliyil, S., Krishnakumar, P. and Narasimha, M. (2011). Spatial, temporal and molecular hierarchies in the link between death, delamination and dorsal closure. *Development* **138**, 3043-3054.

Munoz-Descalzo, S., Terol, J. and Paricio, N. (2005). Cabut, a C2H2 zinc finger transcription factor, is required during Drosophila dorsal closure downstream of JNK signalling. *Dev Biol* **287**, 168-179.

Nellen, D., Burke, R., Struhl, G. and Basler, K. (1996). Direct and long-range action of a DPP morphogen gradient. *Cell* **85**, 357-368.

Noguchi, T., Lenartowska, M. and Miller, K. G. (2006). Myosin VI stabilizes an actin network during Drosophila spermatid individualization. *Mol Biol Cell* **17**, 2559-2571.

Nusslein-Volhard, C. and Wieschaus, E. (1980). Mutations affecting segment number and polarity in Drosophila. *Nature* **287**, 795-801.

Nusslein-Volhard, C., Frohnhofer, H. G. and Lehmann, R. (1987). Determination of anteroposterior polarity in Drosophila. *Science* **238**, 1675-1681.

Padgett, R. W., Wozney, J. M. and Gelbart, W. M. (1993). Human BMP sequences can confer normal dorsal-ventral patterning in the Drosophila embryo. *Proc Natl Acad Sci U S A* **90**, 2905-2909.

Palm, W., Swierczynska, M. M., Kumari, V., Ehrhart-Bornstein, M., Bornstein, S. R. and Eaton, S. (2013). Secretion and signalling activities of lipoprotein-associated hedgehog and non-sterol-modified hedgehog in flies and mammals. *PLoS Biol* **11**, e1001505.

Pashmforoush, M., Pomies, P., Peterson, K. L., Kubalak, S., Ross, J., Jr., Hefti, A., Aebi, U., Beckerle, M. C. and Chien, K. R. (2001). Adult

mice deficient in actinin-associated LIM-domain protein reveal a developmental pathway for right ventricular cardiomyopathy. *Nat Med* **7**, 591-597.

Penton, A., Chen, Y., Staehling-Hampton, K., Wrana, J. L., Attisano, L., Szidonya, J., Cassill, J. A., Massague, J. and Hoffmann, F. M. (1994). Identification of two bone morphogenetic protein type I receptors in Drosophila and evidence that Brk25D is a decapentaplegic receptor. *Cell* **78**, 239-250.

Perez-Garijo, A., Shlevkov, E. and Morata, G. (2009). The role of Dpp and Wg in compensatory proliferation and in the formation of hyperplastic overgrowths caused by apoptotic cells in the Drosophila wing disc. *Development* **136**, 1169-1177.

Petritsch, C., Tavosanis, G., Turck, C. W., Jan, L. Y. and Jan, Y. N. (2003). The Drosophila myosin VI Jaguar is required for basal protein targeting and correct spindle orientation in mitotic neuroblasts. *Dev Cell* **4**, 273-281.

Pickering, K., Alves-Silva, J., Goberdhan, D. and Millard, T. H. (2013). Par3/Bazooka and phosphoinositides regulate actin protrusion formation during Drosophila dorsal closure and wound healing. *Development* **140**, 800-809.

Raftery, L. A., Twombly, V., Wharton, K. and Gelbart, W. M. (1995). Genetic screens to identify elements of the decapentaplegic signalling pathway in Drosophila. *Genetics* **139**, 241-254.

Ramet, M., Lanot, R., Zachary, D. and Manfruelli, P. (2002). JNK signalling pathway is required for efficient wound healing in Drosophila. *Dev Biol* **241**, 145-156.

Ramirez-Weber, F. A. and Kornberg, T. B. (1999). Cytonemes: cellular processes that project to the principal signalling center in Drosophila imaginal discs. *Cell* **97**, 599-607.

Rauzi, M., Lenne, P. F. and Lecuit, T. (2010). Planar polarized actomyosin contractile flows control epithelial junction remodelling. *Nature* **468**, 1110-1114.

Rebay, I. and Rubin, G. M. (1995). Yan functions as a general inhibitor of differentiation and is negatively regulated by activation of the Ras1/MAPK pathway. *Cell* **81**, 857-866.

Reed, B. H., Wilk, R. and Lipshitz, H. D. (2001). Downregulation of Jun kinase signalling in the amnioserosa is essential for dorsal closure of the Drosophila embryo. *Curr Biol* **11**, 1098-1108.

Riesgo-Escovar, J. R. and Hafen, E. (1997). Drosophila Jun kinase regulates expression of decapentaplegic via the ETS-domain protein Aop and the AP-1 transcription factor DJun during dorsal closure. *Genes Dev* **11**, 1717-1727.

Riesgo-Escovar, J. R., Hafen, E., Hou, X. S., Goldstein, E. S., Perrimon, N., Glise, B., Noselli, S., Kockel, L., Zeitlinger, J., Staszewski, L. M. et al. (1997). Connecting up the pathways in Drosophila development. *Trends Cell Biol* **7**, 421-422.

Rios-Barrera, L. D. and Riesgo-Escovar, J. R. (2013). Regulating cell morphogenesis: the Drosophila Jun N-terminal kinase pathway. *Genesis* **51**, 147-162.

Rios-Barrera, L. D., Gutierrez-Perez, I., Dominguez, M. and Riesgo-Escovar, J. R. (2015). acal is a long non-coding RNA in JNK signalling in epithelial shape changes during drosophila dorsal closure. *PLoS Genet* **11**, e1004927.

Rodriguez-Diaz, A., Toyama, Y., Abravanel, D. L., Wiemann, J. M., Wells, A. R., Tulu, U. S., Edwards, G. S. and Kiehart, D. P. (2008). Actomyosin purse strings: renewable resources that make morphogenesis robust and resilient. *HFSP J* **2**, 220-237.

Rogat, A. D. and Miller, K. G. (2002). A role for myosin VI in actin dynamics at sites of membrane remodeling during Drosophila spermatogenesis. *J Cell Sci* **115**, 4855-4865.

Roth, S., Stein, D. and Nusslein-Volhard, C. (1989). A gradient of nuclear localization of the dorsal protein determines dorsoventral pattern in the Drosophila embryo. *Cell* **59**, 1189-1202.

Rousset, R., Bono-Lauriol, S., Gettings, M., Suzanne, M., Speder, P. and Noselli, S. (2010). The Drosophila serine protease homologue Scarface regulates JNK signalling in a negative-feedback loop during epithelial morphogenesis. *Development* **137**, 2177-2186.

Roy, S., Hsiung, F. and Kornberg, T. B. (2011). Specificity of Drosophila cytonemes for distinct signalling pathways. *Science* **332**, 354-358.

Roy, S., Huang, H., Liu, S. and Kornberg, T. B. (2014). Cytoneme-mediated contact-dependent transport of the Drosophila decapentaplegic signalling protein. *Science* **343**, 1244624.

Ruberte, E., Marty, T., Nellen, D., Affolter, M. and Basler, K. (1995). An absolute requirement for both the type II and type I receptors, punt and thick veins, for dpp signalling in vivo. *Cell* **80**, 889-897.

Rushlow, C., Frasch, M., Doyle, H. and Levine, M. (1987). Maternal regulation of zerknullt: a homoeobox gene controlling differentiation of dorsal tissues in Drosophila. *Nature* **330**, 583-586.

Ryoo, H. D., Gorenc, T. and Steller, H. (2004). Apoptotic cells can induce compensatory cell proliferation through the JNK and the Wingless signalling pathways. *Dev Cell* **7**, 491-501.

Saias, L., Swoger, J., D'Angelo, A., Hayes, P., Colombelli, J., Sharpe, J., Salbreux, G. and Solon, J. (2015). Decrease in Cell Volume Generates Contractile Forces Driving Dorsal Closure. *Dev Cell* **33**, 611-621.

Sakuma, T., Hosoi, S., Woltjen, K., Suzuki, K., Kashiwagi, K., Wada, H., Ochiai, H., Miyamoto, T., Kawai, N., Sasakura, Y. et al. (2013).

Efficient TALEN construction and evaluation methods for human cell and animal applications. *Genes Cells* **18**, 315-326.

Samakovlis, C., Hacohen, N., Manning, G., Sutherland, D. C., Guillemin, K. and Krasnow, M. A. (1996). Development of the Drosophila tracheal system occurs by a series of morphologically distinct but genetically coupled branching events. *Development* **122**, 1395-1407.

Sekelsky, J. J., Newfeld, S. J., Raftery, L. A., Chartoff, E. H. and Gelbart, W. M. (1995). Genetic characterization and cloning of mothers against dpp, a gene required for decapentaplegic function in Drosophila melanogaster. *Genetics* **139**, 1347-1358.

Selcen, D. and Engel, A. G. (2005). Mutations in ZASP define a novel form of muscular dystrophy in humans. *Ann Neurol* **57**, 269-276.

Shen, J. and Dahmann, C. (2005). Extrusion of cells with inappropriate Dpp signalling from Drosophila wing disc epithelia. *Science* **307**, 1789-1790.

Simin, K., Bates, E. A., Horner, M. A. and Letsou, A. (1998). Genetic analysis of punt, a type II Dpp receptor that functions throughout the Drosophila melanogaster life cycle. *Genetics* **148**, 801-813.

Sokolow, A., Toyama, Y., Kiehart, D. P. and Edwards, G. S. (2012). Cell ingression and apical shape oscillations during dorsal closure in Drosophila. *Biophys J* **102**, 969-979.

Solon, J., Kaya-Copur, A., Colombelli, J. and Brunner, D. (2009). Pulsed forces timed by a ratchet-like mechanism drive directed tissue movement during dorsal closure. *Cell* **137**, 1331-1342.

Song, Z., McCall, K. and Steller, H. (1997). DCP-1, a Drosophila cell death protease essential for development. *Science* **275**, 536-540.

Spahn, P. and Reuter, R. (2013). A vertex model of Drosophila ventral furrow formation. *PLoS One* **8**, e75051.

Spencer, F. A., Hoffmann, F. M. and Gelbart, W. M. (1982). Decapentaplegic: a gene complex affecting morphogenesis in Drosophila melanogaster. *Cell* **28**, 451-461.

St Johnston, D. (2002). The art and design of genetic screens: Drosophila melanogaster. *Nat Rev Genet* **3**, 176-188.

St Johnston, R. D. and Gelbart, W. M. (1987). Decapentaplegic transcripts are localized along the dorsal-ventral axis of the Drosophila embryo. *EMBO J* **6**, 2785-2791.

Staehling-Hampton, K., Laughon, A. S. and Hoffmann, F. M. (1995). A Drosophila protein related to the human zinc finger transcription factor PRDII/MBPI/HIV-EP1 is required for dpp signalling. *Development* **121**, 3393-3403.

Steward, R. (1989). Relocalization of the dorsal protein from the cytoplasm to the nucleus correlates with its function. *Cell* **59**, 1179-1188.

Stronach, B. (2014). Extensive nonmuscle expression and epithelial apicobasal localization of the Drosophila ALP/Enigma family protein, Zasp52. *Gene Expr Patterns* **15**, 67-79.

Stronach, B. and Perrimon, N. (2002). Activation of the JNK pathway during dorsal closure in Drosophila requires the mixed lineage kinase, slipper. *Genes Dev* **16**, 377-387.

Struhl, G., Johnston, P. and Lawrence, P. A. (1992). Control of Drosophila body pattern by the hunchback morphogen gradient. *Cell* **69**, 237-249.

Su, Y. C., Maurel-Zaffran, C., Treisman, J. E. and Skolnik, E. Y. (2000). The Ste20 kinase misshapen regulates both photoreceptor axon targeting and dorsal closure, acting downstream of distinct signals. *Mol Cell Biol* **20**, 4736-4744.

Tabata, T. and Kornberg, T. B. (1994). Hedgehog is a signalling protein with a key role in patterning Drosophila imaginal discs. *Cell* **76**, 89-102.

Takatsu, Y., Nakamura, M., Stapleton, M., Danos, M. C., Matsumoto, K., O'Connor, M. B., Shibuya, H. and Ueno, N. (2000). TAK1 participates in c-Jun N-terminal kinase signalling during Drosophila development. *Mol Cell Biol* **20**, 3015-3026.

Tan, Y., Yamada-Mabuchi, M., Arya, R., St Pierre, S., Tang, W., Tosa, M., Brachmann, C. and White, K. (2011). Coordinated expression of cell death genes regulates neuroblast apoptosis. *Development* **138**, 2197-2206.

te Velthuis, A. J. and Bagowski, C. P. (2007). PDZ and LIM domain-encoding genes: molecular interactions and their role in development. *ScientificWorldJournal* **7**, 1470-1492.

Tipping, N. and Wilson, D. (2011). Chick amniogenesis is mediated by an actin cable. *Anat Rec (Hoboken)* **294**, 1143-1149.

Torrado, M., Senatorov, V. V., Trivedi, R., Fariss, R. N. and Tomarev, S. I. (2004). Pdlim2, a novel PDZ-LIM domain protein, interacts with alpha-actinins and filamin A. *Invest Ophthalmol Vis Sci* **45**, 3955-3963.

Toyama, Y., Peralta, X. G., Wells, A. R., Kiehart, D. P. and Edwards, G. S. (2008). Apoptotic force and tissue dynamics during Drosophila embryogenesis. *Science* **321**, 1683-1686.

Tsuneizumi, K., Nakayama, T., Kamoshida, Y., Kornberg, T. B., Christian, J. L. and Tabata, T. (1997). Daughters against dpp modulates dpp organizing activity in Drosophila wing development. *Nature* **389**, 627-631.

Vallenius, T., Luukko, K. and Makela, T. P. (2000). CLP-36 PDZ-LIM protein associates with nonmuscle alpha-actinin-1 and alpha-actinin-4. *J Biol Chem* **275**, 11100-11105.

Vallenius, T., Scharm, B., Vesikansa, A., Luukko, K., Schafer, R. and Makela, T. P. (2004). The PDZ-LIM protein RIL modulates actin stress fiber

turnover and enhances the association of alpha-actinin with F-actin. *Exp Cell Res* **293**, 117-128.

Vatta, M., Mohapatra, B., Jimenez, S., Sanchez, X., Faulkner, G., Perles, Z., Sinagra, G., Lin, J. H., Vu, T. M., Zhou, Q. et al. (2003). Mutations in Cypher/ZASP in patients with dilated cardiomyopathy and left ventricular non-compaction. *J Am Coll Cardiol* **42**, 2014-2027.

Vincent, S., Perrimon, N. and Axelrod, J. D. (2008). Hedgehog and Wingless stabilize but do not induce cell fate during Drosophila dorsal embryonic epidermal patterning. *Development* **135**, 2767-2775.

Vincent, S., Ruberte, E., Grieder, N. C., Chen, C. K., Haerry, T., Schuh, R. and Affolter, M. (1997). DPP controls tracheal cell migration along the dorsoventral body axis of the Drosophila embryo. *Development* **124**, 2741-2750.

Wells, A. L., Lin, A. W., Chen, L. Q., Safer, D., Cain, S. M., Hasson, T., Carragher, B. O., Milligan, R. A. and Sweeney, H. L. (1999). Myosin VI is an actin-based motor that moves backwards. *Nature* **401**, 505-508.

Wells, A. R., Zou, R. S., Tulu, U. S., Sokolow, A. C., Crawford, J. M., Edwards, G. S. and Kiehart, D. P. (2014). Complete canthi removal reveals that forces from the amnioserosa alone are sufficient to drive dorsal closure in Drosophila. *Molecular biology of the cell* **25**, 3552-3568.

Williams-Masson, E. M., Malik, A. N. and Hardin, J. (1997). An actin-mediated two-step mechanism is required for ventral enclosure of the C. elegans hypodermis. *Development* **124**, 2889-2901.

Winick, J., Abel, T., Leonard, M. W., Michelson, A. M., Chardon-Loriaux, I., Holmgren, R. A., Maniatis, T. and Engel, J. D. (1993). A GATA family transcription factor is expressed along the embryonic dorsoventral axis in Drosophila melanogaster. *Development* **119**, 1055-1065.

Wood, W., Jacinto, A., Grose, R., Woolner, S., Gale, J., Wilson, C. and Martin, P. (2002). Wound healing recapitulates morphogenesis in Drosophila embryos. *Nat Cell Biol* **4**, 907-912.

Young, P. E., Richman, A. M., Ketchum, A. S. and Kiehart, D. P. (1993). Morphogenesis in Drosophila requires nonmuscle myosin heavy chain function. *Genes Dev* **7**, 29-41.

Zecca, M., Basler, K. and Struhl, G. (1995). Sequential organizing activities of engrailed, hedgehog and decapentaplegic in the Drosophila wing. *Development* **121**, 2265-2278.

Zhou, Q., Ruiz-Lozano, P., Martone, M. E. and Chen, J. (1999). Cypher, a striated muscle-restricted PDZ and LIM domain-containing protein, binds to alpha-actinin-2 and protein kinase C. *J Biol Chem* **274**, 19807-19813.

Zhou, Q., Chu, P. H., Huang, C., Cheng, C. F., Martone, M. E., Knoll, G., Shelton, G. D., Evans, S. and Chen, J. (2001). Ablation of Cypher, a PDZ-LIM domain Z-line protein, causes a severe form of congenital myopathy. *J Cell Biol* **155**, 605-612.

ANNEXES EN FRANCAIS

THÈSE DE DOCTORAT
DE L'UNIVERSITE DE LYON

Préparée à l'Ecole Normale Supérieure de Lyon

Ecole Doctorale n°340 - Biologie Moléculaire Intégrative et Cellulaire (BMIC)

Discipline : Sciences de la Vie

par

Antoine Ducuing

Signalling and morphogenesis during Drosophila dorsal closure

Voies de signalisation et morphogénèse pendant la fermeture dorsale de la Drosophile

---

Thèse présentée et soutenue publiquement à l'Ecole Normale Supérieure de Lyon, le 11 mars 2016

Directeur de thèse : Dr. Stéphane Vincent

Devant le jury composé de:

Dr. Yohanns Bellaïche, Directeur de Recherche, Institut Curie, Paris	Rapporteur
Dr. Krzysztof Jagla, Directeur de Recherche, GReD, Clermont-Ferrand	Rapporteur
Dr. Stéphane Vincent, Maître de Conférences, LBMC, ENS de Lyon	Directeur de Thèse
Pr. Arezki Boudaoud, Professeur, RDP, ENS de Lyon	Examinateur
Dr. Muriel Grammont, Chargée de Recherche, LBMC, ENS de Lyon	Examinatrice
Dr. Raphaël Rousset, Chargé de Recherche, IbV, Nice	Examinateur

INTRODUCTION

La fermeture dorsale est un événement majeur de l'embryogénèse de la drosophile durant lequel les cellules les plus dorsales de l'épiderme se différencient et agissent de concert pour refermer une ouverture dorsale temporairement recouverte par l'amnioséreuse. Ce processus présente de nombreuses similarités avec la cicatrisation cellulaire. Pendant la fermeture dorsale, les cellules de la marge active ont un cytosquelette extrêmement dynamique : les cellules sont polarisées, elles accumulent de fortes jonctions adhérentes et un réseau de microtubule dense. Les cellules de la marge active produisent également un câble d'actine ainsi que des protrusions appelées filopodes. Pendant la fermeture dorsale, les cellules de la marge active sont régulées par les voix JNK et DPP (homologue à la voie TGB-ß), où JNK induit DPP. Ces deux voies sont nécessaires à la fermeture dorsale. En effet, dans les mutants de la voie JNK ou DPP, la fermeture dorsale ne se fait pas. Les embryons présentent un phénotype d'ouverture dorsale. Cependant, on ne connaît pas comment les signaux de la voie JNK et DPP sont intégrés par les cellules de la marge active pour permettre une fermeture dorsale robuste. J'ai montré que les voies JNK et DPP forment une boucle cohérente appelée « feed-forward loop » (boucle d'anticipation) qui contrôle la différentiation des cellules de la marge active. La branche DPP de cette boucle filtre les signaux non désirés de la voix JNK quand les embryons sont soumis à un stress thermique. DPP joue un rôle ici de tampon contre les variations environnementales, ce qui est une nouvelle fonction par rapport à son rôle bien décrit de morphogène.

Je me suis ensuite concentré sur le câble d'actine, une structure supra-cellulaire produite par les cellules de la marge active lors de la fermeture dorsal. Les cellules autour d'une plaie dans des embryons de Drosophile, de poulet ou même de souris produisent également ce câble d'actine. En me servant de Zasp52, l'une des

cibles de la boucle de régulation JNK / DPP, j'ai montré que le câble d'actine est une structure discontinue qui n'est pas nécessaire pour la fermeture dorsale ou pour la cicatrisation cellulaire. Ceci remet en cause le modèle principal selon lequel le câble d'actine agit comme un cordon de bourse qui se ferme. J'ai montré que le câble ne confère par une force contractile pendant la fermeture. Le câble d'actine homogénéise les forces et stabilise la géométrie cellulaire pour que la fermeture se fasse de manière parfaite et sans cicatrice. Sans le câble, les cellules ont une forme irrégulière, associé à des défauts de patterning et des défauts de polarité planaire qui ressemblent aux défauts que l'on trouve lors de la formation d'une cicatrice. Nous proposons donc que le câble empêche la formation de cicatrice en « congelant » les propriétés mécaniques des cellules afin de les protéger des forces qui agissent au niveau tissulaire lors de la fermeture dorsale.

J'ai également montré que lors de la fermeture dorsale, DPP ne protège pas contre la mort cellulaire induite par JNK. J'ai également montré que c'est plus vraisemblablement la mort cellulaire dans l'amnioséreuse qui participe à l'apparition du phénotype d'ouverture dorsale dans les mutants de la voie DPP.

Enfin, j'ai montré que les tensions anormales / le stress peuvent déclencher l'activation de la voie JNK. Cette activité de JNK induite par le stress est cruciale pour la cicatrisation cellulaire chez l'embryon.

En conclusion, mon travail apporte un regard neuf sur la signalisation et la morphogenèse lors de la fermeture dorsale de l'embryon de Drosophile.

SOMMAIRE

ABSTRACT 7

INTRODUCTION 9

SOMMAIRE 11

CHAPITRES 21

I. De Thomas Hunt Morgan à nos jours : la Drosophile comme modèle d'étude pour comprendre les voies de signalisation et la morphogénèse 21

I.1 Thomas Morgan et sa pionière 'Fly Room' 21

I.2 Facile a élever : les Drosophiles comme modèle versatile 22

I.3 Un petit mais instructif génôme 23

I.4 Génétique de la drosophile 25

I.5 Live imaging et techniques in vivo 26

II. Le développement embryonaire de la Drosophile 29

II.1 Stades précoces (Stade 1 – Stade 5) 29

II.2 Gastrulation (Stade 6 – Stade 7) 32

II.3 Extension de la bandelette germinale (Stade 8 – Stade 10) 35

II.4 Segmentation et invagination des trachées (Stade 11) 37

II.5 Rétraction de la bandelette germinale (Stade 12) 41

II.6 Fermeture dorsale (Stade 13 – Stade 15) 43

II.7 Embryogénèse tardive (Stade 16 – Stade 17) 44

III. Morphogénèse pendant la fermeture dorsale 45

III.1 Généralités 47

III.2 L'amnioséreuse 50

III.3 Le cable d'actine 53

III.4 Les filopodes 59

III.6 La fermeture dorsale comme un modèle de cicatrisation cellulaire 63

IV. Voies de signalisation lors de la fermeture dorsale 65

IV.1 La voie JNK. 65

IV.2 La voie DPP. 70

V. Jupiter, Jaguar et Zasp52: 3 protéine du cytosquelette qui définissent l'identité de la marge active pendant la fermeture dorsale 77

V.1 Jupiter, une protéine associée aux microtubules 78

V.2 JAGUAR, l'homologue de la Myosine VI 81

V.3 Z band alternatively spliced PDZ-motif containing protein 52 83

PAPIERS 87

1. A DPP-mediated feed-forward loop canalizes morphogenesis during Drosophila dorsal closure 87

1.1. L'Article 87

1.2. Figures additionnelles 88

2. Le papier Zasp52 105

3. L'histoire sur JNK induit par le stress 141

4. Le papier mort cellulaire 154

Autres Papiers 196

1. Absolute requirement of cholesterol binding for Hedgehog gradient formation in Drosophila. 197

2. Cholesterol-free and cholesterol-bound Hedgehog: Two sparring-partners working hand in hand in the Drosophila wing disc? 199

DISCUSSION 212

1. JNK and DPP forment une boucle d'anticipation cohérente. 215

2. Qu'est-ce que la marge active ? 219

3. Zasp52 contrôle la formation du câble d'actine 221

4. Le cable d'actine n'est pas un cordon de bourse. 223

5. Est-ce que JNK agit comme un médiateur du stress dans l'embryon ? 227

6. Conclusion 231

Méthodes 233

1. Collection des embryons 233

2. Lignées de Drosophile 235

3. Immunofluorescence 239

3.1 Immunofluorescence classique 239

3.2. Marquage à la phalloidine 241

3.3 Anticorps 244

4. Live imaging et techniques in vivo 247

4.1. Aligner les embryons pour le Spinning disc 247

4.2 Régler le Spining disc 249

4.3. Ablation laser 253

5. Quantifications 255

5.1. Vitesse de fermeture 255

5.2. Expériences de recoil 255

5.3. Droiture de la marge active. 256

5.4 Statistiques. 256

6. Travail sur les images 257

6.1 Live imaging 257

6.2 Immunofluorescence 258

REFERENCES 259

RESUME DES CHAPITRES

Chapitre 1 : De Thomas Hunt Morgan à nos jours : la Drosophile comme modèle d'étude pour comprendre les voies de signalisation et la morphogénèse

La drosophile est un modèle puissant pour l'étude des voies de signalisation et de la morphogénèse. Ces petites mouches ont un cycle de vie court, s'élèvent facilement, donne naissance à une grande quantité de descendants. De nombresues lignées sont disponibles, et les outils génétiques puissants permettent de contrôler l'expression de transgénèse avec une résolution spatiale et temporelle. L'embryon de drosophile peut s'observer en live avec des protéines fluorescentes (GFP), ce qui en fait un outil très puissant

Chapitre 2 : Le développement embryonnaire de la Drosophile.

Le développement embryonnaire de la Drosophile est un événement qui dure 24 heures au cours duquel l'œuf subit des changements majeurs pour donner naissance à une larve qui est un organisme fonctionnel. Après une phase précoce durant laquelle les cellules se divisent de manière synchrone pour former un syncytium, l'embryon s'organise en trois feuillets pendant la gastrulation. A l'issue de la gastrulation, l'extension de la bandelette germinale se met en place. Plus tard, l'embryon se régionalise en segments, et les trachées se forment. La bandelette germinale se rétracte ensuite, laissant place à la fermeture dorsale. Une fois la fermeture dorsale terminée, la condensation du système nerveux se met en place pour donner naissance à une larve.

Chapitre 3 : Morphogénèse pendant la fermeture dorsale

La fermeture dorsale est un événement majeur de l'embryogénèse de la Drosophile durant lequel les cellules de la marge active de l'épiderme se différencient et agissent de concert pour refermer un trou dorsal recouvert par l'amnioséreuse. L'amnioséreuse est un moteur de la fermeture dorsale : ses cellules pulsent, se contractent et délainent afin de réduire la surface apicale de l'amnioséreuse. Pendant la fermeture dorsale, les cellules de la marge activent ont un cytosquelette dynamique. D'une part, ces cellules s'allongent et accumulent des microtubules orientés le long de l'axe dorso-ventral. D'autre part, ces cellules accumulent des filopodes qui vont permettre la fusion des deux bords. Les cellules de la marge active produisent également un câble d'actine qui encercle l'amnioséreuse. Sa fonction reste discutée. La fermeture dorsale présente de nombreuses similitudes avec la cictarisation cellulaire, c'est pourquoi c'est un modèle de choix pour comprendre comment les organismes vivants cicatrisent.

Chapitre 4 : Voies de signalisation pendant la fermeture dorsale

Les cellules de la marge activent reçoivent les signaux de la voie JNK, une voie anciennement de réponse au stress qui est une sous classe de la voie des MPAK. La voie JNK se composent d'une série de Kinases qui se phosphorylent en cascade. Cependant, on ne connaît pas le signal en amont activateur de la voie JNK. En aval, JNK induit quelques cibles dont DPP, l'exemple le plus frappant de morphogène. DPP agit en réprimant Brinker, un répresseur transcriptionnel. De plus, DPP donne aussi un signal activateur pour certaines cibles. En aval, on ne connaît pas de cibles de DPP. Pourtant, on sait que les voies JNK et DPP sont cruciales pour la fermeture dorsale car dans des embryons où la voie JNK ou la voie DPP est affectée ne peuvent pas se fermer.

Chapitre 5 : Jupiter, Jaguar et Zasp52: 3 protéine du cytosquelette qui définissent l'identité de la marge active pendant la fermeture dorsale.

On sait que les voies JNK et DPP sont cruciales pour la fermeture dorsale. En parallèle, on sait que le cytosquelette des cellules de la marge active dépend de ces deux voies. Cependant, on ne connaît pas de cibles des voies JNK et DPP qui agissent directement sur le cytosquelettes. Pendant ma thèse, j'ai mis en évidence que jupiter, Jaguar et Zasp52 sont trois gènes spécifiquement exprimés dans les cellules de la marge active au cours de la fermeture dorsale. De plus, ces protéines interagissent directement avec le cytosquelette des cellules de la marge active. Ce sont donc d'excellents marqueurs de la marge active. J'ai utilisé ces marqueurs pour comprendre comment les cellules de la marge activent interprètent les signaux des voies JNK et DPP. Je me suis ensuite focalisé sur Zasp52 et sa fonction lors de la fermeture dorsale.

Chapitre 6 : Résultats

Je présente ici mes résultats (un papier publié, un papier en revue, deux papier en future soumission). J'ai montré que les voies JNK et DPP forment une boucle cohérente appelée « feed-forward loop » (boucle d'anticipation) qui contrôle la différentiation des cellules de la marge active. La branche DPP de cette boucle filtre les signaux non désirés de la voix JNK quand les embryons sont soumis à un stress thermique. DPP joue un rôle ici de tampon contre les variations environnementales, ce qui est une nouvelle fonction par rapport à son rôle bien décrit de morphogène.

Je me suis ensuite concentré sur le câble d'actine, une structure supra-cellulaire produite par les cellules de la marge active lors de la fermeture dorsal. Les cellules autour d'une plaie dans des embryons de Drosophile, de poulet ou même de

souris produisent également ce câble d'actine. En me servant de Zasp52, l'une des cibles de la boucle de régulation JNK / DPP, j'ai montré que le câble d'actine est une structure discontinue qui n'est pas nécessaire pour la fermeture dorsale ou pour la cicatrisation cellulaire. Ceci remet en cause le modèle principal selon lequel le câble d'actine agit comme un cordon de bourse qui se ferme. J'ai montré que le câble ne confère par une force contractile pendant la fermeture. Le câble d'actine homogénéise les forces et stabilise la géométrie cellulaire pour que la fermeture se fasse de manière parfaite et sans cicatrice. Sans le câble, les cellules ont une forme irrégulière, associé à des défauts de patterning et des défauts de polarité planaire qui ressemblent aux défauts que l'on trouve lors de la formation d'une cicatrice. Nous proposons donc que le câble empêche la formation de cicatrice en « congelant » les propriétés mécaniques des cellules afin de les protéger des forces qui agissent au niveau tissulaire lors de la fermeture dorsale.

J'ai également montré que lors de la fermeture dorsale, DPP ne protège pas contre la mort cellulaire induite par JNK. J'ai également montré que c'est plus vraisemblablement la mort cellulaire dans l'amnioséreuse qui participe à l'apparition du phénotype d'ouverture dorsale dans les mutants de la voie DPP.

Enfin, j'ai montré que les tensions anormales / le stress peuvent déclencher l'activation de la voie JNK. Cette activité de JNK induite par le stress est cruciale pour la cicatrisation cellulaire chez l'embryon.

De plus, j'ajoute également mes deux papiers sur Hedgehog, publiés au début de ma thèse.

Conclusion

Pendant mon doctorat, je essayé de mieux comprendre la fermeture dorsale d'un point de vue des voies de signalisation et de la morphogénèse. J'ai trouvé que les voies JNK et DPP forment une boucle de feed-forward cohérente, où JNK est le signal instructif, et DPP filtre les signaux de JNK indésirables pour assurer une fermeture dorsale robuste et canalisée. Deuxièmement, j'ai montré que le câble actine produit par les cellules de la marge active n'est pas nécessaire pour la fermeture dorsale. Plus précisément, le câble de l'actine ne fournit pas une force contractile majeure, mais impose plutôt de fortes tensions afin d'équilibrer les forces et de stabiliser la géométrie des cellules de sorte que la fermeture laisse place à un tissu parfaitement structuré et sans cicatrice. J'ai également montré que JNK peut répondre à des tensions mécaniques et peut agir pendant la cicatrisation embryonnaire. Cependant, il est peu probable que DPP protège les cellules de la marge active de la mort cellulaire induite par JNK

Pour concluure, je voudrais donner une vision synthétique de la façon dont la fermeture dorsale pourrait simplement fonctionner, en tenant compte de toutes les données que je généré (cela est strictement mon opinion et peut ne pas refléter la réalité). Lors de la fermeture dorsale, les cellules de l'amnioséreuse pulsent et délaminent. Ceci est incontestablement la principale force motrice de la fermeture dorsale. Les filopodes jouent un rôle important puisqu'ils assurent la progression dorsale des cellules de la marge active. Ils peuvent agir à la place de l'amnioséreuse, comme cela est le cas au cours de la cicatrisation cellulaire. Le câble de l'actine ne produit pas une force contractile lors de la fermeture dorsale. A contario, il maintient la marge active droite afin de permettre une fermeture parfaite. Il peut également aider au zipping des filopodes en en limitant l'angle de chaque canthus. D'un point de vue de la signalisation, le cytosquelette des cellules de la marge active est contrôlé

par la boucle de feed-forward JNK / DPP. Le but principal d'un tel motif est de filtrer les signaux de JNK indésirables. En effet, l'activité de JNK non voulue est délétère pour la fermeture dorsale (voir le phénotype mutant PUC par exemple). J'ai trouvé que la température et le stress mécanique peuvent conduire à une activité de JNK ectopique, et je crois que d'autres contraintes pourraient déclencher l'activation de JNK. Par conséquent, cette boucle JNK / DPP permet aux cellules de la marge active de n'interpréteur que la composante développementale de la voie JNK.

La fermeture dorsale est donc un exemple frappant de la façon dont les voies de signalisation et des composants du cytosquelette agissent de concert pour promouvoir une action parfaite, robuste et coordonnée de centaines de cellules.